

V.E. LEVIN

Nuclear
Physics
and
Nuclear
Reactors

MIR PUBLISHERS
MOSCOW

The book is based on the lectures of the author at the Obrinsk Polytechnical School. The textbook is divided into two parts, "Atomic and Nuclear Physics" and "Nuclear Reactors". Part one describes the fundamentals of atomic physics, as well as the structure of the atomic nucleus and radioactivity, the registration and dosimetry of ionizing radiations, and their interaction with matter. Methods for accelerating charged particles, the properties of cosmic radiation and the physics of neutrons are also discussed. An introduction to atomic power engineering is presented in the second part. The construction, physics and operation of nuclear reactors, the development and economics of atomic power are also considered. The textbook is intended for students in physics technical schools, for technicians working in physics laboratories or servicing nuclear reactors and other atomic installations.



В. Е. ЛЕВИН

ЯДЕРНАЯ ФИЗИКА
И ЯДЕРНЫЕ РЕАКТОРЫ

ИЗДАТЕЛЬСТВО «АТОМИЗДАТ»
МОСКВА

V. E. LEVIN

Nuclear
Physics
and
Nuclear
Reactors

Translated from the Russian
by L. N. Bell

MIR PUBLISHERS
MOSCOW

**First published 1981
Revised from the 1979 Russian edition**

На английском языке

**© Издательство «Атомиздат», 1979
© English translation, Mir Publishers, 1981**

CONTENTS

PART ONE ATOMIC AND NUCLEAR PHYSICS

Chapter 1. ATOMIC PHYSICS

- 1.1 Matter and Electricity 11
- 1.2 Probability and Spectra 15
- 1.3 Mass and Energy 20
- 1.4 Electromagnetic Radiation 23
- 1.5 Structure of the Atom 27
- 1.6 Atomic Spectra 31

Chapter 2. FUNDAMENTALS OF QUANTUM MECHANICS

- 2.1 The Subject of Quantum Mechanics 38
- 2.2 Quantum States of Electrons in Atoms 41
- 2.3 Uncertainty Principle 45

Chapter 3. ATOMIC NUCLEUS

- 3.1 Properties of the Atomic Nucleus 49
- 3.2 Binding Energy of the Nucleus 54
- 3.3 Energy Levels of Nuclei 58
- 3.4 Nuclear Forces. Stability of the Nucleus 60
- 3.5 Models of the Nucleus 65

Chapter 4. RADIOACTIVITY

- 4.1 General Properties of Radioactivity 69
- 4.2 Radioactive Series 76
- 4.3 Law of Radioactive Decay 77
- 4.4 Alpha Decay 81
- 4.5 Beta Decay 84
- 4.6 Internal Conversion. Nuclear Isomerism 87
- 4.7 Applications of Radioactive Substances 90

Chapter 5. INTERACTION BETWEEN IONIZING RADIATIONS AND MATTER

- 5.1 Particle Flux Density and Intensity of Ionizing Radiation 96**
- 5.2 Interaction Between Heavy Charged Particles and Matter 99**
- 5.3 Range of Heavy Particles in Matter 102**
- 5.4 Interaction Between β -Particles and Matter 105**
- 5.5 Interaction Between Electromagnetic Radiation and Matter 108**
- 5.6 Radiation Doses 117**
- 5.7 Characteristics of γ -Radiation Sources 120**
- 5.8 Calculation of Protective Shields for Point γ -Sources 123**

Chapter 6. MEASUREMENT OF IONIZING RADIATIONS

- 6.1 Ionization Methods for Measurement of Radiations 126**
- 6.2 Volt-Ampere Characteristic of a Gas Discharge 128**
- 6.3 Ionization Chamber 131**
- 6.4 Proportional Counters 133**
- 6.5 Geiger-Muller Counters 138**
- 6.6 Scintillation Counters 141**
- 6.7 Semiconductor Detectors 143**
- 6.8 Other Techniques for Measuring Radiations 147**

Chapter 7. ACCELERATORS OF CHARGED PARTICLES

- 7.1 Applications of Accelerators 152**
- 7.2 Linear Accelerators 154**
- 7.3 The Cyclotron and Synchrocyclotron 156**
- 7.4 Electron Accelerators 159**
- 7.5 Proton Synchrotron 163**

Chapter 8. NUCLEAR REACTIONS

- 8.1 General Definition. Nuclear Reaction Equations 166**
- 8.2 Laws of Conservation of Energy and Momentum in Nuclear Reactions 168**
- 8.3 The Compound Nucleus 171**

8.4 Effective Cross Section and Yield of a Nuclear Reaction	173
8.5 Nuclear Reactions Induced by Charged Particles. The Nuclear Photoeffect	178
8.6 Nuclear Reactions at High Energies	180
8.7 Thermonuclear Reactions	182
8.8 Transuranic Elements	189

Chapter 9. COSMIC RADIATION

9.1 Nature of Cosmic Radiation	193
9.2 Radiation Belts of the Magnetosphere	198
9.3 Elementary Particles	200

Chapter 10. NEUTRON PHYSICS

10.1 Properties of Neutrons	205
10.2 Neutron Sources	206
10.3 Neutron Spectrometers	209
10.4 Neutron-Induced Nuclear Reactions	213
10.5 Neutron Detection	216
10.6 General Law of Attenuation of the Neutron Flux Density. The Macroscopic Cross Section	221
10.7 Neutron Diffusion	224
10.8 Neutron Slowing-Down	229
10.9 Thermal Neutrons	235
10.10 Nuclear Fission	237
10.11 Nuclear Fission Chain Reaction	243

PART TWO

NUCLEAR REACTORS

Chapter 11. DESIGN AND CLASSIFICATION OF REACTORS

11.1 Reactor Design	251
11.2 How Reactors Are Used	258
11.3 Homogeneous and Heterogeneous Reactors	263
11.4 Thermal, Fast and Intermediate Neutron Reactors	267
11.5 Classification of Power Reactors with Respect to Coolants and Moderators	269
11.6 Reactor Structural Materials	272

Chapter 12. REACTOR PHYSICS

- 12.1 Neutron Multiplication Factor 279**
- 12.2 Neutron Flux Density. Neutron Leakage 289**
- 12.3 Parameters of a Critical Bare Reactor 292**
- 12.4 Reactor with Reflectors 297**

Chapter 13. REACTOR OPERATION

- 13.1 Reactivity and Reactor Period 301**
- 13.2 Reactivity Temperature Coefficient 307**
- 13.3 Changes in Nuclear Fuel Composition 309**
- 13.4 Control Devices of the Safety Control System 315**
- 13.5 Reactor Start-Up and Shutdown 321**
- 13.6 Heat Generation and Heat Exchange in Reactors 327**

Chapter 14. ATOMIC POWER ENGINEERING

- 14.1 Development of Atomic Power Engineering 333**
- 14.2 Atomic Power Economics 340**
- 14.3 Research and Experimental Reactors 344**
- 14.4 Graphite-Water Reactors 350**
- 14.5 Vessel Water-Water Power Reactors (WWPR) 358**
- 14.6 Fast Neutron Reactors 361**

Appendix

- 1. International System of Units (SI) 367**
- 2. Fundamental Constants 368**
- 3. Physical and Nuclear Properties of Some Elements 369**
- 4. Physical Properties of Some Moderators 370**
- 5. Half-lives of Some Radioactive Substances 370**
- 6. Values of e^{-x} and e^x Functions 371**

Subject Index 372

PART ONE

ATOMIC AND NUCLEAR PHYSICS

CHAPTER 1

ATOMIC PHYSICS

1.1 Matter and Electricity

Matter is a form of nature, of the material world. Every substance consists of minute particles (atoms, molecules) which possess all chemical properties of the substance. Molecules of simple substances consist of one or several identical atoms whereas those of complex substances are composed of atoms of different chemical elements.

Atoms of a chemical element which differ with respect to mass are called *isotopes* of that element (see Sec. 3.1). Natural carbon has two isotopes. The *atomic mass unit* (amu) is defined as being 1/12 of the mass of the lighter isotope of natural carbon.

The mass of an atom (or molecule) is of the order of 10^{-26} kg. Special instruments, which were invented comparatively recently, are employed to measure such small masses. Before the advent of such devices the masses of atoms and molecules were expressed in relative units. The ratio of the mass of an atom (molecule) to the atomic mass unit is called the *relative atomic (molecular) mass* (or briefly, the *atomic (molecular) mass*)*. By definition this is a dimensionless quantity. It shows how many times the mass of an atom (molecule) exceeds the atomic mass unit. The atomic mass is denoted by *A* and the molecular mass, by μ .

* The ratio of the mass of an atom (molecule) to the atomic mass unit is also referred to as the *atomic (molecular) weight*.

A chemical element is a mixture of isotopes. The relative amount of an isotope in a chemical element is called the *isotope content*. It is expressed as a fraction or in per cent. The atomic mass of an element (Table 1.1) is the mean value of the atomic masses of the isotopes of that element. As an example, natural boron consists of two isotopes with contents 18.8% ($A = 10.0129$) and 81.2% ($A = 11.0093$) and hence its atomic mass $A = 10.8220$.

Table 1.1

Atomic Masses of Some Elements

Element	Symbol	Atomic mass	Element	Symbol	Atomic mass
Hydrogen	H	1.00797	Sodium	Na	22.9898
Helium	He	4.0026	Iron	Fe	55.847
Lithium	Li	6.9390	Nickel	Ni	58.71
Beryllium	Be	9.0122	Zirconium	Zr	91.22
Boron	B	10.8220	Indium	In	114.82
Carbon	C	12.01115	Thorium	Th	232.038
Oxygen	O	15.9994	Uranium	U	238.03

The mass of an atom (molecule) in atomic mass units is numerically equal to the atomic (molecular) mass. Thus the mass of the helium atom is 4.0026 amu and that of the oxygen atom, 15.9994 amu.

In molecular physics, chemistry and other fields of science a subsidiary mass unit, the kilogram-mole (kmole), is used for homogeneous substances, i.e. those which are composed of particles with identical properties. This is the amount of a homogeneous substance in kilograms which is numerically equal to its molecular (atomic) mass. A kilogram-mole of carbon, for example, is 12.01115 kg and that of beryllium, 9.0122 kg and of water, 18.0154 kg.

The number of molecules in a kilogram-mole of any homogeneous substance N_A is the same and is 6.02×10^{23} . This quantity, N_A , is called *Avogadro's number*. Knowing Avogadro's number and the kilogram-mole for carbon one can determine the atomic mass unit:

$$1 \text{ amu} = \frac{1}{72} \frac{A_C}{N_A} = \frac{1}{72} \frac{12}{6.02 \times 10^{23}} = 1.66 \times 10^{-27} \text{ kg}$$

The number of particles (molecules, atoms) in a cubic metre of a homogeneous substance is termed the particle density N . It can be found if the density ρ (kg/m^3), molecular mass μ (atomic mass A) and Avogadro's number are known,

$$N = \frac{\rho}{\mu} N_A; \quad N = \frac{\rho}{A} N_A \quad (1.1)$$

In the calculations of N approximate values of μ and A are usually employed, the first three figures being sufficient. Thus the approximate atomic mass of beryllium $A_{\text{Be}} \approx 9.01$ and the approximate molecular mass of water $\mu_{\text{H}_2\text{O}} \approx 18.0$.

Example. Find the molecular density of water H_2O . The density of water $\rho = 1000 \text{ kg/m}^3$ and molecular mass $\mu \approx 18$. According to formula (1.1)

$$N_{\text{H}_2\text{O}} = \frac{1000}{18} 6.02 \times 10^{26} = 3.34 \times 10^{28} \text{ molecules/m}^3$$

The number of atoms of any element in a cubic metre of the substance can easily be evaluated if the chemical formula of the molecule of the substance and the density of the latter are known:

$$N_i = n_i \frac{\rho}{\mu} N_A \quad (1.2)$$

where n_i is the number of element i in the molecule.

Example. How many boron atoms are there in 1 m^3 of boron carbide, B_4C , if its density is $2.3 \times 10^3 \text{ kg/m}^3$? The molecular mass of boron carbide $\mu \approx 10.8 \times 4 + 12.0 = 55.2$. There are four boron atoms in each molecule ($n_{\text{B}} = 4$).

According to formula (1.2)

$$N_{\text{B}} = 4 \frac{2.3 \times 10^3}{55.2} 6.02 \times 10^{26} = 1.00 \times 10^{29} \text{ atoms/m}^3$$

Impurities are usually present in various materials. The concentration of an impurity is defined as the amount of it in a unit volume of the material. It can be expressed in kilograms (or number of atoms, molecules) per unit volume or in per cent etc. The impurity concentration m (kg/m^3) and N (particles/m^3) are related by formula (1.1) in which the density of the substance ρ should be replaced by the impurity concentration m . If the mass concentration of the impurity

expressed in per cent is P then $m = P\rho_m \times 10^{-2}$, where ρ_m is the density of the mixture of substances. The impurity concentration N can then be calculated by the formula

$$N = P \frac{\rho_m}{\mu} N_A \times 10^{-2} \quad (1.3)$$

where μ is the molecular (atomic) mass of the impurity.

Example. Calculate the concentration of boron N_B in carbon if $P = 2 \times 10^{-4}\%$ and carbon density $\rho_C = 1.8 \times 10^{-3} \text{ kg/m}^3$. Since the concentration of boron in the carbon is low we may assume $\rho_m \approx \rho_C$ and hence according to formula (1.3)

$$N_B = 2 \times 10^{-6} \frac{1.8 \times 10^3}{11} 6.02 \times 10^{26} \approx 2.0 \times 10^{23} \text{ atoms/m}^3$$

The molecules in solids and liquids are arranged close to each other. Hence the volume V per molecule in such substances is comparable to the volume of the molecules. As an example, consider the volume of a molecule of water. Since the molecular density for water is $N_{H_2O} = 3.34 \times 10^{28} \text{ molecules/m}^3$, the volume of a single molecule

$$V_{H_2O} \approx 1/3.34 \times 10^{28} \approx 3 \times 10^{-29} \text{ m}^3$$

Assuming that the molecule can approximately be regarded as a sphere, the diameter of a water molecule can be calculated to be

$$d \approx \sqrt[3]{6V/\pi} \approx 3.86 \times 10^{-10} \text{ m}$$

The unit of length usually employed in atomic physics is the *angstrom* (\AA) which is 10^{-10} m . In these units the diameter of a water molecule, d , is approximately 3.86 \AA .

Atomism is not only a trait of matter but of electricity as well. The elementary electric charge $e = 1.60 \times 10^{-19} \text{ C}$. No other electric charge can be smaller than e and must be a multiple of it. Both positive and negative electric charges exist. The carrier of the elementary negative charge is the electron whose mass $m_e = 9.1 \times 10^{-31} \text{ kg} = 5.5 \times 10^{-4} \text{ amu}$ and specific charge $e/m_e = 1.76 \times 10^{11} \text{ C/kg}$. The elementary positive charge is the positron. Its mass and specific charge are the same as those of the electron. The positron is designated by the symbol e^+ and the electron by e^- .

1.2 Probability and Spectra

Natural events (phenomena) can be divided into certain and random events. A *certain event* is one which necessarily occurs if some S conditions exist. Thus, the boiling of water in a vessel is a certain event if the temperature of the water is 100°C and the gas pressure above the surface of the water $p = 1 \text{ atm}$. Events which do not occur under the given S conditions are termed impossible events. Water, for example, does not boil at temperatures $t < 100^{\circ}\text{C}$ and a pressure $p = 1 \text{ atm}$.

An event is called a *random event* if it does or does not occur under some certain conditions. Thus a falling coin may land with heads or tails up. Either of these possibilities, heads or tails, is a random event.

The laws governing the behaviour of random events occurring under certain conditions are studied in probability theory. One of the main concepts in this theory is that of the probability of an event.

Suppose that under identical conditions random events A_i ($i = 1, 2, \dots, k$) occur. Let event A_1 occur n_1 times, event A_2 n_2 times etc. and the total number of events $n = n_1 + n_2 + \dots + n_k$, n being a sufficiently large number. The probability of event A_i is defined as the quantity $f(A_i)$ equal to the ratio of the number of events A_i to the total number of events,

$$f(A_i) = n_i/n$$

The possibility of event A_i occurring can be predicted if $f(A_i)$ is known. For a coin thrown upwards under identical conditions the probability for it landing with heads or tails up is 0.5.

From the definition of the probability $f(A_i)$ it follows that the sum of all probabilities is unity,

$$\sum_{i=1}^k f(A_i) = f(A_1) + f(A_2) + \dots + f(A_k) = 1$$

This means that if the prescribed conditions are met, one of the k events certainly occurs. It may be noted that the probability of a certain event is unity and that of an impossible event, zero.

Random physical quantities are defined in a similar manner. The values of these quantities under a given set of conditions may vary. An example of a random physical quantity is the velocity of a gas molecule. At a gas pressure of 1 atm a molecule experiences about 10^8 collisions per second and after each collision its velocity changes. Hence one may speak only about the probability for the molecule to possess a certain velocity.

Probability theory is applied in statistical physics which studies the laws governing systems containing a large number of particles. In such systems the particles are kept together by attractive forces or by other means. An example of such a system of particles is a gas contained in a closed vessel.

Under normal conditions (pressure $p = 760$ mm Hg, temperature $t = 0^\circ\text{C}$) a kilogram-mole of any gas occupies a volume of 22.4 m^3 . In these conditions the molecular density of all gases is the same. It can be found by dividing Avogadro's number by the volume of a kilogram-mole and is $2.7 \times 10^{26} \text{ molecules/m}^3$. A comparison of the molecular densities of a gas and its liquid shows that the distance between the molecules in the gas is much greater than the size of the molecules.

An enormous amount of random events (e.g., the motion of each particle, alteration of its energy) may take place in a particle system. A result of the superposition of all these events is the emergence of certain laws which are called *statistical laws* and govern the behaviour of the particle system.

Statistical laws involve the mean values of physical quantities. These values characterize the state of the system and the processes occurring in it. They can either be measured directly or determined from the spectrum of the physical quantity. The spectrum of a physical quantity (mass spectrum, energy, velocity, frequency spectra etc.) is defined as the distribution of the system particles with respect to the values of the physical quantity.

Molecules of matter are in a state of continuous motion called *thermal motion*. As a result of this motion the molecules of a gas frequently collide. Under normal conditions the average distance a gas molecule travels between collisions

is 10^{-8} m. During the collisions energy exchange takes place between the molecules, the faster ones transferring part of their energy to the slower ones. As a consequence of the large number of collisions an equilibrium velocity distribution (velocity spectrum) is set up in a gas in a closed vessel.

Two types of spectra may be distinguished. If the distribution of the particles of a system with respect to a given physical quantity is continuous, the spectrum is called a *continuous* spectrum. If the distribution is not continuous and the particles can acquire only certain discrete values of the physical quantity, the spectrum is called a *discrete (line)* spectrum. An example of a discrete spectrum is the mass spectrum of an element which consists of atoms with certain values of mass. The distribution of molecules of a gas with respect to their velocities (velocity spectrum) is a continuous spectrum.

Spectra of physical quantities can be studied by theoretical methods or measured by using instruments called *spectrometers*. Spectra can be plotted as graphs, presented in tables or be expressed by analytic functions.

Suppose the particles of a system can be characterized by a random quantity L which varies continuously. Since L is random it is meaningless to speak about the number of particles with an exact value of L . This number is indefinite and may even be zero. However, the number of particles possessing values of L in an interval between L and $L + dL$ is definite and may be denoted $dN(L)$. Thus $dN(L)$ is the number of particles in an interval dL near the given value of L . The number $dN(L)$ is proportional to the number of particles in the system, N_0 , and to the width of the interval dL ,

$$dN(L) = f(L)N_0 dL$$

The proportionality coefficient

$$f(L) = \frac{1}{N_0} \frac{dN(L)}{dL}$$

defines the *probability density*. It depends on L and is the fraction of particles in the system contained in a unit interval near L . The function $f(L)$ is thus the probability that a particle possesses a value of the physical quantity in a unit range near L . Moreover, it is the continuous spectrum

of the physical quantity L . The spectrum is normalized to unity which means that the integral of $f(L)$ over all possible values of L is unity,

$$\int_0^{\infty} f(L) dL = \frac{1}{N_0} \int_0^{N_0} dN = 1$$

The properties of a system are determined by the mean values of the physical quantities, \bar{L} , which can be determined from the spectrum of the physical quantity,

$$\bar{L} = \int_0^{\infty} L f(L) dL / \int_0^{\infty} f(L) dL$$

Since function $f(L)$ is normalized to unity it follows

$$\bar{L} = \int_0^{\infty} L f(L) dL$$

The velocity spectrum $f(v)$ of gas molecules in a restricted volume was first studied by Maxwell. The function $f(v)$ is therefore called the *Maxwell spectrum* or *Maxwell distribution function*. Analytically the Maxwell spectrum has the form

$$f(v) = 4\pi \left(\frac{m}{2\pi kT} \right)^{3/2} v^2 \exp \left(-\frac{mv^2}{2kT} \right)$$

where v is the velocity of the molecule in m/s, m is the mass of the molecule in kg, $k = 1.38 \times 10^{-23}$ J/K is the Boltzmann constant and T is the temperature of the gas in Kelvin degrees, K.

The Maxwell spectrum $f(v)$ is depicted in Fig. 1.1. The molecular velocities range from zero to very large values. However most of the molecules move with velocities close to the most probable value v_p at which the spectrum is maximum. About 42% of the molecules move with velocities $v < v_p$. Consequently, the mean molecular velocity is 1.128 times greater than v_p . The fraction of molecules in an interval dv near a velocity v is represented in Fig. 1.1 by the crosshatched column. The base of the column is dv and its mean height $f(v)$.

The energy spectrum $f(E)$ of the molecules of a gas is

$$f(E) = \frac{2}{\sqrt{\pi}} \frac{\sqrt{E}}{(E_T)^{3/2}} \exp\left(-\frac{E}{E_T}\right)$$

The maximum of the Maxwell energy spectrum is located at the energy

$$E_M = E_T/2 = kT/2$$

The mean kinetic energy of the molecules \bar{E} and the kinetic energy E_T corresponding to the most probable velocity

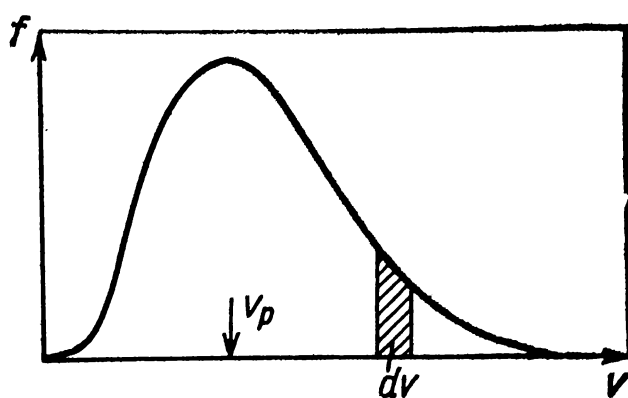


Fig. 1.1 Velocity distribution of molecules

city v_p are proportional to the temperature of the gas T :

$$E = \frac{3}{2}kT, \quad E_T = kT$$

Heating of a gas results in an alternation of the velocity distribution. A consequence of this is that the maximum in the Maxwell distribution shifts toward higher velocities and the temperature of the gas increases.

Suppose now that the random quantity L for a system of N_0 particles can assume only discrete values L_i ($i = 1, 2, \dots, k, \dots$), and let N_i be the number of particles possessing values L_i . The probability that a particle has a value L_i is equal to fraction of particles with that particular value L_i .

$$f(L_i) = N_i/N_0$$

The discrete spectrum $f(L_i)$ is normalized to unity since

The mean value of a discrete quantity is

$$\bar{L} = \sum_{i=1}^{\infty} L_i f(L_i)$$

To illustrate, the atomic mass of an element (see Table 1.1), which is the mean atomic mass of the isotopes of that element, can be found from the mass spectrum of the element.

1.3 Mass and Energy

The mechanical motion of bodies is always studied in inertial coordinate systems. These systems are fixed to other bodies which are regarded as being at rest. In studies of mechanical motion on the earth the laboratory coordinate system fixed to the earth's surface is usually employed. However all bodies, including the earth, are in motion, and hence only relative, but not absolute, motion of bodies can be observed.

The laws of mechanics are the same in all inertial coordinate systems. Thus the laws of free fall of bodies to the earth are the same as those for free fall in a uniformly moving train, steamship, airplane etc. This is the essence of the principle of relativity of motion discovered by Galilei.

According to the laws of classical mechanics the mass of a body is not dependent on its velocity of relative motion. These laws have been verified for body velocities much smaller than the velocity of light. However in a number of experiments it was subsequently observed that the masses of particles increase at high velocities. The dependence of the mass of a particle on its velocity was first observed by Kaufmann on measuring the specific charge of the electron.

Many experimental results which were inconsistent with the laws of classical mechanics were explained in 1905 by Albert Einstein in his theory of relativity. Underlying the first part of the theory, which has been termed the *special theory of relativity*, are two postulates based on experimental results.

1. No experiments carried out in any inertial system can ever detect whether the system is moving uniformly or is in a state of rest. In other words absolute uniform motion of bodies cannot be detected.

2. In all reference systems the velocity of light in vacuum is the same and equal to 3×10^8 m/s.

The conclusions of the special theory of relativity are very important for an understanding of the physical processes encountered in atomic and nuclear physics. It is precisely in these fields of physics that the speed of particles is close to that of light. We shall now consider two conclusions of the special theory of relativity.

1. The mass of any body m depends on its velocity v in accordance with the formula

$$m = \frac{m_0}{\sqrt{1 - v^2/c^2}} \quad (1.4)$$

where m_0 is the *rest mass* (mass of the body at $v = 0$). The mass of a moving body is called its *relativistic mass*. For $v/c \ll 1$ the mass $m \approx m_0$.

The ratio m/m_0 for various values of v/c is presented in Table 1.2. It can be seen that the mass of a body appreciably increases with approach of the velocity to the velocity of light.

Table 1.2

Relative Increase of the Mass of a Body on Increase of Its Velocity

v/c	0.006	0.06	0.55	0.990
m/m_0	1.00002	1.002	1.20	22.4

2. The mass m and energy W of a body are related by the equation

$$W = mc^2 \quad (1.5)$$

where m is the relativistic mass of the body. The mass of a body at rest $m = m_0$, and its energy $W_0 = m_0c^2$ (*rest energy*). Equation (1.5) shows that energy and mass do not exist separately. For an energy W of any form there corresponds a mass $m = W/c^2$. The energy W of a body is the sum of the rest energy W_0 and kinetic energy E .

$$W = W_0 + E$$

The unit of energy employed in atomic and nuclear physics is the **electronvolt** (eV) which is the energy an electron acquires on passing through a potential difference of one volt. It is related to the joule as follows,

$$1 \text{ eV} = 1.6 \times 10^{-19} \text{ J}$$

A larger energy unit is the **mega-electronvolt** (MeV),

$$1 \text{ MeV} = 10^6 \text{ eV} = 1.6 \times 10^{-13} \text{ J}$$

As an example let us determine the kinetic energy and velocity of an electron with an energy $W = 5 \text{ MeV}$. The rest energy of an electron $W_0 = m_0 c^2 = 9.1 \times 10^{-31} \times 9 \times 10^{16} = 8.19 \times 10^{-14} \text{ J} = 0.51 \text{ MeV}$. It may be noted that the masses of resting particles are frequently expressed in terms of the rest mass of the electron. In order to find out how many times the rest mass of a particle exceeds that of the electron it is sufficient to divide the rest energy of the particle by the rest energy of the electron. Thus the rest energy of the hydrogen atom $W_H = 937 \text{ MeV}$ and its rest mass $m_H = 1837 m_e$.

The kinetic energy of the electron $E = W - W_0 = 5 - 0.51 = 4.49 \text{ MeV}$. From equations (1.4) and (1.5) we find

$$v/c = \sqrt{1 - (W_0/W)^2} \approx 0.99$$

and the electron velocity is

$$v \approx 0.99c = 2.97 \times 10^8 \text{ m/s}$$

If the velocity of a body is small compared to that of light ($v/c \ll 1$), the binomial formula yields

$$\left[1 - \left(\frac{v}{c} \right)^2 \right]^{-1/2} \approx 1 + \frac{1}{2} \left(\frac{v}{c} \right)^2$$

and according to formula (1.4)

$$m = m_0 + \frac{1}{2} m_0 \left(\frac{v}{c} \right)^2$$

Inserting this expression for the mass into formula (1.5) we get

$$W = m_0 c^2 + \frac{1}{2} m_0 v^2$$

The first term is equal to the rest energy of the body W_0 and the second to the kinetic energy of the body,

$$E = \frac{1}{2} m_0 v^2$$

1.4 Electromagnetic Radiation

Electromagnetic waves are emitted by charges moving with acceleration. If a charge oscillates with a constant frequency ν it excites an electromagnetic wave of the same frequency. The electric E and magnetic H intensities of the electromagnetic field are numerically equal. They are perpendicular to each other and to the direction of propagation of the wave and oscillate with the same frequency ν . If electrons oscillate in an antenna with a frequency ν , radio waves will be emitted. Another example of accelerated motion of electrons is when they revolve in a circle with a frequency ν .

The oscillation period T and wavelength λ of electromagnetic radiation are related by the equations

$$T = 1/\nu; \quad \lambda = c/\nu$$

Electromagnetic radiation can be divided into several types (Table 1.3)

Table 1.3

Types of Electromagnetic Radiation

Radiation	Frequency range, Hz	Wavelength range, m
Radio waves	10^4-10^{11}	$3 \times 10^4-0.3 \times 10^{-2}$
Infrared	$10^{11}-4 \times 10^{14}$	$0.3 \times 10^{-2}-7.5 \times 10^{-7}$
Visible light	$4 \times 10^{14}-7.5 \times 10^{14}$	$7.5 \times 10^{-7}-4 \times 10^{-7}$
Ultraviolet	$7.5 \times 10^{14}-3 \times 10^{18}$	$4 \times 10^{-7}-10^{-10}$
X-ray	$3 \times 10^{16}-3 \times 10^{20}$	$10^{-8}-10^{-12}$
Gamma	$3 \times 10^{19}-3 \times 10^{22}$	$10^{-11}-10^{-14}$

The properties of electromagnetic radiation depend only on its frequency ν but not on the way it is generated. Infrared light produces a feeling of warmth in man and hence is frequently called heat radiation. X-rays are used in medicine for diagnosis of diseases due to its high penetrating power.

The wave properties of electromagnetic radiation are confirmed by various experiments and in particular by experiments on the diffraction of waves. Diffraction of radiation is observed when the radiation interacts with bodies whose size is comparable to that of the wavelength λ . As a result of diffraction alternating maxima and minima of the radiation intensity are formed. As an example consider the diffraction of X-rays on reflection from the surface of a single crystal

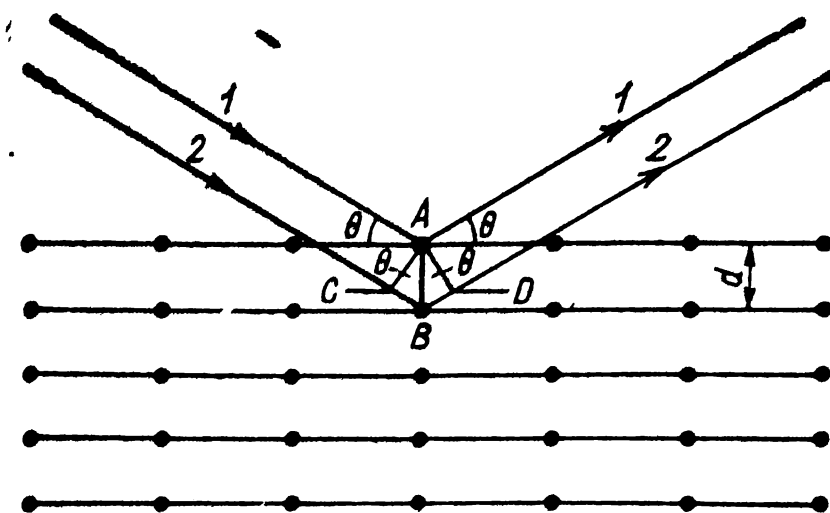


Fig. 1.2 Reflection of X-rays by a crystal plane

(Fig. 1.2). The single crystal consists of atoms arranged in a regular pattern. The distance between the atoms (lattice constant) is approximately equal to the size of the atoms (10^{-10} m) and of the same order of magnitude as the wavelength of X-rays.

All atoms lying in the same plane form a crystal plane. For X-rays incident on the surface of a single crystal at an angle θ the crystal planes are effectively semitransparent mirrors. They reflect part of the rays and transmit the remaining ones. A single crystal is therefore an array of such reflecting planes.

Suppose the radiation is reflected from two neighbouring crystal planes (beams 1 and 2, Fig. 1.2). The path difference of the beams in the crystal, l , is the sum of the segments CB and BD . The angle of incidence of the radiation is equal to the angle of reflection. The right triangles ABC and ABD are therefore congruent. Hence $BC = BD = d \sin \theta$. The intensity of the radiation will be enhanced if the reflected

beams leave the crystal in the same phase. This condition is met if the path difference l is equal to an integral number of wavelengths,

$$n\lambda = 2d \sin \theta$$

where $n = 1, 2, 3, \dots$ This equation was derived independently by the Russian physicist Vul'f and the English physicist Bragg and is therefore called the *Vul'f-Bragg equation*.

If the path difference is equal to a nonintegral number of wavelengths the reflected rays will leave the crystal in different phases and therefore will be partially or completely quenched. Complete quenching occurs when l is equal to an uneven number of half wavelengths and is observed at an angle θ such that

$$\frac{2n+1}{2} \lambda = 2d \sin \theta$$

The wave theory of light satisfactorily explains such phenomena as diffraction, interference etc. However, it yields erroneous results for the photoelectric effect.

The *photoelectric effect* consists in the ejection of electrons from a substance as a result of irradiation by light. A minimum light frequency ν_0 exists below which the effect does not occur. This frequency is called the *photoelectric threshold frequency*. The lowest threshold frequency is observed in the alkali metals, particularly in caesium, which are used to cover the cathodes of photocells.

The wave theory of light explains the ejection of electrons from a metal as follows. The periodic electric field of the light wave produces a periodic force in the metal which "rocks" the electron and conveys energy to it which may be sufficient for its ejection (the minimum amount of energy required to eject an electron is called the work function). The higher the intensity of the light the greater one would expect the electron to be rocked and the higher would be its velocity. According to the wave theory photoelectrons should appear only a certain time after the beginning of illumination of the metal. This is the time required for the electrons to be rocked sufficiently to acquire an amount of energy which exceeds the work function. The wave theory predicts that a time of several hours would be required for this amount of energy to be accumulated at low light intensities. However,

these predictions of the wave theory are not in agreement with the experimental data. First of all, the velocities of the photoelectrons depend on the frequency and not on the intensity of the light, and secondly the emission of photoelectrons commences immediately after the beginning of illumination of the metal.

In 1905 Einstein showed that all regularities of the photo-effect could be explained by the *corpuscular theory of light*. In this theory light is regarded as a stream of electrically neutral particles called *photons*. The energy of a photon E_{ph} is proportional to frequency of the light ν

$$E_{ph} = h\nu$$

where $h = 6.62 \times 10^{-34} \text{ J}\cdot\text{s} = 4.13 \times 10^{-15} \text{ eV}\cdot\text{s}$ is the *Planck constant*.

A photon always moves with the velocity of light and its relativistic mass

$$m_{ph} = E_{ph}/c^2 = h\nu/c^2$$

The rest mass of a photon is zero since a photon cannot be at rest as an electron, atom etc. can.

According to the corpuscular theory of light the photons incident on the surface of a metal are absorbed by the electrons in the metal. Part of the photon energy $E_{ph} = h\nu$ is spent on overcoming the work function W_e and the other part is spent in imparting kinetic energy to the photoelectron E . In accordance with the law of conservation of energy

$$h\nu = W_e + E$$

Since the work function W_e is equal to the least energy of a photon sufficient to eject an electron, $h\nu_0$, we may substitute $h\nu_0$ for W_e and hence

$$h\nu = h\nu_0 + E$$

where ν_0 is the threshold frequency. This equation can be useful in explaining the experimental results on the photo-effect. Thus the energy and hence the velocity of the photoelectron is seen to be dependent on the energy $E_{ph} = h\nu$ of the photon absorbed by the electron in the metal. Since energy is transmitted to the electrons instantaneously, the photoelectrons are emitted immediately after commencement of illumination of the metal.

The photoelectron energy is a linear function of the frequency ν and this permits an experimental determination of the Planck constant h . For this purpose the energy of photoelectrons in a photocell is measured at various light frequencies. The dependence $E = f(\nu)$ is then plotted and should be a straight line. The slope of the line is equal numerically to the Planck constant h .

A study of the properties of electromagnetic radiation revealed that some of the experimental data could be explained by the wave theory and others by the corpuscular theory of light. Neither of these theories can separately explain all the experimental facts. Thus *dualism* in the nature of electromagnetic radiation is observed. The quantum theory of radiation, which embraces both the wave and corpuscular properties of light, is now employed by scientists to explain a variety of natural phenomena.

1.5 Structure of the Atom

Up to the end of XIX century the atom was considered indivisible. However, some phenomena indicated that the atom may possess a complex structure. Several models of the atom were proposed at the beginning of the XX century. These models, it was hoped, would be useful in explaining a number of puzzling experimental results such as the line structure of the emission spectra of gases at high temperatures and the electric neutrality of the atom and its stability.

A planetary model of the atom similar to that of the solar system was proposed by Ernest Rutherford in 1911. In this model a small nucleus of about 10^{-14} m in size is located in the centre of the atom whose size is approximately 10^{-10} m. Almost all the mass of the atom is concentrated in the nucleus. The nucleus has a positive charge Ze , where Z is the atomic (ordinal) number of the element in the Mendeleev periodic system. Electrons move around the nucleus in circular orbits. Their charge compensates the positive charge of the nucleus, which explains why the atom is neutral.

Each moving electron experiences a centripetal force equal to the coulomb force of attraction between the electron and nucleus. This force presumably ensures stable orbital motion

of the electron in the atom, which is similar to the orbital motion of planets about the sun.

The planetary model however turned out to be untenable. Indeed, the electron moves in the atom with acceleration. It should therefore emit energy and after having lost all its energy it should fall onto the nucleus. Thus, under any conditions the atom should emit electromagnetic waves according to the planetary model and hence be unstable. Actually the atom is a very stable system and does not emit radiation at low temperatures. Atoms begin to emit radiation appreciably only at high temperatures and the emission spectrum of gases is linear.

A solution to this problem was suggested by the Danish physicist Niels Bohr in 1913. He developed a new model in which some of the main features of the planetary model were retained. He assumed that the motion of electrons in the atom and the emission and absorption of electromagnetic waves by the atom do not obey the classical laws of physics, as assumed in the planetary model, but are governed by novel quantum laws. These laws were formulated as two postulates.

1. Electrons moving in the atom in definite stationary orbits do not emit electromagnetic waves and the energies of the electrons are discrete values W_1, W_2, \dots, W_n .

2. When an electron jumps from one orbit to another its energy changes by a discrete value

$$\Delta W = W_{n_2} - W_{n_1}$$

where W_{n_2} and W_{n_1} are the final and initial energies of the electron. If $\Delta W > 0$ the atom absorbs energy, and if $\Delta W < 0$, it emits a photon with a frequency $\nu = -\Delta W/h$.

According to Bohr's theory the orbital electrons in the atom are grouped together in electron shells to which numbers may be ascribed, the numbers increasing with the distance from the nucleus. These shell numbers $n = 1, 2, 3, \dots$ are called *quantum numbers*. Electron shells with quantum numbers $n = 1, 2, 3, 4, 5, 6, \dots$ are designated respectively as *K, L, M, N, O, P, ... shells*. Thus the first shell ($n = 1$) is the *K*-shell etc. All electrons of an n th shell have the same energy W_n which is usually referred to the total rest energy of the nucleus and all atomic electrons.

The electron is not only attracted by the nucleus but repulsed by the other electrons which weaken its attraction to the nucleus. This effect is called *screening*. It is greater for the farthermost shells. Electrons of the *K*- and *L*-shells are almost not screened in many-electron atoms. These electrons are most strongly bound in the atom.

In general there is an infinite number of electron shells in an atom. However only a few of them are filled completely or partially by the Z electrons and the remaining are empty. In the absence of external forces the electrons fill in the shells closest to the nucleus. In each n th shell there may be up to $2n^2$ electrons. This array corresponds to a minimum energy of the atom and hence ensures its stability. This state is called the *ground state* and the respective energy—the *ground energy level* (ground level). If external forces act on the atom (for example, as a result of inelastic collisions* with other atoms or free electrons etc.) a certain amount of energy may be imparted to an electron which may jump into a vacancy in one of the outer shells. The atom is then said to be in an *excited state* and its energy is referred to as an *excited energy level* (excited level). The atom is ionized if an electron in some shell n_1 is completely removed from the atom ($n_2 = \infty$).

The excited atom is unstable. Its lifetime is approximately 10^{-8} s. The electron jumps to an orbit in a shell closer to the nucleus and the atom returns to the ground state. A photon is emitted on transition of an excited atom from the excited to ground state.

The nucleus and atom are bound-particle system. In such systems the particles are held together by attractive forces. The bond of a particle a in a system can be characterized by the *binding energy* e_a . This is the energy required to remove particle a from the system (e.g. an electron from the atom). The *binding energy of a system of particles*, W_b , is the energy required to break the bonds between all particles of the system. If particle a returns to the bound-particle system an

* In inelastic collisions of two particles part of the kinetic energy is spent in altering the inner state of the particles. In elastic collisions only a redistribution of kinetic energy occurs between the particles, their internal state remaining the same.

amount of energy ϵ_a is released and if the whole system is resynthesized the energy liberated is W_s . According to formula (1.5), during the synthesis of a bound system of particles part of the rest energy is transformed into other types of energy. This transformation of rest energy into other types of energy may shortly be termed *energy liberation* (or *release*).

The binding energy of electrons in atoms can be measured by bombarding the atoms with fast electrons. At a certain accelerating potential difference U_i , the energy of the bombarding electrons E_i becomes equal to the binding energy of electrons in the outermost shell W_i , and ionization of the atoms commences. The potential difference U_i is the *ionization potential*.

The chemical properties of elements depend on the number of electrons in the outer shell. These electrons are bound to the nucleus more weakly than those of the inner shells. In chemical reactions the outer shell electrons, which are also called valence electrons, are transferred from one atom to another. Electrons of the outer, but filled, shells are more strongly bound in the atom than are the electrons of outer but not completely filled shells. This is why the noble gases (helium, neon etc.) are chemically inert under normal conditions. The noble gases are monoatomic precisely because the outer shells of the atoms are filled.

Consider now the order of filling of the atomic shells. Hydrogen has a single electron in the K -shell and is univalent. In helium the K -shell is filled and it is an inert gas. Since not more than $2n^2 = 2$ electrons can be in the K -shell, the L -shell begins to be filled in univalent lithium. This shell is completely filled in the atoms of the inert gas neon.

Building-up of the M -shell begins in sodium, the first element of the third row of the Mendeleev periodic table. There is one electron in the outer M -shell and the chemical properties of sodium are therefore similar to those of lithium. Beryllium and magnesium, which have two electrons in the outer shell, are divalent elements. An interesting feature of the structure of the electron shells in the rare-earth elements (lanthanides) which occupy a single group in the periodic table ($Z = 57-71$) should be noted. Despite the fact that their atomic numbers are different, the chemical properties of all the lanthanides are similar. In the atoms of

these elements the binding energy is maximal if the usual order of filling up of the shells is violated. The first three shells in cerium ($Z = 58$) are completed shells; there are 19 electrons in the N -shell ($n = 4$), 9 in the O -shell and 2 in the outermost P -shell. In the praseodymium atom ($Z = 59$) the N -shell has 21 electrons, the O -shell 8 and the P -shell, as in cerium, 2 electrons etc. Thus with increase of the atomic number of the lanthanides the vacancies in the inner shells are filled, only two electrons being in the outer shell. A similar pattern is observed in the actinides ($Z = 90-103$), the P -shell of which also contains two electrons.

The physical essence of the Mendeleev periodic law is defined by the structure of the electron shells. According to the law, the properties of the elements should repeat periodically with increase of the atomic mass. However exclusions from this law had to be invoked. Nickel ($A = 58.71$), for example, had to be arranged behind cobalt ($A = 58.93$) in accordance with the chemical properties. The cause of such deviations was explained by the Bohr theory: the properties of the elements should repeat periodically not on increase of the atomic mass but on increase of the atomic number Z . The structure of the external shell repeats periodically with increase of Z and hence the chemical properties of the elements should also vary periodically.

1.6 Atomic Spectra

Line spectra of atoms reflect the structure of the atomic electron shells. Certain regularities are observed in any atomic spectrum. The latter consists of a number of optical and X-ray series of lines. With increase of frequency of the emitted radiation the lines become closer together, their intensity falls and a limit is reached at which the series terminates.

Atoms emit electromagnetic radiation only in the excited state. On transition of an electron from a shell with quantum number n_2 to a shell with n_1 ($n_2 > n_1$), a photon with energy $h\nu = -\Delta W$ is emitted. As n_1 increases the frequency of the photon emitted approaches the limiting value $v_1 = e_0/h$, where e_0 is the binding energy of the electron in shell n_1 .

The energies of electrons in atomic shells can be repre-

Periodic Table of the

Period	I		GROUPS OF ELEMENTS				
			II	III	IV	V	
1	(H)						
2	Li 3 6.941 Lithium	Be 4 9.01218 Beryllium	5 10.81 Boron	6 12.011 Carbon	7 14.0067 Nitrogen		
3	Na 11 22.98977 Sodium	Mg 12 24.305 Magnesium	13 26.98154 Aluminium	14 28.08 Silicon	15 30.97376 Phosphorus		
	K 19 39.098 Potassium	Ca 20 40.08 Calcium	Sc 21 44.9559 Scandium	Ti 22 47.90 Titanium	V 23 50.9414 Vanadium		
4	29 Cu 63.548 Copper	30 Zn 65.38 Zinc	31 Ga 69.72 Gallium	32 Ge 72.59 Germanium	33 As 74.9216 Arsenic		
	Rb 37 85.4678 Rubidium	Sr 38 87.62 Strontium	Y 39 88.9059 Yttrium	Zr 40 91.22 Zirconium	Nb 41 92.9064 Niobium		
5	47 Ag 107.868 Silver	48 Cd 112.40 Cadmium	49 In 114.82 Indium	50 Sn 118.69 Tin	51 Sb 121.75 Antimony		
	Ca 55 132.9054 Cesium	Ba 56 137.34 Barium	La* 57 138.9055 Lanthanum	Hf 72 178.49 Hafnium	Ta 73 180.9479 Tantalum		
6	79 Au 196.9665 Gold	80 Hg 200.59 Mercury	81 Tl 204.37 Thallium	82 Pb 207.2 Lead	83 Bi 208.9804 Bismuth		
7	Fr 87 [228] Francium	Ra 88 226.0254 Radium	Ac** 89 [227] Actinium	Ku 104 [261] Kurchatovium	(Nc) 105 [261] (Nielsborium)		

* LANTH

Ce 58 140.12 Cerium	Pr 59 140.9077 Praseo- dymium	Nd 60 144.24 Neodym- ium	Pm 61 [145] Prome- thium	Sm 62 150.4 Samar- ium	Eu 63 151.96 Europium	Gd 64 157.25 Gado- linium
---------------------------	--	-----------------------------------	-----------------------------------	---------------------------------	-----------------------------	------------------------------------

** ACT

Th 90 232.0381 Thorium	Pm 91 231.0359 Protactinium	U 92 238.026 Uranium	Np 93 237.0482 Neptu- nium	Pu 94 [244] Pluto- num	Am 95 [243] Americum	Cm 96 [247] Curium
------------------------------	-----------------------------------	----------------------------	-------------------------------------	---------------------------------	----------------------------	--------------------------

Chemical Elements

		VII		VIII	
VI		1 1.0079 Hydrogen	H	2 4.00260 Helium	He
8 15.9994	O Oxygen	9 18.99840	F Fluorine	10 20.179	Ne Neon
16 32.06	S Sulphur	17 35.453	Cl Chlorine	18 39.948	Ar Argon
Cr 51.996	24 Chromium	Mn 54.9380	25 Manganese	Fe 55.847	26 Iron
34 78.96	Se Selenium	35 79.904	Br Bromine	36 93.80	Kr Krypton
Mo 95.94	42 Molybdenum	Tc 98.9062	43 Technetium	Ru 101.07	44 Ruthenium
52 127.60	Te Tellurium	53 126.9045	I Iodine	54 131.30	Xe Xenon
W 183.85	74 Tungsten	Re 186.207	75 Rhenium	Os 190.2	76 Osmium
84 [209]	Po Polonium	85 [210]	At Astatine	86 [222]	Rn Radon
				Symbol of element	
				<div style="border: 1px solid black; padding: 5px; display: inline-block;"> Li 3 6.941 Lithium </div>	
				Atomic number Atomic mass	

ANIDES

Tb 158.9254	Dy 162.59	Ho 164.9304	Er 167.28	Tm 169.0342	Yb 173.01	Lu 174.97
Terbium	Dysprosium	Holmium	Erbium	Thulium	Ytterbium	Lutetium

NITRUM

Bk [247]	Cf [251]	Mg [254]	Pm [257]	Md [258]	(No) [259]	(Lr) [260]
Berkelium	Californium	Magnesium	Promethium	Mandelshtamium	(Nobelium)	(Lawrencium)

sented by a diagram (Fig. 1.3). This electron energy level diagram consists of a number of horizontal lines arranged at different heights. The distance between some n th horizontal line and a given reference line is plotted to be proportional to the energy W_n . The energies W_n and quantum numbers n are written near each line. Possible electronic transitions in the excited atom are designated by the vertical arrows.

Lines of the K -series are emitted when electrons jump

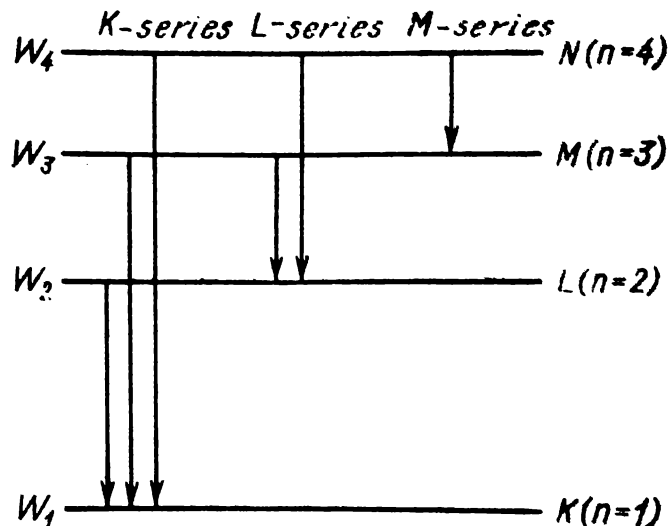


Fig. 1.3 Energies of electrons in atomic shells and X-ray series

into the K -shell; the L -series is emitted when an electronic transition to the L -shell occurs etc. The K -series consists of K_{α} , K_{β} and other lines, the L -series of L_{α} , L_{β} and other lines.

Suppose that there is a vacancy in the K -shell and that electrons from outer shells may occupy the vacancy. It has been found that the probability for an electronic transition to the K -shell from any other shell, and hence the intensity of the respective line, decreases with increase of the quantum number n of the outer shell. The most probable is a transition from the L -shell which is the closest to the K -shell. Correspondingly the K_{α} -line is the most intense in the K -series. The set of electronic transitions to the K -shell from all possible excited states of the atoms yields the K -series. The other spectral series are produced in a similar way.

Each transition of an electron in an excited atom involves the emission of a single photon. Several photons can be

emitted if the transition is accompanied by other transitions. If an electron from the outer shell jumps directly into the *K*-shell only one photon will be radiated. If, however, an electron from the *L*-shell first moves into the *K*-shell and then an electron from an outer shell moves into the *L*-shell, two photons will be emitted etc. It should be noted that the transition of an electron from an atomic shell to another shell corresponds to the transition of the atom from a certain energy level to another level, the energies of the electron and atom being altered by the same amount.

The hydrogen atom is the simplest. The nucleus is the proton designated by *p*. The proton mass $m_p = 1.007276$ amu is 1836 times greater than the electron mass. The positive charge of the proton is equal to the elementary electric charge 1.60×10^{-19} C. According to the Bohr theory the emission spectrum of hydrogen can be expressed by the formula

$$\nu = cR (1/n_1^2 - 1/n_2^2) \quad (1.6)$$

where $R = 1.097 \times 10^{-7}$ m⁻¹ is the *Rydberg constant* and *c* is the velocity of light in m/s.

The so-called Balmer series is emitted in transitions from shells with $n_2 = 3, 4, 5, \dots$ to the *L*-shell ($n_1 = 2$). This series was established experimentally before the appearance of Bohr's theory. On the basis of formula (1.6) Bohr predicted several other spectral series for hydrogen which were subsequently observed experimentally. The agreement between the theory and experiments for the hydrogen atom seemed to prove the validity of the Bohr postulates regarding the motion of electrons in atoms.

The spectra of many-electron atoms are very complex. This is due to electron screening in the atom which varies on increase of the distance of the shell from the nucleus.

X-rays are emitted in transitions of the electrons to the inner shells. Optical radiation is connected with electronic transitions in the outer shells. Optical radiation can be divided into ultraviolet, visible and infrared light.

Consider the effect of electron screening on the properties of the optical and X-ray spectra. It has been mentioned that electrons of the outermost shell are weakly bound to the nucleus. Only an effective nuclear charge *e* but not the total charge acts on an electron of the outer shell. The remaining

part of the nuclear charge is neutralized by the $(Z - 1)$ other electrons of the atom. Hence the properties of the optical spectrum are almost completely determined by the structure of the external shell and only weakly depend on the atomic number Z . Since the structure of the outer shell varies periodically, the properties of the optical spectrum vary in a similar manner. As an example, the outer shells of the alkali metal atoms contain only one electron. These electrons emit light whose frequencies are much the same for the various alkali metals. Thus there is no appreciable dependence of the frequency on the atomic number.

The X-ray frequency varies in a different manner. It strongly depends on the nuclear charge. As an example consider the K_{α} -line. An effective nuclear charge equal to $(Z - 1) e$ acts on the electrons of the K - and L -shells. According to the Bohr theory the frequency of the K_{α} -line can be found by applying formula (1.6), which should first be multiplied by $(Z - 1)^2$, and by assuming $n_1 = 1$, $n_2 = 2$,

$$\nu = \frac{3}{4} cR (Z - 1)^2$$

For atomic numbers $Z \gg 1$ the frequency of the K_{α} -line is proportional to Z^2 . Thus with increase of the atomic number no periodicity in the properties of the X-ray spectrum is observed as in the case of the optical spectrum.

Taking the square root of both sides of the last equation and substituting $1/\lambda$ for ν/c we get

$$\sqrt{1/\lambda} \approx \sqrt{(3/4) R} (Z - 1)$$

The square root of the inverse wavelength of the K_{α} -line is thus a linear function of the atomic number. A linear dependence of $\sqrt{1/\lambda}$ on Z is observed for the K -, L - and M -series of lines in the X-ray spectrum. This regularity was first observed experimentally in 1913 by the English physicist Moseley and hence has been called the *Moseley law*. The nuclear charge has been determined with greater precision by measuring the K_{α} -line frequencies of various elements and applying the Moseley law.

The line spacing in the X-ray spectrum is specific for each element. The structure of the X-ray spectrum, which is a reflection of the properties of the inner electron shells, is

characteristic of the atom. The X-ray line spectrum of elements has therefore been termed the *characteristic spectrum*.

Bohr's theory gave insight into the structure of the atom. The results of the theory pertaining to the emission of radiation by the hydrogen atom were in brilliant agreement with the experimental results. The Bohr theory could explain the origin of the line spectra of complex elements, Mendeleev's periodic law and Moseley's law. However it was puzzling why the motion of electrons in atoms obeys the two postulates. The latter were introduced by Bohr without any proof and the justification was that theoretical predictions could be made which were in agreement with the experimental results. A theoretical study of the structure of the atom was continued in quantum mechanics in which the laws of motion in atoms and other quantum systems were established on a new basis.

CHAPTER 2

FUNDAMENTALS OF QUANTUM MECHANICS

2.1 The Subject of Quantum Mechanics

The laws of the macroscopic world (macrocosm) are studied in classical physics. This world consists of bodies formed by enormous numbers of atoms and molecules. Almost all of the experimental results seemed to have been explained by the end of the XIX century due to the discoveries made by Galilei, Newton, Lomonosov and other scientists. However the nature of the photoeffect and of some other phenomena remained to be clarified. The study of these phenomena initiated the penetration of physics into the secrets of the microscopic world (microcosm) in which the properties of atoms, electrons and other microparticles are of particular importance. The investigations of Planck and Einstein on the interaction between light and matter laid the foundations of the quantum theory of electromagnetic radiation. According to the quantum theory, light is a stream of photons possessing an energy E and momentum p ,

$$\left. \begin{array}{l} E = h\nu \\ p = h/\lambda \end{array} \right\} \quad (2.1)$$

The left-hand sides of these equations (energy, momentum) are characteristics of particles (corpuscles), whereas the right-hand sides (frequency, wavelength $\lambda = c/\nu$) are characteristics of electromagnetic waves. Thus equation set (2.1), as written, reflects the dualism of light (wave-particle). On the one hand light resembles a gas consisting of photons with an energy E and momentum p , and on the other it may be regarded as a continuous electromagnetic wave of frequency ν . Depending on the experimental conditions light exhibits either corpuscular or wave properties.

In 1923 the French physicist Louis de Broglie proposed the hypothesis, which was soon confirmed experimentally,

that any moving body possesses both corpuscular and wave properties. The kinetic energy and momentum of a body are related to the frequency and wavelength in accordance with equations (2.1). The wavelength of a moving body can be found from the second equation in which the momentum p is replaced by the product of the relativistic mass m and the velocity v ,

$$\lambda = h/mv \quad (2.2)$$

With increase of mass of the body its wavelength tends to zero. The wavelength of macroscopic bodies is incomparably smaller than the sizes of the bodies themselves even at very low velocities. Consequently the wave process does not affect the interaction between macroscopic bodies.

The mass of microparticles (electron, proton, neutron, atoms etc.) is comparable to the atomic mass unit and the wavelength of the microparticle may be significant even at low velocities. Thus the wavelength of an electron with a kinetic energy 100 eV is 1.33 Å and comparable to the crystal lattice constant d . If the surface of a crystal is irradiated with an electron beam of wavelength $\lambda \approx d$ (see Fig. 1.2) it will be found that the electrons in the reflected beam are diffracted. Experiments on the reflection of electrons from the surface of crystals supplied the first proof of the correctness of the de Broglie hypothesis.

The particle wavelength decreases with increase of the velocity v . For velocities close to that of light the wavelength is very small. For electrons with energies of 100 MeV the wavelength $\lambda \approx 3 \times 10^{-8}$ Å which is about 1000 times smaller than the lattice constant. No diffraction is observed for such electron beams.

The wave properties of particles appreciably affect their motion in quantum phenomena. The wavelength of the particles is of the same order of magnitude as the sizes of the atoms and molecules, particularly if the velocity is not high. Thus interacting microparticles behave in some cases as waves and in others (at high velocities) as particles. This is one of the features of the microcosm.

Another feature of the microcosm is the discreteness of the mechanical and magnetic quantities (energy, angular momen-

tum etc.) in bound-particle systems (atoms, nuclei etc.). Whereas these quantities vary continuously in the macroscopic world, they may assume only discrete values in the microcosm.

The laws of motion in the microcosm are one of the main objects of study in quantum mechanics. Quantum mechanics reflects a qualitatively new stage of understanding of nature and correspondingly employs novel concepts. Some concepts, such as that of momentum, angular momentum, magnetic moment are borrowed from classical physics. However in quantum mechanics their meaning is somewhat different.

In quantum mechanics information on motion in the microcosm is contained in the wave function Ψ (psi function). This function can be found by solving the wave equation first derived by the Austrian physicist Schrödinger and called the *Schrödinger equation*. It describes quantum phenomena for velocities $v \ll c$. Relativistic quantum processes ($v \approx c$) are described by the *Dirac equation*. One of the problems of quantum mechanics is the solution of the Schrödinger or Dirac equation for concrete quantum systems (atom, nuclei etc.). The wave function yields the distribution of particles with respect to quantum states characterized by discrete values of the energy, angular momentum and other quantities. The wave function is therefore a function of state of a particle in the microcosm. In the general case the wave function Ψ is a complex quantity. Its physical significance is that the square of the wave function $|\Psi(r, t)|^2$ is the probability density for finding the particles in a certain state near a point r at a time t .

Planck's constant plays a special role in quantum mechanics. It is found in all expressions for quantities characterizing quantum processes (photon energy, particle wavelength etc.). If these quantities can be neglected in considering some certain motion, it can be asserted that the motion is governed by the classical laws. Thus there is no sense in taking into account the wavelength $\lambda = h/mv$ of macroscopic bodies. The laws of classical mechanics are limiting cases of the laws of quantum mechanics on transition from the microcosm to macrocosm.

2.2 Quantum States of Electrons in Atoms

The quantum state of an electron in an atom is characterized by its energy, angular momentum and magnetic moment which can have only discrete values. In other words, these quantities are quantized. Electrons in a shell with a given number n move with the same energy. As in the Bohr theory the number $n = 1, 2, 3, \dots$ characterizes the discrete energy states of the electrons and the number of the electron shell. In quantum mechanics n is called the *principal quantum number*.

The motion of an electron in its orbit is characterized by its orbital angular momentum \mathbf{L} . It is directed along the axis of rotation of the electron perpendicular to the plane of the orbit (Fig. 2.1).

The absolute value of the orbital angular momentum can only have values such that $L = \hbar\sqrt{l(l+1)}$, where $\hbar = h/2\pi$. The integer l is called the *azimuthal quantum number*. For a shell with a principal quantum number n , it may have values ranging from 0 to $n - 1$. Thus the azimuthal quantum number for an electron in the n th shell may have n different values. The only value of the azimuthal quantum number for the K -shell is zero. This would seem to be impossible for orbital motion. Actually an electron with $l = 0$ does not have a definite orbit. It can be found with equal probability at any point on the surface of a sphere with a radius equal to that of the shell. Since the orbital angular momentum is directed in space its mean value in the case of an electron moving over the surface of a sphere with equal probability in different directions will be zero. In the L -shell ($n = 2$) the azimuthal quantum number may have two values, 0 and 1. As in the case of K -orbit an electron with $l = 0$ can be found with equal probability at any point on

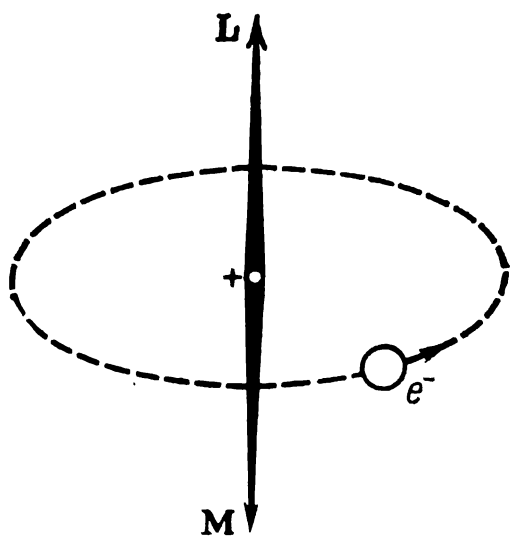


Fig. 2.1 Relative position of the orbital momentum \mathbf{L} and magnetic moment \mathbf{M} of an electron

the sphere in the L -shell. The orientation of the electron orbital motion for $l = 1$ is more pronounced.

The mean absolute value of L for $n = 1$ is $\hbar\sqrt{2}$. In the M -shell ($n = 3$) the absolute value of the angular momentum may be 0, $\hbar\sqrt{2}$ and $\hbar\sqrt{6}$.

The states of electrons in an n th shell with unequal azimuthal quantum numbers are somewhat different. A consequence is that the n th shell splits up into n subshells. They have the same principal quantum number but different azimuthal quantum numbers.

The orbital motion of an electron may be viewed as a circulating electric current. It may be mentioned that the direction of the current is accepted to be that of the positive charge flow. Therefore the orbital current flows opposite the movement of the electron. A circulating current produces a magnetic field (see Fig. 2.1) with a magnetic moment M . The moment is directed from the south to north pole and hence is opposite to the direction of the angular momentum L . The magnetic moment M is also quantized. Its absolute value is proportional to the Bohr magneton $\mu_0 = e\hbar/2m_e = 9.27 \times 10^{-24}$ J/T. The magnetic moment and orbital angular momentum are proportional to each other and the possible values of the magnetic moment are

$$M = \mu_0 \sqrt{l(l+1)} = eL/2m_e$$

Consider now what will happen if an atom is in a magnetic field directed along the z -axis. The magnetic field orientates the orbital magnetic moments in certain directions. There is only one stable direction for a compass needle and that is when the magnetic moment is directed along the field. However the situation in the microcosm is quite different. The magnetic moment is directed in such a way that the projection of the orbital angular momentum on the z -axis can only have values which are multiples of \hbar . The orbital angular momentum $L = \hbar\sqrt{12}$ ($l = 3$), for example, can have only seven directions, the projection of the orbital angular momentum on the direction of the field having the values $-3\hbar, -2\hbar, -\hbar, 0, \hbar, 2\hbar$ and $3\hbar$ (Fig. 2.2). The projection of the angular momentum on the z -axis L_z can briefly be denoted $m\hbar$. The number m is the *magnetic quantum number*.

It has $2l + 1$ integral values for an orbital angular momentum with an azimuthal quantum number l . The values of the magnetic quantum number vary from $-l$ to $+l$.

The dimension of the constant \hbar is the same as that for action (product of energy by time or angular momentum). The constant serves as a unit of measurement of action and is called the *quantum of action*. Experimentally it is not the absolute value of the angular momentum L which is measured but its projection L_z which is always a multiple of \hbar .

The electron rotates about its own axis with an angular momentum S called its *spin*. Roughly one may visualize

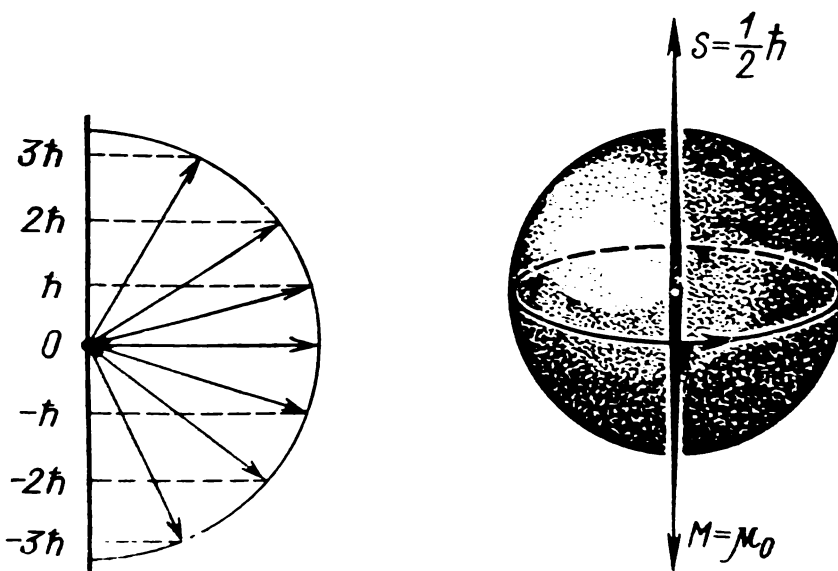


Fig. 2.2 Possible values of the projections of the orbital momentum $L = \hbar\sqrt{12}$ on the magnetic field direction ($l = 3$)

Fig. 2.3 Relative position of the intrinsic angular momentum (spin) and magnetic moment of an electron

the electron as a spinning top. The electron spin can have only one value, $\hbar\sqrt{3/2}$. Rotation of the electron, which is an electric charge, effectively produces a circulating electric current. Hence the electron has a magnetic moment which is directed opposite to the spin and is equal to $\mu_0\sqrt{3}$.

The orientation of the electron spin in an external magnetic field is determined by the orientation of the electron magnetic moment. This orientation is such that in an external magnetic field the projection of the spin S on the direction of the magnetic field may equal either $+\hbar/2$ or $-\hbar/2$. These possible values of the spin component may be expressed by

the formula $S_z = \hbar m_s$. The number m_s , which is either $1/2$ or $-1/2$, is called the *spin quantum number*.

In discussions regarding the motion of coupled electrons and other particles the angular momenta and magnetic moment \mathbf{L} , \mathbf{S} and \mathbf{M} are usually replaced by their maximum projections $\hbar l$, $\hbar/2$, $\mu_0 l$ etc. This simplification will also be used in the present book and is usually employed in other books for designation of the particle spins in tables or on depiction of the particles on the basis of models.

As an example, the electron is depicted in Fig. 2.3, and the maximum projections of the spin $\hbar/2$ and of the intrinsic magnetic moment μ_0 are indicated.

Depending on their spins elementary particles can be divided into fermions and bosons. Fermions are particles with half-integral spins ($\hbar/2, 3\hbar/2, \dots$). Such are the electron, proton and neutron which all have a spin $\hbar/2$. The spin of bosons is a multiple of \hbar ($0, \hbar, 2\hbar, \dots$). A typical representative of the bosons is the photon which has a spin equal to \hbar .

The quantum states of electrons in atoms are characterized by four quantum numbers, the principal quantum number n , azimuthal l , magnetic m and spin m_s . In order to explain the composition and structure of the electron shells of atoms the Austrian physicist Pauli formulated in 1924 a general principle which has been called the *Pauli principle* (or *Pauli exclusion principle*). According to this principle no two electrons in an atom can be in the same quantum state. This means that the quantum states of any two electrons in an atom must differ with respect to at least one quantum number. As an example, in the K -shell ($n = 1$) the only possible values for the electrons are $l = 0$ and $m = 0$. Therefore there may be only two electrons in the shell, one of which has $m_s = 1/2$ and the other $m_s = -1/2$. In this case the principal, azimuthal and magnetic quantum numbers are the same but the spin quantum numbers are different. In the L -shell ($n = 2$) l may have two values, 0 and 1. As for the K -shell there cannot be more than two electrons if $l = 0$ and $m = 0$. For $l = 1$ the magnetic quantum number may have three values ($2l + 1 = 3$); $-1, 0, +1$. In each state there may be two electrons with opposite spins. The total number of electrons in the L -shell with $l = 1$ is therefore

$2(2l + 1) = 2 \cdot 3 = 6$. Altogether there cannot be more than $2 + 6 = 8$ electrons in the L -shell: two with $l = 0$ and six with $l = 1$.

Let us find the maximum number of electrons in some n th shell. There can be two electrons in a state with $l = 0$, six electrons for $l = 1$, ten for $l = 2$ etc. In a state with $l = n - 1$ there can be $2(2n - 1)$ electrons. The sum of all the electrons $2 + 6 + 10 + \dots + 2(2n - 1)$ is an increasing arithmetic progression with a difference 4 and containing n terms. The maximum number in the n th shell is the sum of all terms of the progression, viz.

$$\frac{2 + 2(2n - 1)}{2} n = 2n^2$$

As mentioned above not only electrons but other fermions obey the Pauli principle. This is the main difference between fermions and the bosons which are not governed by the Pauli principle. Thus the physical essence of the Mendeleev periodic law, which is a reflection of the distribution of electrons in discrete quantum states in atoms, was elucidated by the exclusion principle.

In the present section of this chapter use was made of the classical term *electron orbit*. We shall now inquire what meaning should be attached to this term in the microcosm.

2.3 Uncertainty Principle

In classical mechanics the trajectory of a moving body may be characterized by exact values of its coordinates and momentum at any given time t , the two quantities being interrelated. Uniform rectilinear motion of a body of mass m and velocity v is described, for example, by the coordinate $x(t) = vt$ and momentum $p = mv$. Hence $x(t) = pt/m$.

In the microcosm particles display wave properties under some conditions and corpuscular properties under other. The exact position of a particle can be found only if the corpuscular properties are predominant, as in the Bohr theory of the atom. However if the wave properties are significant this should not be possible. Wave processes occur in a large part of space and hence it is meaningless to speak of the coordinate of a wave.

In quantum mechanics it is shown that if the wave properties of particles are taken into account, no particle can simultaneously possess exact coordinate and momentum values and that these two quantities are not interrelated. If the momentum of a particle is known exactly its position is uncertain and vice versa. This behaviour is described by the *uncertainty principle* or the *Heisenberg principle*, as it is often called after the German physicist who first formulated it. According to this principle the product of the uncertainty in the momentum, Δp , and the uncertainty in the coordinate, Δx , is of the same order of magnitude as the Planck constant \hbar ,

$$\Delta p \Delta x \approx \hbar$$

Dividing both sides by the particle mass m and taking into account that $\Delta p = m\Delta v$, we obtain the Heisenberg relation for the uncertainties in the velocity Δv and coordinate Δx ,

$$\Delta v \Delta x \approx \hbar/m$$

The Heisenberg relation reflects the nature of the microcosm and limits the simultaneous determination of the position and momentum of a particle. This indeterminacy is not due to the errors caused by the measuring instruments. Since exact momenta and coordinates of a particle do not exist simultaneously, it is not possible to speak strictly about the trajectory of the particle. Thus an exact orbit cannot be ascribed to an electron in an atom. Indeed, the indeterminacy in the electron coordinate in the atom is comparable to the size of the atom, i.e. $\Delta x \approx 10^{-10}$ m. According to the Heisenberg uncertainty relation the indeterminacy in the electron velocity

$$\Delta v \approx \frac{\hbar}{m_e \Delta x} \approx \frac{1.05 \times 10^{-34}}{9.11 \times 10^{-31} \times 10^{-10}} \approx 1.15 \times 10^6 \text{ m/s}$$

The velocity of an electron in an atom v is approximately 1.0×10^6 m/s and is of the same order as the uncertainty Δv . Thus there is no sense in speaking about the orbit of an electron. Nevertheless most of the time atomic electrons move near the Bohr orbits. The Bohr theory was able to explain some properties of the atom simply because the most probable positions of the electrons in the atom were involved in the theory.

The Heisenberg relationship is of no practical importance for bodies with large masses. As an example suppose the indeterminacy in the coordinate of a flying tennis ball $\Delta x \approx 10^{-10}$ m and its mass is $m = 0.06$ kg. Then

$$\Delta v \approx 1.05 \times 10^{-34} / 0.06 \times 10^{-10} = 1.75 \times 10^{-23} \text{ m/s}$$

With such uncertainties Δx and Δv , the coordinate and velocity can be determined with a high degree of accuracy simultaneously.

The Heisenberg relation can be written for another pair of variables, energy and time. If the uncertainty in the energy of a system is ΔW over a time Δt , then:

$$\Delta W \Delta t \approx \hbar$$

The time spent in measuring the energy (mass) of stable particles may be arbitrarily large. Thus for $\Delta t > 10^{-6}$ s the energy uncertainty $\Delta W < 10^{-28}$ J = 6.25×10^{-14} MeV. Even for the lightest particle, the electron, ΔW is so small that it cannot affect the results of the energy (mass) measurements.

For unstable particles the time for measurement of the rest energy is restricted by their lifetime τ . Therefore for such particles the indeterminacy in the energy is not less than $\Delta W = \hbar/\tau$. Excited atoms may be regarded as unstable particles. On the average their lifetimes $\tau \approx 10^{-8}$ s. Hence the energy of the excited level of an atom is not defined exactly. The mean indeterminacy in its energy $\Delta W \approx \approx 10^{-7}$ eV is called the *level width* and designated by Γ . Some atoms have excited levels with a width $\Gamma \ll 10^{-7}$ eV. The lifetimes τ of such excited states, which are called *metastable* levels, are very large compared to 10^{-8} s. When metastable atoms go over to the ground state, photons with a very small energy (and hence wavelength) spread are emitted. This fact is exploited in metrology in defining the standard length, the metre. In the SI system the metre is defined as being equal to $\sim 1.65 \times 10^6 \lambda$, where λ is the wavelength of light emitted by krypton and equal to 6057 Å.

The energy-time Heisenberg relation underlies the theory of exchange forces in the microcosm. We shall consider the main features of this theory for the special case of interaction between two resting electric charges.

According to the classical laws a resting electric charge produces an electric field whose intensity varies continuously in space. If another electric charge is introduced into the field a coulomb force will act on the first charge. The action of one charge on another is transmitted via the electric field. In quantum theory the description of the interaction between electric charges is quite different. The electric field is assumed to have a discrete structure and consists of photons. In order to create an electric field the charge must emit photons. The action of one charge on another thus involves exchange of photons.

The question now arises as to where resting charges acquire the additional energy required for photon emission. According to the $\Delta W \Delta t \approx \hbar$ indeterminancy relation the rest energy of the particle may differ from the mean value W_0 during a time interval Δt by ΔW . Consequently for a time less than Δt the charges may exchange photons with energies $\hbar v < \Delta W$. The average distance R at which photon exchange occurs cannot exceed $c\Delta t$. With increase of the time Δt the energy of the emitted photons decreases. Because of this the interaction between charges is attenuated with increase of the distance between them.

What is the difference between exchange photons and real photons? Exchange processes may be regarded as virtual (imaginary) processes occurring in the microcosm. Hence the exchanged photons are called virtual photons since they cannot be observed experimentally. Charges emit virtual photons on the condition that a deviation from the law of conservation of energy by a certain amount ΔW occurs, this being forbidden under real conditions, of course. Real photons which can be detected with suitable instruments arise only if the law of conservation of energy is obeyed rigidly. For example in collisions between charges part or all of the kinetic energy of the charges may be expended in the emission of real photons.

In the theory of exchange forces the interaction of any two particles is envisaged as being due to the exchange of a third, virtual, particle. In other words each field is characterized by its own exchange particle. This hypothesis was first formulated by the Soviet physicist Tamm in 1934.

CHAPTER 3

THE ATOMIC NUCLEUS

3.1 Properties of the Atomic Nucleus

Composition of the nucleus. The nucleus is composed of Z protons and N neutrons. The neutron n is an electrically neutral particle. Its mass ($m_n = 1.008665$ amu), as that of the proton, does not differ much from the amu.

The number of protons and neutrons in the nucleus $A = Z + N$. The number A is called the *mass number* since the mass of the atom and its nucleus is approximately equal to A amu. The mass of the beryllium atom ($A = 9$), for example, is 9.0122 amu and differs from 9 by about 1.4%.

The nucleus and the physical properties of the atom can be studied only if the nucleus exists for a sufficiently long time. Among the many energy states of the nucleus there are a few which are long-lived, i.e. possess a relatively long lifetime (see Sec. 3.3). The ground and metastable energy states are states of this type.

An atom with a definite mass number, atomic number and with its nucleus in the ground or metastable energy state is labelled a *nuclide*.

Nuclides with the nucleus in the ground state are denoted ${}^A_Z X$, and nuclides with the nucleus in the metastable state ${}^{A^m}_Z X$, where X is the symbol of the element. The notations ${}^A_Z X$ and ${}^{A^m}_Z X$ designate the composition of the nucleus (Z protons and $A - Z$ neutrons), the energy state of the nucleus and number of electrons in the nuclide (Z). As an illustration, the carbon nuclide, 1/12 mass of which is chosen as the amu, and also the nucleus of this nuclide are denoted ${}^{12}C$ (carbon six-twelve). The ${}^{12}C$ nucleus contains six protons and six neutrons, it is in the ground state and six electrons revolve around the nucleus. Since each chemical element has a definite atomic number the latter is frequently omitted from the nuclide symbol. Thus one writes simply ${}^{12}C$ (carbon 12) or ${}^{16}O$ (oxygen 16) etc.

As an exclusion the hydrogen nuclides are frequently designated by symbols which do not indicate the atomic and mass numbers. Thus hydrogen 1H is usually denoted by H,* deuterium 2H by D and the artificial nuclide tritium 3H by T. Hydrogen, deuterium, tritium and helium 4He nuclei are employed for bombarding other nuclei. The hydrogen nucleus is the proton, the deuterium nucleus is called the deuteron and the tritium nucleus the triton. The nucleus of helium 4He is the alpha particle. These nuclei are denoted by p , d , t and α respectively.

The chemical properties of atoms are related to the number of electrons in the electron shells. i.e. the atomic number, and do not depend on the mass number. As a consequence nuclides with the same atomic numbers but different mass numbers have the same chemical properties. They are called *isotopes* of the chemical element. Thus the nuclide ${}^{12}C$ is the isotope of carbon, 12C . Natural chemical elements contain from one to almost a dozen isotopes. Carbon, for example, has two isotopes, oxygen three, tin ten and antimony only one.

Isobars are nuclides with equal mass numbers but different atomic numbers. Examples are ${}^{108}_{47}Ag$ and ${}^{108}_{48}Cd$, 1H and 2He .

Nuclides with identical atomic and mass numbers but with different long-lived energy states of the nucleus are called *nuclear isomers*. Thus ${}^{80}_{36}Br$ and ${}^{80m}_{35}Br$ are bromine nuclear isomers.

Mass of the nucleus. One of the main characteristics of the A_ZX atomic nucleus is its mass denoted as $M_n(Z, A)$ or $M_n({}^A_ZX)$. It is very difficult to measure directly the mass of a nucleus since all electrons should first be removed from the atom. A simpler way is to first measure the mass of the singly charged ion of the atom and on the basis of these measurements to calculate the mass of the atom and the nucleus.

The mass of a nuclide $M(Z, A)$ is approximately equal to the sum of the nuclear mass $M_n(Z, A)$ and the masses of the electrons Zm_e . The approximation is due to the fact that the mass equivalent to the binding energy of the electrons in the nuclide is not taken into account. On synthesis of the nuclide from the nucleus and electrons an energy W_b equal

* In chemistry the hydrogen isotope 1H is frequently called protium (from the Greek *proto* which means first).

to the binding energy of the electrons in the nuclide is liberated. The nuclide mass is therefore smaller than the sum of the masses of the free nucleus and Z electrons by $\Delta M = -W_b/c^2$. Since ΔM is very small compared to m , it will be assumed in the following that

$$M(Z, A) = M_n(Z, A) + Zm_e \quad (3.1)$$

The mass of a nuclide can be measured with a high degree of accuracy. Several means of measurement exist. In one case an instrument called the mass spectrometer is employed (Fig. 3.1). This consists of an ion source, vacuum chamber and ion detector. Nuclides ionized in the ion source are accelerated by an electric field. The kinetic energy of the ions entering the vacuum chamber through a slit is equal to the energy imparted to the ions in the electric field

$$M_i(Z, A) v^2/2 = eU$$

where M_i is the ion mass and U the accelerating voltage. The velocity of the ions v is inversely proportional to $\sqrt{M_i}$ and hence for a given accelerating voltage U ions of heavier nuclides move with a lower speed than those of lighter nuclides. The vacuum chamber is arranged in the uniform magnetic field in such a way that the magnetic induction vector B is perpendicular to the ion velocity v . As a result the ions in the vacuum chamber move in a circle of radius R . The centripetal forces acting on the ions are balanced by the Lorentz force

$$M_i v^2/R = evB$$

Excluding from the last two equations the velocity v we obtain

$$M_i = eB^2R^2/2U$$

The charge detector in the vacuum chamber is located on a circle with a radius R_d . Ions with a mass M_i therefore hit

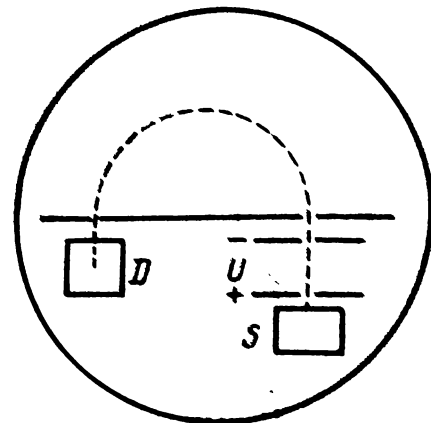


Fig. 3.1 Sketch of the mass-spectrometer

D —ion detector, U —accelerating voltage, S —ion source

the detector only if the radius of their orbit is equal to R_d , $R = R_d$. Consequently, the ion current in the detector will grow only when the accelerating voltage is such that

$$U = a/2M_1 (Z, A)$$

where $a = eB^2R_d^2$ is a constant.

The mass spectrum of molybdenum is shown in Fig. 3.2. It is composed of seven peaks of the ion current. The height of each peak is proportional to the amount of each isotope in the element.

Measuring instruments are characterized by their resolving power. This is the difference ΔL between the two closest

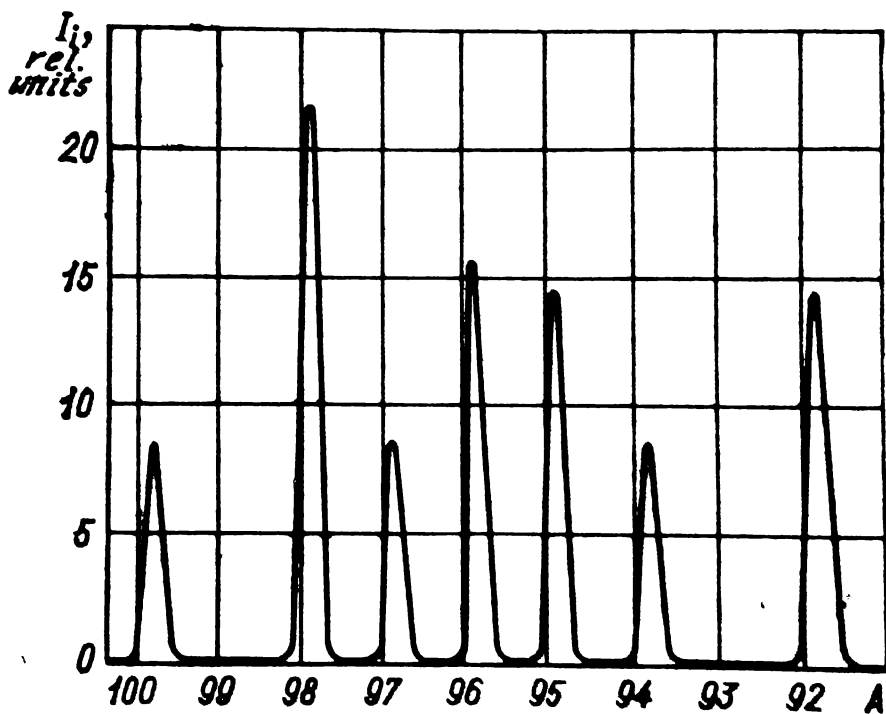


Fig. 3.2 Mass spectrum of molybdenum

values of a physical quantity L which can be resolved (separated) by the instrument. The smaller the difference ΔL the higher is the resolving power of the instrument. Very often the relative resolution $\Delta L/L$ is used. In modern spectrometers $\Delta M/M = 10^{-4}-10^{-5}$. Such mass-spectrometers can be used to measure ion masses with an accuracy to within $10^{-4}-10^{-5}\%$.

Spin and magnetic moment of the nucleus. Protons and neutrons are fermions, their spin being $\hbar/2$. The relative (orbital) motion of particles in the nucleus, like electrons in

the atom, is characterized by integral orbital moments. The total angular momentum of the nucleus is the sum of the particle spins and the orbital angular momenta. It is usually referred to as the *nuclear spin*.

Experiments show that the nuclear spin depends on the mass number A . Nuclei with an even A have whole number spins ($0, \hbar, 2\hbar$ etc.) whereas the spins of nuclei with odd A are half-integral ($\hbar/2, 3\hbar/2$ etc.). The spin of nuclei with even values of Z and N is zero.

Protons and neutrons are also characterized by their *magnetic moments* M . The spin and magnetic moment of the

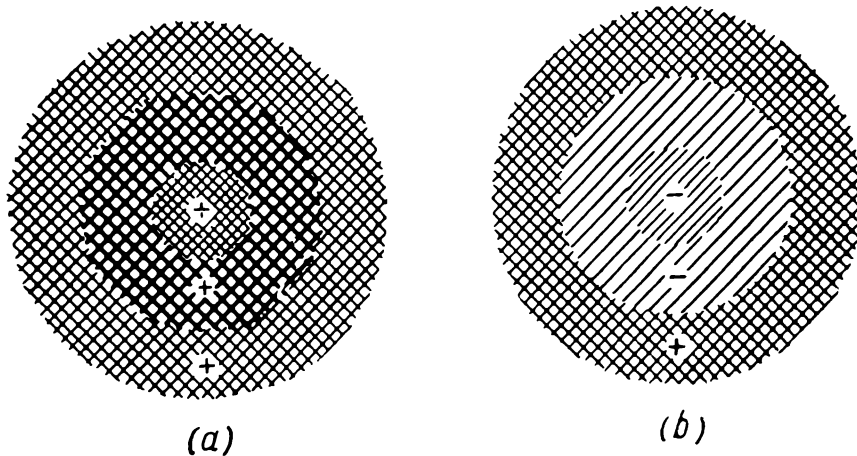


Fig. 3.3 Models of the proton (a) and neutron (b)

proton are oriented in the same direction and those of the neutron—in opposite directions. The mutual orientation of these two quantities indicates the sign of the magnetic moment. It is positive for the proton and negative for the neutron. The presence of a magnetic moment in the neutron, which does not have an electric charge, is due to the specificity of the charge distribution within the neutron.

Models of the proton and neutron are depicted in Fig. 3.3. The positive charge of the proton is distributed throughout the volume of the particle. A heavy core is located at the centre of the proton, about 10% of the charge being contained in the core. The remaining part of the charge is distributed in the middle region and outer shell. The core and middle part of the neutron are charged negatively and the outer shell, positively. The positive and negative charges are equal and the total charge is therefore zero in the neutron.

There is no sharp boundary between the different regions in the proton and neutron and the charge density gradually varies in the bulk of the particles.

Nuclear magnetic moments are measured in terms of nuclear magnetons μ . This unit is $1/1836$ of the Bohr magneton μ_0 . The orbital and proper magnetic moments of the electron are multiples of μ_0 but the nuclear magnetic moments are not integral values of μ . Even the magnetic moments of the proton and neutron are not integral values of the nuclear magneton. According to the measurements $M_p = 2.79 \mu$ for the proton and $M_n = -1.913 \mu$ for the neutron.

3.2 Binding Energy of the Nucleus

The synthesis of nuclei from protons and neutrons involves the release of energy. The mass equivalent to this energy ΔM is called the *mass defect*. It is the difference between the mass of the Z protons and $A - Z$ neutrons and the mass of the nucleus

$$\Delta M (Z, A) = Zm_p + (A - Z)m_n - M_n (Z, A)$$

Usually it is the nuclide masses which are presented in the tables. It is therefore more convenient to employ in the calculations a formula in which the nuclear masses are replaced by the nuclide masses in accordance with formula (3.1),

$$\Delta M = Zm_H + (A - Z)m_n - M (Z, A) \quad (3.2)$$

where m_H is the mass of the H nuclide, and $M (Z, A)$ is the mass of nuclide ${}^A_Z X$. For all nuclei studied ΔM is found to be positive and this signifies that the synthesis of nuclei from protons and neutrons involves the release of energy, i.e. part of the rest energy is transformed into kinetic energy. This is somewhat similar to the synthesis of atoms from nuclei and electrons and to exothermal chemical reactions. In the latter case only about 10^{-10} of the rest energy of the molecule is released as a result of rearrangement of the outer electron shells. In the synthesis of a nucleus from protons and neutrons the amount of energy liberated may be 10^{-4} of the rest energy of the nucleus. Thus the particles in the nucleus are bound together by forces which exceed by millions of times the forces which bind atoms in molecules.

Knowing the mass defect it is easy to determine the binding energy of the nucleus, i.e. the energy required for disrupting the nucleus into its constituent particles,

$$W_b = \Delta M c^2$$

Recalling that $1 \text{ amu} = 1.66 \times 10^{-27} \text{ kg}$, we find the energy corresponding to an atomic mass unit,

$$W_b = 1.66 \times 10^{-27} \times (3 \times 10^8)^2 = 1.492 \times 10^{-10} \text{ J} = \\ = 931 \text{ MeV}$$

If the mass defect is expressed in atomic mass units then

$$W_b = 931 \Delta M \text{ MeV} \quad (3.3)$$

Values of the nuclide masses and nuclear binding energies are presented in Table 3.1. The binding energy grows with

Table 3.1

Nuclide Masses and Binding Energies of Nuclei

${}^A_Z X$	Mass number A	Nuclide mass, amu	Binding energy of nucleus, MeV
n	1	1.008665	—
H	1	1.007825	—
D	2	2.014102	2.2246
T	3	3.016049	8.4822
${}^3_2 \text{He}$	3	3.016029	7.7184
${}^4_2 \text{He}$	4	4.002603	28.296
${}^6_3 \text{Li}$	6	6.015123	31.995
${}^7_3 \text{Li}$	7	7.016004	39.245
${}^9_4 \text{Be}$	9	9.012182	58.167
${}^9_5 \text{B}$	9	9.013300	56.050
${}^{10}_5 \text{B}$	10	10.012938	64.752
${}^{11}_5 \text{B}$	11	11.009305	76.208
${}^{12}_6 \text{C}$	12	12.000000	92.165
${}^{13}_6 \text{C}$	13	13.003355	97.111
${}^{14}_7 \text{N}$	14	14.003074	104.662
${}^{15}_7 \text{N}$	15	15.000109	115.494
${}^{16}_8 \text{O}$	16	15.994915	127.624
${}^{17}_8 \text{O}$	17	16.999133	131.766
${}^{18}_8 \text{O}$	18	17.999160	139.813

increase of the number of particles in the nucleus and is insensitive to the nature of the particles. Thus addition of a neutron to the deuteron d results in the formation of triton t whereas the addition of a proton yields the helium nucleus ^3He . In the first case the increase in the binding energy is 6.259 MeV and in the second 5.500 MeV. The difference in the binding energy increments (0.759 MeV) can be ascribed to weakening of the binding in the ^3He nucleus as a result of coulomb repulsion between the protons.

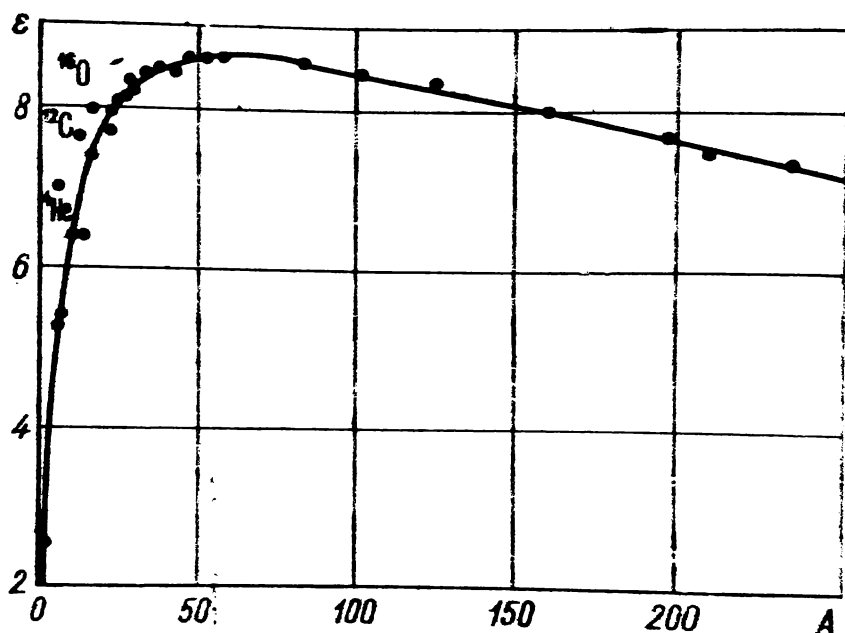


Fig. 3.4 Dependence of mean binding energy per nucleon ϵ on mass number A

The increase of the binding energy with growth of the mass has some characteristic features. They can be appreciated if one considers the dependence of the mean binding energy $\epsilon = W_b/A$ per nuclear particle (nucleon) on the mass number (Fig. 3.4); ϵ first increases and reaches a maximum value of 8.7 MeV at $A \sim 60$. Further increase of number of nucleons results in a gradual weakening of the particle binding. In the heavy nucleus region ($A > 200$) ϵ drops to 7.5 MeV.

Most values of the mean energy ϵ lie on a smooth curve. Exceptions are nuclei with 2, 8, 14, 20, 50 or 82 protons or 2, 8, 14, 20, 50, 82 or 128 neutrons. These numbers of protons and neutrons and the nuclei which contain them are called

magic numbers or **nuclei** respectively. Protons and neutrons in the magic nuclei are more tightly bound. Because of this the values of ϵ for the magic nuclei are greater than those of nuclei with close values of the mass number.

The lightest magic nuclei are ${}^4_2\text{He}$ and ${}^{16}_8\text{O}$. Enhanced values of ϵ are also observed in light nuclei containing equal numbers of protons and neutrons (e.g. ${}^{12}_6\text{C}$) although these are not magic nuclei. For all nuclei with $A > 20$ the mean energy ϵ only weakly varies and on the average is about 8 MeV. The binding energy of the nucleus in this region is therefore an almost linear function of the mass number A : $W_b = 8A$ MeV.

Another important conclusion can be drawn on the basis of the dependence of $\epsilon = W_b/A$ on A . If a heavy nucleus ($A \approx 240$) is divided into two intermediate nuclei ($A \approx 120$) or if a single nucleus is synthesized from two light nuclei, the resulting nuclei in both cases will be more stable than the initial ones. This means that such processes (fission or synthesis) must involve the liberation of energy. The energy released in nuclear processes (nuclear fission or synthesis, radioactive decay etc.) is called *atomic* (or *nuclear*) *energy*.

The binding energy of a single proton ϵ_p or neutron ϵ_n is not equal to the mean energy ϵ . The removal of a neutron from the ${}^9\text{Be}$ nucleus, for example, requires an energy $\epsilon_n = 1.665$ MeV whereas $\epsilon = 6.5$ MeV.

The binding energy of a particle a in a nucleus, ϵ_a can be determined in the same way as the binding energy of the nucleus is evaluated. If the ${}^A_Z X$ nucleus is regarded as a bound system consisting of the ${}^{A_1}_{Z_1} Y$ nucleus and a particle a then

$$\epsilon_a = 931 [M(Z_1, A_1) + m_a - M(Z, A) + (Z - Z_1)m_e]$$

where m_a is the mass of particle a , $M(Z, A)$, $M(Z_1, A_1)$ are the masses of nuclides with mass numbers A and A_1 and atomic numbers Z and Z_1 respectively.

Fusion of particle a with the nucleus results in the release of an amount of energy which is equal to the binding energy of the particle in the compound nucleus. Thus addition of a neutron to the ${}^9\text{Be}$ nucleus leads to the formation of the ${}^{10}\text{Be}$ nucleus and release of an energy of 1.665 MeV.

3.3 Energy Levels of Nuclei

The rest energy of a nucleus W can have only discrete values $W_0, W_1, W_2, W_3, \dots, W_n, \dots$. These *nuclear energy levels* can be divided into the ground and excited levels. A nucleus is in the ground state (ground level) if no external forces act on it. The energy of a nucleus in the ground state W_0 is minimum.

A nucleus interacting with a particle may acquire a discrete portion of energy and goes over to an excited state involving one of the excited levels W_i ($i = 1, 2, \dots, n$). The excited state of a nucleus is unstable. After a period of time called the *lifetime* ($\tau \approx 10^{-14}-10^{-13}$ s) the excited nucleus returns to the ground state.

The mode of transition to the ground state depends on the excitation energy W_{ex} . This is the difference between the energies of the nucleus in the excited and ground states. If the excitation energy W_{ex} exceeds the binding energy for some particle a (neutron, proton, α -particle etc.) the excited

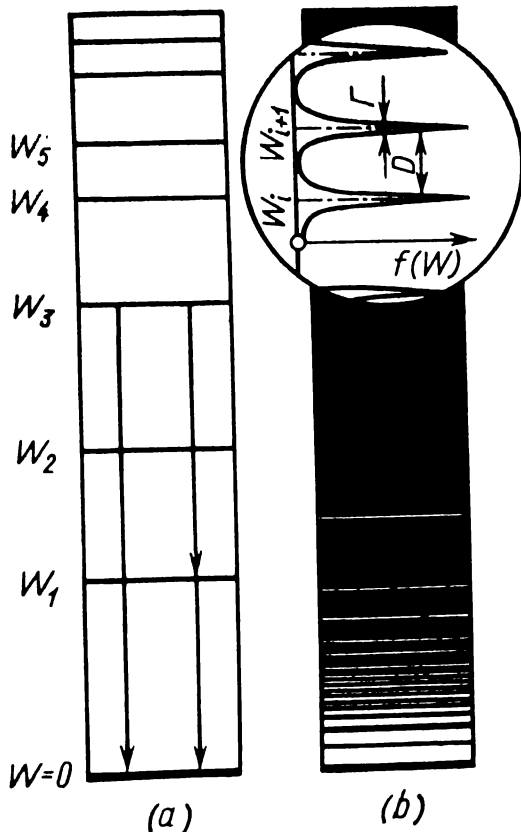


Fig. 3.5 Energy level diagram for a light (a) and heavy (b) nucleus

nucleus may emit gamma-quanta (γ -quanta), i.e. photons of nuclear origin, or particle a . Only γ -quanta are emitted if the excitation energy is lower than the binding energy of particle a .

Energy levels of a nucleus may be depicted diagrammatically (Fig. 3.5). This energy level scheme is similar to that for the energy levels in atoms (see Sec. 1.6). Since the energy of a nucleus $W \gg W_{\text{ex}}$, it is convenient to choose the ground state energy as the reference point. In this case the energy level is identical to the excitation energy of the nucleus.

The level energies $W_0, W_1, W_2, \dots, W_n, \dots$ are represented at the left of the horizontal lines in the diagram. The vertical arrows pointing downward indicate the transitions between energy levels taking place with the emission of γ -quanta. The energy of a γ -quantum corresponds to the difference of the energies of the levels located at the beginning and end of the arrow on the diagram.

The energy of an excited nucleus in the i th excited state, W , is located in a narrow energy interval near the most probable value of the energy of the level W_i . The probability density $f(W)$ for a nucleus excited to the i th level having an energy W is a function with a sharp peak (Fig. 3.5). With increase of the energy W the function $f(W)$ first sharply rises, reaches a maximum $f(W_i)$ and then sharply drops. The level width Γ is taken to be the width of the peak at a height $(1/2)f(W_i)$.

With increase of the excitation energy and mass number the distance between neighbouring energy levels D decreases. In light nuclei ($A < 50$) and for excitation energies $W_{\text{ex}} = 1-3$ MeV one finds $D \approx 1$ MeV; for $W_{\text{ex}} \approx 8$ MeV, $D \approx 10$ keV. In heavy nuclei ($A > 200$) D is approximately 0.1 MeV and 10 eV respectively. For excitation energies $W_{\text{ex}} \gg 8$ MeV the distance D is smaller than the width of the energy level Γ . Thus at high excitation energies the energy levels overlap.

The γ -radiation spectrum of excited nuclei (γ -spectrum) consists of lines for energies $W_{\text{ex}} \leq 20$ MeV. If the nucleus goes over to the ground state directly from the excited level it emits a single γ -quantum with an energy $E_\gamma = W_{\text{ex}}$. However, successive transition via part or all intermediate excited levels is also possible (see Fig. 3.5). In this case a whole series of γ -quanta is emitted, the total energy of the quanta being W_{ex} . For excitation energies $W_{\text{ex}} \gg 20$ MeV the γ -spectrum is continuous.

A study of γ -spectra is one of the ways investigating the energy levels of nuclei. After measuring the γ -spectra they are analyzed and the nuclear energy levels are determined.

The energy level width Γ can be measured with a high degree of accuracy. Widths $\Gamma > 5 \times 10^{-6}$ eV have been determined. Lifetimes of excited nuclei $\tau \approx 10^{-14}-10^{-15}$ s

cannot be measured with existing instruments. However if the level width Γ is known the lifetime can be estimated on the basis of the Heisenberg relationship $\tau \approx \hbar/\Gamma$.

For most excited levels the width $\Gamma = 0.01\text{-}0.1\text{ eV}$ and the lifetime $\tau = 10^{-14}\text{-}10^{-13}\text{ s}$. However, long-lived excited nuclei exist for which the width of one or several of the excited levels $\Gamma \leq 10^{-15}\text{ eV}$. The lifetimes of such excited states, which are called *metastable states*, may vary between a fraction of a second and dozens of days. When τ is sufficiently long the properties of the metastable nuclei may be investigated experimentally. Over 200 nuclei with one or two metastable levels are known at present. As an example, the $^{124}_{51}\text{Sb}$ nucleus has two metastable levels with lifetimes 1.9 and 30.3 minutes.

3.4 Nuclear Forces. Stability of the Nucleus

The nuclei of most natural elements are very stable systems. The neutrons and protons are confined in the nucleus by powerful nuclear attractive forces which surpass the repulsive coulomb forces between the protons. Let us now consider some of the properties of nuclear forces.

The interaction between two protons ($p-p$), two neutrons ($n-n$) or between a proton and neutron ($p-n$) is the same, i.e. the nuclear forces do not depend on the electric charge. This is the essence of charge independence of nuclear forces. A corollary is that the nature of nuclear forces is different from that of electric forces. A single nuclear charge is ascribed to the proton and neutron and they are considered as being nuclear particles of essentially the same type, viz., *nucleons*. The stability of the deuteron, which consists of a proton and neutron, is explained by the charge independence of the nucleons.

Nuclear forces are saturating forces (each nucleon can interact with only a few neighbouring nucleons). This follows from an analysis of the binding energy of nuclei. Suppose that each nucleon interacts with all $A - 1$ nucleons. Then the total number of interactions will be $A(A - 1)$ and the binding energy of the nucleus should be proportional to $A(A - 1) \approx A^2$. However, it was mentioned in the

previous section that the binding energy is proportional to the mass number A .

In light nuclei with mass numbers $A < 12$ the strongest binding is in the α -particle. The two protons and two neutrons in this nucleus form a saturated system. If a nucleon is added to the α -particle the product will be an unstable nucleus.

Nuclear forces are short-range forces. Their range of action is of the order of a fermi (the *fermi* is a unit of length equal to 10^{-15} m and named after the Italian physicist Enrico Fermi).

We shall now consider briefly the dependence of the interaction between a proton or neutron and the nucleus on the distance between the particle and the nucleus. If the distance between the proton and nucleus exceeds 1 fermi the coulomb repulsion will be predominant. The coulomb force, it may be noted, is a nonsaturated, long-range force. The potential energy of coulomb interaction between the nucleus and proton

$$V(r) = Ze^2/4\pi\epsilon_0 r$$

where $\epsilon_0 = 8.85 \times 10^{-12}$ F/m is the electric constant and r is the distance.

The constant $b_0 = 1/4\pi\epsilon_0 = 9 \times 10^9$ m/F is numerically equal to the potential energy of interaction between two particles with charges of 1 C in vacuum and separation $r = 1$ m. As the proton approaches the nucleus repulsion increases (Fig. 3.6). If there were no attractive nuclear forces the interaction energy would continue to increase with decreasing distance r (ascending line in Fig. 3.6). However, as soon as the proton enters the region where the nuclear forces are effective ($r \approx R$, where R is the radius of the nucleus) repulsion is rapidly replaced by attraction and the potential energy becomes negative. The graph $V(r)$ can be divided into two parts: a potential barrier ($r > R$) with a height V_b and a potential well ($r < R$) with a depth V_w . The height of the potential barrier V_b is equal to the maximum potential energy of the proton at the boundary of the nucleus. An expression for V_b in mega-electronvolts can be derived as follows. For any particle with a charge $Z_1 e$ the height of the barrier of a nucleus

with a charge Ze is

$$V_h = b_0 Z_1 Z e^2 / R$$

Taking $R = 1.4 \times 10^{-15} \sqrt{A}$ m (see formula (3.4)) and substituting

$$b_0 \times \frac{e^2}{1.4 \times 10^{-15}} = 9 \times 10^9 \frac{1.6^2 \times 10^{-30}}{1.4 \times 10^{-15}} = \\ = 1.64 \times 10^{-13} \text{ J} \approx 1 \text{ MeV}$$

we obtain

$$V_h = \frac{Z_1 Z}{A^{1/3}} \text{ MeV}$$

Interaction between the neutron and nucleus begins at a distance close to the nuclear radius R . The potential energy

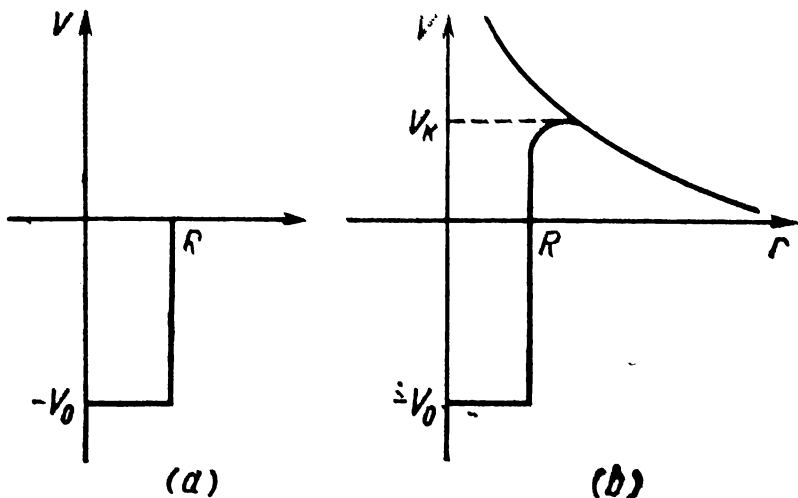


Fig. 3.6 Dependence of the potential energy of a neutron (a) and proton (b) on distance from the nucleus

of interaction between the neutron and nucleus is characterized exclusively by the depth of the potential well V_0 .

Nucleons in the nucleus are in motion but are confined by powerful attractive forces. The kinetic energies of the nucleons are less (in absolute value) than the depth of the potential well by a quantity equal to its binding energy ε_n .

The nuclear field has its exchange particles—the unstable π -mesons (pi-mesons) also called *pions*. The existence of pions was predicted in 1936 by the Japanese physicist Hideki Yukawa. The particles were discovered in 1947.

Pions are divided into three types differing with respect

to charge, mass and lifetime. The positive and negative pions (π^\pm -mesons) have a rest mass $m_{\pi^\pm} = 273.2m_e$, charges $q = \pm e$ and lifetime $\tau = 2.5 \times 10^{-8}$ s. The rest mass of the neutral pion (π^0 -meson) $m_{\pi^0} = 264.2m_e$ and the lifetime $\tau = 1.9 \times 10^{-16}$ s. The spin of all three pions is zero.

Exchange interactions between two nucleons occur in time periods of approximately 4×10^{-24} s. For such short periods the uncertainty in the nucleon energy exceeds the rest mass of the pions by several times. The range of the nuclear forces is equal to the maximum distance which a virtual pion covers in 4×10^{-24} s moving with a speed close to that of light: $R \approx 4 \times 10^{-24} \times 3 \times 10^8 = 1.2 \times 10^{-15}$ m.

Two protons, two neutrons or a proton and neutron can exchange neutral pions. In this case the nucleons do not change. The interaction between a neutron and proton can also occur by negative pion exchange. The neutron which emits the negative pion becomes a proton and the proton which absorbs the negative pion turns into a neutron, its positive charge being neutralized by the negative pion charge. Finally proton-neutron interaction may occur via positive pion emission by the proton.

The stability of nuclei is intimately connected with the nature of nuclear forces. There are about 300 stable nuclei in nature, each of which contains certain amounts of protons and neutrons. The neutron-proton diagram in Fig. 3.7 illustrates the dependence of the number of neutrons N on number of protons Z in nuclei. The black points in the diagram denote stable nuclei. They occupy a relatively narrow band called the stable nucleus region.

Light stable nuclei lie near the line $N = Z$. With increase of Z the weakening of the nuclear forces due to coulomb repulsion between protons begins to manifest itself. In order to compensate this weakening the nucleus must contain a larger amount of neutrons. Consequently after $Z = 20$ the ratio N/Z in the stable nucleus region begins to deviate from a straight line and for the last stable nucleus $^{209}_{83}\text{Bi}$ it is 1.52. This is the upper limit for stable nuclei. In nuclei with $Z > 83$ the nucleon interaction cannot completely compensate the coulomb repulsion and the nuclei are radioactive.

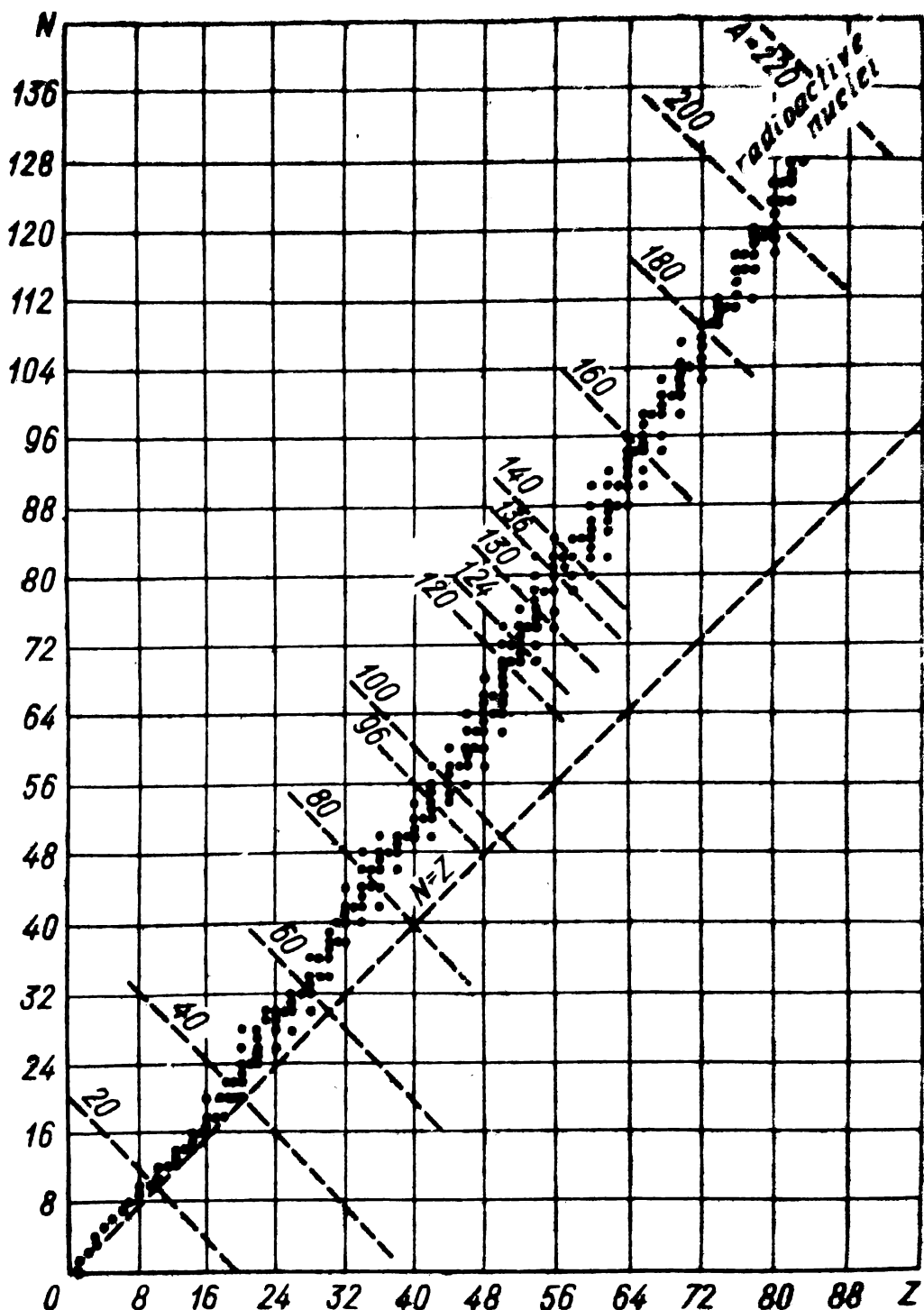


Fig. 3.7 Neutron-proton diagram of nuclei
 N —number of neutrons; Z —number of protons in the nucleus

3.3 Models of the Nucleus

To develop a theory of the nucleus one must know in detail the properties of the nuclear forces. However, the nature of these forces has not been elucidated sufficiently. Therefore simplifying assumptions are made in attempts to build models of nuclear processes. The usefulness of any particular model is judged by comparing the theoretical and experimental results. If agreement between the theory and experiments is observed the nuclear model may be considered as correctly imparting the main features of the structure of the nucleus. At present several nuclear models are in usage. None of them is universal in the sense that all experimental facts can be understood on the basis of a single model. Each of the models is suitable in the study of a restricted number of nuclear processes. Of the numerous models proposed we shall describe here only two—the liquid-drop and shell models of the nucleus.

Liquid-drop model of the nucleus. There is a certain similarity in the properties of the nucleus and those of a liquid drop, and it is on this basis that the liquid-drop model of the nucleus has been developed. A drop of liquid is usually spherical. Short-range intermolecular forces are operative, i.e. each molecule interacts only with its immediate neighbours. The molecules are in random motion and experience frequent collisions with each other. The surface molecules are attracted to the inner molecules in a unilateral fashion and the result is the presence of surface tension. The density of a drop does not depend on its size. The nucleus possesses similar properties, the molecules and intermolecular forces being replaced by nucleons and nuclear forces. Thus according to the drop model the nucleus may be envisaged as a drop of liquid. According to the liquid-drop model the nucleons are in rapid random motion and undergo frequent collisions. Each collision involves violent interaction between the nucleons and an exchange of energy and momentum between them. The nuclear drop is prevented from flowing by the forces of surface tension.

If a certain amount of energy is imparted to the nucleus it goes over to the excited state. Due to the frequent collisions between nucleons this energy may be redistributed

rapidly among the nucleons. Some of this energy may be transferred to a surface particle (nucleon, α -particle). If the energy of the particle is greater than its binding energy in the nucleus, the particle may overcome the surface tension (nuclear forces) and leave the nucleus. According to this model the expulsion of a particle from the nucleus is analogous to the evaporation of a molecule from a liquid drop. Evaporation of a surface molecule can take place only if the molecule receives enough energy from the other molecules to permit it to surmount the surface tension barrier. However, in contrast to a liquid drop, the excited nucleus may go over to the ground state by emitting one or several γ -quanta.

The liquid-drop model can be applied, for example, to explain fission of heavy nuclei (see Sec. 10.10). It can also be used to calculate the nuclear radius.

The nucleus-drop may be regarded as being filled with nucleons as a liquid drop is filled with molecules. Hence the volume of the nucleus V should be proportional to the mass number A and the radius of the nucleus $R = \alpha A^{1/3}$. The proportionality factor α can be found by various experimental methods. We shall consider one of them.

The radius of the orbit of a charged particle revolving about the nucleus is inversely proportional to its mass. Hence if some heavy negative particle is in the K -shell, the radius of the orbit should be approximately the same as the radius of the nucleus. The most suitable particles for such experiments are negative muons which are particles with a mass of 207 electron masses, a spin $\hbar/2$; being fermions they obey the Pauli principle. The negative muon is an unstable particle with a lifetime 2.2×10^{-6} s. Its charge is the same as that of the electron and it interacts with the nucleus as electrons do. However the atomic energy states of the negative muon and the electron are different. As a result all possible quantum states are available and the muon may occupy any of them.

A fast negative muon interacting with matter is slowed down and may be captured by an atom and begin to move in some outer shell. Since all quantum states are free, the muon will move in the K -shell which is closest to the nucleus. An atom with a muon in one of its shells is called a

mesic atom. This is an unstable system and exists only a millionth part of a second. Nevertheless transitions of muons in a mesic atom can be detected on the basis of the X-ray photons which are emitted in such transitions. By measuring the X-ray emission spectrum of a mesic atom one can determine the binding energy of the muon in the *K*-shell, ϵ_μ . Then from the equation for the binding energy $\epsilon_\mu = b_0 Ze^2/2r_1$ the radius r_1 is determined. Assuming r_1 to be equal to the nuclear radius R , one can find the coefficient α from the equation $R = \alpha A^{1/3}$.

The value of α measured by various methods varies between 1.2 and 1.5 fermi. For the sake of definiteness we will assume that $\alpha = 1.4$ fermi and hence

$$R = 1.4A^{1/3} \text{ fermi} \quad (3.4)$$

We can now calculate the density of the nuclear fluid. The volume of the nucleus

$$V = (4/3) \pi R^3 = (4/3) \pi \alpha^3 A$$

The mass of the nucleus $M_n(Z, A) \approx Am_n$, where A is the mass number and m_n is the nucleon mass which is assumed to be approximately one amu. The density of the nuclear fluid, which is the ratio of the mass to volume of the nucleus,

$$\rho = \frac{M_n(Z, A)}{V} \approx \frac{Am_n}{(4/3) \pi \alpha^3 A} = \frac{1.66 \times 10^{-27}}{(4/3) \pi \alpha^3} \text{ kg/m}^3$$

The density of the nuclear fluid, as that of a liquid drop, is independent of the nuclear size, and is identical for all nuclei. On substituting $\alpha = 1.4 \times 10^{-15}$ m, we obtain

$$\rho = \frac{3 \times 1.66 \times 10^{-27}}{4 \times 3.14 (1.4 \times 10^{-15})^3} \approx 1.45 \times 10^{17} \text{ kg/m}^3$$

Shell model of the nucleus. The stability of the magic nuclei is found to be particularly high. It is found to repeat periodically for proton magic numbers 2, 8, 14, 20, 50 and 82 and neutron magic numbers of 2, 8, 14, 20, 50, 82 and 126. If the chemical properties of elements are compared with the nuclear properties the following may be noted. The chemical properties vary periodically with variation of the atomic number Z whereas the magic properties of nuclei repeat on variation of the mass number A .

Precisely this periodicity in the properties of nuclei was the basis of the shell model of the nucleus. According to the model, nucleons in the nucleus are arranged in shells, each shell containing, in accordance with the Pauli principle, only a restricted number of nucleons. With increase of the number of nucleons the first shell is filled, then the next nucleon shell etc.

The magic properties are observed when the outer nucleon shell is completely filled. The first shell is filled in ${}^4_2\text{He}$ which consists of two protons and two neutrons; the next shell is filled in ${}^{16}_8\text{O}$ etc. The enhanced stability of magic nuclei resembles the chemical inertness of helium, neon etc. in which the outer electron shell is filled.

According to the shell model of the nucleus each nucleon moves in the field of the other nucleons just as an atomic electron moves in the electric field of the nucleus and other electrons. On excitation of the nucleus a nucleon or several nucleons move into excited levels. Transition to the ground state is accompanied by the emission of γ -quanta.

CHAPTER 4

RADIOACTIVITY

4.1 General Properties of Radioactivity

In 1896 the French physicist Henri Becquerel discovered radioactivity of uranium. This phenomenon, as everything else new in science, attracted the attention of many scientists. The outstanding physicists Pierre and Marie Curie, Ernest Rutherford and others began to study radioactivity.

Radioactivity is the property of certain nuclei (radioactive nuclei, nuclides) to emit spontaneously particles (α -particles, electrons, γ -quanta etc.) or X-rays accompanied by the capture of an orbital electron by the nucleus, or to divide into two lighter nuclei. This spontaneous transmutation of radioactive nuclei is called *radioactive decay*. After radioactive decay of a nucleus occurs a nuclide is formed which differs from the initial one with respect to its physical and chemical properties. Radioactivity is completely determined by the internal structure of the nucleus and is independent of the external conditions (pressure, temperature, state of aggregation etc.). All attempts to alter the course of radioactive decay by varying the external conditions have met with failure: the laws of radioactive decay remained intact.

The nuclei of radioactive elements contain an excess either of neutrons or of protons compared with the number in the stable nuclei of the same element. Nuclei arranged above the stable nucleus region (see Fig. 3.7) are supersaturated with neutrons whereas nuclei below the stable nuclei region possess an excess of protons. This means that in the former type of nuclei there are more (n - n) interactions than are required for stability of the nucleus whereas in the latter type there is an excess of (p - p) interactions. By altering spontaneously their composition, the nuclei are transformed ultimately into stable nuclei (see Fig. 3.7).

Radioactive decay can be divided into α -decay, β -decay, spontaneous fission of nuclei and γ -decay. In α -decay the radioactive nuclei emit α -particles. The α -particle has a charge of $+2e$ and a mass $m_\alpha = 4.0026$ amu. In β -decay β^- -particles (electrons) or β^+ -particles (positrons) are expelled or an orbital electron is captured by the nucleus (electron capture). The electrons and positrons emitted by radioactive nuclei are called β -particles. They are not constituents of the nucleus but arise during the β -decay.

Spontaneous fission of nuclei is observed in heavy nuclei with mass numbers $A \approx 240$ (uranium, neptunium, plutonium etc.). The nuclei of such elements break up spontaneously into two lighter nuclei called fission fragments whose mass numbers range between 70 and 170. Besides fragments, from 2 to 3 neutrons on the average may be produced.

γ -Decay consists in the emission of γ -quanta by metastable nuclei. The latter are distinguished by the long lifetime of their excited states. Metastable nuclei arise in certain α - or β -decaying nuclei or when nuclei interact with particles. In γ -decay the nucleus goes over from one energy state to another and the composition of the nucleus remains unchanged.

A radioactive nucleus may change into other nuclei by several pathways (types of radioactive decay). Thus in heavy elements undergoing spontaneous fission of the nucleus, α -decay may alternatively take place. Such nuclei are thus transformed into those of other elements by two pathways, by spontaneous fission and by α -decay.

Radioactive nuclei are usually divided into *natural* and *artificial* ones. The natural radioactive nuclei are found in nature and comprise only a small fraction of the total number of known radioactive nuclei.

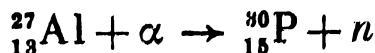
Most radioactive nuclei are obtained by artificially altering the composition of stable nuclei. They are therefore called *artificial radioactive nuclei*. The only difference between natural and artificial radioactive nuclei is their origin. Their radioactive decay is governed by the same laws.

How are artificial radioactive nuclei obtained? It can be seen from the neutron-proton diagram (see Fig. 3.7) that the

region of stable nuclei is located between regions in which the unstable nuclei have either an excess of neutrons (upper region) or an excess of protons (lower region). If one or several neutrons are added to a stable nucleus the product nucleus will be shifted from the stable region upward and will be radioactive. If the charge of the nucleus is increased the product nucleus will be in the lower unstable region. Nuclei with a neutron excess expel β^- -particles and those with a proton excess, β^+ -particles.

Artificial radioactive nuclei can be produced in nuclear reactions. A nuclear transformation, i.e. a change in composition of the initial nucleus, occurs in a nuclear reaction.

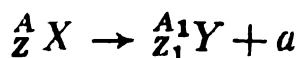
Artificial radioactivity was discovered by Irene and Frederic Joliot-Curie in 1934. By irradiating aluminium with α -particles they observed the nuclear reaction



The notation of a nuclear reaction is similar to that of a chemical reaction. Thus the nucleus and particle which interact are written at the left and the reaction products are written at the right. In the particular reaction cited the artificial β^+ -active $^{30}_{15}\text{P}$ nucleus is produced. Since 1934 over a thousand different radioactive nuclei have been obtained artificially.

An experimental study of radioactive decay revealed that the rate of disintegration obeys a certain law. Each radioactive element is characterized by its *half-life period* $T_{1/2}$. The half-life is the time required for half of the radioactive nuclei to decay. Depending on the radioactive species the half-lives range from a small fraction of a second to many billions of years.

Radioactive decay can be described by an equation of the form



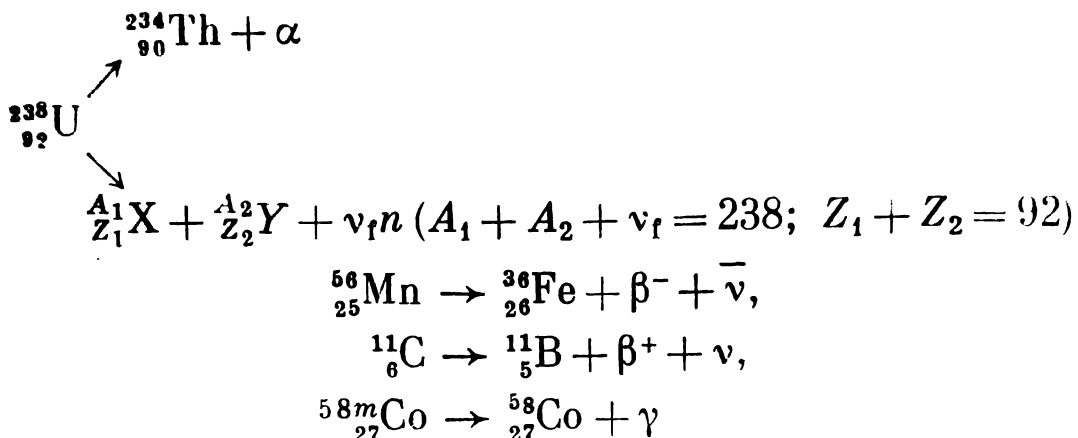
or in abbreviated form



where $^{A}_{Z}X$ is the parent radioactive nucleus and $^{A_1}_{Z_1}Y$ is the product (daughter) nucleus produced in the decay of the

parent nucleus; a denotes the particle emitted (α -particle, β -particle, γ -quantum).

Below are presented some examples of radioactive disintegrations:



where v_f is the number of neutrons emitted, ν denotes the neutrino, $\bar{\nu}$ denotes the antineutrino. The half-lives for spontaneous fission of ${}^{238}_{92}\text{U}$ nuclei into ${}^{A_1}_{Z_1}\text{X}$ and ${}^{A_2}_{Z_2}\text{Y}$ fragments or for α -decay are respectively 8×10^{15} and 4.5×10^9 years. Spontaneous fission of the ${}^{238}_{92}\text{U}$ nucleus is thus less probable than its α -decay: only one fission occurs per 2×10^6 α -decays.

In the β -decay of the ${}^{56}_{25}\text{Mn}$ and ${}^{11}_{6}\text{C}$ nuclei emission of a charged particle (electron or positron) is accompanied by the expulsion of an electrically neutral particle (neutrino ν or antineutrino $\bar{\nu}$, see Sec. 4.5).

If the product nucleus is produced in the excited state it emits γ -quanta after radioactive decay. As an example, the fraction of excited nuclei produced in the radioactive transformation ${}^{235}_{92}\text{U} \xrightarrow{\alpha} {}^{231}_{90}\text{Th}$ is 90%.

The law of conservation of energy is obeyed in radioactive decay. Accordingly the energy of the parent nucleus is equal to the energy of the decay products. For a parent nucleus at rest the law of conservation of energy may be expressed as follows,

$$M_n(Z, A) c^2 = [M_n(Z_1, A_1) + m_a] c^2 + W_d$$

The quantity W_d is the *total decay energy*. It is that part of the rest energy of the parent nucleus which is transformed into the kinetic energy of the product nucleus, of particle a .

and of the γ -quanta: $W_d = E_n + E_a + E_\gamma$. In many cases it is presented in the right hand side of the disintegration equation. The sum of the kinetic energies of the daughter nucleus and particle a , $E_d = E_n + E_a$ is called the *decay energy*. It is liberated at the instant of decay of the parent nucleus and is equal to W_d if the product nucleus is produced in the ground state. It may be mentioned that for a certain type of radioactive decay E_d may assume one or several values.

If masses are expressed in amu and energy in megaelectronvolts, we may write

$$W_d = 931 [M_n (Z, A) - M_n (Z_1, A_1) - m_a]$$

Replacing the nuclear masses by the nuclide masses in accordance with formula (3.1), the latter equation can be transformed into the equation

$$W_d = 931 [M (Z, A) - M (Z_1, A_1) - m_a - (Z - Z_1) m_e] \quad (4.1)$$

The decay energy W_d cannot be negative. From this fact and from equation (4.1) one obtains the energy condition for radioactivity of nuclei,

$$M (Z, A) - M (Z_1, A_1) - m_a - (Z - Z_1) m_e > 0 \quad (4.2)$$

Besides the law of conservation of energy, other laws which are obeyed in radioactive decay are those of conservation of momentum, electric charge and number of nucleons. The law of conservation of momentum can be written as a vector equation,

$$M_n (Z, A) \mathbf{v} = M_n (Z_1, A_1) \mathbf{v}_1 + m_a \mathbf{v}_2$$

where \mathbf{v} and \mathbf{v}_1 are the velocities of the parent and product nuclei and \mathbf{v}_2 is the velocity of the particle a .

Under ordinary conditions the parent nucleus may be considered to be at rest and hence $v = 0$. In this case the product nucleus and particle a fly apart in opposite directions and their velocities are inversely proportional to their masses,

$$v_2/v_1 = M_n (Z_1, A_1)/m_a$$

Let us find the kinetic energy of an α -particle, E_α , and of the product nucleus, E_n , after α -decay. Squaring both

sides of the last equation and taking into account that $M_n (Z_1, A_1) \approx A_1$ amu, $m_\alpha \approx 4$ amu, $A = A_1 + 4$, $v_2 \ll c$, $E_\alpha + E_n = E_d$, we find

$$E_\alpha = (A_1/A)E_d; E_n = (4/A)E_d$$

For α -active nuclei the mass number $A \geq 210$ and hence approximately 98% of the decay energy E_d is imparted to the α -particle.

In β -decay the product nucleus and β -particle move in opposite directions only if the neutrino energy $E_\nu = 0$. The fraction of decay energy which is transferred to the product nucleus when $E_\nu = 0$ can be estimated as follows. Since the mass of the daughter nucleus $M_n (Z_1, A_1) \approx \approx A_1$ amu = $1836A_1 m_\beta$, we find that even in the extreme case when A_1 is minimal, viz., when $A_1 = 1$ (neutron), the ratio

$$m_\beta/M_n (Z_1, A_1) = 1/1836A_1 < 5.5 \times 10^{-4}$$

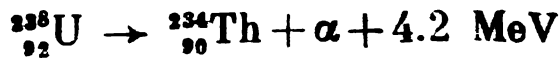
Thus in β -decay less than 0.06% of the decay energy is imparted to the product nucleus. Even less energy is transmitted to the product nucleus in γ -decay.

The amount of energy released in spontaneous nuclear fission $E_d \approx 169$ MeV. It is divided between the two fission fragments inversely proportional to their mass numbers.

$$E_1/E_2 = A_2/A_1, \quad E_1 + E_2 = E_d$$

As an example, if the mass numbers are $A_1 = 95$ and $A_2 = 139$, then $E_1 = 100$ MeV and $E_2 = 69$ MeV.

The laws of conservation of number of nucleons and electric charge can be illustrated by the following case of α -disintegration,



The number of nucleons at the left is 238 and is equal to the number of nucleons at the right, $234 + 4 = 238$. At the left the charge is $92e$ and at the right, $90e + 2e = 92e$.

During α - and β -disintegration the charge of the nucleus and hence the chemical properties of the elements change. The displacement law can be established on the basis of the change of the nuclear charge. In α -decay the atomic number of an atom decreases by two units and therefore

the product atom is shifted to the left by two places in the periodic table. In β^+ -decay the Z of the product atom decreases by one and the atom is shifted one place to the left. In β^- -decay Z increases by one and the atom is displaced one place to the right.

It is convenient to depict radioactive disintegration diagrammatically. Diagrams of α -decay of $^{235}_{92}\text{U}$ and of β^- -decay of $^{60}_{27}\text{Co}$ are presented in Fig. 4.1. The energies are

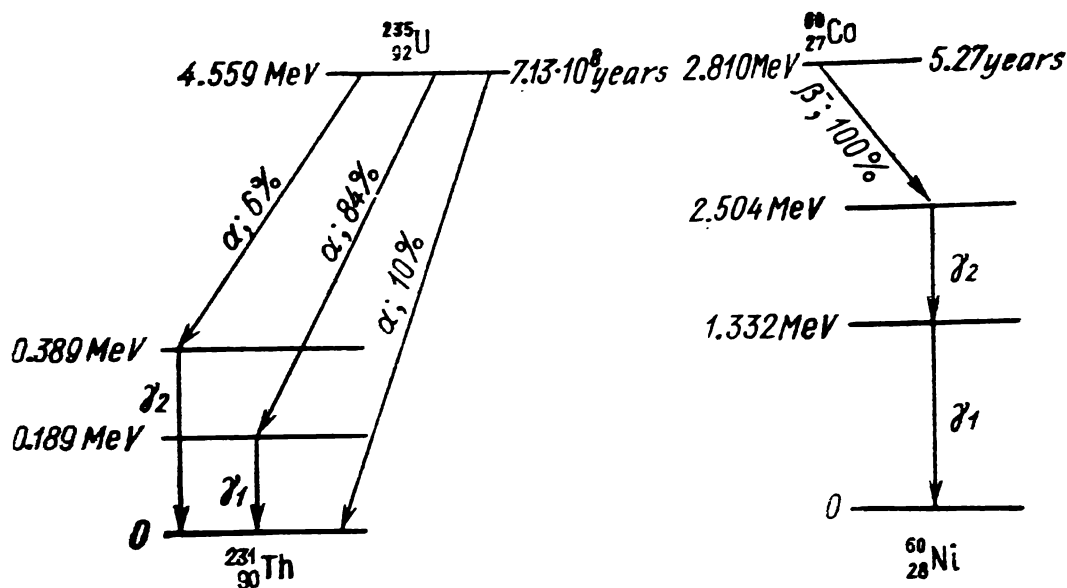


Fig. 4.1 Diagram of α -decay of $^{235}_{92}\text{U}$ and β^- -decay of $^{60}_{27}\text{Co}$

referred to the total rest energy of the product nucleus and charged particle a in the ground states. With the reference point chosen in this way, only the change in the rest energy during radioactive disintegration, W_d , is taken into account. The energy levels of the parent and product nuclei are denoted by the horizontal lines. The half-lives and energy levels in mega-electronvolts referred to the zero energy as chosen above are indicated near each line. Radioactive disintegrations (α , β^+) in which the nuclear charge decreases are depicted by arrows pointing downward and to the left; β^- -decay is depicted by arrows pointing downward and to the right and γ -transitions by vertical arrows pointing downward. The type of decay is indicated along each arrow. The decay energy E_d is the difference between energies of the levels at the beginning and end of the arrows.

As an example, six of every hundred ^{238}U nuclei are transmuted into ^{234}Th nuclei with an excitation energy of 0.389 keV. An energy $E_d = 4.17 \text{ MeV}$ is released in the α -decay. The excited product nucleus may then emit a 0.389 keV γ -quantum and go over to the ground state.

4.2 Radioactive Series

Radioactive disintegration does not always terminate with the formation of a stable nucleus. In many cases a

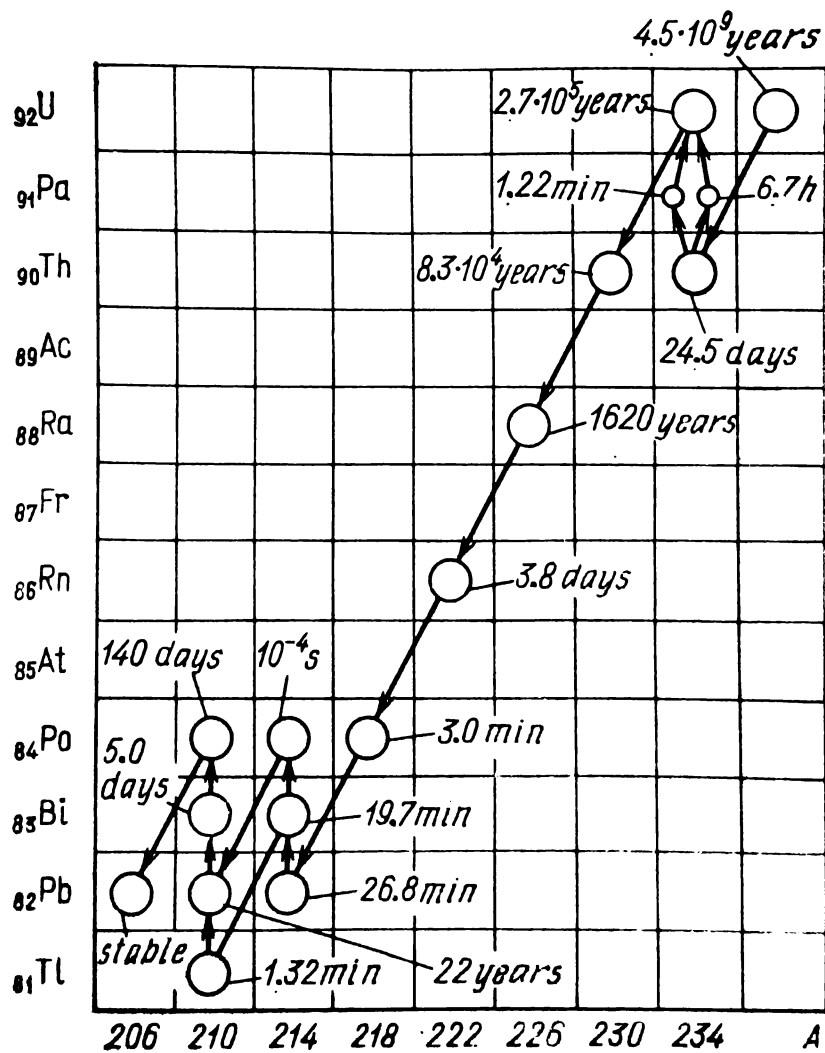


Fig. 4.2 Uranium radioactive series
 α -decay is denoted by slanting arrows and β^- -decay by vertical arrows

chain of radioactive decays is observed in which the nuclei are related to each other. These radioactive chains are called *radioactive series*.

Three natural radioactive substances exist which have half-lives comparable to the lifetime of the earth, which is approximately 4.5×10^9 years. These are $^{238}_{92}\text{U}$ ($T_{1/2} = 4.5 \times 10^9$ years), $^{235}_{92}\text{U}$ ($T_{1/2} = 7.13 \times 10^8$ years) and $^{232}_{90}\text{Th}$ ($T_{1/2} = 1.4 \times 10^{10}$ years). These elements are all located at the end of the periodic table and belong to the actinide group of elements. The three substances are the parents of the three natural radioactive series, the uranium ($^{238}_{92}\text{U}$), actinium ($^{235}_{92}\text{U}$) and thorium ($^{232}_{90}\text{Th}$) series.

The uranium radioactive series and the half-lives of the respective radioactive substances are shown in Fig. 4.2. The end product of the uranium series is the stable $^{206}_{82}\text{Pb}$ nucleus. The end products of the actinium and thorium series are the stable $^{207}_{82}\text{Pb}$ and $^{208}_{82}\text{Pb}$ nuclei respectively.

In any of the series the mass number A changes only as a result of α -decay in which case A is reduced by four units. Consequently the mass numbers of the nuclei of any series can be expressed by a single formula

$$A = 4n + C$$

where n and C are whole numbers.

For the uranium series $C = 2$ and n lies between 51 and 59. For the actinium series $C = 3$, $51 \leq n \leq 58$ and for the thorium series $C = 0$, $51 \leq n \leq 58$. The value of the constant C in the expression for A is thus either 0, 2 or 3. A radioactive neptunium series with $C = 1$ has been obtained artificially. The most long-lived element in this series is $^{237}_{93}\text{Np}$ with a half-life of 2.2×10^6 years.

4.3 Law of Radioactive Decay

The radioactive decay law is a statistical law. One of its characteristics is the *radioactive decay constant* or simply *decay constant*. It is denoted λ and has the dimension s^{-1} . It yields the fraction of radioactive nuclei decaying per unit time.

Let $N(t)$ be the number of radioactive nuclei at some initial time t . Then the fraction of nuclei $dN/N(t)$ disintegrating in a time dt is

$$dN/N(t) = -\lambda dt$$

The minus sign in the differential equation indicates that the number of radioactive nuclei decreases over the time period dt . Integration of the equation yields

$$N(t) = Be^{-\lambda t}$$

The integration constant B can be found from the initial disintegration conditions: at $t = 0$ the number of radioactive nuclei was N_0 and hence $B = N_0$. Insertion into the latter equation yields the equation which expresses the *law of radioactive decay*

$$N(t) = N_0 e^{-\lambda t} \quad (4.3)$$

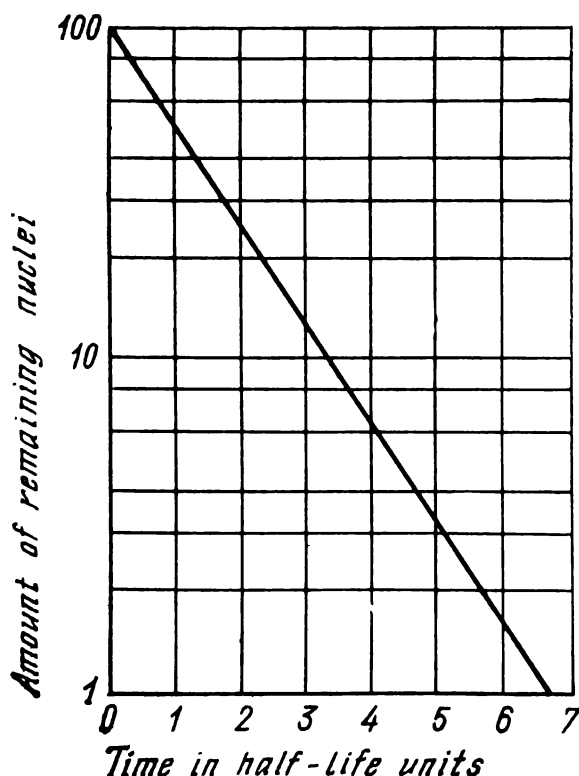


Fig. 4.3 Law of radioactive decay

This law is valid if the number of radioactive nuclei is sufficiently large. The function $\ln N(t)$ depends linearly on t . A plot of the function is shown in Fig. 4.3. After a time equal to the half-life $T_{1/2}$ the number of radioactive nuclei is halved. The relation between λ and $T_{1/2}$ can be found in the following way. Since

$$N(T_{1/2})/N_0 = 1/2 = e^{-\lambda T_{1/2}}$$

it follows

$$T_{1/2} = 0.693/\lambda \quad (4.4)$$

The number of nuclei disintegrating in the time interval between t and $t + dt$ is $\lambda N dt$, each of the nuclei having lived a time t . The total lifetime of these nuclei is $t\lambda N dt$ and the total lifetime of all N_0 nuclei can be found by integrating $t\lambda N dt$ from zero to infinity. The mean lifetime of the radioactive nuclei, τ , is the ratio of the integral to N_0 .

$$\tau = \frac{1}{N_0} \int_0^\infty t \lambda N dt = \lambda \int_0^\infty t e^{-\lambda t} dt$$

The integration yields

$$\tau = 1/\lambda \quad (4.5)$$

Formula (4.5) shows that the larger the decay constant, the higher is the rate of decay of the radioactive nuclei. Substitution of $\lambda = 1/\tau$ into formula (4.4) gives the relation between the half-life $T_{1/2}$ and the mean lifetime τ ,

$$T_{1/2} = 0.693\tau$$

In tables of radioactive substances the values of the decay constant λ , half-life $T_{1/2}$ (or one of the values) and also the decay energy and type of emitted particle are usually given. The characteristics of some radioactive nuclides are presented in Table 4.1.

Table 4.1

Characteristics of Some Radioactive Nuclides

Nuclide	Half-life	Decay constant, s ⁻¹	Particle	Total decay energy W_d . MeV
$^{238}_{92}\text{U}$	4.5×10^9 years	4.84×10^{-18}	α	4.2
$^{234}_{92}\text{U}$	2.48×10^6 years	8.17×10^{-14}	α	4.75
$^{210}_{83}\text{Bi}$	4.97 days	1.61×10^{-6}	β^-	1.17
$^{210}_{81}\text{Tl}$	1.32 min	8.75×10^{-3}	β^-	1.80

Example. What fraction of $^{210}_{83}\text{Bi}$ nuclei disintegrates in one hour? According to equation (4.3)

$$N/N_0 = e^{-3600\lambda} = e^{-1.61 \times 10^{-6} \times 3600} = 0.994$$

The fraction of $^{210}_{83}\text{Bi}$ nuclei which disappears in an hour is $1 - N/N_0 = 1 - 0.994 = 0.006$, i.e. 0.6% of the $^{210}_{83}\text{Bi}$ nuclei decay in one hour.

Experimentally it is the *activity of a substance* that is measured. The activity a is the number of nuclei decaying per second. It can be calculated from the equation

$$a = |dN/dt| = \lambda N$$

The unit of activity is one disintegration per second (dis./s) and is called the *becquerel* (Bq). Very often a subsidiary unit, the *curie*, or fractions of it, is employed. By definition:

1 curie (Ci) = 3.7×10^{10} dis./s;

1 millicurie (mCi) = 3.7×10^7 dis./s;

1 microcurie (μCi) = 3.7×10^4 dis./s.

The concentration of radioactive substances in gases or liquids can be expressed in curies per litre (Ci/l).

A relationship exists between the mass of a radioactive substance, m , with an activity of 1 Ci and its half-life $T_{1/2}$ and atomic mass A . According to formula (1.1) there are $N = (m/A) N_A$ radioactive atoms in the mass m and the activity is therefore $a = (\lambda m/A) N_A$. Here N_A is Avogadro's number. Since it is assumed that $a = 3.7 \times 10^{10}$ dis./s, we obtain

$$m = 8.86 \times 10^{-17} A T_{1/2} \quad (4.6)$$

if m is expressed in kilograms and $T_{1/2}$ in seconds.

The activity of a kilogram of a radioactive substance in curies is

$$a = 1.13 \times 10^{16} / A T_{1/2}$$

Example. Determine the activity of 10 g of ^{238}U . In accordance with formula (1.1) the number of atoms in 10 g of ^{238}U is

$$N = (0.01/238) 6.02 \times 10^{26} = 2.53 \times 10^{22} \text{ atoms}$$

The decay constant $\lambda = 4.84 \times 10^{-18} \text{ s}^{-1}$. The activity of the uranium $a = 4.84 \times 10^{-18} \times 2.53 \times 10^{22} = 1.22 \times 10^5 \text{ dis./s} = 3.31 \mu\text{Ci}$.

Example. Calculate the mass of ^{60}Co ($T_{1/2} = 5.27$ years) if the activity is 1 Ci.

According to formula (4.6)

$$\begin{aligned} m &= 8.86 \times 10^{-17} \times 60 \times 3.15 \times 10^7 \times 5.27 \approx \\ &\approx 8.82 \times 10^{-7} \text{ kg} = 0.882 \text{ mg} \end{aligned}$$

The accumulation of radioactive product nuclei depends on the disintegration rate of both the parent and product nuclei. Denote by $N_1(t)$ and $N_2(t)$ the number of parent and product radioactive nuclei and by λ_1 and λ_2 their decay constants. If at some initial time $t = 0$ the number of parent nuclei was N_{01} and there were no product nuclei, then at a time t the number of product nuclei $N_2(t)$ will be

$$N_2(t) = \frac{\lambda_1}{\lambda_2 - \lambda_1} N_{01} (e^{-\lambda_1 t} - e^{-\lambda_2 t})$$

Two special cases may be considered.

(a) $\lambda_1 \ll \lambda_2$. The mean lifetime of the parent substance is so large that the number of its nuclei is virtually invariable in time. After a time $t \gg 1/\lambda_2$ the second exponential term may be neglected and $\lambda_2 N_2(t) = \lambda_1 N_1(t)$. This relationship is called the *law of secular equilibrium*.

The parent and product substances are in radioactive equilibrium over a very long period of time, the activity of each of them being proportional to its half-life $T_{1/2}$. The secular equilibrium law can be employed to determine the amount of a radioactive substance in a mixture. In the uranium series, for example, the ^{238}U nuclei ($T_{1/2} = 4.5 \times 10^{10}$ years) are in prolonged equilibrium with the ^{234}U nuclei ($T_{1/2} = 2.48 \times 10^5$ years). The amount of ^{234}U in natural uranium can be found from the relation

$$N_1(t)/N_2(t) = T_{1/2}^{234}/T_{1/2}^{238} = 0.54 \times 10^{-4}$$

and hence is $5.4 \times 10^{-3}\%$.

(b) $\lambda_1 \gg \lambda_2$. The parent nuclei are transmuted to the product nuclei almost completely over a short period of time during which only few product nuclei disintegrate. Hence approximately, $N_{02} \approx N_{01}$. The variation of $N_2(t)$ occurs according to the law

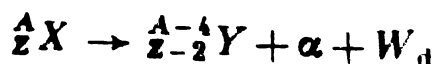
$$N_2(t) = N_{01} e^{-\lambda_2 t}$$

Thus in the uranium series the ^{238}U and ^{234}U nuclei are in prolonged equilibrium via two short-lived nuclei, ^{234}Th and ^{234}Pa (see Fig. 4.2). The lifetimes of the latter nuclei are very short and it may be assumed that approximately ^{238}U is instantaneously transformed into ^{234}U without any intermediate decay stages being involved.

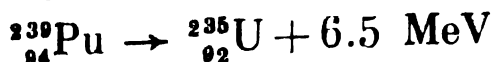
4.4 Alpha Decay

Alpha decay was discovered in studies of the radioactivity of some natural elements. The natural α -active nuclides are located at the end of the periodic system. Altogether about 40 natural and 100 artificial α -emitters are known.

The equation for α -decay is



After expulsion of an α -particle the charge of the nucleus is reduced by two units and the mass number by four. An example of α -decay is



The energy condition for α -decay can be obtained if we take into account that $m_a = m_\alpha$ and $Z - Z_1 = 2$ and substitute $M(^4\text{He})$ for $m_\alpha + 2m_e$ in equation (4.2),

$$M(Z, A) = M(Z - 2, A - 4) + M(^4\text{He}) + W_d/c^2$$

Since the energy $W_d > 0$, α -decay is possible only if the mass of the parent nuclide exceeds the masses of the product and ^4He nuclides taken together. In the example considered the mass of ^{239}Pu exceeds the sum of the $^{235}_{92}\text{U}$ and ^4He masses by $\Delta M = 0.007$ amu.

Two features of α -decay may be mentioned which were discovered experimentally.

1. The decay constant λ and α -particle energy E_α are related by the equation

$$\ln \lambda = B_1 \ln E_\alpha + B_2$$

which expresses the *Geiger-Nutall law*. The constant B_1 is the same for all series whereas B_2 varies from series to series. The Geiger-Nutall law shows that the shorter the lifetime of an α -emitter the greater the energy of the α -particle.

2. The energies of α -particles emitted by various substances lie between 4 and 9 MeV. This is much less than the energy an α -particle would possess as a result of acceleration in the electric field of the nucleus.

For example, the potential energy of repulsion of an α -particle at the boundary of the thorium nucleus in the α -decay $^{238}_{92}\text{U} \xrightarrow{\alpha} ^{234}_{90}\text{Th}$ is about 30 MeV. Therefore after surmounting the potential barrier the α -particle should be accelerated to an energy of approximately 30 MeV. Actually the α -particle energy observed is only 4.2 MeV.

How can the Geiger-Nutall law be explained? Why is the energy of the emitted α -particles so relatively low? The answers to these questions can be found in quantum mechanics. In many nuclei an α -particle exists prior to the commencement of α -decay. They move with a certain

energy E'_α . If there were no potential barrier the α -particle would leave the nucleus with an energy E_α ($E_\alpha = V_0$) (Fig. 4.4), where V_0 is the depth of the potential well. This is precisely the α -particle energy observed experimentally. The α -particle escapes from the nucleus as if no potential barrier existed.

According to the laws of quantum mechanics α -particles possess wave properties. Hence on colliding with the wall of the potential barrier they are reflected, just as waves would

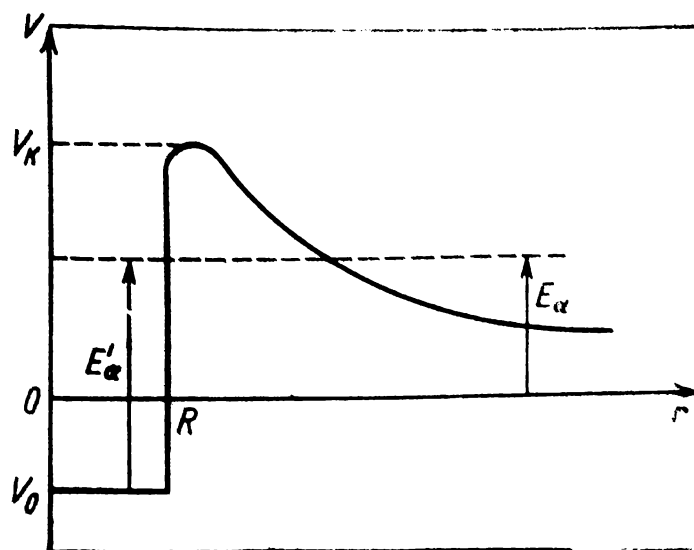


Fig. 4.4 Diagram illustrating the penetration of a potential barrier by an α -particle

be. However not all of the α -particles are reflected back from the wall. Some of them penetrate the wall and escape from the radioactive nucleus with an energy E'_α . This escape of α -particles through the potential barrier at energies below the height of the barrier is called the *tunnel effect*. This effect explains the low α -particle energies observed in α -decay.

The width of the potential barrier decreases with increase of the energy E'_α (see Fig. 4.4). The narrower the potential barrier the greater is the probability that an α -particle will escape from the nucleus. This, briefly, is the physical explanation of the Geiger-Nutall law.

The fraction of α -particle collisions with the potential barrier which results in α -particle emission is called the *transmission coefficient D*. With increase of the α -particle

energy the transmission coefficient increases and becomes unity at energies E_α exceeding the height of the potential barrier V_h . It may be mentioned that in the case of irradiation of a nucleus by charged particles α possessing an energy $E_\alpha < V_h$ the transmission coefficient determines the fraction of particles penetrating into the nucleus through the potential barrier. These particles then interact with the nucleus.

The energy of an α -particle depends on the energy state of the product nucleus after the α -disintegration. If the product nucleus is formed only in the ground state, mono-energetic α -particles will be emitted. However, if the product nuclei are formed in the ground and excited states, several energy groups of α -particles and γ -quanta will be emitted. The α -particle spectrum is therefore discrete.

The disintegration diagram of $^{235}_{92}\text{U}$ which illustrates the emission of several groups of α -particles is shown in Fig. 4.1. Three groups of α -particles with energies of 4.559, 4.370 and 4.170 MeV are observed in the α -decay of $^{235}_{92}\text{U}$. The product nucleus $^{231}_{90}\text{Th}$ is formed either in the ground state or in one of two excited states. The further transformation of thorium from the excited state to the ground state is accompanied by γ -quantum emission.

4.5 Beta Decay

In β -decay one isobar is transformed into another. On the neutron-proton diagram (Fig. 3.7) the chains of radioactive isobars are located on lines for which $A = \text{constant}$. One of the characteristic features of β -decay is that the energy spectrum of the β -particles $f(E_e)$ is continuous (Fig. 4.5). The energy of β -particles varies between zero and the decay energy E_d which in this case is also called the maximal or end-point energy, E_e^{\max} . This energy is usually indicated in the β -decay schemes (see Fig. 4.1).

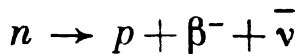
The β -particle spectra are measured with magnetic beta-ray spectrometers. With respect to design and operation they resemble conventional mass-spectrometers.

Along with the positron (or electron) a neutrino ν (or antineutrino $\bar{\nu}$) is emitted in β -decay. The neutrino has a

spin $\hbar/2$ and like γ -quanta moves with the speed of light and has no rest mass or charge. The penetrating power of neutrinos is enormous and hence it is difficult to detect them.

The β -particle energy $E_e = E_e^{\max} - E_\nu$. It depends on the energy of the neutrino E_ν which may have any value between 0 and E_e^{\max} . Precisely because of this the β -particle spectrum is continuous. On the average the β -particles carry an energy $E_e^{\max}/3$ which can be measured experimentally. Before anything was known about the existence of the neutrino it seemed that the law of conservation of energy was being violated in β -decay and some scientists began to doubt the validity of the law in the microcosm. In 1933 the Swiss physicist Pauli predicted theoretically the emission of neutrinos and the applicability of the law of conservation of energy in β -decay.

Modern theory regards the emission of β -particles and neutrinos (antineutrinos) in β -decay as being the result of nucleon transformations in the nucleus. Electrons arise in the transformation of a neutron into a proton, and positrons in the transformation of a proton into a neutron. If the number of neutrons in a nucleus exceeds that found in the stable nuclei with the same atomic number Z , β^- -decay will occur in which a neutron in the nucleus is replaced by a proton,



The charge of the nucleus in this case is increased by one whereas the mass number remains unchanged. The β^- -decay energy can be found from equation (4.1) in which it should be assumed that $Z - Z_1 = -1$ and $m_a = m_e$:

$$W_d = 931 [M(Z, A) - M(Z + 1, A)]$$

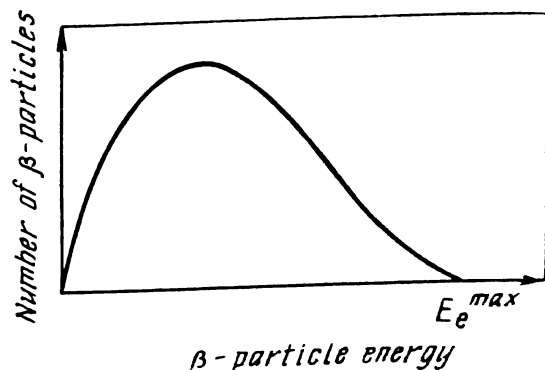
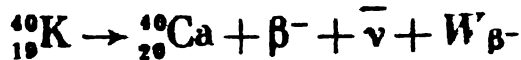


Fig. 4.5 Energy spectrum of β -particles

The decay energy is positive and hence β^- -decay is possible on the condition that the mass of the parent nuclide M (Z, A) exceeds that of the product nuclide M ($Z + 1, A$).

Example. Find the energy of the β^- -decay



The masses of the parent and product nuclides are

$$M({}_{19}^{40}\text{K}) = 39.9640 \text{ amu}; \quad M({}_{20}^{40}\text{Ca}) = 39.9626 \text{ amu}$$

The decay energy

$$W_d = 931 (39.9640 - 39.9626) \approx 1.3 \text{ MeV}$$

If the nucleus contains an excess of protons it is transmuted as a result of transformation of a proton into a neutron,



A transformation of this type can occur only in the nucleus. Free protons are stable particles. The mass number does not change in β^+ -decay whereas the nuclear charge decreases by one. In written form the energy conditions for β^+ -decay and β^- decay are quite different. Inserting $Z - Z_1 = 1$ and $m_a = m_e$ into equation (4.1) we get

$$W_d = M(Z, A) - M(Z - 1, A) - 2m_e$$

Thus positron decay occurs only if the mass of the parent nuclide exceeds that of the product nuclide by at least two electron masses.

Example. Find the energy of the β^+ -decay ${}_{6}^{11}\text{C} \rightarrow {}_{5}^{11}\text{B} - + \beta^+ + \nu$. The nuclide and electron masses are

$$M({}_{6}^{11}\text{C}) = 11.0114 \text{ amu}, \quad M({}_{5}^{11}\text{B}) = 11.0093 \text{ amu}.$$

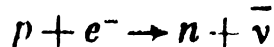
$$m_e = 0.00055 \text{ amu}$$

The decay energy is

$$W_d = 931 (11.0114 - 11.0093 - 0.0011) \approx 0.931 \text{ MeV}$$

The third type of β -decay is electron capture. A nucleus with an excess of protons may capture an electron from one of the atomic orbits. The capture is followed by the emission of characteristic X-rays and, as in positron decay, a nuclear

proton is transformed into a neutron,

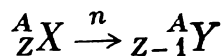


Electron capture is designated in accordance with the orbit from which the electron is acquired. Thus capture of an electron from the *K*-orbit is called *K*-capture, that from the *L*-orbit is called *L*-capture etc. and the electrons involved are respectively denoted e_K^- , e_L^- etc.

In electron capture the atomic number decreases by one ($Z - Z_1 = +1$) and an electron disappears ($m_a = -m_e$). Thus according to equation (4.1) the decay energy

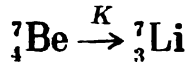
$$W_{dn} = [M(Z, A) - M(Z - 1, A)] c^2$$

where the subscript $n = K, L, \dots$ denotes the type of electron orbit. Electron capture can therefore be observed if the mass of the parent nuclide exceeds that of the product nuclide. The equation for electron capture is



The shell from which the electron is captured is indicated by the symbol above the arrow.

An example of *K*-capture is



in which the ${}^7_4 \text{Be}$ nucleus captures a *K*-electron with a capture energy $W_{dK} = 0.886$ MeV.

4.6 Internal Conversion. Nuclear Isomerism

Internal conversion. Excited nuclei with excitation energies lower than the binding energy of the nucleon may go over to the ground state and emit γ -quanta. However, the excitation energy may be liberated in other ways. In a process called internal conversion the excitation energy of the nucleus is transferred directly to an orbital electron which may then be ejected from the atom. The vacancy in the inner shell is then filled by an electron from an outer shell and the atom emits a characteristic X-ray photon.

During internal conversion part of the excitation energy of the nucleus is expended in breaking the bond between

the electron and nucleus, ϵ_e , and the other part is transformed into the kinetic energy of the electron, E_e .

$$W_{ex} = \epsilon_e + E_e$$

Since the excitation energy of the nucleus and the binding energy of the electron in each atomic shell have discrete values, the electrons ejected in internal conversion will also possess discrete energy values. In this respect β^- -decay, which has a continuous spectrum, differs significantly from internal conversion.

The discrete energy spectrum of the internal conversion electrons observed in the radioactive decay $^{214}_{82}\text{Pb} \xrightarrow{\beta^-} {}^{214}_{83}\text{Bi}$ is presented in Table 4.2. The product nucleus $^{214}_{83}\text{Bi}$ is pro-

Table 4.2

Spectrum of Internal Conversion Electrons Emitted in Radioactive Decay

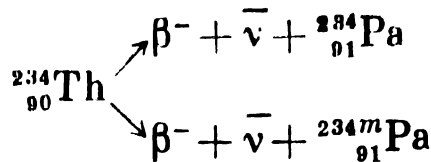
Electron energy E_e , MeV	Electron shell	Electron binding energy ϵ_e , MeV	Quantum energy E_γ , MeV
0.0368	L	0.0161	0.0529
0.1510	K	0.0887	0.240
0.1617	K	0.0887	0.257
0.2041	K	0.0887	0.293
0.2605	K	0.0887	0.350

duced in excited states. Some of the excited nuclei decay to the ground state by internal conversion and some emit γ -quanta.

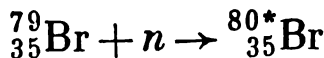
The quantities E_e , ϵ_e and E_γ can be measured. The sum of the energies $E_e + \epsilon_e$ (first and third columns) is close to the energy of the γ -quanta (fourth column) and this confirms the internal conversion origin of the electrons.

Nuclear isomerism. Nuclear isomers are nuclei with the same atomic number and mass number but with different energy states. The phenomenon of existence of nuclear isomers is referred to as *nuclear isomerism*. Isomers may be formed in β -decay or in nuclear reactions. They were first detected by the German chemist Hahn in 1931. Among the β^- -decay products of $^{232}_{90}\text{Th}$ he observed two protactinium

isomers with lifetimes of 6.7 hours and 1.22 minutes:



Bromine isomers were discovered in 1935 by Academician I. V. Kurchatov. Irradiation of natural bromine by neutrons results in the nuclear reaction



The ${}^{80*}_{35}\text{Br}$ nucleus is formed in the excited state (indicated by the asterisk). If the neutron energy is close to zero, the excitation energy is equal to the binding energy of the

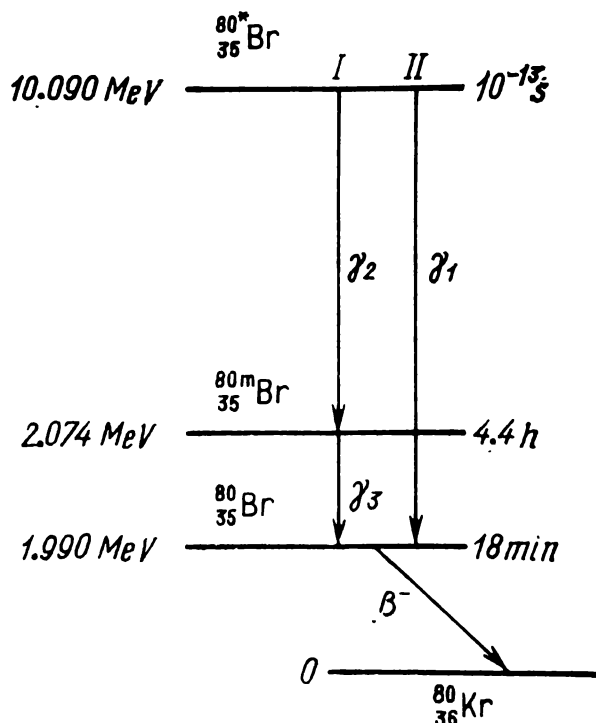


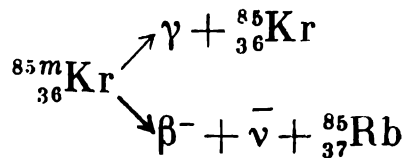
Fig. 4.6 Formation of ${}^{80m}_{35}\text{Br}$ and ${}^{80}\text{Br}$ isomers

neutron in the ${}^{80}_{35}\text{Br}$ nucleus. Part of the excited nuclei emits γ -quanta (Fig. 4.6, I) and goes over to a metastable level whereas the others make transitions to the ground state (Fig. 4.6, II). The half-life of the ${}^{80}\text{Br}$ isomer is 18 minutes. Therefore the ${}^{80}\text{Br}$ nuclei produced in the nuclear reaction disappear in a comparatively short time.

The excitation energy of the ${}^{80m}_{35}\text{Br}$ nucleus is removed in two competing processes with a half-life of 4.4 hours. These

processes are γ -decay (${}^{80m}_{38}\text{Br} \rightarrow \gamma + {}^{80}_{38}\text{Br}$) and internal conversion (${}^{80m}_{38}\text{Br} \rightarrow e^- + {}^{80}_{38}\text{Br}$). The emission of conversion electrons ($T_{1/2} = 4.4$ h) and β^- -particles ($T_{1/2} = 18$ min) is what is observed experimentally.

Transformation of the metastable β -active nuclei into their products may occur along several lines. Thus the ${}^{85m}_{36}\text{Kr}$ nucleus undergoes either γ -decay or β^- -decay:



4.7 Applications of Radioactive Substances

The production of radioactive substances is steadily rising in many countries of the world. This is due to the fact that the application of radioactive substances has been helpful for solving various complex problems.

In the studies of many processes the *labelled atom technique* has been useful. The chemical properties of isotopes of a certain element are identical. If the stable isotope of an element in a chemical compound is replaced by a radioactive isotope (tagged or labelled atom), the role of that element in the chemical or physical processes of interest may be ascertained in some cases by studying the movement of the isotope.

Labelled atoms are used in medicine for diagnostic purposes and treatment of sicknesses. Two examples may be considered. The blood circulation of a patient can be checked by introducing a small amount of radioactive sodium into the vein. The sodium does not become evenly distributed in the body instantaneously. The radioactive atoms initially move through the blood vessels in a concentrated form. The radiation emitted by the radioactive sodium atoms is measured by a γ -quantum counter placed near the foot of the patient. In a healthy organism the counting rate increases rapidly after introduction of the isotope and is maximum in less than an hour. If the circulatory system is not functioning satisfactorily the counting rate increases slowly. By measuring the counting rate at various parts of the patient's body one may detect the accumulation of the

tagged atoms and hence the sites of blood vessel occlusion.

Enhanced amounts of iodine are found in the thyroid glands of patients afflicted by Basedow's disease. To study the functioning of the thyroid gland radioactive iodine is introduced. The seriousness of the sickness may be established by measuring the counting rate near the thyroid gland.

Biologists use the tracer technique to study the uptake and distribution of elements in organisms. As an example, radioactive phosphorus is included in compounds fed to plants. The plant is then pressed upon a photographic film and covered with light-proof paper. After development the film yields the distribution pattern of the phosphorus in the stems and leaves of the plant.

Wear-proof of piston rings, bearings etc. is studied in the engineering industry by means of labelled atoms. For this purpose radioactive iron isotopes are introduced into the parts under investigation. During operation of the engine some of the atoms appear in the lubricating oil. The wear of the particular part may be determined by periodically measuring the activity of the oil.

In industry γ -sources are employed to check the quality of finished parts, integrity of welded joints etc. The machine part is placed between a γ -quantum source and photographic film. After development cavities and other defects may be detected in rejects. Gamma-ray emitters are useful for measuring continuously the metal thickness in rolling mills.

The absorption of the charged particles and γ -rays emitted by radioactive substances is accompanied by the liberation of heat. Radioactive substances employed as sources of heat are called *radioisotope fuels*. They are used in radioisotope thermoelectric power generators.

The main components of the generator are the radioisotope fuel capsule, battery of thermocouples, thermal insulation, construction parts and cooler (Fig. 4.7). Part of the fuel capsule is covered with thermocouples and the other part by heat insulating material.

An amount of heat Q_1 flows from the radioisotope capsule to the thermoelectric couple battery (Fig. 4.8) and part of this heat Q_2 is then transferred to the cooler with cooling fins which facilitate the discharge of the heat to the ambient

medium. The difference between these two heat flows $\Delta Q = Q_1 - Q_2$ is used to generate electric energy.

The radioisotope fuel is usually a metal or chemical compound with a high specific power (energy released per

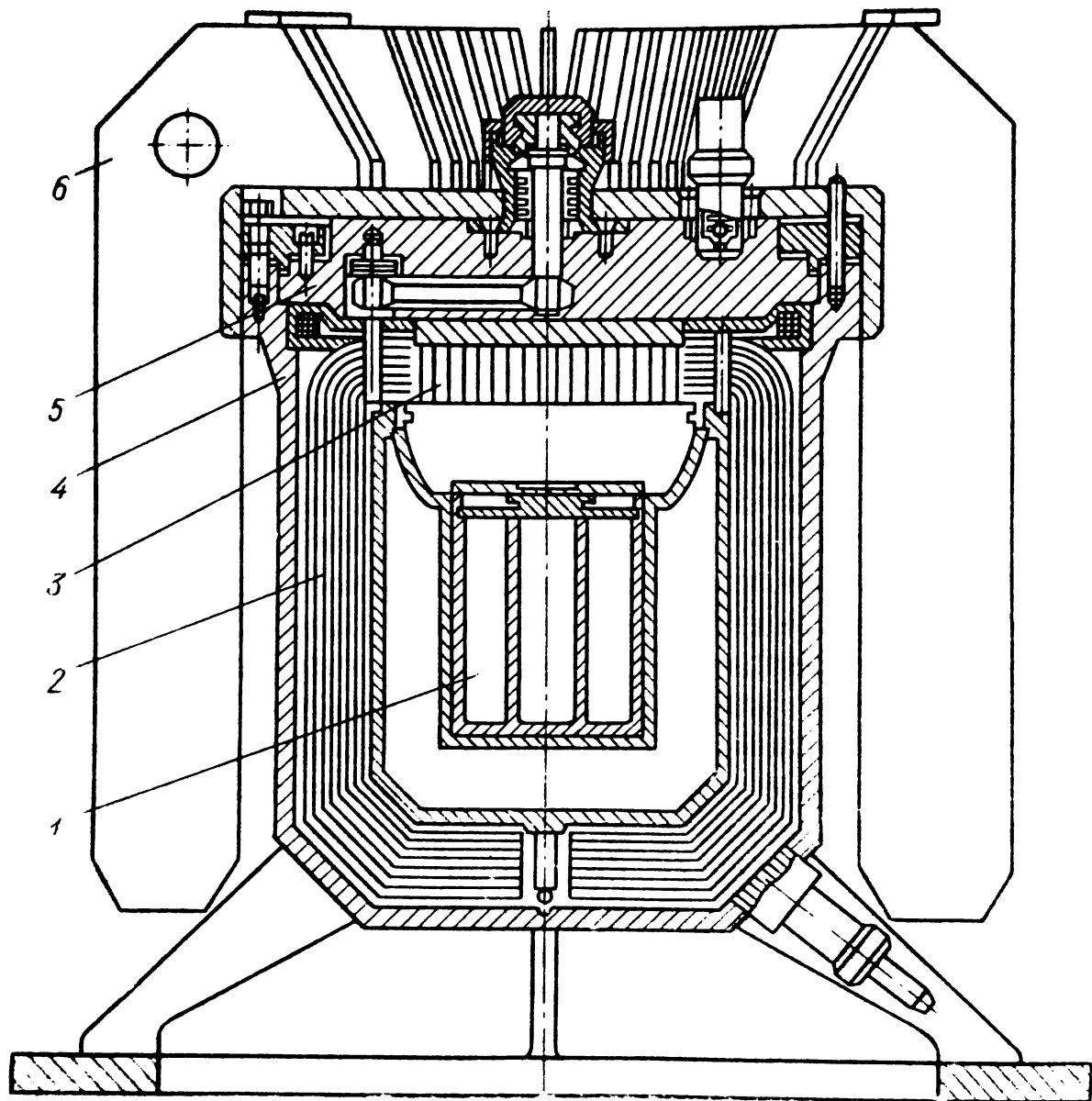


Fig. 4.7 "Beta-3" radioisotope generator

1—radioisotope fuel capsule; 2—thermal insulation; 3—thermobattery; 4—casing;
5—lid; 6—cooler

unit mass or unit volume per second), high heat conductivity (Table 4.3) and melting point of not less than 500°C. The demands on the radioisotope fuel and construction parts are rigid. They are dictated by the constraints on the size and mass of the generator as well as by the radiation safety

required in case of breakdown during operation or accidents in transportation of the generator.

Other restrictions on radioactive metals are that they should not be toxic, nor react chemically with the air,

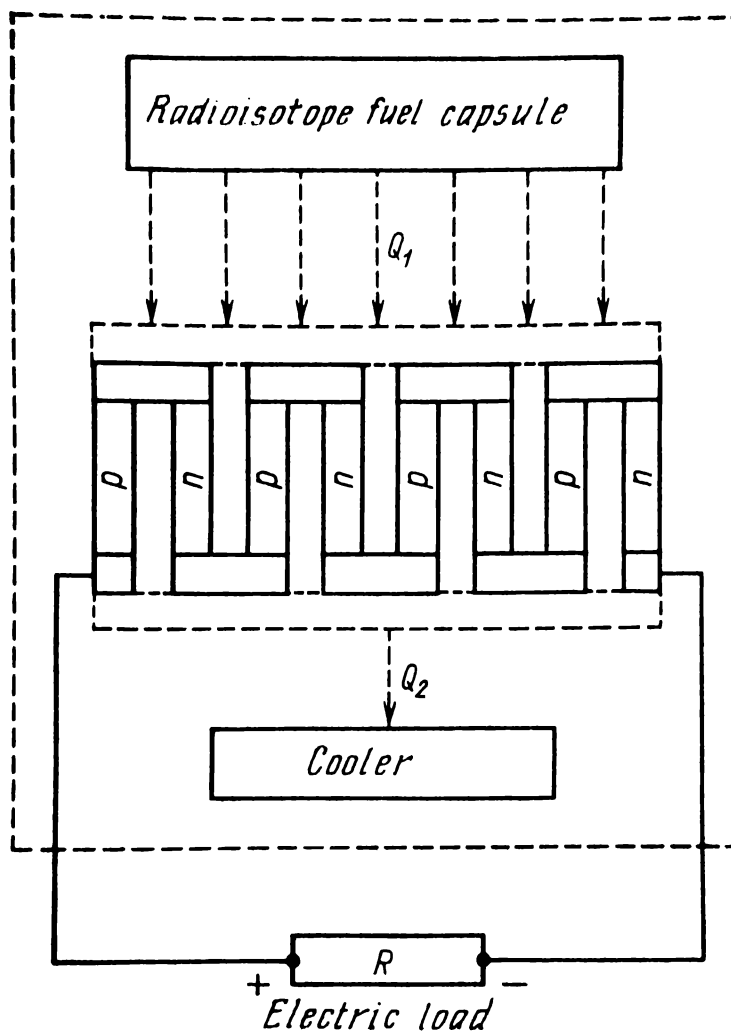


Fig. 4.8 Schematic drawing of a radioisotope thermoelectric generator

water or material of the fuel capsule and should possess a sufficiently high melting point. Therefore the metals are usually replaced by compounds containing them. Examples are strontium titanate SrTiO_3 and cerium molybdate $\text{Ce}_2(\text{MoO}_4)_3$.

The thermocouple battery consists of a large number of thermocouples connected in series. The junctions to which the heat flows from the radioisotope capsule are called hot junctions and the junctions in contact with the cooler are the cold junctions. A thermocouple consists of two semi-

Characteristics of Some Types of Metallic Radioactive Fuels

Fuel	Density, 10 ³ kg/m ³	Melting point, °C	Decay	Half-life, years	Specific power, kW/kg
⁹⁰ Sr	2.6	770	β^-	27.7	0.936
¹⁴⁴ Ce	6.7	804	β^-	0.78	26.7
¹³⁷ Cs	1.87	28.5	β^-	30	0.411
⁶⁰ Co	8.7	1495	β^-	5.27	17.5
²⁴² Cm	13.5	950	α	0.44	122.5
²¹⁰ Po	9.4	254	α	0.38	144
²³⁸ Pu	16.5	640	α	86.4	0.58

conducting rods. One rod is a semiconductor with electronic conductivity (*n*-type semiconductor) and the other is a semiconductor with hole-type conductivity (*p*-type semiconductor).

The heat ΔQ is expended in the battery in the formation of free electrons (in the *n*-type semiconductor) or positive ions (*p*-semiconductor), the amount of the charges increasing with the temperature. Since the temperature of the hot junction t_1 exceeds that of the cold junction t_2 the charge distribution is not uniform in the rods and an electromotive force arises. Materials particularly suited for making thermocouples are the solid solutions $\text{Bi}_2\text{Te}_3\text{-Sb}_2\text{Te}_3$ and $\text{Bi}_2\text{Te}_3\text{-Bi}_2\text{Se}_3$ (operation temperature range 200-600 K) and the alloys Pb-Te (600-1000 K) and Si-Ge (900-1300 K).

The main characteristics of the generator are the electric power P_e , service life τ , output voltage U and efficiency η . The power $P_e(t)$ is proportional to the activity of the radioisotope fuel. The service life τ varies between $0.2T_{1/2}$ and $T_{1/2}$ depending on the generator. The half-life $T_{1/2}$ is usually chosen to lie between 100 days and 100 years.

The voltage U is proportional to the temperature drop $\Delta t = t_1 - t_2$ and to the number of thermocouples in the battery. The efficiency η depends on the temperature drop Δt , temperature of the hot junction and properties of the semiconducting materials. The electric power of generators of the "Beta", "Efir" and "Penguin" types in operation

in the USSR and of the "SNAP-7" type in the USA is around 100 W, the output voltage being 4-12 V and efficiency is not higher than 10%.

Radioisotope thermoelectric generators have been employed for powering automatic radiometeorological stations, radio beacons, apparatus in artificial satellites of the earth etc. Miniature generators have also been applied in medicine such as for powering heart pacemakers.

CHAPTER 5

INTERACTION BETWEEN IONIZING RADIATIONS AND MATTER

5.1 Particle Flux Density and Intensity of Ionizing Radiation

Any radiation which on interacting with matter produces electric charges of opposite signs is called ionizing radiation. Ionizing radiation (or simply, radiation) can be divided into charged radiation (electrons, protons, α -particles etc.), electromagnetic (γ -quanta) and neutral (neutrons, neutrinos etc.) radiation. Charged particles ionize molecules by interacting with the electrons of their atoms. Gamma-rays and neutrons produce charged particles in matter through which they pass and these particles then ionize the molecules of the matter.

Quantitative characteristics of any radiation are the *particle flux density* and *radiation intensity*. We shall define these quantities for radiation whose particles move in a given direction. The particle flux density ϕ is the number of particles incident per unit time on a unit area perpendicular to the direction of propagation of the radiation. Suppose that the density of a particle flux striking a plane target, ϕ , is constant and let n denote the number of particles in a unit volume moving toward the target. This number is called the *particle density*.

Assume that all particles moving in a given direction have the same velocity v . The number of particles passing through a unit area of the target per second will be the product of the velocity and unit area. Hence the particle flux density

$$\phi = nv$$

The unit of particle flux density is particles/ $\text{m}^2 \cdot \text{s}$.

Radiation consisting of particles of a single kind and possessing identical energies is called *monoenergetic radiation*. The number of particles striking a target of area S per unit time is called the *particle flux* Φ . If the particle

flux density over an area S is constant, the particle flux will be $\Phi = \varphi S$. For example, if the area $S = 10 \text{ cm}^2$ and the particle flux density of a neutron beam $\varphi = 10^{17} \text{ neutr./m}^2 \cdot \text{s}$, the neutron flux will be

$$\Phi = 10^{17} \times 10^{-3} = 10^{14} \text{ neutr./s}$$

The *radiation intensity* I is defined as the energy of the radiation incident per unit time on a unit area perpendicular to the direction of propagation of the radiation. Some units of radiation intensity are the watt per square metre (W/m^2), mega-electronvolt per square metre per second ($\text{MeV/m}^2 \cdot \text{s}$).

The intensity expressed in $\text{MeV/m}^2 \cdot \text{s}$ units exceeds numerically that in W/m^2 by 6.25×10^{12} times:

$$I \text{ MeV/m}^2 \cdot \text{s} = 6.25 \times 10^{12} I \text{ W/m}^2$$

For monoenergetic radiation consisting of particles with kinetic energy E the particle flux density and radiation intensity are related by the simple formula

$$I = \varphi E$$

If the radiation consists of nonmonoenergetic particles the kinetic energy E in the formula should be replaced by the mean kinetic energy of the particles, \bar{E} ,

$$I = \varphi \bar{E}$$

In many cases the direction of motion of the particles is not unique. However as a rule the interaction between the particles and medium is independent of the direction of motion of the particles. Therefore for calculation of a number of quantities more general definitions of particle flux density and radiation intensity are introduced. The intensity of radiation $I(r)$ (or particle flux density $\varphi(r)$) at a point r is defined as the energy of the radiation (number of particles) entering in a unit time a sphere with a unit cross section and centre at the point r .

The definitions of the particle flux density and radiation intensity given above for a directed beam of radiation are particular cases of this definition.

The expression for the flux density of a nondirected beam of particles in terms of the particle density and velocity is similar to that for a beam of particles with a given direction.

In this case, however, the particle density n refers to all particles with velocity v moving in a unit volume along all possible directions.

Nonmonoenergetic radiation consists of particles with different energies. As an example, the electrons emitted in β^- -decay possess energies ranging from zero to E_e^{\max} . Nonmonoenergetic radiation is specified by the particle flux density $\psi(r, E)$ referred to a unit energy interval near energy E at the point r . It is briefly called the particle flux density for the energy E at point r and is measured in units $\text{part./m}^2 \cdot \text{s} \cdot \text{MeV}$. The particle flux density in a narrow energy interval dE between E and $E + dE$ is

$$\varphi(E, r) = \psi(E, r) dE$$

The total particle flux density at point r can be found by integrating with respect to energy:

$$\varphi(r) = \int_0^{\infty} \psi(E, r) dE$$

The intensity of nonmonoenergetic radiation in a narrow interval dE near energy E is

$$I(E, r) dE = \psi(E, r) E dE$$

and the total intensity of radiation at point r

$$I(r) = \int_0^{\infty} \psi(E, r) E dE$$

Usually radiation interacts with the medium over a finite time t . In order to characterize the radiation in this case the quantities *particle fluence* $F(r)$ and *integral intensity of radiation* $I_t(r)$ are introduced. They are defined as the number of particles (energy of radiation) entering a sphere with unit cross section and centre at point r during the time t . If the particle flux density $\varphi(r)$ is independent of time, the particle fluence $F(r) = \varphi(r) t$ and the integral intensity of radiation $I_t(r) = I(r) t$.

The particle fluence and integral radiation intensity are measured in particles per square metre (part./m^2) and megaelectronvolts per square metre (MeV/m^2) respectively.

If the particle flux density or radiation intensity vary with time the integral quantities are found by taking into account the time dependences:

$$F(r) = \int_0^t \varphi(r, t) dt; \quad I_t(r) = \int_0^t I(r, t) dt$$

5.2 Interaction Between Heavy Charged Particles and Matter

Heavy particles are defined as those whose mass exceeds by hundreds of times the electron mass. On passage through matter they interact predominantly with atomic electrons since the nucleus occupies a much smaller space in the atom. Hence the nucleus does not play a significant role in the slowing down of heavy particles.

Consider (Fig. 5.1) the interaction between a heavy particle (with velocity v , charge $q > 0$) with a free electron at rest and let us find the dependence of the energy lost by the particle on v and q .

On passing near an electron at rest the particle exerts a coulomb force whose absolute value is

$$F = b_0 q e / \epsilon r^2$$

where r is the distance in metres between the charges and depends on time; $b_0 = 9 \times 10^9 \text{ m/F}$ is a constant and ϵ is the relative dielectric constant of the medium, which shows how many times the interaction is weaker in the medium than in vacuum.

The coulomb force F acting on the electron (see Fig. 5.1) is directed along the radius r . It may be resolved into two components: $F = F_1 + F_2$. Force F_1 is parallel to the velocity v and force F_2 perpendicular to it. At points symmetric with respect to point O the absolute value of component F_1 is the same but the signs of F are opposite. Hence

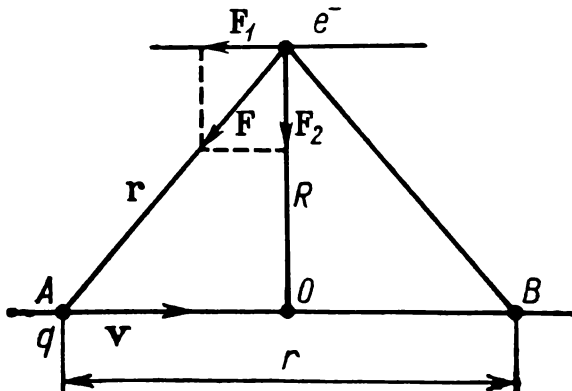


Fig. 5.1 Collision between a heavy charged particle and electron

deviations of the electron in the horizontal direction mutually compensate each other at symmetric points before and after point O and the electron is deflected as a result of the collision only in the vertical direction.

The coulomb force is inversely proportional to r^2 . It is significant only over a small part of the trajectory l located near point O . On this section the distance r is nearly constant and is approximately equal to R .

According to the law of conservation of momentum $m_e v_e = F_2 t$, where m_e and v_e are the electron mass and velocity respectively. The time of interaction between the particle and electron $t = l/v$. On section l , $F_2 \approx F$. The kinetic energy acquired by the electron in a time t is

$$E_e = \frac{m_e v_e^2}{2} = B \frac{q^2 l^2}{v^2 R^4}$$

where B is a proportionality coefficient. A positive charge attracts the electron which thus moves toward the particle trajectory. If the heavy particle is negative the electron will move away from the particle trajectory as a result of the collision. For identical velocities v and distances R an α -particle will lose 4 times more energy in a collision than a proton or deuteron. With increase of the velocity v the time t , and hence the energy loss of the particle in collision with an electron, will be smaller.

Actually electrons are not free in matter and are bound in the atoms. Hence only energies sufficient for the ionization or excitation of the atom may be imparted to the electron. As a consequence, for distances R exceeding some R_0 the particle effectively does not interact with a definite electron but rather with the atom as a whole. In this case an elastic collision between the particle and atom is said to occur. The distance R_0 at which the atom can still be excited depends on the atomic number Z , i.e. on the binding strength of the electrons in the atom.

The energy which a charged particle loses in inelastic (excitation or ionization) or elastic collisions with atoms is usually referred to as an ionization loss. It can be characterized by the specific ionization N_1 which is the number of ion pairs (electron plus positive ion) produced per unit path length of the particle in the medium. The

energy expended in the formation of an ion pair in a certain substance, e_1 , is on the average the same for various charged particles. This energy is called the *energy of formation of an ion pair*. Approximately half of the energy e_1 is spent in ionization and the other half in excitation and elastic collisions with the atoms (molecules). In air, for example, 36 eV are expended in the formation of an ion pair.

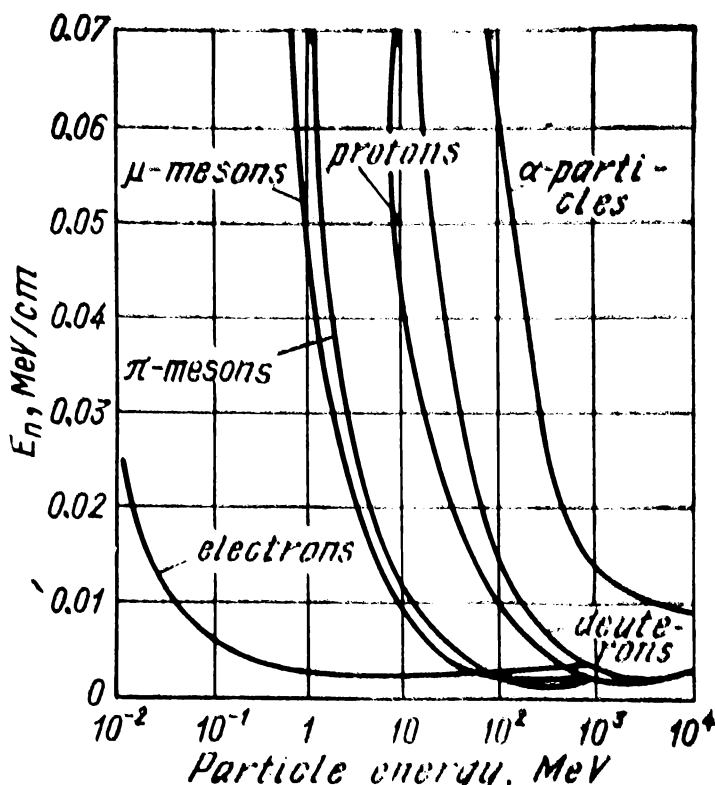


Fig. 5.2 Dependence of specific energy loss in air on the energy of a charged particle

The specific ionization can readily be determined on the basis of the specific energy loss E_1 which is the decrease in the kinetic energy of the particle per unit path length in the medium. The number of ion pairs per unit length is simply the specific energy loss divided by the energy of formation of an ion pair e_1 :

$$N_1 = E_1/e_1$$

The specific energy loss is also called the *stopping power* of the particular substance. It depends on the square of the particle charge and on the square of the particle velocity. It is also proportional to the number of electrons encountered

by the particle per unit length and hence to the density of atomic electrons of the substance N_a ,

$$E_i \sim N_a q^2/v^2$$

The dependences of the specific energy loss on particle energy are shown in Fig. 5.2 for mesons, protons, deuterons and α -particles moving through air. The curves have similar shapes but are shifted with respect to each other along the energy axis. With increase of particle energy the time of interaction with the electrons is shorter and hence the ionization losses are lower. The ionization losses begin to rise when the kinetic energy of the particle is about double its rest energy. The explanation is that the electric field of charged particles with velocities $v > 0.9c$ begins to deform and is stronger in the direction perpendicular to the particle trajectory. A result of this deformation of the electric field is that the range of action of the electric forces of the particle is greater and more electrons are acted on than at the lower velocities.

5.3 Range of Heavy Particles in Matter

A charged particle traverses a certain distance in matter prior to losing its kinetic energy. The total length of the path of a charged particle is called its *linear range* R . The linear range depends on the specific energy loss. The higher the density of the atomic electrons and the particle charge, the greater are the energy losses and hence the smaller is the range. Heavy charged particles mainly interact with the atomic electrons and are weakly deflected from the initial direction of motion. For this reason the range of a heavy particle can be measured by the distance between the particle source and point of stoppage.

A good idea as to how α -particles are slowed down in air can be obtained from the curve in Fig. 5.3 obtained in 1905 by the English physicist Bragg for monoenergetic α -particles with an initial energy of 7.68 MeV. With increase of the distance from the source the specific ionization of the particles slowly rises, then increases abruptly and further out begins to drop sharply. This type of behaviour can be explained by the variation of the particle velocity. The α -particle initially moves with a high velocity and the specific

ionization is correspondingly low. Due to the ionization losses the α -particle is slowed down and interacts a longer time with the electrons. Consequently the specific ionization increases. The ionization losses are particularly high near the end of the α -particle path. However, when the particle moves very slowly it begins to capture electrons from the orbits of the atoms of the medium and is transformed into a singly ionized and then neutral helium atom. As a result the ionization losses drop off very rapidly.

The α -particle flux density is almost independent of the distance of the particles from the source whereas the energy intensity of the α -particles decreases with increase of the distance from the source as a result of the ionization losses.

The interaction between α -particles and electrons is governed by statistical laws and hence there is a certain spread of the ranges (straggling). A small fraction of the α -particles have ranges exceeding somewhat those of the other particles.

The mean range of monoenergetic α -particles, R_α , can be calculated by empirical formulas. In air under normal conditions

$$R_\alpha = aE_\alpha^n \quad (5.1)$$

where R_α is the range in cm and E_α the kinetic energy of the α -particles in MeV. For α -particles emitted by natural α -emitters ($4 < E_\alpha < 9$ MeV), $a = 0.318$, $n = 1.5$. For α -particles with higher energies ($E_\alpha \leq 200$ MeV), $a = 0.148$, $n = 1.8$. Thus for α -particles with an energy $E_\alpha = 5$ MeV the distance covered is 3.51 cm; for an energy $E_\alpha = 30$ MeV, $R_\alpha = 68$ cm.

The ratio of the linear ranges of two different types of particles possessing identical initial velocities in air is

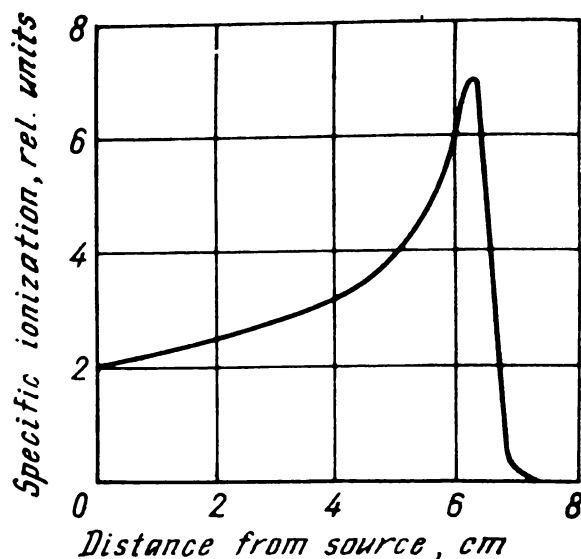


Fig. 5.3 Variation of specific ionization on slowing down of an α -particle in air (Bragg curve)

proportional to the ratio of the specific energy losses of the particles,

$$\frac{R_1}{R_2} = \frac{m_1}{m_2} \left(\frac{q_2}{q_1} \right)^2 \quad (5.2)$$

where m_1 and m_2 are the particle masses and q_1, q_2 the particle charges.

Example. Determine the linear range of a proton with an energy $E_p = 10$ MeV in air.

We shall first find the kinetic energy of an α -particle possessing the same initial velocity as the proton:

$$\frac{E_p}{E_\alpha} = \frac{m_p v_p^2}{m_\alpha v_\alpha^2} = \frac{m_p}{m_\alpha} \approx \frac{1}{4}$$

The linear range of α -particles with an energy $E_\alpha = 40$ MeV in air is

$$R_\alpha = 0.148 E_\alpha^{1.8} = 114 \text{ cm}$$

The linear range of a proton with an energy $E_p = 10$ MeV (see formula (5.2)) is

$$R_p = \frac{1}{4} \left(\frac{2}{1} \right)^2 R_\alpha = 114 \text{ cm}$$

Capture of electrons by moving fission fragments, in contrast to charge exchange involving α -particles, occurs over the whole range of the fragment and not only at the end. The fragment fills its electron shells by capturing electrons from the medium and thus decreases its charge. The linear range in air R_f of a fission fragment with a mass number A under normal conditions can be calculated by the formula

$$R_f \approx 4 - 1.35 \times 10^{-2} A \text{ cm}$$

Fission fragments with a mass number $A = 120$ travel a distance in air $R_f \approx 2.4$ cm. In solids the linear range of a fission fragment is approximately 10^3 to 10^4 times smaller than in air.

In experimental physics the *mass range* of a charged particle, R_m , expressed in kilograms per square metre (kg/m^2) is frequently employed instead of the linear range. Numerically the mass range is equal to the mass of matter in a cylinder whose height is equal to the linear range of

the particle in metres, R , and cross section is 1 m^2 ,

$$R_m = \rho R \quad (5.3)$$

where ρ is the density of the matter in kg/m^3 .

An empirical formula for the mass range of α -particles with energies lying between 4 and 9 MeV is

$$R_{m\alpha} = \sqrt{AE_\alpha^s} \text{ g/m}^2 \quad (5.4)$$

where A is the mass number of matter and E_α is the α -particle energy in MeV.

Example. Find the mass and linear ranges of α -particles with an energy $E_\alpha = 5 \text{ MeV}$ in beryllium ($A = 9$, $\rho = 1800 \text{ kg/m}^3$).

According to formula (5.4) the mass range

$$R_{m\alpha} = \sqrt{9 \times 125} = 33.5 \text{ g/m}^2$$

According to formula (5.3) the linear range

$$R_\alpha = 33.5 \times 10^{-3} / 1800 = 1.85 \times 10^{-5} \text{ m} = 18.5 \mu\text{m}$$

5.4 Interaction Between β -Particles and Matter

The energy losses of electrons moving in matter may be divided into ionization and radiative losses.

The energy dependence of the specific ionization losses for electrons is similar to that for heavy charged particles (see Fig. 5.2). The energy loss curve decreases with increase of the velocity up to kinetic energies equal to about twice the electron rest energy and then begins to rise slowly.

Radiative energy losses occur as a result of acceleration of a free charged particle in the electric field of a nucleus. On passing near the nucleus the particle is deflected by the coulomb force $F = b_0 Ze^2 / \epsilon r^2$. This force is also related to the particle mass m and its acceleration a in accordance with Newton's second law, $F = ma$. Any free charge moving with acceleration a emits photons whose total energy is proportional to the square of the acceleration. Since $a^2 = F^2 / m^2$, i.e. $a^2 \sim 1/m^2$, the radiative losses of heavy charged particles will be considerably lower than those of light charged particles (electrons or positrons). Thus the radiative losses of electrons exceed those of protons subject-

ed to the same force by $(m_p/m_e)^2 = 3.5 \times 10^6$ times. Radiative losses of heavy particles are insignificant compared to ionization losses up to very high particle energies and usually are not taken into account. However the radiative losses of light particles may be appreciable, particularly on passage through media with high atomic numbers Z .

The radiation emitted as a result of radiative losses is called *bremsstrahlung*. This is the radiation produced by the deceleration of charged particles in the electric field of a nucleus. Bremsstrahlung is also emitted by electrons moving in circular orbits in electron accelerators (betatrons and synchrotrons). The radiation in these cases is therefore called *betatron* and *synchrotron radiation*.

The specific radiative losses E_r are proportional to the electron energy E_e and square of the atomic number of the medium:

$$E_r \sim Z^2 E_e$$

Ionization losses of electrons E_i predominate at comparatively low energies. With increase of kinetic energy the relative contribution of the ionization losses to the total energy loss diminishes. Since $E_i \sim Z$, the ratio of the specific radiative to ionization losses, k , is proportional to ZE_e ,

$$k = 1.25 \times 10^{-3} Z E_e$$

where E_e is expressed in mega-electronvolts.

The electron energy for which $E_i = E_r$ ($k = 1$) is called the *critical energy*. For iron ($Z = 26$) the critical energy is 31 MeV and for lead ($Z = 82$) approximately 9.8 MeV. Above the critical energy radiative losses exceed the ionization losses. Thus in iron the radiative energy losses of 100 MeV electrons exceed the ionization losses by 3.25 times and in lead by 10.2 times.

Bremsstrahlung radiation with frequencies in the X-ray range is obtained in special X-ray tubes with a high vacuum and heavy anticathode. It is applied in medicine for diagnostics of diseases. The electrons in the tubes are accelerated up to 30-100 keV (1 keV = 10^3 eV) and then stopped by the heavy anticathode. The X-rays emitted on deceleration of the electrons possess a continuous spectrum.

The electron mass is much smaller than that of heavy particles and this determines the character of their motion in matter. Electrons are strongly deflected on colliding with atomic electrons or nuclei. They do not move along a straight line as heavy particles do but in a tortuous path. The total path length of electrons greatly exceeds the ranges of heavy charged particles. Of practical interest, however, is the effective electron range. This is the thickness of a layer of matter which completely stops the electron. The effective mass range of electrons R_{me} in aluminium can be found by the empirical formulae

$$\left. \begin{aligned} R_{me} &= 5.43E_e - 1.60, \text{ for } 1.0 \leq E_e \leq 2.5 \text{ MeV} \\ R_{me} &= 5.30E_e - 1.06, \text{ for } E_e \geq 2.5 \text{ MeV} \end{aligned} \right\} \quad (5.5)$$

where R_{me} is in kg/m^2 and E_e is the maximum β -particle energy or the energy of monoenergetic electrons in MeV units. Formulae (5.5) may be used with an accuracy to about 10% for estimation of R_{me} in air and iron.

Example. Find the thickness of an aluminium layer absorbing electrons with an energy 2 MeV.

The density of aluminium is 2700 kg/m^3 . According to the first of formulae (5.5)

$$R_{me} = 5.43 \times 2 - 1.60 = 9.26 \text{ kg/m}^2$$

$$R_{Al} = R_{me}/\rho_{Al} = 9.26/2700 = 3.43 \times 10^{-3} \text{ m} = 0.343 \text{ cm}$$

Fast positrons lose their energy just as electrons do by ionizing and emitting bremsstrahlung. The slowed down positrons can pull out electrons from the outer shells of the atom since they are more weakly bound than the inner electrons. The electron-positron pair may form the lightest of hydrogen-like atoms, which is called *positronium*. In such atoms the electron and positron revolve around a common centre of mass. The lifetime of positronium is of the order of a billionth of a second after which the positron and electron annihilate to produce two or three γ -quanta. The total energy of the γ -quanta is 1.02 MeV which is twice the rest energy of an electron. Electrons and positrons may also annihilate without forming positronium. The radiation produced in electron-positron annihilation is called *annihilation radiation*.

5.5 Interaction Between Electromagnetic Radiation and Matter

Law of attenuation of radiation in matter. X-rays, betatron, synchrotron and gamma-radiations are electromagnetic waves and their behaviour depends on their frequency. They are identical if their frequencies are the same. Thus it will be sufficient to consider the interaction between gamma radiation and matter. The properties of the other radiations in the same frequency range are identical.

Gamma radiation is a strongly penetrating radiation. On passing through matter γ -quanta interact with the atoms,

electrons and nuclei and their intensity is attenuated.

The attenuation law for a parallel monoenergetic beam of primary γ -quanta striking a plane target will be considered. By definition *primary particles* are those which did not interact with the electrons, nuclei or atoms on passage through matter.

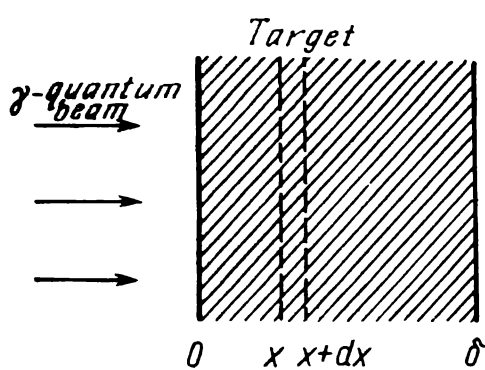


Fig. 5.4 Beam of γ -quanta incident on a plane target

Let a parallel (collimated) beam of γ -quanta be incident on a plane target at right angles (Fig. 5.4). The intensity of the primary beam is diminished as a result of absorption and scattering of the γ -quanta. A γ -quantum scattered by an electron loses part of its energy and changes its direction of motion. At a distance x from the front surface the flux density of the primary γ -quanta is reduced to a value $\varphi(x)$. In a thin layer of the target, dx , the γ -quantum flux density is reduced from $\varphi(x)$ to $\varphi(x+dx)$. Since the thickness of the layer is assumed to be small the difference between the flux densities $\varphi(x)$ and $\varphi(x+dx)$ is not great. Under these conditions the number of interactions between the γ -quanta and matter in the thin layer is proportional to the flux density $\varphi(x)$ at the surface of the layer and to the layer thickness dx ,

$$d\varphi = -\mu\varphi dx \quad (5.6)$$

The minus sign in the right-hand part of the equation shows that the flux density of the γ -quanta is decreased by $d\phi$ in the layer dx . The proportionality coefficient μ is called the *total linear attenuation coefficient*. Its dimension is m^{-1} and numerically the coefficient is equal to the fraction of monoenergetic γ -quanta removed from the parallel beam per unit length in the material. The value of μ depends on the density and atomic number of the material as well as on the energy of the γ -quanta,

$$\mu = \mu (\rho, Z, E_\gamma)$$

The solution of a differential equation similar to (5.6) was considered in Sec. 4.3. If ϕ_0 denotes the γ -quantum flux density at the front surface of the target, the attenuation law for a parallel beam of monoenergetic primary γ -quanta passing through matter may be expressed by the formula

$$\phi (x) = \phi_0 e^{-\mu x} \quad (5.7)$$

The value of μ is equal to $1/d$, where d is the thickness of a layer of material which reduces the γ -quantum flux density by $e = 2.72$ times. For practical purposes a more convenient quantity is the half-value thickness $d_{1/2}$. This is the thickness of a layer of matter which reduces the flux density by two times. The relationship between μ and $d_{1/2}$ is the same as that between the half-life and the decay constant,

$$\mu = 0.693/d_{1/2}$$

The total linear attenuation coefficient is proportional to the density of the material. If we divide μ by the density of the material we obtain the *mass attenuation coefficient* $\mu_m = \mu/\rho$, which is measured in square metres per kilogram (m^2/kg). This is the fraction of monoenergetic γ -quanta removed from the beam on passage through a target layer thickness of 1 kg/m^2 . The coefficient μ_m depends on the atomic number of the material and on the γ -quantum energy,

$$\mu_m = \mu_m (Z, E_\gamma)$$

After substituting $\mu = \mu_m \rho$ the attenuation law (5.7) assumes the form

$$\phi (x) = \phi_0 e^{-\mu_m M_x} \quad (5.8)$$

where $M_x = \rho x$ is the mass of a target of area 1 m² and thickness x .

Example. Calculate: (a) the half-value thickness for a parallel beam of $E_\gamma = 1$ MeV γ -quanta in lead ($Z = 82$) and aluminium ($Z = 13$); (b) the mass of lead and aluminium layers (in kilograms per square metre) which diminish the beam flux density by two times.

The total linear attenuation coefficients $\mu_{\text{Pb}} = 80 \text{ m}^{-1}$, $\mu_{\text{Al}} = 15 \text{ m}^{-1}$ and densities $\rho_{\text{Pb}} = 11\,340 \text{ kg/m}^3$, $\rho_{\text{Al}} = 2700 \text{ kg/m}^3$.

The half-value thickness is
for lead

$$d_{1/2} = 0.693/\mu_{\text{Pb}} = 0.693/80 \approx 8.65 \times 10^{-3} \text{ m}$$

for aluminium

$$d_{1/2} = 4.6 \times 10^{-2} \text{ m}$$

The mass attenuation coefficient is
for lead

$$\mu_m = \mu/\rho = 80/11\,340 \approx 7 \times 10^{-3} \text{ m}^2/\text{kg}$$

for aluminium

$$\mu_m = 5.55 \times 10^{-3} \text{ m}^2/\text{kg}$$

The mass of a lead target which reduces the beam flux density two times is

$$M_{\text{Pb}} = \rho_{\text{Pb}} d_{1/2} = 11\,340 \times 8.65 \times 10^{-3} = 98.7 \text{ kg/m}^2$$

of aluminium target

$$M_{\text{Al}} = 12.4 \text{ kg/m}^2$$

The removal of γ -quanta from a beam is due to three major and independent processes: to the photoelectric effect, Compton effect and pair production. These effects involve the interaction of γ -quanta with atoms, electrons or nuclei respectively. Consequently the total linear attenuation coefficient is equal to the sum of three independent linear coefficients: that due to photoelectric absorption μ_{ph} , to Compton interaction μ_C and to pair production μ_{pp} .

$$\mu = \mu_{\text{ph}} + \mu_C + \mu_{\text{pp}}$$

Each of these coefficients depend in their own specific way on the atomic number and energy of the γ -quantum.

Photoelectric effect. This is a type of interaction between a γ -quantum and atom in which the γ -quantum is absorbed (disappears) and an electron is ejected from the atom. Part of the energy of the γ -quantum, E_γ , is spent in breaking the bond between the electron and nucleus and the other part is imparted to the electron as kinetic energy E_e ,

$$E_\gamma = E_e + e_e^{(n)}$$

The photoelectric effect involving an electron in some n th atomic shell occurs only if the energy of the γ -quantum exceeds the binding energy of the electron in the shell, $e_e^{(n)}$. If the γ -quantum energy is smaller than the binding energy of an electron in, say, the K -shell but greater than that in the L -shell, the photoelectric effect may take place in all shells of the atom besides the K -shell.

The direction of the photoelectron is almost perpendicular to the direction of propagation of the absorbed γ -quantum (Fig. 5.5) and almost coincides with the direction of the electric intensity vector of the electromagnetic field. This signifies that photoelectrons are ejected from the atom by electric forces.

Photoelectric absorption of γ -quanta in an n th shell decreases with growth of the γ -quantum energy. It is maximum for an energy E_γ close to the binding energy $e_e^{(n)}$. For energies $E_\gamma \gg e_e^{(n)}$ the probability for photoelectric absorption in the n th shell is reduced by thousands of

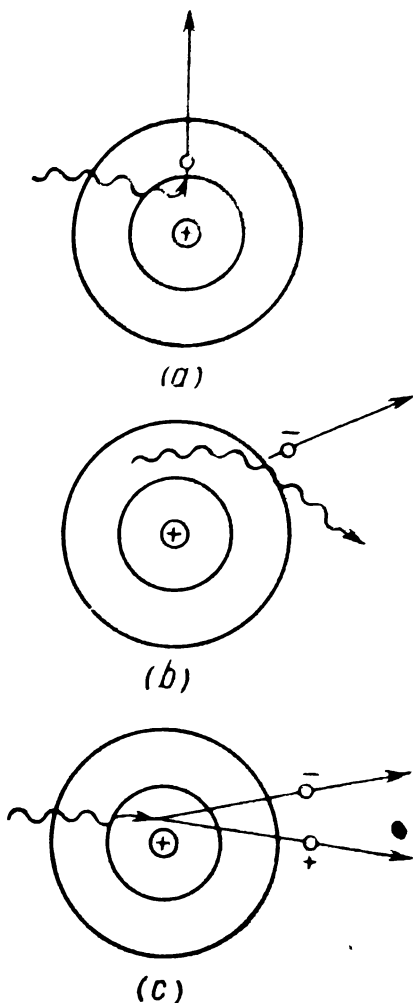


Fig. 5.5 Main modes of interaction between γ -quanta and matter

a—photoelectric effect; b—Compton effect; c—pair production

times. It might be mentioned that a free electron cannot absorb a γ -quantum since the laws of conservation of energy and momentum would then be violated.

The linear coefficient of photoelectric absorption μ_{ph} is proportional to the ratio Z^5/E_γ^3 .⁵ The dependence of coefficient μ_{ph} on γ -quantum energy in lead is shown in Fig. 5.6. It drops off rapidly with increase of the energy and for $E_\gamma > 10$ MeV practically no photoelectrons arise in lead.

Compton effect. The scattering of γ -quanta by atomic electrons is called the *Compton effect*. The interaction

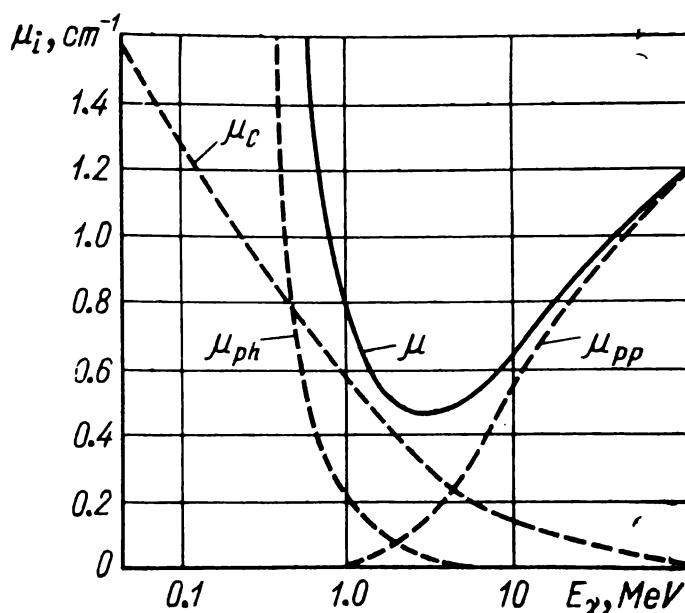


Fig. 5.6 Dependence of linear attenuation coefficient on γ -quantum energy in lead

μ —total; μ_{ph} —photoelectric absorption; μ_C —Compton interaction; μ_{pp} —pair production

between the γ -quantum and electron in the Compton effect is viewed as the collision of two elastic spheres (see Fig. 5.5) with masses $m_\gamma = h\nu/c^2$ and m_e . In each elastic collision the γ -quantum transmits part of its energy to the electron and is scattered. Since the scattering of the γ -quanta depends on the density of the atomic electrons $N_e \sim Z$, the Compton effect is dependent on the atomic number Z of the material. Scattering of the γ -quanta takes place mostly as a result of interaction with weakly bound electrons of the outer shells. The linear Compton interaction coefficient μ_C is proportional to Z/E_γ . Hence with increase of quantum energy the fraction of γ -quanta scattered decreases.

In lead the Compton effect supersedes the photoelectric effect at energies $E_\gamma > 0.5$ MeV (see Fig. 5.6). The decrease of the coefficient μ_C with increasing energy is more gradual than of μ_{ph} and more Compton electrons are produced in lead at $E_\gamma > 0.5$ MeV than photoelectric electrons. At energies above 50-100 MeV the Compton effect is insignificant.

Pair production. A γ -quantum in the field of a nucleus may produce a pair of particles and in particular an electron and positron (see Fig. 5.5). The energy of the γ -quantum is transformed into the rest energy of the electron and positron $2m_e c^2$, into their kinetic energy E_{e+} , E_{e-} and into the kinetic energy of the nucleus E_n ,

$$h\nu = 2m_e c^2 + E_{e+} + E_{e-} + E_n$$

The particle pair is formed only if the γ -quantum energy is greater than twice the rest energy of the electron which is 1.02 MeV. The γ -quantum cannot be transformed into a particle pair outside the bounds of the nucleus since this would be a violation of the law of conservation of momentum. Conceivably a 1.02 MeV γ -quantum could create an electron and positron but their momentum would be zero whereas that of the γ -quantum is $h\nu/c$.

In the field of a nucleus the momentum and energy of a γ -quantum are distributed between the electron, positron and nucleus without violation of the laws of conservation of energy and momentum. The nuclear mass greatly exceeds the electron and positron masses and hence a very insignificant part of the energy is transmitted to the nucleus. Practically all energy of the γ -quantum is transformed into energy of the electron and positron.

The linear pair production coefficient μ_{pp} is proportional to $Z^2 \ln E_\gamma$. Pair production is appreciable in heavy substances at high γ -quantum energies. The coefficient μ_{pp} is not zero only at energies exceeding the threshold energy $E_\gamma = 1.02$ MeV. With increase of energy μ_{pp} rapidly rises. Beginning at 8 MeV most of the absorption of the γ -quanta is due to pair production.

The total linear attenuation coefficient μ is the sum of the three coefficients μ_{ph} , μ_C and μ_{pp} and hence with increase of the quantum energy it decreases (see Fig. 5.6) reaching

a minimum at 3 MeV after which it begins to increase. This type of dependence is due to the fact that at low energies $\mu(E_\gamma)$ is determined by the photoelectric effect and Compton effect and at energies exceeding 8 MeV the main contribution to μ is from the pair production process. Lead is most transparent to γ -quanta with energies of about 3 MeV. A similar dependence of $\mu(E_\gamma)$ is also observed in other heavy elements.

Energy transfer coefficient. The energy of gamma radiation interacting with matter is transformed into the kinetic energy of electrons and into the energy of secondary γ -radiation (which includes the X-rays emitted in the photoelectric effect, γ -quanta scattered in the Compton effect and annihilation radiation). The coefficient μ may thus be expressed as the sum

$$\mu = \mu_a + \mu_s$$

The coefficient μ_a is called the *linear energy transfer coefficient*. It is equal to the fraction of energy of the γ -radiation which is transferred to the electrons liberated in a layer of matter of unit thickness. The fraction of energy of the γ -radiation which is transformed into the energy of secondary γ -radiation in a unit layer of matter is referred to as the *linear scattering coefficient* μ_s . Coefficient μ_a is of great importance in radiation dosimetry (see Sec. 5.6) since the absorbed radiation dose is proportional to the radiation intensity and coefficient μ_a of the material irradiated. The mass energy transfer coefficient for air (Table 5.1) varies only slightly in the 0.2 to 1.5 MeV energy range.

Table 5.1

Mass Energy Transfer Coefficient for Air

E_γ , MeV	μ_{am} , m^2/kg	E_γ , MeV	μ_{am} , m^2/kg	E_γ , MeV	μ_{am} , m^2/kg
0.05	0.384	0.40	0.296	4.0	0.194
0.08	0.236	0.60	0.296	6.0	0.172
0.10	0.233	1.0	0.280	8.0	0.160
0.15	0.251	1.5	0.256	10.0	0.153
0.30	0.288	3.0	0.211		

In γ -radiation dosimetry complex substances are characterized by an effective atomic number Z_{eff} . This is the atomic number of such an element for which the energy transfer coefficient referred to an electron of the element is the same as that of the given substance. Thus the values of Z_{eff} for water, air and living tissues are almost the same and close to 7.5.

Attenuation by distance. The attenuation of the flux density of primary γ -quanta occurs not only as a result of absorption or scattering in the medium. If a point source is placed in vacuum the γ -quantum flux density will decrease with increase of the distance from the source. A source is considered to be a point source if its size is one-fourth of the distance between the source and the observation point.

Suppose a source in vacuum emits isotropically (uniformly in all directions) Q γ -quanta per second. The total number of quanta should be the same at any distance from the source. Hence the γ -quantum flux density at a distance r from the source, $\varphi(r)$, passing through the surface of a sphere of area $S = 4\pi r^2$ is

$$\varphi(r) = Q/4\pi r^2$$

The ratio of the flux densities at spherical surfaces with radii $r = R$ and $r = 1$ cm

$$\varphi(R)/\varphi_0 = 1/R^2 \quad (5.9)$$

where φ_0 is the γ -quantum flux density at a distance $r = 1$ cm from the source. With increase of the distance from a point source the γ -quantum flux density in vacuum diminishes as $1/R^2$.

If a point source is located in a medium, attenuation of the flux density of a beam of monoenergetic γ -quanta and of the intensity will also be affected by interaction of the quanta with the material of the medium and thus

$$\varphi(R) = \varphi_0 e^{-\mu R}/R^2 \quad (5.10)$$

Accumulation factor. The laws expressed by formulae (5.7) and (5.10) are valid for attenuation of the primary γ -radiation. The contribution of scattered radiation to the intensity is not taken into account by these formulae.

Scattered γ -quanta after multiple collisions with the electrons may leave the absorbing medium. Both primary and scattered γ -quanta may pass through some point A located behind the protective layer (Fig. 5.7). The total

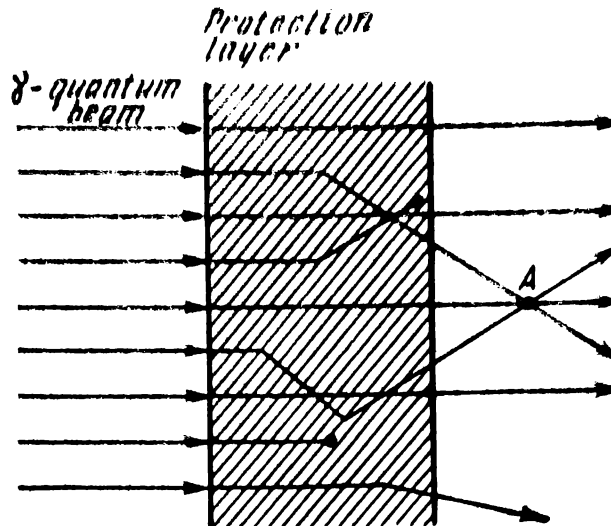


Fig. 5.7 Passage of a collimated γ -quantum beam through a layer of matter

intensity of the radiation at point A is therefore the sum of the intensities of the primary I_p and scattered I_s radiations,

$$I = I_p + I_s$$

The ratio of the total intensity to the intensity of the primary radiation is called the *accumulation factor* B ,

$$B = I/I_p$$

It takes into account the contribution of scattered γ -quanta to the intensity.

The intensity and flux density of the primary radiation are proportional to each other. Thus from the latter relationship and formulae (5.7) and (5.10) it follows that

$$I(R) = BI_0 e^{-\mu R} / R^n$$

where the exponent n is zero for an extended plane source and two for a point γ -quantum source.

The accumulation factor is usually determined experimentally. It depends on the geometry of the source, on the

energy of the primary γ -quanta, on the absorbing and scattering properties of the material and its thickness. In the tables the accumulation factor for a given geometry is usually presented as a function of the product $\mu\delta$ where δ is the thickness of the protective layer. Thus the value of B for lead surrounding a point source of 1 MeV γ -quanta varies between 1.35 ($\mu\delta = 1$) and 5.25 ($\mu\delta = 20$).

5.6 Radiation Doses

The personnel working in atomic stations or manipulating radioactive preparations can be subjected to irradiation by γ -quanta, neutrons, electrons or other particles. The ionization produced in living tissues by the radiations evoke a biological effect in the human organism.

The degree of irradiation of any material can be characterized by the *absorbed radiation dose D* (or briefly, *radiation dose* or simply *dose*). This is defined as the energy of the radiation absorbed by a kilogram of the material. The unit of radiation dose is the rad. It equals a radiation dose such that 1 kg absorbs an energy of 10^{-2} J. In the SI system the unit of radiation dose is the gray: 1 Gr = 100 rads.

It is practically impossible to measure directly the γ -radiation dose in a living tissue. However the absorption of γ -radiation in matter, including living tissues, depends on the effective atomic number Z_{eff} . Materials which have values of Z_{eff} close to that of tissue are called tissue-equivalent materials. They are used to measure the γ -radiation dose in a tissue.

The easiest way to determine the radiation dose is to measure the ionization produced in air which is a tissue-equivalent substance. It has been found that about 36 eV of the radiation energy must be expended to ionize an air molecule. By measuring the ionization in the air it is simple to determine the radiation dose.

Since the γ -radiation dose is measured on the basis of the ionization it produces, in practical dosimetry the so-called *exposure dose* is usually employed. The unit in this case is the roentgen (R) which is the dose of X-rays or γ -radiation that produces in 1 cm³ of air at 0 °C and a pressure of 760 mm Hg ions of one sign carrying a charge of

3.33×10^{-10} C. Referred to the absorbed dose in air 1 R = 0.89 rad and in living tissue 1 R = 0.93 rad. Thus a 1 R dose is slightly smaller than a dose of 1 rad. The exposure dose is convenient for all practical purposes since the ionization in air can easily be measured with an ionization chamber.

The biological effect of radiation on living tissue depends not only on the ionization but also on the specific ionization. Equal doses of protons, α -particles and neutrons evoke a much greater biological effect than those of X-rays or γ -radiation.

The biological effect caused by prolonged irradiation of the human body is taken into account by the radiation *quality factor* Q (Table 5.2). It shows how many times the

Table 5.2
Radiation Quality Factor

Type of radiation	Q	Type of radiation	Q
X- and γ -rays	1	Neutrons with energies:	
β	1	5 keV	2.5
Protons ($E_p \leq 10$ MeV)	10	20 keV	5
α ($E_\alpha \leq 10$ MeV)	10	100 keV	8
Heavy recoil nuclei	20	500 keV	10
Thermal neutrons	3	1 MeV	10.5
		5 MeV	7.0
		10 MeV	6.5

biological effect of some given type of radiation exceeds the effect evoked by γ -radiation of the same dose.

The product of the absorbed dose D for a given type of radiation by the quality factor Q is the *equivalent dose*,

$$D_{eq} = QD$$

The unit of the equivalent dose is rem (*roentgen equivalent man*) which is defined as the amount of radiation that causes the same biological effect as a dose of 1 rad of X-rays or γ -radiation.

The radiation dose referred to a unit time is called the *dose rate*. If the dose conveyed to the medium during a period

of time from t_1 to t_2 is D , the mean dose rate will be

$$W = D/(t_2 - t_1)$$

The biological effect of radiation on organisms also depends on the dose rate. For identical radiation doses the biological effect is the greater the smaller the time interval $t_2 - t_1$. Because of this not only the radiation dose but the dose rate as well are monitored in nuclear energy installations.

A *maximum permissible dose* (MPD) has been set up for personnel working in an irradiation field. It has been chosen so that the annual level of uniform irradiation over a period of 50 years does not evoke any unfavourable changes in the health of the irradiated person or in its progeny. This condition has led to a MPD of 5 rem/year or 100 mrem per working week.

The maximum permissible dose rate

$$W_{mp} = 100/t \text{ mrem/h}$$

where t is the length of the working week in hours. If $t = 36$ h then $W_{mp} = 2.8$ mrem/h.

The maximum permissible doses for internal irradiation have been chosen on the same basis as those for external irradiation. The biological effect of an internal source depends on the chemical properties of the material of the source, on its half-life, type of radiation emitted and energy of the radiation. The chemical properties affect the distribution of radioactive atoms in the organism and the time required for their discharge from the organism. Mean annual permissible concentrations (APC) of radioactive substances in the air in working rooms, in outside air or in water have also been established. The APC predetermine the annual maximum permissible uptake (MPU) of radioactive substances by the human body. If the concentration of radioactive substances in the air of a working room is constant, the MPU ($\mu\text{Ci}/\text{y}$) and APC (Ci/l) are related by the formula

$$\text{MPU} = 2.5 \times 10^{12} \text{ APC}$$

The APC depends on the properties of the radioactive substance. Thus for ^{239}Pu and ^{131}I the APC in working

rooms are 1.7×10^{-16} and 1.0×10^{-10} Ci/l respectively. In the outside air and in water the APC is smaller by several orders of magnitude than that accepted for working rooms.

In order to lower the radiation dose to the MPD, radiation protection is employed. For this purpose a protective shield is used. The shield is made of substances which strongly absorb radiations. Radioactive substances in the air are removed by the ventilation system.

5.7 Characteristics of γ -Radiation Sources

After α - and β -decays of radioactive substances the product nuclei may be in the excited state. Such substances are sources of γ -radiation (γ -sources). Gamma sources are characterized by their half-lives, activities and γ -quantum spectra (γ -spectra). The latter are discrete (line) spectra. The number of lines in a spectrum may vary between one and several dozens. Thus about 50 lines are observed in the γ -spectrum of ^{226}Ra in radioactive equilibrium with its major decay products. In most complex γ -spectra a few lines are particularly intense. In the ^{226}Ra γ -spectrum, for example, six such lines with energies between 0.3 and 1.76 MeV are observed; in the ^{24}Na spectrum there are two intense γ -lines with energies of 1.37 and 2.75 MeV.

The sizes d of γ -sources are usually small. At distances $r \geq 4d$ the γ -source may be regarded with sufficient accuracy as a point source and its size d may be neglected in various problems. Moreover point γ -sources are isotropic sources which emit γ -quanta in various directions with an equal probability.

The radioactive substance is contained in an air-tight ampule with metal walls which alter the spectrum of the γ -rays. The walls and also materials used specially for absorption of part of the γ -lines are called filters.

The exposure dose rate in air produced by an isotropic point source can be characterized by its *ionization γ -constant* K_γ . The gamma constant is the exposure dose rate (R/h) of unfiltered γ -radiation from an isotropic point γ -source of activity of 1 mCi at a distance of 1 cm from the source. K_γ is measured in $\text{R} \cdot \text{cm}^2/\text{h} \cdot \text{mCi}$. It can be determined from the decay diagram of the radioactive nucleus or mea-

sured experimentally and is usually presented in the manuals (Table 5.3).

Filtering of γ -radiation reduces the value of K_γ to a certain $K_\gamma(\delta)$, where δ is the filter thickness. The change

Table 5.3

Ionization γ -Constants and γ -Equivalents of Some Radioactive Substances

Substance	$T_{1/2}$	$K_\gamma, \frac{R \cdot \text{cm}^2}{\text{h} \cdot \text{mCi}}$	γ -Equivalent of 1 mCi of material, mg-eq Ra
^{24}Na	14.9 h	18.55	2.20
^{60}Co	5.27 y	12.93	1.54
^{75}Se	127 d	1.84	0.23
^{134}Cs	2.2 y	8.58	1.02
^{226}Ra	1622 y	9.36	1.11

in K_γ is taken into account in calculations by a correction factor α which is less than one, i.e. $K_\gamma(\delta) = \alpha K_\gamma$. For lead, iron and aluminium capsules of 0.1-0.3 cm thickness the value of α varies between 0.85 and 0.98 for γ -quantum energies $E_\gamma > 1$ MeV. The values of K_γ cited in the manuals in the case of unfiltered radiation overestimate the dose and thickness of the protective shield.

Calculation of the exposure dose rate at a distance r from an unprotected point γ -source $W(R)$ is considerably simplified by using K_γ . Since the γ -radiation intensity, according to formula (5.9), is proportional to $1/R^2$, we get

$$W(R) = a K_\gamma / R^2 \quad (5.11)$$

where $W(R)$ is the exposure dose rate in R/h, a is the γ -source activity in mCi and R is the distance from the γ -source in cm.

In dosimetry γ -sources are frequently compared on the basis of the ionization they produce in air. Two radioactive substances which produce under identical measurement conditions equal exposure dose rates are said to have equal γ -equivalents. The γ -equivalent is measured in milligram equivalents of radium (mg-eq Ra). This unit is equal to the

amount of radioactive substance whose γ -radiation for the given filtration and identical measurement conditions produces the same exposure dose rate as the γ -radiation from a milligram of radium does on passing through a 0.5 mm thick platinum filter.

The exposure dose rate due to a point source with a γ -equivalent of 1 mg-eq Ra at a distance of 1 cm is 8.4 R/h. The γ -equivalent of a substance, m (mg-eq Ra), is related to its activity a (mCi) and K_γ (R·cm²/h·mCi) by the formula $m = aK_\gamma/8.4$. Substituting $aK_\gamma = 8.4m$ into formula (5.11) we get

$$W(R) = 8.4m/R^2 \quad (5.12)$$

where $W(R)$ is the exposure dose rate in R/h, m is the γ -equivalent of the substance in mg-eq Ra and R is the distance from the source in air (in cm).

Example. At what distance R from a ⁶⁰Co point source with a mass 10^{-6} g is the dose during a 6 hour working day equal to the MPD? Calculate the γ -equivalent of the material.

According to formula (1.1) the number of atoms in 10^{-6} g of ⁶⁰Co is

$$N = \frac{1.0 \times 10^{-6}}{60} \times 6.02 \times 10^{26} = 1.0 \times 10^{18} \text{ atoms}$$

The activity of cobalt ($T_{1/2} = 5.27$ years)

$$a = \lambda N = \frac{0.693}{5.27 \times 3.15 \times 10^7} \frac{1.0 \times 10^{18}}{3.7 \times 10^7} = 1.13 \text{ mCi}$$

The maximum permissible dose rate for a six hour working day $W_{mp} = 2.8 \times 10^{-3}$ rem/h. Since K_γ (⁶⁰Co) = 12.93 R·cm²/h·mCi, we find from formula (5.11)

$$R = \sqrt{aK_\gamma/W_{mp}} = \sqrt{1.13 \times 12.93/2.8 \times 10^{-3}} \approx 72 \text{ cm}$$

The γ -equivalent of the radioactive substance

$$m = aK_\gamma/8.4 = 1.13 \times 12.93/8.4 \approx 1.74 \text{ mg-eq Ra}$$

5.8 Calculation of Protective Shields for Point γ -Sources

The exposure dose from a point γ -source can be reduced to the MPD by various ways: by increasing the distance between the source and working site, by enclosing the source in a protective shield, by reducing the working time etc.

It is quite easy to calculate the thickness of a protective shield for a given degree of attenuation by using suitable universal tables or the data in handbooks on radiation protection. An example of the table used is Table 5.4.

Table 5.4

Thickness of Protective Shields, cm

Attenuation ratio K_0	Lead ($\rho = 11.34 \text{ g/cm}^3$ for $E_\gamma =$)			Iron ($\rho = 7.89 \text{ g/cm}^3$ for $E_\gamma =$)			Concrete ($\rho = 2.3 \text{ g/cm}^3$ for $E_\gamma =$)		
	1 MeV	2 MeV	3 MeV	1 MeV	2 MeV	3 MeV	1 MeV	2 MeV	3 MeV
2	1.3	2.0	2.1	3.3	3.9	4.4	12.9	14.1	15.3
10	3.8	5.9	6.5	8.5	11.0	12.2	29.9	37.7	43.4
10^2	7.0	11.3	12.2	14.5	19.5	22.1	50.5	65.7	77.5
10^3	10.2	16.5	18.0	20.5	27.5	31.7	70.4	92.7	110.9
10^4	13.3	21.3	23.5	26.0	35.5	40.9	89.2	118.6	143.2
10^5	16.5	26.2	28.9	31.5	43.2	50.0	106.8	144.4	173.8
10^6	19.5	31.0	34.3	37.0	50.6	58.8	124.4	171.4	205.4

The attenuation ratio K_0 shows how many times the measured or calculated exposure dose rate W must be reduced in order to obtain a given exposure dose rate W_1 ,

$$K_0 = W/W_1$$

For a given attenuation ratio the thickness of the protective shield can be determined by means of universal tables such as Table 5.4.

The thickness of a protective shield is frequently expressed in kilograms per square metre,

$$\delta_m = \rho \delta \quad (5.13)$$

Example. Calculate the thickness of a lead shield required to obtain maximum permissible working conditions from a ^{60}Co point source (γ -equivalent $m = 400 \text{ mg-eq Ra}$) at a distance of 1 metre from the source, the duration of the working week being 30 hours.

According to formula (5.12) the exposure dose rate

$$W = 8.4m/R^2 = 8.4 \times 400/10^4 = 0.336 \text{ R/h}$$

The maximum permissible dose rate

$$W_{mp} = 100/t = 100/30 = 3.3 \text{ mrem/h}$$

The attenuation ratio

$$K_0 = W/W_{mp} = 336/3.3 \approx 100$$

For ^{60}Co the γ -quantum energy is about 1.25 MeV. By interpolating the data in Table 5.4, a thickness $\delta \approx 8.1 \text{ cm}$ for the protective shield is obtained.

From formula (5.13) we obtain for the thickness

$$\delta_m = 11.34 \times 8.1 \approx 92 \text{ g/cm}^2 = 9.2 \text{ kg/m}^2$$

The thickness of a protective shield can also be determined from the half-value layer $d_{1/2}$. This is the shield thickness which halves the exposure dose rate. The value of $d_{1/2}$ varies with the thickness of the shield since both primary and scattered γ -rays contribute to the exposure dose rate. With increase of the shield thickness $d_{1/2}$ first grows and subsequently starts to drop off. For approximate calculations of the shield thickness the mean value $\bar{d}_{1/2}$ is frequently used. For ^{226}Ra and ^{60}Co sources the $\bar{d}_{1/2}$ value for lead is 1.3 cm, for iron 2.2 cm and for concrete 6.9 cm.

A thickness corresponding to one half-value layer reduces the exposure dose rate by two times, two half-value layers by $2^2 = 4$ times and n layers by $2^n = K_0$ times. Thus in order to reduce the dose rate K_0 times the number of half-value layers in the shield thickness is

$$n = \log K_0 / \log 2 \approx 3.32 \log K_0$$

The thickness of the shield is therefore

$$\delta = n \bar{d}_{1/2}$$

Example. Find the thickness of the lead shield in the previous example assuming that the half-value layer for lead $\bar{d}_{1/2} = 1.3$ cm.

The number of half-value layers

$$n = 3.32 \log 10^2 = 6.64$$

and hence the thickness of the lead shield

$$\delta = n\bar{d}_{1/2} = 6.64 \times 1.3 = 8.62 \text{ cm}$$

CHAPTER 6

MEASUREMENT OF IONIZING RADIATIONS

6.1 Ionization Methods for Measurement of Radiations

The interaction between radiation and matter is accompanied by a number of effects such as the formation of ions, emission of photons and liberation of heat. All these effects can be used to detect radiations, measure the particle flux density or intensity and the radiation spectra. The operation of many measuring devices (detectors) is based on the ability of radiations to ionize molecules. Each ion pair produced by the radiation in the detector consists of a positive molecular ion and an electron. The ionization produced by the radiation is called the *primary ionization*. Charged particles directly ionize molecules. Gamma quanta, on the other hand, first eject electrons from the molecules in the photoeffect or impart energy to Compton electrons or produce electron-positron pairs and these electrons subsequently produce the ionization in the detector. By measuring the charge in the detector one can study the properties of the radiation passing through the detector.

The detectors most commonly used are ionization chambers, proportional counters and Geiger-Muller counters. The operation and design of these detectors are similar. Essentially they consist of a container with two electrodes to which an electric voltage is applied. The space between the electrodes is filled with a dry gas.

To illustrate the operation of gas-filled detectors we shall consider the operation and circuit of a flat ionization chamber. This detector is a parallel-plate capacitor in which a potential difference U is applied to the plates (Fig. 6.1).

Dry gas is a good insulator. However irradiation of the gas considerably alters the conductance. The radiation ionizes the molecules and the gas acquires the ability to conduct an electric current. This closes the electric circuit and a current can pass through it. The current can be mea-

sured directly with a microammeter (Fig. 6.1a) which indicates the mean current flowing through the detector. Detectors operating under such conditions are called *current detectors*.

If it is desirable to record each particle separately then *pulse detectors* are employed. They are connected to circuits which permit pulses from the detector to be measured. A particle makes the gas a conductor over a short period of

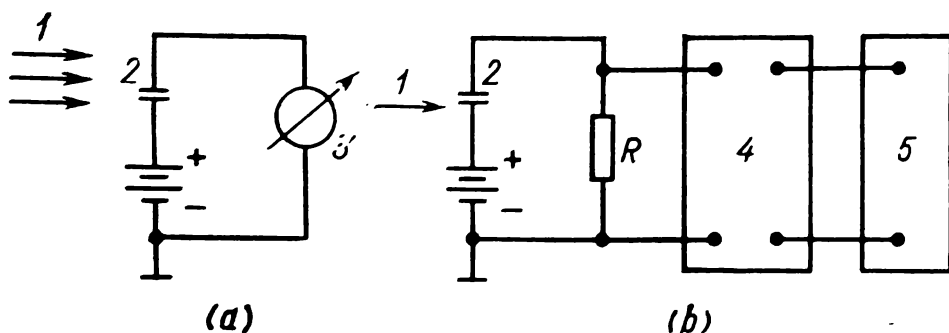


Fig. 6.1 Connection of a flat ionization chamber for current (a) or pulsed (b) operation

1—particle beam; 2—ionization chamber; 3—microammeter; 4—amplifier; 5—recorder

time. The voltage on a load resistance R changes (Fig. 6.1b). The voltage pulse is fed to an amplifier which increases the amplitude of the pulse by hundreds or more times. The amplified pulse then enters the recording system (or register). The pulse counting rate (number of pulses recorded per unit time) is a measure of the particle flux density in the detector.

Pulse detectors can also be used to measure the energy spectra of particles. In some detectors the amplitude of the voltage pulse on the load resistance is proportional to the particle energy provided the particle is stopped completely in the detector. From the amplitude distribution of the pulses one may determine the energy distribution of the particles.

In some experiments it is necessary to separate a certain phenomenon from the rest (e.g. to determine the direction of a fast particle). In such cases coincidence circuits are used. The outputs of two detectors are connected to the circuit. If a particle passes through both detectors simulta-

neously a voltage pulse is sent to the register. In the anti-coincidence circuits the pulses from two detectors are also accepted however the circuit is triggered only if a voltage pulse arrives from only one of the detectors.

6.2 Volt-Ampere Characteristic of a Gas Discharge

The passage of an ionization current through a gas-filled detector (gas discharge) depends on the properties of the gas, on the magnitude of the voltage applied and on the shape of the electrodes. The main characteristic of a gas

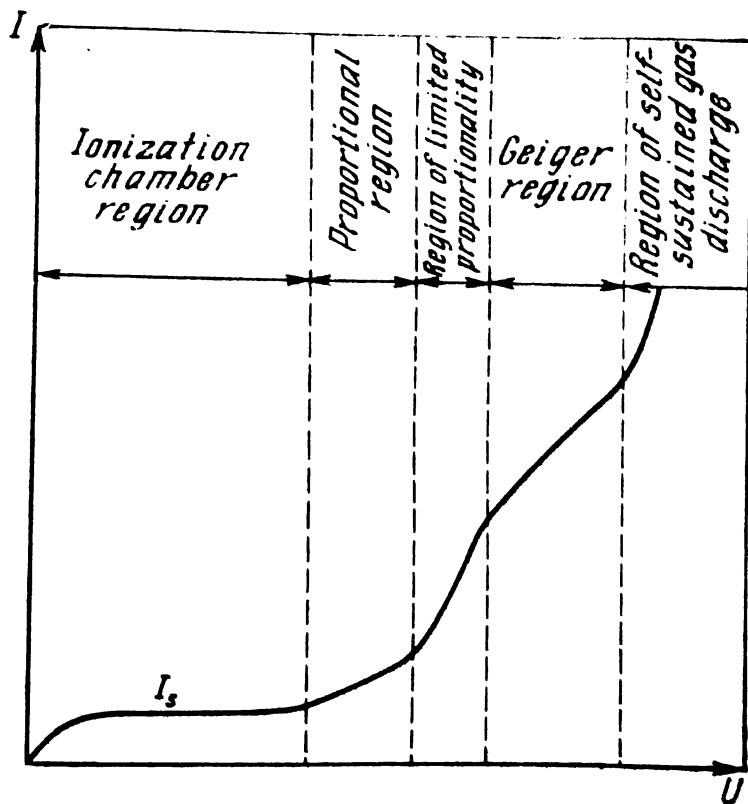


Fig. 6.2 Volt-ampere characteristic of a gas discharge

discharge is the dependence of the current I on voltage U for a constant radiation intensity in the detector—the *volt-ampere characteristic* (Fig. 6.2). With increase of the voltage the current initially rises, then for a certain range of voltage remains constant and finally begins to increase again.

Let us analyze the cause of such behaviour. Since there is an electric field in the gas between the electrodes the

ions move to the oppositely charged electrodes. The ion velocity v is proportional to the electric field strength E , $v = uE$. The proportionality coefficient u is called the *ion mobility*. Numerically it is the ion velocity (m/s) for a unit field strength $E = 1$ V/m and is measured in $\text{m}^2/\text{s}\cdot\text{V}$. The ion mobility is a characteristic of the gas filling. The higher the ion mobility of a gas the faster the charges are collected at the electrodes. Molecules of electronegative gases, such as the halogens, attach electrons in collisions and form negative ions. In such gases the mobility of both the positive and negative ions is of the order of $(1-10) \times 10^{-4} \text{ m}^2/\text{s}\cdot\text{V}$. Atoms of electropositive gases (argon, helium etc.) do not attach electrons. The negative ions in such gases are electrons whose mobility may reach $1.5 \text{ m}^2/\text{s}\cdot\text{V}$. Due to the large difference in the mobilities electrons are first collected at the anode (which is also called the collecting electrode) during a short time interval of about 10^{-7} s. Afterwards the slower heavy ions begin to be collected, the positive ions at the cathode and the negative at the anode.

At low voltages the velocity of directional movement of the ions is low and does not affect significantly the movement of the ions. Random thermal motion of the ions is predominant in this case. Two phenomena—recombination and diffusion of the ions, occur as a result of the numerous collisions between the ions and molecules.

Collisions between electrons and positive ions at low speeds may result in ion recombination, i.e. in the formation of neutral molecules. The recombination rate depends on the ion density in the gas. The higher the density of the electrons, positive ions and molecules the higher the recombination rate. However with increase of ion velocity the time of interaction between them decreases and hence ion recombination becomes less frequent.

The density of the ions produced by radiation is not uniform throughout the gas volume. It is higher in some parts and lower in other. Due to this difference in density and to the thermal motion the ions move from points of higher density to those of lower density. This type of movement of ions in the gas is termed *ion diffusion*.

Recombination and diffusion of ions reduce the current in a detector since not all of the ions reach the electrodes.

Of the two phenomena ion diffusion exerts the least effect on the gas discharge.

With increase of voltage applied to the electrodes the diffusion and recombination decrease and the amount of charges reaching the electrodes increases. At a certain voltage all primary ions are collected by the electrodes. Further increase of the voltage then does not affect the current. The current is saturated and is correspondingly called the *saturation current* I_s .

In the region of saturation elastic scattering of the ions by the gas molecules takes place. The kinetic energy conveyed to the ions by the electric field is still insufficient to ionize the molecules. However at a certain voltage (boundary of the saturation region) the mobile electrons are accelerated between two collisions to such a kinetic energy which is sufficient for ionization of the gas molecules. This type of ionization is called *secondary ionization*. In further collisions the electrons ionize other molecules etc. An avalanche type of ion formation occurs. The additional ions formed in the gas in this manner lead to an increase of the current which is the greater the higher the voltage. This phenomenon is called gas amplification. It is characterized by the *gas amplification factor* k equal to the ratio of the charge collected at the electrode to the primary charge.

In the current saturation region $k = 1$. With further increase of the voltage U the coefficient k sharply rises and in a certain range depends only on the voltage. This signifies that to each value of U there corresponds a certain value of k and that the final charge is proportional to the primary charge at the given value of U . The voltage region in which k is independent of the primary charge is the *proportional region*. At the end of the proportional region k may acquire a value of 10^3 to 10^4 .

Following the proportional region is the *region of limited proportionality*. The gas amplification factor in this region depends on both the voltage and magnitude of the primary charge.

In a region of sufficiently high U the gas discharge ceases to depend on either the primary charge or on the type of radiation. The formation of only one ion pair in the gas is now sufficient for initiation of the discharge. This is

the *Geiger region* of voltage. A gas discharge arising in the Geiger region cannot cease spontaneously and must be quenched by any of the suitable methods which will be discussed later. The Geiger region terminates in the *region of self-sustained gas discharge*.

Ionization chambers operate in the first voltage region and in the saturation region. This range of voltages is also called the ionization chamber region. Proportional counter operate in the proportional region and Geiger-Muller counters in the Geiger region.

6.3 Ionization Chamber

The ionization chamber is one of the most commonly used detectors. It can be employed for measurement of any type of radiation. Depending on their design ionization chambers are divided into flat, cylindrical and spherical.

In the flat chamber the electrodes (plates) are separated by the gas and enclosed in a container. The voltage leads to the electrodes are isolated from the container by materials with a high resistance of 10^9 - 10^{14} ohms (amber, polyethylene, textolite, Getinaks etc.). An homogeneous electric field of strength $E = U/d$ is produced in the space between the plane electrodes to which a voltage U is applied (d is the distance between the plates). Homogeneity of the electric field is violated near the edges of the plates (edge effect). In these parts of the chamber the electric field is weaker. The fraction of ions collected at the electrode from the edge regions is smaller than that from the central regions. This is one of the shortcomings of flat chambers since it becomes difficult to determine the operating volume, i.e. the volume contributing primary ionization charges to the electrodes.

The resistance of insulators employed in the experiments, R , does not ordinarily exceed 10^{14} ohms. If the current in the chamber is 10^{-10} A, that flowing through an insulator with $R = 10^{18}$ ohms at $U = 200$ V is

$$I = U/R = 2 \times 10^{-11} \text{ A}$$

The measuring instrument will record a current 1.2×10^{-10} A and hence the error in measuring the primary

ionization will be 20%. Accordingly the voltage applied to the electrodes of flat chambers is usually chosen near the beginning of the saturation region.

One of the major characteristics of a detector is its *sensitivity*. This is the minimum primary ionization which the detector can measure. The sensitivity of a chamber can be increased either by increasing its volume or the gas pressure.

In the first case the path length of a charged particle in the chamber is enhanced whereas in the second the range of a charged particle is decreased. In both cases the number of ion pairs formed by the particle in the chamber is higher and the current is larger. Flat chambers can be employed to measure currents as low as 10^{-12} A. The sensitivity of large chambers is limited by the currents induced by cosmic rays, radioactive contaminations etc.

Another important characteristic of a detector is its *efficiency*. This is the ratio of the number of particles recorded by the detector to the total number of particles entering the detector. The efficiency depends on the type and construction of the detector and on the properties of the particles.

A cylindrical ionization chamber (Fig. 6.3) consists of a hollow air-tight cylinder with a metal rod along the axis which is the collecting electrode. A high voltage is applied to the collecting electrode and the cylindrical container is grounded. Sensitive cylindrical chambers measure currents down to 10^{-18} - 10^{-16} A. To make the leakage currents much below 10^{-16} A the high voltage is applied to both the collecting electrode and a guard ring arranged in the middle of the electric insulator. The potential difference between the collecting electrode and guard ring is almost zero and hence

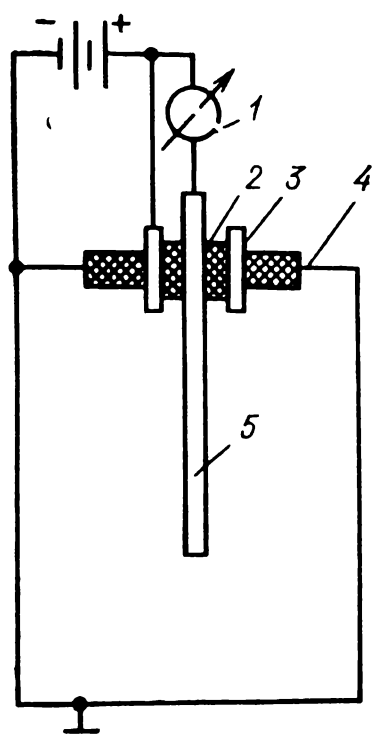


Fig. 6.3. Cylindrical ionization chamber

1—microammeter; 2—electric insulation; 3—guard ring; 4—container; 5—collecting electrode

low air-tight cylinder with a metal rod along the axis which is the collecting electrode. A high voltage is applied to the collecting electrode and the cylindrical container is grounded. Sensitive cylindrical chambers measure currents down to 10^{-18} - 10^{-16} A. To make the leakage currents much below 10^{-16} A the high voltage is applied to both the collecting electrode and a guard ring arranged in the middle of the electric insulator. The potential difference between the collecting electrode and guard ring is almost zero and hence

the major part of the leakage current flows from the guard ring to the container without passing through the microammeter. The presence of a guard ring considerably lowers the demands on the insulating materials and increases the accuracy of the measurements.

Finally, the last type of ionization chambers is the spherical chamber. The container is made of metal (aluminium, copper, steel). The collecting electrode is a small metal ball located at the centre of the chamber. The voltage is applied to the ball via a glass insulator.

Depending on their purpose and construction ionization chambers may work in a pulse or current regime. Pulse chambers are employed for recording single heavy charged particles (protons, α -particles, fission fragments etc.). The specific ionization of light particles (electrons, positrons etc.) is comparatively low and they cannot be recorded efficiently by pulse chambers.

Pulse detectors are characterized by their resolving time τ_r . It is defined as the minimum time interval between pulses during which each pulse from the load resistance can be recorded. Knowing the resolving time one can easily calculate the resolving power of a pulse detector, $N_r = 1/\tau_r$. The resolving power is the maximum number of particles which the detector can record per unit time.

Current chambers are used to measure the average intensity of various types of radiation. The intensity is proportional to the mean current flowing through the chamber.

6.4 Proportional Counters

The voltage pulses produced even in the most sensitive ionization chambers are so small that high-gain amplifiers are needed to record them. An advantage of proportional counters as compared to ionization chambers is that the primary ionization is amplified within the counter itself. Since the gas amplification factor k in the proportional region may reach 10^3 - 10^4 , the voltage pulse amplitude for a given primary ionization in a proportional counter will exceed that from an ionization chamber by k times. Consequently much simpler amplifier circuits may be employed in conjunction with proportional counters,

Proportional counters are designed in such a way as to obtain a high gas amplification factor in a small size counter at low voltages. Cylindrical counters have been found to be the most suitable for this (Fig. 6.4). It consists of a cylindrical case which is the cathode and a metal wire, stretched

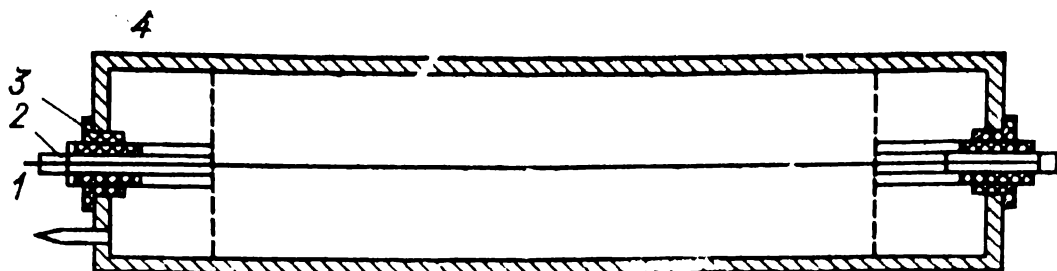


Fig. 6.4 Cylindrical counter

1—collecting electrode; 2—guard ring; 3—insulator; 4—counter body

along the axis, which is the collecting electrode. A high voltage is applied to the collecting electrode and the counter body is grounded.

The electric field between the electrodes in a cylindrical counter is not uniform. The field strength E varies inversely proportional to the distance r from the counter axis in accordance with the law

$$E = \frac{U}{\ln(R/a)} \frac{1}{r} \quad (6.1)$$

where R is the radius of the counter body, a is the radius of the collecting electrode and U is the voltage applied to the electrodes.

After passage of a charged particle through the counter the mobile electrons move toward the collecting electrode. Far away from the collecting electrode the field strength E is not great and the electrons experience elastic collisions with the gas molecules. In this region the interaction between the electrons and gas molecules is similar to that in ionization chambers. However in a small space surrounding the wire, which is called the critical space, the field strength E rapidly rises. In the critical space the energy of the accelerated electrons exceeds the threshold energy E_{th} at which molecule ionization begins. It is in this space that gas amplification of the charges occurs and an electron avalanche strikes the collecting electrode,

High values of k can be obtained by applying a voltage $U > 1000$ V. The diameter of the wire varies between 0.05 and 0.3 mm. The upper limit of the wire diameter is chosen so that the applied voltage will not be unnecessarily high. The lower limit is determined by the fragility of the wire. Collecting electrode wires are usually made of tungsten or steel. The surface is polished since even small roughnesses may strongly distort the electric field near the wire surface. The counter is filled with a gas to a pressure of 50-760 mm Hg. With decrease of pressure the electron path in the gas increases and hence the energy imparted to the electrons by the electric field increases. Thus at lower pressures gas amplification sets in at lower voltages.

The highly mobile electrons are collected at the anode in about 10^{-7} s. During this short time the heavy positive ions in the critical space do not move significantly. They form a positively charged sheath around the wire in that part of the critical region in which the particle has passed. The positive ions appreciably weaken the electric field strength in the critical space during a time τ_d called the *dead time of the counter*.

No significant gas amplification takes place in the weak electric field during τ_d . Therefore if a second charged particle passes through the proportional counter during a time τ_d the pulse amplitude on the resistor R will be smaller than the sensitivity threshold of the amplifier and the voltage pulse will not be recorded. In proportional counters the dead time $\tau_d \geq 10^{-5}$ s.

On approach of the positive ions to the cathode the potential difference in the critical space tends to its initial value. After a certain time τ_r the gas amplification factor becomes sufficiently large for the pulse amplitude on the resistor R to exceed the sensitivity threshold of the amplifier and a new particle may now be recorded. Conditions in the counter are completely restored after the positive ions are neutralized at the cathode. The time τ_{rc} reckoned from the end of the dead time during which the counter properties are restored is called the *recovery time*. In proportional counters $\tau_{rc} \sim 10^{-4}$ s.

The resolving time of a counter τ_r depends on τ_d and on the threshold sensitivity of the amplifier. For propor-

tional counters $\tau_r \geq 10^{-6}$ s and the resolving power $N_r \leq 10^6$ counts per second.

The filling gas affects the course of the gas discharge in a counter. If the gas is electrically negative (O_2 , Cl_2 etc.) the collecting time of the negative ions will be longer and the resolving power of the counter will be low. Therefore electrically positive gases are preferred (argon etc.). Such gases ensure rapid collecting of electrons at the anode.

However if the counter is filled with pure argon additional avalanches may occur. On striking the cathode argon ions may expel electrons from the metal and produce excited argon atoms. On transfer to the ground state these atoms emit photons in a broad energy range. Ultraviolet photons may eject electrons from the counter body (anode) and the photoelectric electrons cause a gas discharge in the gas (afterdischarge). This lowers the quality of the counter.

Two methods are used to quench afterdischarges. Depending on the method used proportional counters are divided into *non-self-quenching* and *self-quenching counters*. Non-self-quenching counters are filled with helium, argon or other electropositive gases which do not quench the afterdischarges. These secondary effects are therefore removed by external means. The simplest consists in connecting a load resistor in series with the voltage source and counter electrodes. If the resistance is not smaller than 10^8 ohm the voltage at the anode will appreciably decrease during 10^{-3} - 10^{-2} s. During this large period of time the excited atoms disappear in the gas and no afterdischarges arise. Non-self-quenching counters can work over long periods of time but their resolving time is large and may reach 10^{-2} s.

Self-quenching counters are filled with a mixture of argon atoms and molecules of a polyatomic gas (alcohol, methane etc.). The concentration of the latter molecules in the mixture is about 10-15%. Polyatomic gases are good ultraviolet absorbers. A molecule of a polyatomic gas colliding with an argon ion readily transfers an electron to the atom and thus neutralizes it. At the cathode the heavy molecular ion extracts an electron from the metal and is transformed into an excited molecule. The lifetime of such excited molecules with respect to dissociation into the component

atoms is a hundred times shorter than the photon emission time. The result is that the excitation energy of almost all of the molecules is spent in dissociation and not in photon emission.

The service life of a proportional counter is measured by the number of particles it can record. In non-self-quenching counters the gas discharges do not change the composition of the filling gas. The service life of non-self-quenching counters is therefore determined by design shortcomings (such as violation of air-tightness of the counter container

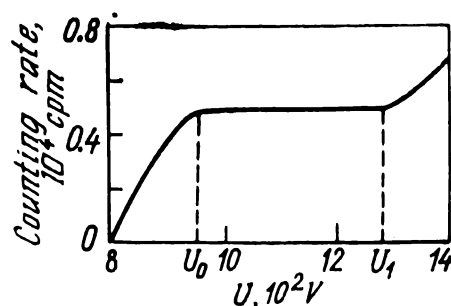


Fig. 6.5 Counting characteristic of a proportional counter

etc.). In self-quenching counters the registration of a single particle involves the dissociation of approximately 10^5 polyatomic molecules. Since there are not more than 10^{20} polyatomic molecules in the filling gas a self-quenching counter can record only about 10^{15} particles and this determines the service life of the counter.

One of the main characteristics of a proportional counter is its counting characteristic (Fig. 6.5). This is the dependence of the counting rate on voltage applied to the electrodes for a constant radiation intensity in the counter and a given sensitivity threshold of the amplifier. Between voltages U_0 and U_1 the counting characteristic is almost horizontal (this part is called the plateau), i.e. the counting rate is constant. The pulse amplitude is proportional to the primary ionization which depends on the direction of motion of the particle in the gas. The path lengths of the particles in the gas depend on their direction and because of this there is a spread of pulse amplitudes. The greater the amplitude spread the higher is the boundary voltage U_0 . For a given sensitivity threshold of the amplifier the magnitude

of U_0 depends on the nature of the radiation. The value of U_0 is smaller for α -particles than for β -particles since the specific ionization of β -particles in a gas is much smaller than that of α -particles. If the threshold of the amplifier is reduced U_0 will be shifted toward smaller values.

The plateau is slightly inclined with respect to the voltage axis. The slope of the plateau is characterized by the relative change in the counting rate per 100 volts. It is approximately 0.1% per 100 volts and is due to gas discharges induced by particles from extraneous sources.

Proportional counters are operated at voltages corresponding to the plateau. They are employed for registration of charged particles and neutrons and also for measuring the energy spectra and activity of radiation sources.

6.5 Geiger-Muller Counters

In practice the region of limited proportionality is not used in work with gas-filled counters. The gas amplification factor in this region depends on the voltage and on the primary ionization which makes the counter inconvenient for recording radiations.

Gas-filled counters operating in the Geiger region are called *Geiger-Muller counters* after the inventors. In design they do not differ significantly from proportional counters. However, the applied voltage is higher and as a result the critical region is broader and the gas amplification factor may increase up to 10^{10} . The Geiger-Muller counter is therefore the most sensitive of gas-filled detectors. Large voltage pulses with amplitudes up to 50 V are produced by the counters.

An enormous number of ions and excited molecules is formed during avalanche multiplication of electrons. Intense ultraviolet radiation is emitted by the excited molecules and photoelectrons are expelled both from the metal of the cathode and from the molecules of the gas. The photoelectrons induce new electron avalanches and the gas discharge rapidly occupies the whole volume of the counter.

A dense sheet of positive ions is formed around the anode after collection of the electrons. The field strength near the anode is correspondingly reduced. In effect the diameter

of the anode becomes equal for a certain period of time to that of the critical volume. The voltage applied to the electrodes is therefore insufficient for avalanche multiplication of electrons to take place. The positive ions are neutralized at the cathode and during this process they emit ultraviolet radiation which ejects electrons from the cathode metal. About 10^{-4} s after the beginning of the discharge afterdischarges arise in the counter. They are quenched in the same way as in proportional counters, i.e. by employing external circuits or adding polyatomic molecules to the filling gas.

The dead time, recovery time and resolving time of Geiger-Muller counters are close to 10^{-4} s.

The service life of self-quenched Geiger-Muller counters is not very long. Not more than 10^{20} alcohol molecules are added to the filling gas. About 10^{10} of them are dissociated in each discharge. Thus not more than 10^{10} charged particles can be recorded.

The service life of self-quenched counters can be increased by filling them with an inert gas (neon, argon) and a small admixture of a halogen element (chlorine, bromine). Counters with such mixtures are called *halogen counters*.

The diatomic halogen molecules readily transfer one of their electrons to the inert gas ions with which they collide and become positively charged ions. On neutralization at the cathode the positive halogen ions are converted into excited molecules which dissociate into their constituent atoms.

The halogens thus play the role of the quenching gas. In contrast to the atoms of other quenching gases the halogen atoms recombine into molecules during the collisions. The amount of quenching molecules in the counter thus remains constant.

The halogens are chemically active substances. This limits the choice of materials which can be used for the counter body. Whereas aluminium, glass or copper may be used in ordinary counters, stainless steel is the material usually used to build the bodies of halogen counters.

The shape of the counting characteristic of Geiger-Muller counters is similar to that of proportional counters. Up to the threshold (boundary) voltage U_0 the counter operates

in the region of limited proportionality. The pulse amplitude still depends on the primary ionization. The external circuit records only those pulses whose amplitude exceeds the sensitivity threshold of the amplifier. With increase of the voltage the amplitudes of all pulses become larger and the counting rate increases. At voltages exceeding the threshold value U_0 , all particles produce pulses with amplitudes exceeding the sensitivity threshold of the external circuit and all of the pulses are recorded.

The threshold voltage depends on the nature of the filling gas. The lowest threshold voltage (350-400 V) is observed in halogen counters filled with neon and an admixture of argon (0.1%) and a halogen (0.1%). Counters with other filling gases operate at 800-1300 V.

The plateau of the counting characteristic of Geiger-Muller counters is the same for all types of radiation since the pulse amplitude is independent of the primary ionization. The length of the plateau may reach several hundred volts. The slight slope of the plateau is caused by spurious counts not related to the particles under investigation. The spurious counts may be due to electrons expelled from the cathode by the electric field or by photons. With increase of voltage the number of spurious pulses also increases and the counting rate increases by 3-4% per 100 volts.

The presence of a plateau in the counting characteristic renders the Geiger-Muller counter a convenient detector. If the working voltage of the counter is chosen somewhere near the middle of the plateau the counting rate will be stable. Small random variations of the voltage applied to the electrodes will not affect the rate significantly.

At the end of the plateau the counting rate begins to increase rapidly. At voltages above U_1 spontaneous discharges begin to dominate. Prolonged operation of the counter in the spontaneous discharge region may spoil the counter.

Geiger-Muller counters are employed for measurement of γ -quanta, β - and α -particles. The pulse amplitude is so large that in some cases amplifiers are not used and the pulses are fed directly to the recorder. Equipment involving Geiger-Muller counters is therefore ordinarily simple and portable.

6.6 Scintillation Counters

The energy of fast particles is expended in ionization and excitation of the molecules of the medium. In the scintillation technique it is the excited molecules which produce the signals to be recorded. In some transparent substances called phosphors part of the radiation emitted by the excited molecules lies in the visible region. The transit of the phosphor by a particle may be accompanied by a light flash (scintillation). The ratio of the light energy emitted by the phosphor to the absorbed energy of the particle is the *conversion efficiency of the phosphor (scintillator)*.

A scintillation counter consists of two main parts (Fig. 6.6), the scintillator and photoelectric multiplier. A small amount of an activator is introduced into the scintillator to increase the conversion efficiency. The activating substance is usually denoted in parenthesis after the symbol of the phosphor. For example NaI(Tl) means that sodium iodide is doped with thallium. Part of the light flash from the scintillator strikes the cathode of the photomultiplier and knocks out photoelectrons. The cathode is made of light-sensitive materials with a high electron emission efficiency. An antimony-cesium cathode, for example, emits from 8 to 15 photoelectrons per 100 incident photons.

A photomultiplier contains 8 to 13 electrodes, called *dynodes*, arranged consecutively. A voltage of 1500-2500 V

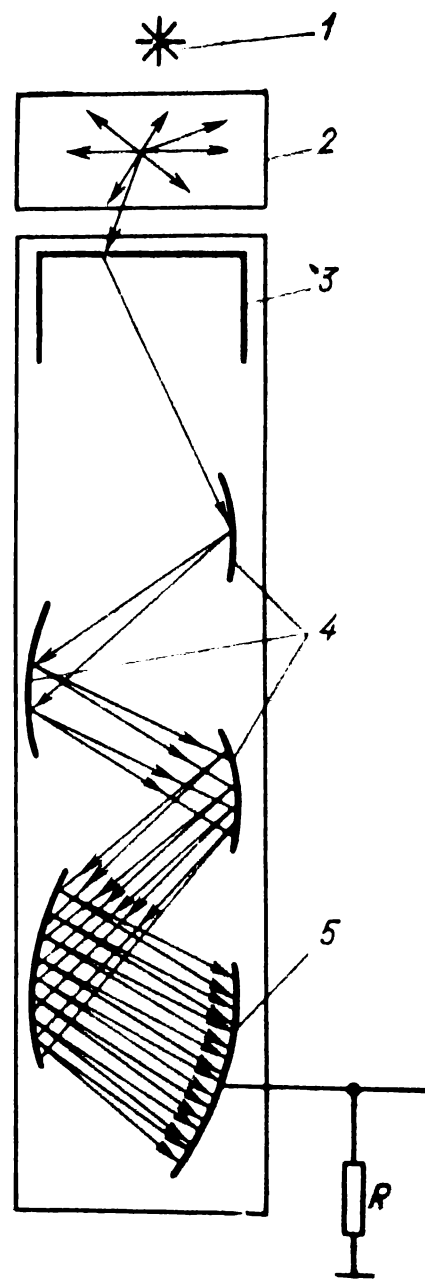


Fig. 6.6) Scintillation counter

1—radiation source; 3—phosphor; 5—photocathode; 4—dynodes; 5—anode

applied between the cathode and anode is distributed between the dynodes by a resistor divider. The photoelectrons from the cathode accelerated to 150-200 eV strike the first dynode and knock out on the average $\sigma = 2-4$ secondary electrons. These, in turn, are accelerated and each knocks out σ electrons from the second dynode etc. If A electrons strike the first dynode, a total of $A\sigma^m$ electrons will be collected at the anode from the m th dynode. The amplification factor of the photomultiplier, $k = \sigma^m$, depends on the material of the dynodes, their number in the photomultiplier and on the voltage between them. In modern photomultipliers k lies between 10^5 and 10^7 .

The output electric pulses from the photomultiplier are measured on a load resistor R . If the pulses are small they are amplified prior to being fed to the recorder.

Phosphors may be made of either organic or inorganic substances possessing a high degree of transparency for the light emitted. This is one of the main characteristics required of phosphors. The greater the amount of light emitted by the phosphor, the larger the number of electrons ejected from the photocathode.

Another characteristic of a phosphor is its emission decay time. A particle passes through a phosphor in about 10^{-10} s. The light flash then follows. In order to keep the resolution time as small as possible phosphors are chosen with decay times of 10^{-6} - 10^{-9} s.

Scintillation counters are used to measure various types of radiation. Accordingly phosphors selectively sensitive to a particular type of radiation are employed. The ZnS (Ag) phosphor, for example, is characterized by its high sensitivity to α -particles, and it can be used to record α -particles accompanied by electrons or γ -quanta.

The NaI(Tl) crystal is a suitable phosphor for γ -quantum counters. Its density is quite high— 3.67 g/cm 3 . The presence of iodine ($Z = 53$) in the crystal raises the efficiency of γ -quantum counting up to 60% whereas the efficiency of Geiger-Muller counters for γ -quanta is only 1-2%.

The resolving time of scintillation counters varies between 10^{-9} and 10^{-6} s. This permits appreciably higher counting rates to be attained than is possible in gas-filled counters.

In some phosphors such as NaI(Tl), anthracene etc., the

intensity of the light flash is proportional to the amount of energy absorbed. Scintillation counters can therefore be used in spectrometers for γ -quanta, electrons or other particles. The energy resolution of scintillation spectrometers does not exceed 7.5-10%.

6.7 Semiconductor Detectors

The smallest size a gas-filled ionization chamber can have is determined by the specific ionization of the particles in the gas. With decrease of size of the chamber its counting efficiency for various types of radiation decreases. If the gas in a chamber could be replaced by a solid the specific ionization would increase by approximately 10^4 times. With a "filling" of this type the detector efficiency would be rather high even for small size detectors. The creation of portable detectors became possible after a study of the properties of semiconductors and the development of technology of their production. Semiconductors are substances whose electric conductivity is intermediate between that of metals (conductors) and dielectrics (insulators). Semiconducting properties are possessed by part of the elements of the III and IV groups of the periodic table. Two elements of the IV group are most suitable for obtaining single crystals to be used in detectors, germanium and silicon.

In order to obtain semiconductors with a prescribed electric conductivity, small admixtures of elements of the III or V group are introduced into pure germanium (silicon) single crystals. Let us elucidate how these admixtures affect the electric properties of the semiconductors.

In each crystal lattice site of a germanium single crystal there is one four-valent atom. Eight electrons are involved in the valency bond of the lattice site atoms in germanium single crystals: the four external electrons of the site atom and four outer electrons of the four neighbouring atoms. Suppose that a germanium atom is replaced by phosphorus, an element of the V group. Phosphorus has five electrons in the outer shell. Four of these compensate the valency bond of the germanium atom removed. The fifth electron revolves around the phosphorus nucleus and collides with

atoms of the crystal which oscillate about their equilibrium position. A result of such collisions is that the bond between the fifth electron and phosphorus nucleus may break. Thus in germanium with phosphorus admixtures or with other elements of the V group there appear free electrons and fixed positive phosphorus ions. Germanium acquires thereby electron conductivity and is called an *n-type semiconductor*.

The electric conductivity will be different if trivalent atoms of the III group (boron, aluminium etc.) are introduced into the crystal. Each boron atom incorporated into the lattice tends to fill all four valency bonds of the germanium atom. Since the boron atom lacks one valency electron to compensate for all four valency bonds, it removes a valency electron from a neighbouring germanium atom and is transferred into a fixed negative ion. Free valency bonds (positive charges) usually termed *holes* arise at the lattice sites.

The free valency bond may be occupied by a valency electron from a neighbouring lattice site. As a result of such transfers the hole (positive charge) moves over the crystal. This hole transition resembles the motion of a positive ion. The only difference is that the positive charge in a single crystal is transferred along a chain of fixed atoms. Germanium single crystals with an admixture of III group atoms are called *p-type semiconductors* and their electric conductivity is called *hole conductivity*.

The number of free electrons in an *n-type semiconductor* or of holes in a *p-type semiconductor* is equal to that of the respective admixture atoms. Both *n*- and *p*-type semiconductors are electrically neutral as the hole and electron charges are compensated by the charges of the fixed ions.

Consider a semiconductor consisting of two parts (Fig. 6.7a), one possessing electron and the other hole conduction. The first part of the semiconductor will contain free electrons and the second, holes. Some electrons will move from the *n*- to the *p*-type semiconductor and neutralize part of the holes in a thin boundary layer. Therefore part of the fixed negative ions remains uncompensated and a thin layer of the *p*-type semiconductor becomes charged negatively. Holes entering the *n*-type semiconductor from the *p*-type semiconductor neutralize part of the electrons

and a thin layer of the *n*-type semiconductor is charged positively. Thus at the contact between an *n*- and *p*-type semiconductor a thin layer is formed which has been termed an *n-p* junction. The layer has relatively few electricity carriers (electrons and holes) and its electric resistance is therefore much higher than in the other parts of single crystal. A contact potential difference producing a field strength E arises at the *n-p* junction and impedes the movement of electrons into the *p*-type semiconductor and holes into the *n*-type semiconductor.

A semiconductor with an *n-p* junction conducts an electric current in only one direction and hence is a semiconductor diode. If the *n*-type semiconductor is connected to the

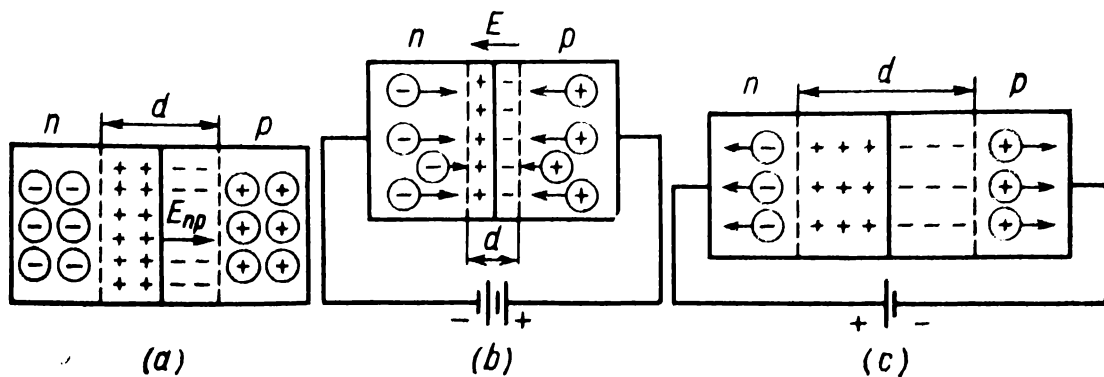


Fig. 6.7 Unidirectional conductivity of an *n-p*-type semiconductor

minus and the *p*-type semiconductor to the plus terminal of a battery (Fig. 6.7b), equilibrium at the *n-p* junction will be disturbed. Under the action of the electric field electrons enter the *p*-type semiconductor and holes enter the *n*-type semiconductor the net effect being the flow of an electric current. On inversion of the polarity (Fig. 6.7c) all free electrons are displaced toward the anode from the *n-p* junction and the holes are shifted toward the cathode. The thickness of the *n-p* junction increases and the single crystal in effect becomes an insulator. It is because of this property of the *n-p* junction that semiconductor diodes can be used as detectors.

An *n-p*-type semiconductor detector is usually a small plate with two plane electrodes attached to it. A high positive potential (several hundred volts) is applied to the *n*-type semiconductor. The *n-p* type semiconductor with

the voltage applied as indicated is an insulator and no current flows in the absence of radiation. Radiation produces free electrons and holes in the *n-p* junction and for a short time the diode becomes a conductor. The time of flow of the current is determined by the time of collection of the electrons and holes at the respective electrodes. The current produces a voltage pulse on the load resistor which is fed into the recording circuit. After removal of the electrons and holes from the *n-p* junction the semiconductor again becomes nonconducting and no current flows.

The energy of formation of an electron-hole pair in germanium and silicon is about 3 eV and therefore approximately ten times more primary charges are produced in a semiconductor detector than in a gas on slowing down the same particles. The sensitivity of semiconductor detectors consequently is higher than that of ionization chambers.

Germanium and silicon *n-p*-type semiconductors possess some properties which make them suitable for detectors. The ions in these semiconductors are sufficiently mobile and do not recombine readily. They can withstand high electric potential differences and hence electric breakdown is excluded. Semiconductor detectors are portable and simple in design.

The thickness of the *n-p* junction in a semiconductor detector depends on the type of radiation. Heavy charged particles are stopped in a layer of about 10 μm . Such miniature detectors are not only capable of recording particles but also of yielding their energy spectra.

Semiconductor detectors with thicker *n-p* junctions are required for the measurement of γ -quanta. The interaction between a γ -quantum and semiconductor involves the production of fast electrons with ranges of approximately 1 mm/MeV. Thus for efficient recording of γ -quanta the thickness of the *n-p* junction should not be less than several millimetres. Such detectors are also suitable for γ -quantum spectrometry. With comparable recording efficiencies the resolution of semiconductor gamma spectrometers is from 20 to 30 times higher than that of scintillation gamma spectrometers.

A valency electron colliding with the crystal lattice atoms executing thermal vibrational motion may obtain an amount of energy sufficient for it to become free. In this

case concurrently with free electrons holes are also formed.

The intrinsic (dark) current of a semiconductor, which is not related to the radiation measured, increases with temperature. The dark current is particularly high in germanium detectors which accordingly are cooled with liquid nitrogen.

6.8 Other Techniques for Measuring Radiations

Cherenkov counters. The velocity of light in a transparent medium $c' = c/n$, where n is the refractive index. If a charged particle moving in vacuum with a speed $v > c/n$ enters such a medium its speed will exceed that of light c' in the medium. The higher the refractive index the smaller the light velocity c' . For water $n = 1.33$ and $c' = 2.26 \times 10^8$ m/s; for glass $n = 1.50$ and $c' = 2.0 \times 10^8$ m/s.

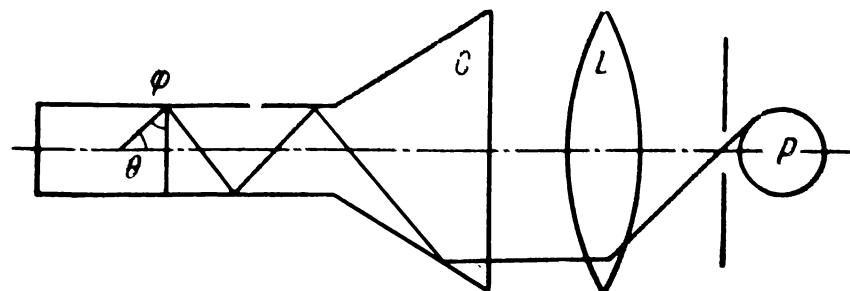


Fig. 6.8 Cherenkov counter

The motion of a charged particle possessing a velocity $v > c'$ in a transparent medium is accompanied by the emission of radiation, part of which is in the visible range of the spectrum. This radiation was discovered by the Soviet physicists S. I. Vavilov and P. A. Cherenkov and named after them.

The *Vavilov-Cherenkov radiation* propagates at an angle $\theta = \arccos(c/nv)$ with respect to the particle trajectory. With increase of v the angle θ increases and at $v = c$ attains its maximum value. This property of the Vavilov-Cherenkov radiation underlies the operation of Cherenkov counters (Fig. 6.8). Fast charged particles with velocities $v > c'$ enter the cylindrical part of a vessel containing a transparent substance C (plexiglas, water). The transparent material

during the short time of motion of the particle in it becomes a light source. The angle of incidence of the light at the interface between the material C and air is close to the angle of total internal reflection. The light therefore cannot leave the medium C and after multiple reflections and focussing with a lens L the light strikes a photomultiplier P .

If the length of the vessel l is 20 cm, the light flash will last $l/c \approx 10^{-9}$ s. As a result Cherenkov counters possess

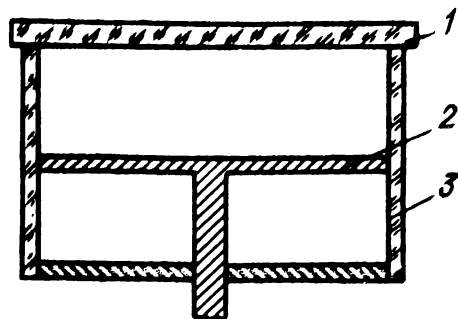


Fig. 6.9 Cloud chamber
1—glass plate; 2—mobile piston; 3—glass cylinder

a very small resolving time and are threshold detectors. They record only charged particles whose velocity exceeds the velocity of light in the transparent medium.

Track chambers. Three types of track chambers are employed in experimental physics. These are the cloud chamber, diffusion and bubble chambers. In these devices particles are detected by the *tracks* they make.

The *cloud chamber* is based on the property of ions to serve as nuclei for condensation of vapour into minute drops of liquid. The simplest cloud chamber consists of a cylindrical chamber with a piston (Fig. 6.9). The chamber is filled with saturated vapour of a liquid (water, alcohol). The piston is then suddenly pulled down. The expansion of the vapour lowers its temperature and it becomes supersaturated. A charged particle passing through the chamber at this moment forms ions on which liquid drops are formed. In this way a visible track is produced. Photographs of the tracks can be made by illuminating them laterally. The sign of the particle charge can be determined by placing the chamber in a homogeneous magnetic field. A photograph of the tracks of an electron and positron is shown in Fig. 6.10.

The two particles emerge from a single point on the surface of a metal plate irradiated by γ quanta. The positron and electron are deflected by the magnetic field in different directions in accordance with their charge.

After 1 or 2 seconds the supersaturated vapour begins to condense throughout the chamber which thus becomes unsuitable for further observations. The chamber is made operative by applying a voltage and removing thereby the ions from it. The piston is returned to its initial position, the chamber is again filled with saturated vapour etc.

Modern chambers employed for investigation of high energy particles are completely automatized. The piston is replaced by a membrane beneath which the pressure can be changed automatically. On reduction of the pressure the membrane bends downward thus expanding the volume of the chamber. Prior to entering the chamber the particles pass through Geiger-Muller counters. The signal from the counters is sent to the mechanism which creates supersaturation of the vapour in the chamber, switches on the light and photographs the tracks. After a certain time interval the charges are removed from the chamber which is then filled with saturated vapour.

In the *diffusion chamber* supersaturation of the vapour is attained as a result of diffusion of the vapour. Unsaturated vapour of a low boiling liquid (alcohol, ether) is introduced in the upper warm part of the chamber. The vapour diffuses toward the lower cold part of the chamber where it condenses. A sensitive layer of supersaturated vapour is located

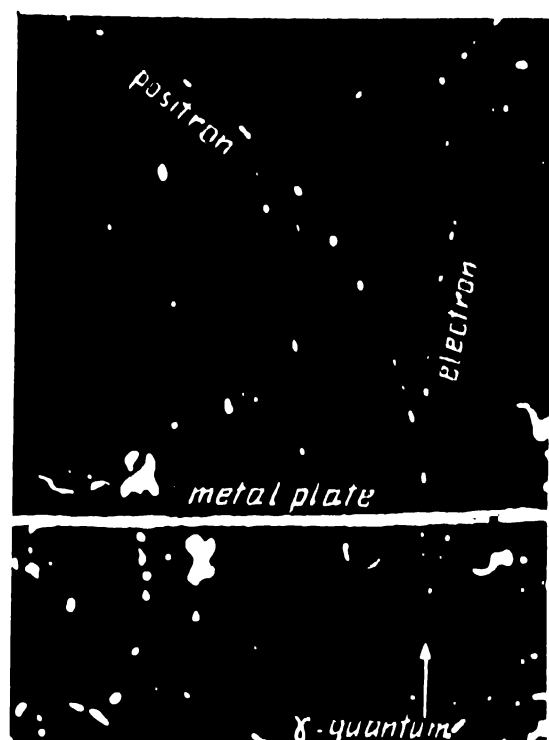


Fig. 6.10 Photograph of positron and electron tracks in a cloud chamber

signal from the counters is sent to the mechanism which creates supersaturation of the vapour in the chamber, switches on the light and photographs the tracks. After a certain time interval the charges are removed from the chamber which is then filled with saturated vapour.

between the cold and hot parts of the chamber. The state of supersaturation is maintained in the cloud chamber for only about 1 or 2 seconds and hence it is quite probable that an interesting event will be missed. In the diffusion chamber the supersaturation state of the vapour in the sensitive layer persists continuously. This is an important advantage of the diffusion chamber over the cloud chamber. However, the increase of operating time of the diffusion chamber is obtained at the expense of a considerable decrease of the thickness of the sensitive layer in the chamber.

The molecule density in the sensitive volume of the cloud and diffusion chambers does not exceed 10^{20} molecules/cm³. If a high energy particle with $E \geq 1$ GeV passes through the gas, a weak intermittent track will be produced from which the properties of the particle can be determined with great difficulty. Investigation of such particles can be carried out with greater efficiency in a bubble chamber which is filled with a liquid of low boiling point (hydrogen, deuterium etc.). Substitution of a liquid for the gas in a chamber increases by over a hundred times the density of the molecules and nuclei. This has made it possible to measure the range of particles with energies $E \geq 1$ GeV, to study the nuclear reactions induced by such particles etc.

The operation of the *bubble chamber* is based on a certain property of liquids, viz. on the fact that the boiling temperature of a liquid in a closed vessel depends on the pressure. The liquid is maintained under pressure at a temperature which slightly exceeds the boiling temperature at atmospheric pressure. A sudden reduction of the pressure to that of the atmosphere renders the liquid superheated. During a short period of time (about 10 ms) the liquid does not boil. If a charged particle passes through the superheated liquid during this time vapour bubbles are formed along its path. The track can be photographed and conveniently studied. Bubble chambers are usually placed at the exit of accelerators producing high energy particles. On entrance of the particles into the chamber the pressure is reduced and a photograph is made of the particle track in the chamber liquid.

Photographic plates. A photographic emulsion layer irradiated by charged particles or photons darkens after

development. This property is used for the recording of radiations. Radiation doses and the recording of single particles can be carried out with photographic plates. The radiation dose is determined on the basis of the degree of darkening of the plate whereas single particles are studied by the tracks they form in the emulsion.

Fine-grain photographic emulsions are employed for investigation of radiations since the sensitivity of an emulsion to radiation depends on the grain size. Stacks of photographic plates are used in studies of fast particles the thickness of the stack being chosen so as to exceed the particle range. Photographic plates are convenient since the particle tracks in the emulsion can be studied in great detail and information can be obtained regarding the nature of the particles, their energy etc.

CHAPTER 7

ACCELERATORS OF CHARGED PARTICLES

7.1 Applications of Accelerators

The properties of atomic nuclei and of elementary particles are studied experimentally by observing nuclear reactions. For a nuclear reaction to occur two nuclei must be made to approach each other so that nuclear forces become operative. The distance between two nuclei (with atomic numbers Z_1 and Z_2) can become sufficiently small only if the potential wall of height V_k MeV is surmounted (see Sec. 3.4). The probability that the nuclei approach each other at energies $E_n < V_k$ is low. The frequency of nuclear reactions therefore can be increased by accelerating the bombarding nuclei to energies $E_n > V_k$.

Light nuclei (or particles) are used as the bombarding particles, viz. protons, deuterons and α -particles. For light nuclei the height of the potential barrier is small and nuclear reactions can be induced at comparatively low accelerating energies.

The first nuclear reactions were observed by bombarding nuclei with α -particles emitted by natural α -emitters. The energies of the α -particles did not exceed 9 MeV. Such particles are suitable for studying nuclear reactions involving nuclei with $Z \leq 20$.

In nature there is one source of very fast charged particles, the cosmic rays (see Chap. 9). Particles of enormous energies (over 10^8 GeV) can be found in the cosmic radiation. Some very valuable information in nuclear physics and the physics of elementary particles has been obtained by studying the interaction between cosmic ray particles and matter. Since the flux density of the cosmic ray particles is low, observation of some events requires time-consuming experiments.

Intense beams of fast particles can be obtained with accelerators in which charged particles move in an electro-

magnetic field. If a particle of charge q moves in an accelerating electric field with a potential difference U its kinetic energy will increase by qU . In some types of accelerators, such as the Van de Graaf electrostatic accelerator, a high voltage is applied, as much as 8 MV. In other types of accelerators energy is imparted to the particle as it passes repeatedly through a field of comparatively low accelerating voltage, about 10 kV.

In modern accelerators the energy of fast particles has been pushed up to 400 GeV. However, even such high energies are not enough for some experiments. New phenomena appear with increase of the particle energy. Therefore, these phenomena can be studied only by employing particles of higher energies.

Such particles as the positron, muon, pion and others were first discovered in the cosmic radiation. Can they be obtained in laboratory conditions and thus be studied in greater detail? According to the relation $W = mc^2$ a particle with a rest mass m_0 can be created only if the kinetic energy is not less than m_0c^2 . However, in a nuclear reaction particles and antiparticles arise simultaneously (see Sec. 9.3), the rest masses being equal. For example, in the electric field of a nucleus a γ -quantum with an energy $E_\gamma = 1.02$ MeV can create an electron (particle)-positron (antiparticle) pair. Therefore, an energy of at least $2m_0c^2$ is required only to obtain a particle-antiparticle pair. Moreover momentum must be conserved in a nuclear reaction, i.e. the total momentum before the reaction must equal the momentum after the reaction. Part of the kinetic energy of the bombarding particles must be spent to conserve momentum.

Proton accelerators are usually employed to obtain such particles as pions, antineutrons, antiprotons etc. The particles are produced in collisions between accelerated protons and nucleons of the target. The threshold energy E_{th} for creation of a particle-antiparticle pair is given by the expression

$$E_{th} = 1.86m_{0a} (m_{0a}/m_{0p} + 2) \text{ GeV}$$

where m_{0a} and m_{0p} are the rest masses of particle a and proton p expressed in amu. The production threshold for

a neutron-antineutron pair ($m_{nn} = m_{\bar{n}\bar{n}} \approx m_{pp}$) is

$$E_{th} = 1.86 \times 3m_{pp} \approx 5.6 \text{ GeV}$$

An energy of 1.879 GeV should be sufficient to produce a resting neutron-antineutron pair. The unproductive expenditure of energy $E = 5.6 - 1.879 \approx 3.7$ GeV is more than 2/3 of the threshold energy. The proton energy in some accelerators has been made as high as 400 GeV. However, only about a tenth, i.e. about 40 GeV, is used productively.

The efficiency of utilization of the particle energy can be increased if two oppositely moving particle beams are made to collide. The total momentum of the particles is zero if the energies of the opposite beams are the same. Hence, unproductive energy losses required for conservation of momentum are reduced to a minimum. Suppose that the amount of energy utilized in a nuclear reaction is the same in an accelerator with a fixed target as in an accelerator with opposite beams. To meet this condition the particles will have to be accelerated to some energy E_1 in the first accelerator and to an energy E_2 in the second. If the rest energy of the particle $W_0 \ll E_2$ then $E_1 \approx 2E_2^2/W_0$.

At present accelerators are in operation in which colliding beams of 3.5 GeV electrons and positrons or colliding beams of 28 GeV electrons interact. In an accelerator with a fixed target the corresponding energies of the electrons (positrons) would have to be 49 000 GeV and of the protons about 1700 GeV.

One of the difficulties in constructing accelerators with opposite moving beams is to obtain beams of a sufficiently high particle density. Only in this case will the yield of nuclear reactions be appreciable.

7.2 Linear Accelerators

A schematic diagram of the Van de Graaf electrostatic generator, which is one of the types of linear accelerators, is shown in Fig. 7.1. Acceleration of the particles occurs in tube T . An ion source made of insulating material (glass, porcelain) and a set of tubular electrodes are located inside the tube. The electrodes are mounted vertically at a small distance from each other. The ion source is placed at one

end of the electrode system and the target M at the other end. The acceleration tube is evacuated to a pressure of 10^{-5} mm Hg. This reduces the probability of collisions between the accelerated ions and air molecules and also of the appearance of gas discharges.

A high voltage (up to 8×10^6 V) is applied to the acceleration tube. The voltage is distributed uniformly between the ion source, tubular electrodes and target by means of a resistor divider.

Ions from the ion source enter the first electrode. In the gap between the source and first electrode the ions obtain their first portion of energy. Within the tubular electrodes the ions move by inertia as there is no electric field there. The second acceleration occurs in the gap between the first and second electrodes etc. The particles striking the target are accelerated to an energy $E = qU$ eV, where q is the particle charge in units of e and U is the voltage applied to the accelerating tube (in volts).

The high voltage is obtained in the following way. By means of a metal brush the charge from a low-voltage generator is applied at point A to an endless belt of insulating material. The charge is collected at point B by a similar brush connected to a metal sphere P called the conductor. The charge accumulates at the outer surface of the sphere and produces a voltage of up to $(5-8) \times 10^6$ V on the conductor which is connected to the accelerating tube.

Notwithstanding the relative simplicity of the Van de Graaff generator it is capable of developing stable particle currents up to 0.1 mA. The generator can be used independently for nuclear investigations or in conjunction with other accelerators as a device for preliminary acceleration.

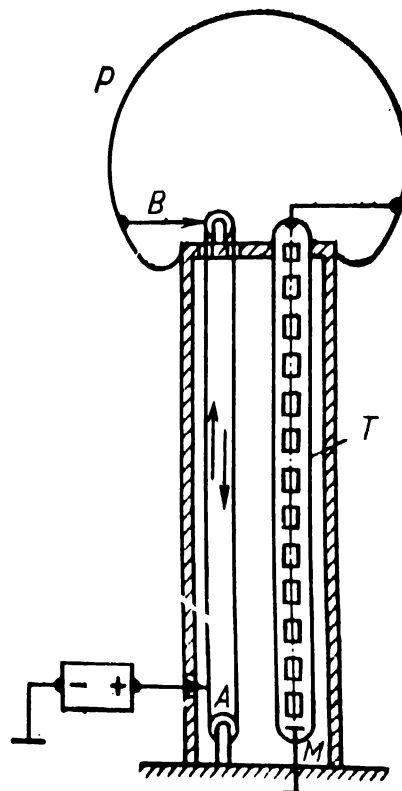


Fig. 7.1 Van de Graaf electrostatic generator

of ions. The particle energy depends on the potential of the conductor which in turn is restricted by charge leakage.

In the accelerating tube of a linear resonance accelerator (Fig. 7.2) the ions are accelerated by repeatedly passing through regions with a potential difference supplied by a high frequency (HF) generator. The length of the cylindrical electrodes increases in the direction of movement of the ions. The time of inertial motion of the ions is the same in

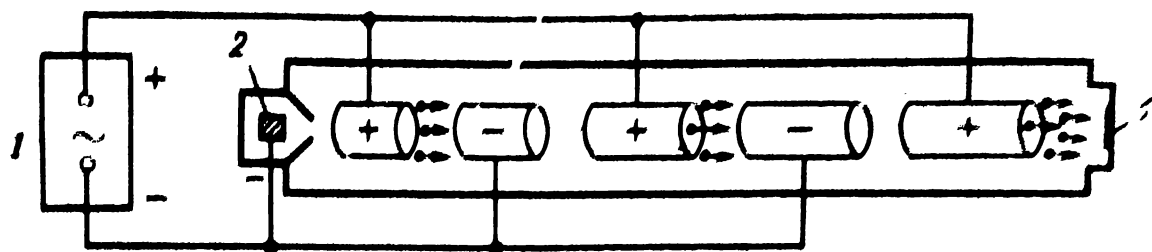


Fig. 7.2 Linear resonance accelerator
1—HF generator; 2—ion source; 3—target

all electrodes and is equal to the half-period of variation of the voltage from the HF generator. The even-number cylindrical electrodes are connected to one terminal of the HF generator and the odd-number electrodes to the other terminal.

Consider a positively charged ion entering the gap between the first and second electrodes. At this instant a positive potential is applied to the odd electrodes and a negative potential to the even electrodes. When the ions begin to move out of the second electrode a positive potential is applied to the even electrodes and a negative potential to the odd ones etc. The time of transit of the ions in each electrode is equal to the period of the alternating potential. For this reason such accelerators are called *resonance accelerators*. Particle energies up to 22 GeV have been attained in linear resonance accelerators. The particles strike the target in pulses at periods equal to that of the HF generator.

7.3 The Cyclotron and Synrocyclotron

If a charged particle moves with a constant velocity in a homogeneous magnetic field perpendicular to its lines of force its path will be a circle. If the mass of the particle is

m , its charge q , velocity v and magnetic flux density B , the radius of the circular path is

$$R = mv/Bq$$

The frequency of revolution v (number of revolutions of the particle per unit time) is equal to the particle velocity divided by the circumference $2\pi R$,

$$v = Bq/2\pi m$$

As long as the mass m is constant the frequency is independent of the particle velocity and this property is exploited for acceleration of particles in the cyclotron.

The cyclotron consists of a magnet with two hollow electrodes (the *dees*) located between the poles of the magnet

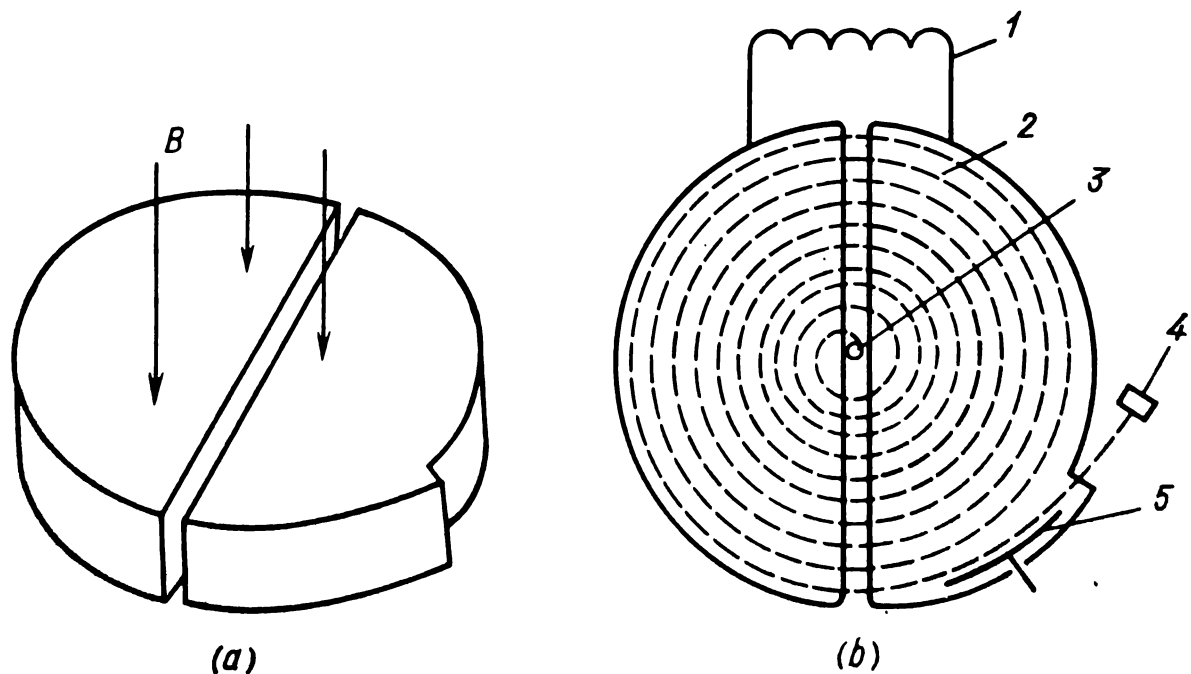


Fig. 7.3 Cyclotron dees (a—general view; b—top view)
1—HF supply; 2—ion trajectory; 3—ion source; 4—target; 5—deflecting electrode

(Fig. 7.3). A comparatively low voltage from a HF generator is applied to the dees and a source of positive ions is placed in the gap between them. The whole system (dees and ion source) is arranged in an evacuated chamber with a pressure of about 10^{-6} mm Hg.

Suppose that the magnetic flux density B is perpendicular to the velocity of the ions, v , and is directed from the reader

to the page and that a positive potential is applied to the right dee. Positive ions emitted from the source are accelerated in the gap and enter the left dee where they move with a constant speed in a circular path in the magnetic field. The frequency of the generator is chosen to equal the frequency of revolution of the ions. After travelling over a semicircle the ions enter the gap between the dees once again and the positive potential is applied to the left dee. A certain amount of energy is imparted to the ions in the gap. After each crossing of the gap the ion velocity increases and the radius of the particle orbit increases correspondingly. The accelerated ions move in a spiral path (Fig. 7.3). At the edge of the device the particle beam is deflected from the chamber onto a target.

Since the particles move in circles the size of the cyclotron is much smaller than that of the linear accelerator and comparatively low voltages may be employed. At the exit of the cyclotron the kinetic energy of the ions is

$$E_a = m_a v_a^2 / 2 = (B^2 R^2 / 2) (q^2 / m_a)$$

Each cyclotron is characterized by the radius of its magnet R and the magnetic flux density B . Therefore, for each given cyclotron the energy of the ions is proportional to the ratio of the squared ion charge to the ion mass. For protons and α -particles the q^2/m_a ratio is the same whereas it is twice as small for deuterons. Hence, the deuteron energy in a cyclotron is one half of that of protons. The final energy of the accelerated ions does not depend on the amplitude of the HF generator. If the voltage applied to the dees is low the ions will execute a larger number of revolutions before leaving the cyclotron than if a higher amplitude voltage is applied. As explained, the energy in both cases will be the same.

At high velocities ($v/c > 0.2$) the ion mass perceptibly increases. Thus the mass of protons with energies of 25 MeV exceeds by 2% the rest mass. With growth of mass the frequency of revolution of the ions decreases and they arrive at the gap at a time which lags behind the time of application of potential to the dees. A result of the difference between the frequencies of the generator and ion revolution is that the ions arrive at the dee gap when the potential is of the wrong

sign and slows down the particles. A limiting energy is thus reached. Protons can be accelerated to 25 MeV and α -particles to 50 MeV.

Higher ion energies can be obtained by applying to the dees a potential whose frequency decreases in step with the frequency of ion rotation. Such accelerators are called *synchrocyclotrons* and they are able to produce ions with energies up to 800 MeV or even more. Acceleration in the cyclotron can be carried out almost continuously since the ions are accelerated at time intervals equal to the period of the HF generator. In the synchrocyclotron only bunches of particles can be accelerated since the generator reduces its frequency with increase of energy of the ions. Protons, deuterons and α -particles are accelerated in the synchrocyclotron. The final energy of the particles is proportional to the square of the radius of the magnet pole faces and hence the magnet of a synchrocyclotron usually weighs several thousand tons. The radius of the synchrocyclotron magnet of the Joint Institute for Nuclear Research in Dubna, for example, is 3 metres and the magnet itself weighs 7000 tons. The device is capable of producing 680 MeV protons, 420 MeV deuterons and 840 MeV α -particles.

7.4 Electron Accelerators

Cyclotrons cannot be employed to accelerate electrons. The electron mass begins to increase noticeably already at 10 keV. Electrons are therefore accelerated in special types of accelerators, in the *microtron*, *betatron* and *synchrotron*.

Microtron. The period of revolution of a charged particle, T , in a stationary magnetic field is proportional to its mass m . If the particle mass could be changed an integral number of times of its rest mass in a small accelerating gap, its period of revolution in a stationary magnetic field would increase by the same number of times. Heavy particles cannot be accelerated in this way as too strong electric fields would be required. However, this method is quite suitable for acceleration of electrons. The accelerator in which this method has been applied is the *microtron* (Fig. 7.4).

A flat vacuum chamber in which electron acceleration occurs is placed between the pole faces of a permanent magnet.

A hollow short tube, the accelerating resonator, is located within the chamber. A HF voltage with a constant frequency $v \approx 3 \text{ GHz}$ is applied to the resonator.

An electron emitter is arranged at the entrance to the resonator. Emission of the electrons is induced by the electric HF field. The electrons obtain the first portion of energy (0.51 MeV) in the resonator; after this they make one revolution in the magnetic field and again enter the resonator in the accelerating phase, the result being an additional 0.51 MeV of energy imparted to them etc. The period of the

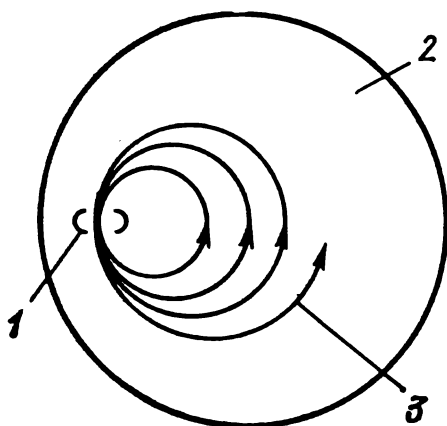


Fig. 7.4 Microtron

1—resonator; 2—region of magnetic field; 3—electron trajectory

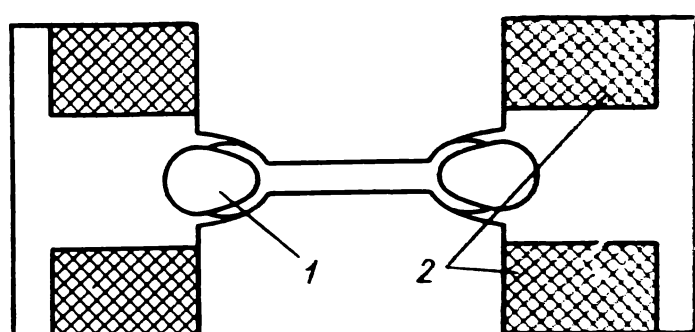


Fig. 7.5 Vertical section of a betatron
1—electron acceleration chamber; 2—electromagnet coil

HF generator, T , is chosen so that it equals the initial period of revolution of the electrons, T_1 . In this case the electrons after each circle enter the resonator in the accelerating phase. The radius of the electron trajectory varies after acceleration in the resonator and approaches the radius of the site of location of the resonator. From the last circle the electrons are deflected out of the microtron. Depending on the design of the microtron the energy increment of the electrons may be 0.51 MeV or a multiple of this quantity.

Electrons can be accelerated up to 50-100 MeV in microtrons. They travel over almost a hundred circles in the vacuum chamber before being deflected out of the microtron. Electrons from the source are pulled out by pulses with a period equal to that of the HF field. The target is therefore bombarded by short electron pulses at intervals of about

3×10^{-4} μ s. The mean electron current is of the order of 100 mA.

Betatron. The betatron works in much the same way as a transformer does. In the latter device two coils of wire are wound around a core. If an alternating electric current is passed through the primary coil an alternating magnetic field will appear in the core. This field induces an electromotive force in the secondary coil and a current will flow if the coil is closed.

In the betatron the secondary coil is replaced by a torus-shaped vacuum chamber. A schematic representation of the cross section of a betatron is shown in Fig. 7.5. The toroid chamber, which is made of glass or porcelain, is placed between the poles of a magnet. The pressure in the chamber is maintained at about 10^{-6} mm Hg. Electrons with an energy of several dozen kilo-electronvolts are injected into the chamber during a time interval up to 0.001 s by means of an "electron gun". The source is a tungsten incandescent filament emitting electrons and an electrode system for focusing and preliminary acceleration of the electrons.

Inside the chamber the electrons move in circles under the action of the electric voltage induced by the varying magnetic field. During acceleration of the electrons the magnetic field strength is increased in such a way as to ensure stability of the electron orbit. Acceleration of the electrons is carried out during the increase of the electric voltage in the coils of the electromagnet from zero to the maximum value, i.e. during a quarter of the period of the power source.

For a stable orbit of radius R the centripetal force F_c is equal to the Lorentz force F_L . The latter force varies along the radius of the accelerating chamber in such a way that for $r > R$, $F_L > F_c$ and for $r < R$, $F_L < F_c$. Hence, any electrons which stray away from the stable orbit are returned to it. During acceleration the electrons execute small oscillations about the stable orbit.

In the first betatron built by Kerst energies of only a few millions of electronvolts were attained. By 1952 betatrons with electron output energies of 300 MeV were in operation. An upper limit to the electron energy obtainable in a betatron exists. Rapidly revolving electrons emit electromagnetic (betatron) radiation. According to the calculations of the

Soviet physicists Pomeranchuk and Ivanenko the energy radiated by an electron during one revolution in the betatron

$$\Delta E \approx 90E_e^4/R \text{ keV}$$

where E_e is the electron energy in GeV and R the orbit radius in metres.

The highest electron energy attainable in the betatron is 500 MeV. Above this energy all energy acquired by the electron during a revolution is lost by betatron radiation.

Synchrotron. An electron with an energy $E_e \geq 2$ MeV moves with a velocity which does not differ appreciably from that of light. Thus the difference between the two velocities is only 2.1% for 2 MeV electrons. This means that for $E_e > 2$ MeV the electron velocity is, for all practical purposes, constant since it cannot exceed the velocity of light. Therefore, further acceleration of the electrons can be carried out as in the cyclotron by using a HF generator. High-energy electrons are obtained in the synchrotron in two stages. In the first the electrons are accelerated in a toroid vacuum chamber, like that in the betatron, up to 2-7 MeV.

The betatron operation is carried out with a small electromagnet in the centre of the chamber. The mass of the magnet is chosen so that saturation of the magnet occurs at electron velocities close to that of light.

After saturation of the inner magnet takes place, synchrotron operation is switched on automatically. The accelerating ring chamber consists of several coupled sections. One of them is replaced by an electric resonator to which a HF generator is connected. On passing through the resonator an electron acquires an energy which is from 4 to 6 times greater than that imparted to an electron making a circle in the betatron. The electrons are confined near the stable orbit by a varying magnetic field in the accelerating chamber in which the ratio of the magnetic flux density B to the electron mass m_e remains constant. The magnetic field is produced by a ring magnet and the accelerating chamber is located between the magnet pieces.

The substitution of a ring magnet for a solid one considerably reduces the mass of the synchrotron magnet. Thus, for acceleration of electrons to 300 MeV in a betatron a

300-400 ton magnet is required whereas the same energy can be obtained in a synchrotron with a 130 ton magnet.

During acceleration the electrons do not move exactly along a stable orbit but oscillate about it. The higher the oscillation amplitude the greater the cross section of the accelerating tube. The cross section area and mass of the ring magnet depend on the sectional area of the accelerating tube. In the earlier synchrotrons considerable deviation of the electrons from the stable orbit were permitted. They were therefore called weak-focusing synchrotrons. Subsequently the oscillation amplitude was considerably reduced and hence magnets with smaller masses could be employed. Such synchrotrons are called strong-focusing synchrotrons. The highest energy which can be obtained in a weak-focusing synchrotron is 1.2-2 GeV; in the strong-focusing synchrotron an energy of 7.5 GeV is attainable.

7.5 Proton Synchrotron

Acceleration of protons in the synchrocyclotron is not rational at energies above 1 GeV as a very heavy magnet would be necessary and the power consumption would be prohibitive. Thus a 10^6 ton magnet would be required to obtain protons with energies $E_p \approx 10$ GeV in the synchrocyclotron. Novel methods of acceleration had to be found in order to push the proton energies still higher. The problem of obtaining fast protons with energies up to 400 GeV was solved in the proton synchrotron (Fig. 7.6).

Protons are accelerated in a toroid vacuum chamber located inside a ring magnet. The magnet consists of four segments connected by linear sectors in which there is no magnetic field. An electric resonator is mounted in one of the linear sectors.

Protons are first accelerated to several million electron-volts in a linear accelerator and then introduced into one of the linear sectors 5 of the toroid chamber. The magnetic field strength is varied at a rate which ensures movement of the protons near a stable orbit. After each passage through the resonator the protons acquire an energy of about 2000 eV. Since the proton velocity increases continuously, whereas the orbit remains the same, the frequency of revo-

lution monotonously increases. Therefore in the first acceleration stage the voltage frequency is varied in the same way as the frequency of revolution of the protons. This stage is analogous to the synchrocyclotron regime of acceleration.

Synchrotron operation is introduced in the second stage after the proton energy exceeds 3 GeV ($v \approx c$). A voltage of

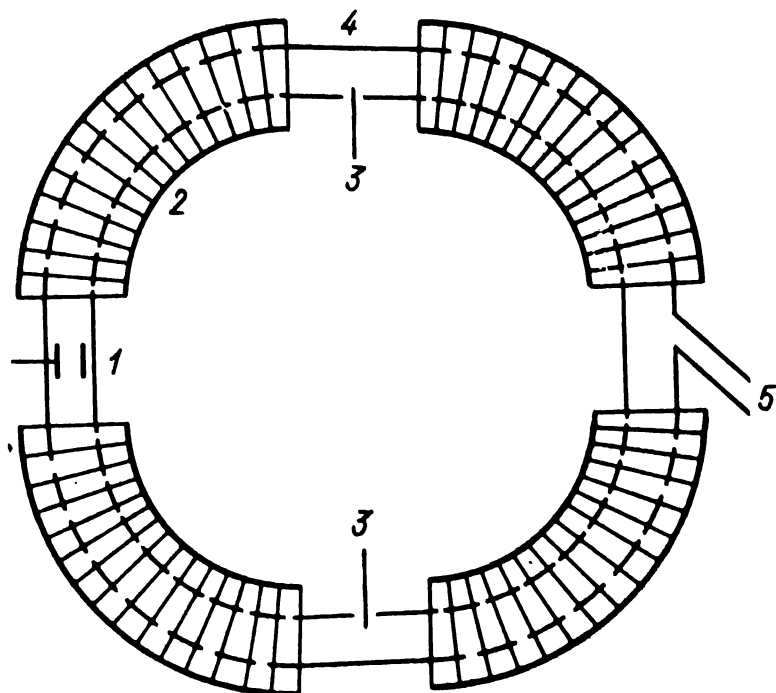


Fig. 7.6 Proton synchrotron

1—resonator; 2—ring magnet; 3—vacuum chamber; 4—proton exit; 5—proton entrance

almost constant frequency is applied to the resonator. Ultimately the proton pulse is deflected out of the device at sector 4 of the proton synchrotron.

The first weak-focusing proton synchrotron was built in the Brookhaven National Laboratory (USA) in 1952. It was called the Cosmotron since the proton energies ($E_p = 3$ GeV) were comparable to those encountered in the cosmic rays. The outer radius of the Cosmotron ring magnet is 10 metres and the mass of the magnet is 2000 tons. A Soviet weak-focusing proton synchrotron began operation in Dubna in 1957. The outer radius of the magnet is 28 metres and the mass of the ring magnet is 36 000 tons. During operation the

accelerator consumes 142 MW. Protons with energies up to 10 GeV can be obtained.

In modern strong-focusing proton synchrotrons energies between 30 and 400 GeV are obtained. The CERN proton synchrotron (Switzerland) delivers 30 GeV protons, the Serpukhov (USSR) accelerator, 76 GeV protons, and the accelerator in Batavia (USA), 400 GeV protons. The average diameter of the Serpukhov accelerator electromagnets is 470 metres and the mass of the electromagnets is 22 000 tons.

CHAPTER 8

NUCLEAR REACTIONS

8.1 General Definition. Nuclear Reaction Equations

Nuclear forces are operative at distances of about 10^{-15} m. If a particle (neutron, proton, deuteron, α -particle or other nuclei) appears within the range of action of nuclear forces a *nuclear reaction* (or simply, a *reaction*) may take place between the nucleus and particle. Just as in the case of radioactive disintegration the number of nucleons and charge are conserved in nuclear reactions. In a nuclear reaction the charge and nucleons are redistributed between the nuclei and particles. On the basis of conservation of charge and number of nucleons one can qualitatively predict the direction of a nuclear reaction.

The first nuclear reaction was observed by Ernest Rutherford in 1919. Nitrogen nuclei were bombarded by 7.7 MeV α -particles from polonium. The potential barrier of the nitrogen nucleus for an α -particle, $V_k = 3.5$ MeV, is almost two times smaller than the kinetic energy of the α -particles. The α -particles therefore easily entered the nitrogen nucleus and induced a nuclear reaction in which $^{17}_8\text{O}$ nuclei and protons were produced. This was the first experimental proof that protons are constituents of the nucleus.

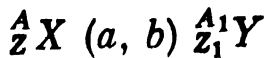
More than ten thousand nuclear reactions have been studied after Rutherford's discovery. What is the purpose of studying nuclear reactions? First of all they yield information on the structure of the nucleus and on the nature of nuclear forces. Secondly, a study of nuclear reactions is important from a practical viewpoint. Thus, the radioactive substances obtained in nuclear reactions are used in many fields of science and engineering.

Nuclear reactions, similar to chemical reactions, can conveniently be represented by an equation. The target nucleus ^{A_Z}X and particle a are shown in the left-hand side of the equation and the products of the reaction, i.e. the nucleus

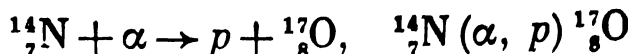
$z_1^A Y$ and emitted particle b , in the right-hand side of the equation:



A shorter notation of a nuclear reaction is



As an example we write down the equation of the first reaction studied in the full and abbreviated forms:



The type of a nuclear reaction is determined by the nature of the bombarding and emitted particles and is denoted as an (a, b) reaction. If the bombarding and emitted particles are identical the (a, a) reaction is said to be one of scattering of particle a . Two types of particle scattering are distinguished. In elastic scattering the nucleus and particle interact as two elastic balls. In a nuclear reaction of this kind the internal state and composition of the nucleus do not change and a redistribution of kinetic energy between the nucleus and particle occurs. The nucleus moving after elastic scattering of a particle is termed a *recoil nucleus*.

Inelastic scattering involves the excitation of the target nucleus without alteration of its composition. Part of the kinetic energy of the inelastically scattered particles is expended in excitation of the nucleus. Since the excited levels of nuclei can assume only discrete energy values, inelastic scattering can occur only if the particle energy exceeds the energy of the first excited energy level. Inelastic scattering is accompanied by emission of γ -quanta by the excited nucleus.

In many experiments with neutrons and in nuclear installations elastic and inelastic scattering are used to slow down neutrons. For example, in experiments designed to study the interaction between matter and slow neutrons ($E_n < 10^3$ eV) the latter are obtained by slowing down fast neutrons ($E_n > 0.1$ MeV), emitted by the source, in materials containing light nuclei ($A \leq 12$) such as those of beryllium, graphite, paraffin.

In the (a, b) reaction the particle a is absorbed and instead of it another particle b is emitted. The composition of the

target nucleus correspondingly changes and hence a nuclear transformation occurs. Some (*a*, *b*) reactions have special names. Thus, the (*a*, γ) reaction is called a reaction of *radiative capture* of particle *a*. Absorption of particle *a* during radiative capture is accompanied by the emission of γ -quanta.

In nuclear reactions involving *inelastic scattering* (or *absorption*)^{*} of particle *a*, nuclei are formed which differ from the target nuclei with respect to their energy state (or composition). Such nuclei are called *product nuclei*.

8.2 Laws of Conservation of Energy and Momentum in Nuclear Reactions

The laws of conservation of energy and momentum are obeyed in nuclear reactions. Let us write down the energy balance for the reaction ${}^A_Z X (a, b) {}^{A_1}_{Z_1} Y$ by taking into account that the total energy of the nuclei and particles is equal to the rest energy plus kinetic energy,

$$M_n (Z, A) c^2 + m_a c^2 + E_1 + E_a = M_n (Z_1, A_1) c^2 + m_b c^2 + E + E_b$$

The subscripts *a* and *b* indicate the particles to which the corresponding quantities refer; E_1 is the kinetic energy of the target nucleus, and E is the kinetic energy of nucleus ${}^{A_1}_{Z_1} Y$. Grouping together the rest energies in the left-hand side and the kinetic energies in the right-hand side we get $[M_n (Z, A) + m_a - M_n (Z_1, A_1) - m_b] c^2 = E + E_b - (E_1 + E_a)$

The change in the kinetic energy, which is equal in absolute value, to the change of the rest energy, is called the *energy of the reaction*, Q . By definition

$$Q = [M_n (Z, A) + m_a - M_n (Z_1, A_1) - m_b] c^2 = \Delta M c^2$$

Replacing the nuclear masses by the masses of the respective nuclides in accordance with formula (3.1) we find that

* Nuclear interactions between particles and nuclei are frequently divided into elastic scattering and nuclear reactions proper. The latter include nuclear interactions in which the energy state of the nucleus is altered (inelastic scattering of particle *a*) or in which the composition of the nucleus is altered (absorption of particle *a*).

the change of the rest mass in the nuclear reaction is

$$\Delta M = M(Z, A) - M(Z_1, A_1) + m_a - m_b - (Z - Z_1)m_e \quad (8.1)$$

If the nuclide and particle masses are expressed in amu units the energy of the reaction will be

$$Q = 931 \Delta M \text{ MeV} \quad (8.2)$$

In an *exoergic* (*exothermic*) reaction ($Q > 0$) part of the rest energy of the target nucleus and bombarding particle is transformed into kinetic energy of the reaction products. As a rule the target nucleus prior to the reaction may be considered as being at rest. Therefore

$$Q = E + E_b - E_a$$

An example of an exoergic reaction is the ${}^5_5\text{B} (n, \alpha) {}^7_3\text{Li}$ reaction. The energy of the reaction, Q , can be calculated for it as follows. The nuclide and neutron masses according to Table 3.1 are

$$M({}^5_5\text{B}) = 10.0129 \text{ amu}, \quad M({}^7_3\text{Li}) = 7.0160 \text{ amu}, \\ m_n = 1.0087 \text{ amu}, \quad M({}^4_2\text{He}) = 4.0026 \text{ amu}$$

The total rest mass before the reaction is 11.0216 amu and after the reaction 11.0186 amu. The decrease in the rest mass $\Delta M = 11.0216 - 11.0186 = 0.0030 \text{ amu}$.

According to formula (8.2)

$$Q = 931 \Delta M = 931 \times 3 \times 10^{-3} \approx 2.8 \text{ MeV}$$

In an *endoergic* (*endothermic*) reaction ($Q < 0$) the sum of the rest mass of the target nucleus and bombarding particle is less than the rest mass of the reaction products by $\Delta M = -Q/c^2$. This mass increment is the result of transformation of the kinetic energy into rest energy. Endoergic reactions take place if the kinetic energy of the particle a exceeds the threshold energy E_{th} . Such reactions are therefore called threshold reactions. The threshold energy ensures the mass increase by ΔM in the nuclear reaction. No endoergic reaction can take place if the energy of the bombarding particle is less than the threshold value. An example of a threshold reaction is that of inelastic scat-

tering of particles or the ${}^1\text{H}(p, n){}^2\text{He}$ reaction for which $Q = -0.783$ MeV.

The law of conservation of momentum in a nuclear reaction involving a target nucleus at rest can be written down in the form of the vector equation

$$m_a \mathbf{v}_a = M_n \mathbf{v}_n + m_b \mathbf{v}_b$$

The law of conservation of momentum can be used to find the relation between the threshold energy E_{th} and energy Q in a threshold reaction. After a collision between the particle and target nucleus a compound nucleus is formed (see 8.3) whose mass $M_C \approx M_n + m_a$. For a target nucleus at rest the momentum of the compound nucleus is equal to that of the particle a . Since the particle a and the compound nucleus C move in the same direction it follows that

$$m_a v_a = M_C v_C$$

Part of the energy E_a which is equal to the kinetic energy E_C of the compound nucleus is spent in fulfilling the law of conservation of momentum. Taking into account that the masses $M_n(Z, A) \approx A$ amu, $m_a \approx A_a$ amu and $M_C \approx A + A_a$ amu, we get

$$E_C = \frac{M_C v_C^2}{2} = \frac{M_C}{2} \left(\frac{m_a}{M_C} \right)^2 v_a^2 \approx \frac{A_a}{A + A_a} E_a$$

That part of the kinetic energy of the particle which is transformed into the rest energy of the compound nucleus is the difference between the kinetic energies of the particle and compound nucleus,

$$\Delta Mc^2 = E_a - E_C = \frac{A}{A + A_a} E_a$$

The smallest mass increment required for the threshold reaction to occur is $\Delta M = -Q/c^2$ and in this case the kinetic energy E_a of the particle is equal to the threshold energy. Substituting in the latter equation

$$\Delta Mc^2 = |Q| \text{ and } E_a = E_{th}$$

we find

$$E_{th} = \frac{A + A_a}{A} |Q| \quad (8.3)$$

If the mass number $A_a \ll A$ then

$$E_{th} \approx |Q|$$

Let us determine the threshold energy for the ${}^4\text{Be}(p,n){}^3\text{B}$ reaction. The nuclide and neutron masses are (see Table 3.1)

$$M({}^4\text{Be}) \approx 9.0122 \text{ amu}, M(\text{H}) \approx 1.0078 \text{ amu},$$

$$m_n \approx 1.0087 \text{ amu}, M({}^3\text{B}) \approx 9.0133 \text{ amu}$$

The increase of the rest mass in the reaction is

$$\Delta M = 9.0133 + 1.0087 - (9.0122 + 1.0078) \approx 0.002 \text{ amu}$$

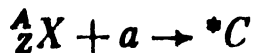
The energy of the reaction $Q = -931 \Delta M \approx -1.9 \text{ MeV}$. The threshold energy for the proton

$$E_{th} = \frac{9+1}{9} \times 1.9 \approx 2.1 \text{ MeV}$$

It would be wrong to substitute A and A_a (in amu) for the masses of the atoms and particles when calculating ΔM and Q as this leads to erroneous results. In the last example such an approximation with $M_n({}^4\text{Be}) \approx 9 \text{ amu}$ and $M(\text{H}) \approx 1 \text{ amu}$ yield $\Delta M = 0$ and $E_{th} = 0$.

8.3 The Compound Nucleus

Investigations of nuclear reactions have yielded much information which underlies the theory of nuclear transformations. One such theory is the theory of the compound (intermediate) nucleus developed by Niels Bohr in 1936. It satisfactorily explains nuclear transformations induced by particles with energies up to 50 MeV. According to this theory a nuclear reaction represented as ${}^A_Z X(a, b){}^{A_1}_Z Y$ takes place in two stages. In the first stage the particle a is captured by the ${}^A_Z X$ nucleus. As a result a compound nucleus C is formed in the excited state



(the asterisk indicates that the nucleus is in the excited state). The excitation energy W_{ex} of the compound nucleus is the sum of the binding energy e_a of particle a in the compound

nucleus and of part of the kinetic energy of the particle, E_a , which is transformed into rest energy of the compound nucleus,

$$W_{ex} = \varepsilon_a + \frac{A}{A+A_a} E_a$$

For $A_a \ll A$

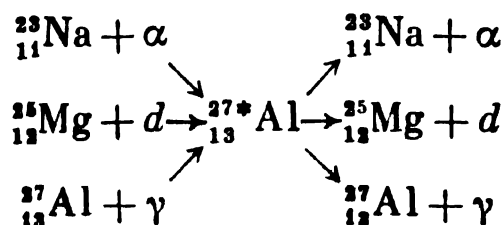
$$W_{ex} \approx \varepsilon_a + E_a$$

In view of the fact that the nucleons interact strongly, the excitation energy is rapidly distributed almost uniformly among the nucleons. Suppose that the excitation energy of nucleus C is sufficient for ejection of a particle b but this does not occur because of the energy being distributed among the nucleons. However, the nucleons collide frequently and a result may be that most of the excitation energy is transferred to a particle b located in the surface layer of the compound nucleus. In the next stage the compound nucleus splits into a nucleus $z_1^A Y$ and the particle b ,

$$*C \rightarrow z_1^A Y + b$$

The lifetime of a compound nucleus, $\tau_C = 10^{-14}-10^{-13}$ s, is much greater than the characteristic nuclear time τ_n during which a particle a travels over a distance comparable to the radius of the nucleus, R . Thus for an α -particle moving at $v_\alpha \approx 10^9$ cm/s, the nuclear time $\tau_n = R/v_\alpha \approx \approx 10^{-12}/10^9 = 10^{-21}$ s which is 10^8 times smaller than the lifetime of a compound nucleus.

A consequence of the long lifetime of the compound nucleus is that its formation and decay are independent events. The mode of decay of the compound nucleus depends only on the excitation energy. The transformation of a nucleus via the compound nucleus can be illustrated by the following example:

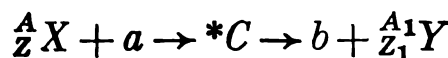


The ${}^{27*}_{13} \text{Al}$ compound nucleus can be formed either as a result of absorption of an α -particle by the ${}^{23}_{11} \text{Na}$ nucleus,

or a deuteron by the $^{25}_{11}\text{Mg}$ nucleus or a γ -quantum by the $^{27}_{13}\text{Al}$ nucleus. If the excitation energy of $^{27*}_{13}\text{Al}$ exceeds the binding energy of an α -particle in it, or of a deuteron, the compound nucleus may emit either of these particles or go over to the ground state with emission of one or several γ -quanta. If, however, the excitation energy of $^{27*}_{13}\text{Al}$ is less than the binding energy of the α -particle or deuteron it can emit only γ -quanta and change into the $^{27}_{13}\text{Al}$ nucleus. The product nucleus $^{A_1}_{Z_1}\text{Y}$ formed after decay of the compound nucleus may also be in the excited state, and in this case it can also emit γ -quanta.

The nuclear interaction leading to a given compound nucleus is referred to as the *input channel* and the mode of decay of the compound nucleus as the *output channel*. In the example presented above there are three input and three output channels of the reaction.

A complete notation of a nuclear reaction which includes the compound nucleus is



As a rule it is the input and output channels which are of interest and hence the compound nucleus $*C$ is usually not indicated in the equation of the reaction.

8.4 Effective Cross Section and Yield of a Nuclear Reaction

The equation of a nuclear reaction gives only a qualitative description of the interaction between the particles and nuclei. It tells nothing about the efficiency of the interaction. In order to define the quantity which characterizes the probability of interaction between a particle and nucleus consider a thin plane target made of homogeneous substance containing N_s nuclei per square metre. Suppose a beam of monoenergetic particles is incident on the target surface in the perpendicular direction (Fig. 8.1). For the sake of simplicity let the bombarding particles be neutrons. Each neutron passing through the square metre of the target can interact with any of the N_s nuclei. If the neutron flux density is ϕ the number of possible neutron-nucleus interactions per second per 1 m^2 target will be ϕN_s . However, the inter-

action between a neutron and nucleus is a random event and not all but only a few of the possible interactions take place. The number of nuclear reactions Π actually occurring each second in 1 m³ of the target is proportional to φN_s ,

$$\Pi = \sigma \varphi N_s$$

The proportionality coefficient σ is numerically equal to the probability of interaction between the neutron and nucleus on condition that a beam of neutrons of unit flux density

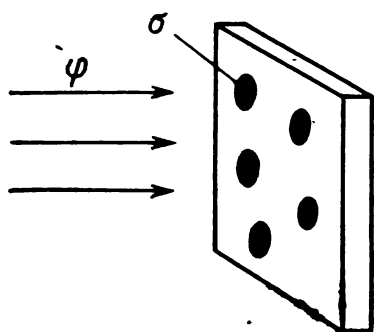


Fig. 8.1 Schematic representation of reaction cross sections (black circles) in a flat target

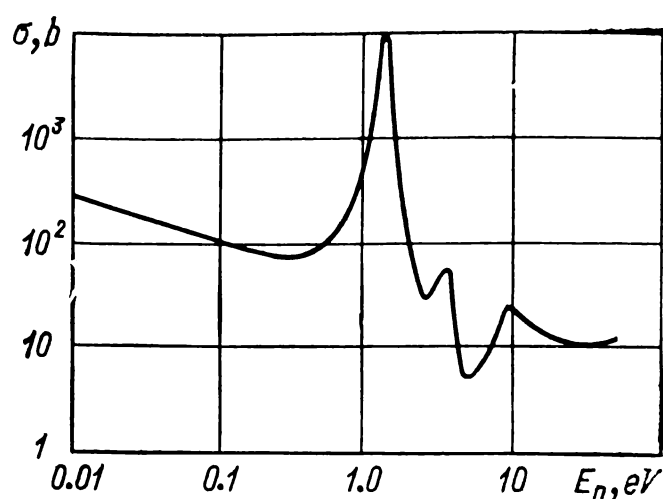


Fig. 8.2 Dependence of the reaction cross section σ for ^{115}In on neutron energy E_n

($\varphi = 1$ neutr./m²·s) is incident on the target surface and there is only one nucleus per 1 m² of the target ($N_s = 1$ nucleus/m²).

The latter equation can be rewritten in the form

$$\sigma = \Pi / \varphi N_s$$

From the dimensions $[\Pi] = \text{m}^{-2} \cdot \text{s}^{-1}$, $[\varphi] = \text{m}^{-2} \cdot \text{s}^{-1}$ and $[N_s] = \text{m}^{-2}$ it can be seen that effectively σ is an area referred to a target nucleus. The neutron induces a nuclear reaction whenever it crosses the surface of a conditional sphere (black circles in Fig. 8.1) with a sectional area σ . The cross section for all nuclei of a 1 m³ target is σN_s . Thus of the φ neutrons uniformly incident per second on 1 m³ of the target, $\sigma N_s \varphi$ neutrons will react with the nuclei.

The quantity σ is called the *effective cross section for the reaction* of interaction between the particles and nuclei (or shorter, the *reaction cross section* or simply *cross section*). The cross section for a reaction and the geometric sectional area of nuclei are of the order of 10^{-28} m^2 . Consequently for the sake of convenience a special unit for nuclear cross sections has been chosen which is called the *barn*, $1 \text{ b} = 10^{-28} \text{ m}^2$.

The reaction cross section σ and geometric cross section of a nucleus in general differ. Thus the reaction cross section for ^{235}U and 0.025 eV neutrons is 705 b whereas the geometric cross section is only about 2.5 b. This difference is due to the wave properties of the particles interacting with the nuclei. Because of this the reaction cross section not only differs from the geometric value but also depends on the particle energy.

The cross section for the reaction between ^{115}In and neutrons as a function of neutron energy is shown on a logarithmic scale in Fig. 8.2. Up to $E_n \approx 0.5 \text{ eV}$ the cross section varies inversely proportional to the neutron velocity v ($1/v$ law). For energies $E_n > 0.5 \text{ eV}$ the energy dependence of σ is similar to that for the probability density $f(W)$ (Sec. 3.3). The cross section peaks σ_{ri} are located at certain neutron energies E_{ri} . The most probable energies of a compound nucleus level $W_i = \varepsilon_n + \frac{A}{A+1} E_{ri}$ correspond to these peaks (ε_n is the binding energy of the neutron in the compound nucleus). The energy range in which the cross section $\sigma(E_n)$ possesses a peak and also the values of σ_r and E_r and finally the cross section peaks themselves are called *resonance* values. The ^{115}In nuclide has several peaks in the resonance region. The highest resonance peak ($\sigma_r = 3 \times 10^4 \text{ b}$) is located at the resonance energy $E_r = 1.44 \text{ eV}$.

With increase of energy the peak heights which correspond to other excited states decrease, and the energy levels become broader. For kinetic energies $E_n \sim 1 \text{ keV}$ the level spacing of heavy nuclei is less than the resolution of the measuring instruments and the levels cannot be separated. As a result the cross section σ measured experimentally decreases and monotonously approaches the geometric cross section of the nucleus πR^2 .

The potential barrier impedes the interaction between a charged particle and the nucleus. If the kinetic energy of the bombarding particles is less than the height of the potential barrier not all particles interacting with the nucleus will induce a nuclear reaction. Some will be scattered by the electric field of the nucleus. The others which do pass through the barrier may evoke a nuclear reaction. The fraction of particles penetrating the potential barrier in collisions with nuclei is equal to the transmission coefficient D .

The energy of charged particles interacting with a nucleus is not equal to the energy E the particle had at the surface of the target. Before encountering the nucleus a charged particle spends part of its energy on ionization and excitation of the target atoms. The longer the path the particle travels before colliding with the nucleus, the higher the ionization losses in the target and the less the energy of the particle. Thus nuclear reactions are induced by charged particles with energies between $E - \Delta E$ and E , where ΔE is the ionization loss of the particle in the target.

Ionization losses are not substantial in thin targets with thicknesses much less than the path length of the particle. In such targets the energy of charged particles is practically constant.

If allowance is made for the transmittance of the nuclear potential barrier, the reaction rate per 1 m^2 of a thin target for a flux density of monoenergetic particles ϕ can be written as

$$\Pi = \sigma D \phi N_s$$

The product σD can be determined on the basis of experimental measurements. This quantity is usually accepted as the reaction cross section and denoted simply as σ . It takes into account the effect of the nuclear and electric properties of the target nucleus and also the properties of the particle of formation of the compound nucleus. The transmission coefficient D rapidly increases with growth of the particle energy and is unity at particle energies exceeding the height of the potential barrier, V_h . The reaction cross section behaves in a similar manner.

A typical dependence of the reaction cross section σ on energy of a charged particle E_a is shown in Fig. 8.3.

The cross section becomes noticeable at an energy $E_a \sim \sim 0.5 V_k$. It then grows rapidly and at energies $E_a > V_k$ gradually approaches the geometric cross section of the nucleus, πR^2 . For some reactions such as $^{27}_{13}\text{Al} (\alpha, p) ^{20}_{14}\text{Si}$ several resonance peaks on the cross section curve are observed at energies up to $E_a \approx V_k$.

Let σ denote the cross section for formation of a compound nucleus. The various modes of decay of the compound nucleus can be characterized by the respective cross sections. Thus σ_s is the elastic scattering cross section, σ_{in} the inelastic scattering cross section and σ_a the particle absorption cross section [for an (a, b) reaction]. The ratios σ_s/σ , σ_{in}/σ and σ_a/σ are the probabilities of compound nucleus decay involving elastic scattering, inelastic scattering or particle absorption respectively. Of a total of Π nuclear reactions $(\sigma_s/\sigma)\Pi$ particles are scattered elastically, $(\sigma_{in}/\sigma)\Pi$ particles are scattered inelastically and $(\sigma_a/\sigma)\Pi$ particles are absorbed by the nucleus. Since the excited compound nucleus must certainly decay via one of the output channels the total probability of its decay

$$\sigma_s/\sigma + \sigma_{in}/\sigma + \sigma_a/\sigma = 1$$

and hence

$$\sigma = \sigma_s + \sigma_{in} + \sigma_a$$

The reaction yield Y is directly related to the cross section of a reaction. It is defined as the fraction of particles which interact with the target nuclei. The reaction yield Y can be found by dividing the reaction rate per square metre of the target by the particles flux density φ . In a thin target the flux density and particle energy do not vary significantly and hence may be regarded as constant quantities. In this particular case the reaction rate per m^2 of target is

$$\Pi_t = \sigma_t N_t \varphi$$

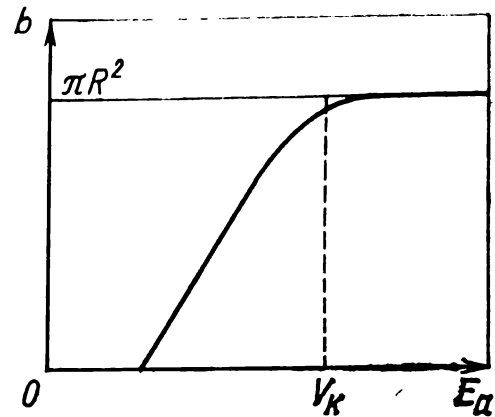


Fig. 8.3 Dependence of reaction cross section σ on energy E_a of a charged particle

where N_s is the number of nuclei per square metre of the target, nucl./m²; σ_i is the cross section for an i th reaction ($i = s, \alpha, a$). Dividing the reaction rate by the flux density φ we obtain the reaction yield for a thin target,

$$Y_i = \sigma_i N_s \quad (8.4)$$

The number of nuclei in a target of 1 m² area and 1 m thickness is equal to the number of atoms in a cube of 1 m³ volume and therefore for a 1 m² target with a thickness δ the number of nuclei will be

$$N_s = \frac{\rho \delta}{A} 6.02 \times 10^{26} \text{ nucl./m}^2$$

Inserting this expression for N_s into formula (8.4) we obtain

$$Y_i = \frac{\sigma_i \rho \delta}{A} 6.02 \times 10^{26}$$

Example. Find the yield of the reaction of absorption of 0.025 eV neutrons in a thin copper target of thickness $\delta = 1$ mm; for copper $\sigma_a = 3.77$ b, $\rho = 8.89 \times 10^3$ kg/m³, $A = 63.5$.

$$N_{Cu} = \frac{8.89 \times 10^3}{63.5} 6.02 \times 10^{26} = 8.42 \times 10^{28} \text{ nucl./m}^3$$

The number of nuclei in a 1 mm thick target of 1 m² area is

$$N_s = 8.42 \times 10^{28} \times 10^{-3} = 8.42 \times 10^{25} \text{ nucl./m}^2$$

The reaction yield according to formula (8.4) is

$$Y_s = 3.77 \times 10^{-28} \times 8.42 \times 10^{25} \approx 3.2 \times 10^{-2}$$

8.5 Nuclear Reactions Induced by Charged Particles. The Nuclear Photoeffect

Reactions induced by α -particles. Information on the structure of the nucleus was first obtained in studies of the (α, b) reaction. By using natural α -emitters physicists were able to establish some regularities pertaining to nu-

clear reactions which later were employed, for example, to develop the model of the compound nucleus.

Besides the first reaction of this kind, $^{14}\text{N}(\alpha, p)^{17}\text{O}$, other important reactions were discovered. Of special importance are the (α, n) reactions. Neutrons were first obtained in the $^{9}\text{Be}(\alpha, n)^{12}\text{C}$ reaction in which beryllium was bombarded by α -particles. Even at present (α, n) reactions are used as laboratory sources of neutrons.

Most (α, n) reactions terminate in the formation of unstable, positron-emitting nuclei. Some artificial radioactive substances have been obtained by means of these reactions.

Reactions induced by protons. The potential barrier of a nucleus is twice as low for protons as for α -particles. The (p, b) reaction can therefore proceed at lower energies. Protons with energies up to 400 GeV can be obtained in particle accelerators.

The splitting of lithium by protons was first observed by Cockcroft and Walton. Protons were accelerated in a linear accelerator up to 700 keV. Under the action of the protons the ^7Li nucleus splits into two α -particles. The $^7\text{Li}(p, \alpha)^4\text{He}$ reaction is exoergic with a reaction energy $Q = 17.3$ MeV. When the reaction proceeds along a different output channel, $^7\text{Li}(p, \gamma)^7\text{Be}$, gamma quanta with an energy $E_\gamma = 17.3$ MeV are emitted.

Reactions induced by deuterons. The deuteron consists of two nucleons, the proton and neutron. Its binding energy is 2.225 MeV which is less than in other multinucleon nuclei. The weak binding of the nucleons in the deuteron explains some features of the (d, b) reaction. This type of reaction may proceed via the compound nucleus, in which case the deuteron is absorbed by the target nucleus; however, it may also proceed without the formation of a compound nucleus by the so-called "direct" reaction. At low deuteron energies the neutron penetrates the nucleus and is stripped from the proton which cannot enter the nucleus because of the repelling coulomb forces. A result of this breaking of the neutron-proton bond is that the direct (d, p) reaction takes place.

With increase of deuteron energy the probability that the proton surmounts the potential barrier and enters the nucleus increases. In this case two competing direct reactions, (d, p) and (d, n) , occur. Radiative capture of deuterons is a rare

event because on absorption of the deuteron the target nucleus is excited to an energy $W_{ex} = \epsilon_n + \epsilon_p - 2.225 \approx 14 \text{ MeV}$, where $\epsilon_n = \epsilon_p \approx 8 \text{ MeV}$ is the proton-neutron binding energy in the compound nucleus. With such a high excitation energy the compound nucleus ejects with a higher probability a nucleon rather than emit a γ -quantum.

Nuclear photoeffect. Absorption of a γ -quantum by a nucleus may induce either the (γ, n) or (γ, p) reaction. These reactions are said to occur in the nuclear photoeffect. Energetically the nuclear photoeffect can occur only if the energy of the γ -quantum is greater than the nucleon binding energy in the nucleus. The threshold of the photoeffect is particularly low for the deuteron in the ^4Be nucleus. The deuteron can be split into a proton and neutron by 2.225 MeV γ -quanta and the threshold energy of the $^9\text{Be}(\gamma, n) ^8\text{Be}$ reaction is only 1.67 MeV.

8.6 Nuclear Reactions at High Energies

Absorption of particles with energies of 10-50 MeV results in the formation of a strongly excited compound nucleus. The excitation energy is so high that it is sufficient for the ejection of several nucleons. For example, 20 MeV neutrons can induce the $^{12}\text{C}(n, 2n) ^{11}\text{C}$ and $^{63}\text{Cu}(n, 3n) ^{61}\text{Cu}$ threshold reactions. The kinetic energy of the neutrons in these cases is used to remove one or two neutrons from the compound nucleus.

For energies $E_a \gg \epsilon_N$, where ϵ_N is the binding energy of a nucleon in the nucleus, the particle practically interacts with a free nucleon. Thus for energies $E_a > 50 \text{ MeV}$ the compound nucleus model cannot yield a correct description of the mechanism of nuclear reactions.

In a collision between a very fast particle and a nucleon the latter may be expelled directly from the nucleus. It is moreover possible that several nucleons will be ejected simultaneously, the number of emitted particles increasing with energy of the bombarding particle. Such a cascade of particles produced by a 300 GeV proton in a photographic emulsion is shown in Fig. 8.4. Nineteen tracks of secondary protons diverge from the point of collision between the impinging proton and the nucleus. The tracks resemble rays from

a star and hence the visible part of the particle cascade is called a star. Neutrons, in contrast to protons, do not pro-

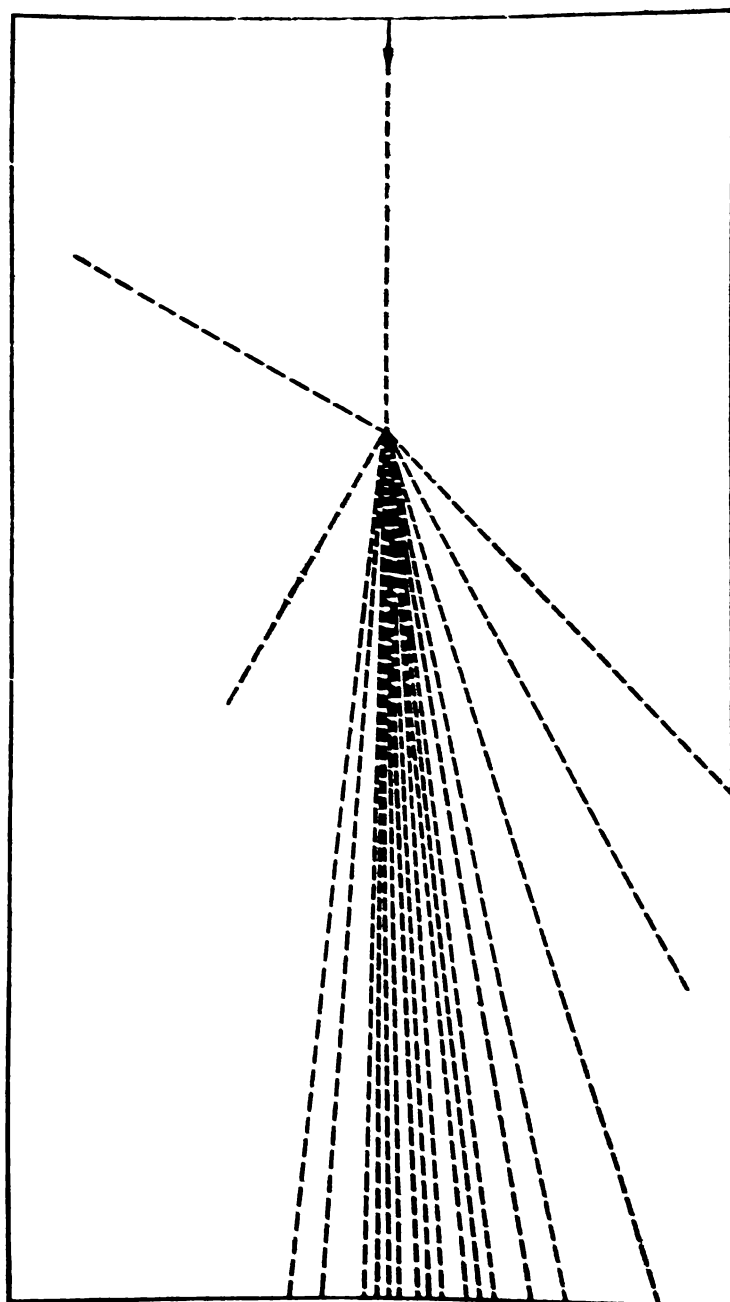


Fig. 8.4 Nuclear star consisting of 19 rays. The energy of the primary proton was 300 GeV

duce any visible track in the photographic emulsion and therefore it is not possible to determine the total number of particles in the cascade by counting the number of star rays.

8.7 Thermonuclear Reactions

Matter heated to several million degrees radically changes its properties. At such temperatures the atoms are completely ionized and an electron-nuclear gas or *plasma* is formed which consists of free nuclei and electrons. Plasmas are usually termed in accordance with the type of nuclei they are

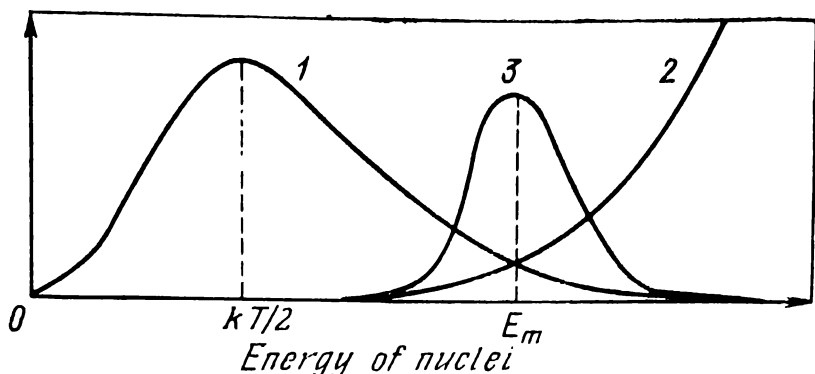


Fig. 8.5 Maxwellian distribution of nuclei in a plasma (1), absorption cross section (2) and reaction yield (3) as a function of energy of nucleus

made of (proton, deuteron etc.) or with the type of atoms yielding the nuclei (deuterium, tritium etc.)

The nuclei and electrons in a plasma move with enormous speeds. As a result of numerous collisions between the particles in the plasma a Maxwellian velocity distribution is established.

The transmittance of a potential barrier for two interacting nuclei depends on their relative kinetic energy E . For two nuclei moving toward each other with the same kinetic energy E_n the value of E will be $4E_n$. If the nuclei move in the same direction their relative kinetic energy will be $E = 0$.

A Maxwellian energy distribution of nuclei in a plasma, $f(E)$, is depicted in Fig. 8.5, curve 1. With increase of energy E the function $f(E)$ at first increases, reaches a maximum at $E = kT/2$ and then rapidly falls off. In a plasma there are slow nuclei with energies $E \ll kT$ as well as a small fraction of "hot" nuclei with $E \gg kT$.

Two light nuclei colliding in a plasma or target may coalesce and form a nucleus which is heavier than either of the two initial nuclei. This process is accompanied by the release

of energy. Reactions of this kind are called *nuclear fusion reactions*. The dependence of the cross section for absorption of one of the nuclei by the other as a function of energy E is shown by curve 2 in Fig. 8.5. With increase of E the transmittance of the potential barrier increases and σ_a sharply rises. For a given energy E the yield $Y(E)$ of a fusion reaction is proportional to the product $\sigma_a(E) f(E)$. Nuclear fusion chiefly occurs near the maximum of the yield $Y(E_m)$ (curve 3). At energies far from E_m ($E \ll E_m$ and $E \gg E_m$), $Y(E) \approx 0$. In the first of these energy ranges the cross section σ_a is small and in the second the relative number of particles is insignificant. The area bounded by curve $Y(E)$ and the energy axis is proportional to the amount of energy released from the plasma. As the temperature of the plasma increases the maximum of the Maxwell spectrum shifts to higher energies. Correspondingly, more nuclei will possess high values of σ_a and hence the energy release will be higher.

At a certain temperature, called the *ignition temperature* T_0 , the fusion process will be self-sustaining. This means that the energy liberated in the plasma is sufficient to keep the plasma temperature constant and to compensate for energy losses and in particular for the energy radiated by the plasma. As the temperature T exceeds more and more T_0 the rate of nuclear fusion increases as does the amount of energy liberated and an explosion might develop. The fusion reaction in a plasma is intimately related to the thermal motion of the nuclei and temperature of the plasma and for this reason such reactions occurring in hot plasma are called *thermonuclear reactions*.

The ignition temperature depends on three factors: on the plasma density, composition and volume. The density of nuclei in a plasma is proportional to the density of the plasma itself. With increase of the plasma density the rate of the thermonuclear reactions also grows and consequently the ignition temperature is reduced. In other words the higher the density the lower is the ignition temperature.

The reaction cross section σ_a depends on the type of nucleus. For a given energy it is greater for deuterons interacting with deuterons than for protons interacting with protons. Therefore, if the densities of the nuclei and the plas-

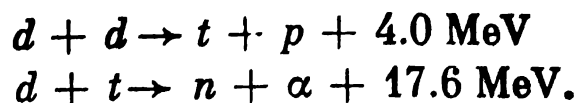
ma temperatures are the same the rate of energy release will be higher in a deuterium plasma than in a proton plasma and the ignition temperature will be lower in the former plasma.

Energy losses from a plasma of infinite volume will be insignificant and the ignition temperature will be minimum. Energy loss through the surface will become appreciable as the plasma volume is decreased. An additional amount of energy must be released in order to compensate for this loss. The ignition temperature of a finite-sized plasma is therefore higher than that of an infinite plasma.

The temperature in the interior of some stars is 20-30 million degrees. Stellar plasmas consists mainly of protons. The plasma is compressed by enormous pressures and the density is about 100 g/cm^3 . This corresponds to a proton density of approximately 6×10^{26} per cubic centimetre. In such dense proton plasmas the synthesis of α -particles occurs and 26.7 MeV of energy per α -particle is liberated. All energy produced in the plasma is expended in radiation through the surface and in maintenance of the star temperature.

Thermonuclear reactions in a hydrogen plasma proceed at a very low rate. Over ten billion years are required for the synthesis of an α -particle in the solar plasma. Thus even in the dense solar plasma the energy yield is only about $2 \times 10^{-4} \text{ W/kg}$.

Scientists from many countries of the world are working on the problem of controlled thermonuclear synthesis of α -particles from deuterons and tritons. The following reactions take place in deuterium-tritium plasmas:



The cross section for the second reaction is much bigger than that for the first reaction. As a result of this the two reactions proceed sequentially in the deuterium plasma whereas the second reaction is predominant in the deuterium-tritium plasma.

Before thermonuclear reactions are made to serve the needs of man quite a few complex problems will have to be solved. A controlled thermonuclear reaction will occur in a device called a *thermonuclear or fusion reactor*. On the earth it is difficult to obtain a plasma as dense as that in the sun because

no materials exist which can withstand pressures of several million atmospheres. In a fusion reactor the plasma density will necessarily be small and the temperature will be maintained at tens or hundreds of millions of degrees. It is hoped that at such temperatures a satisfactory rate of energy release will be achieved. The heated plasma must be confined in some way in the compressed state and be insulated thermally from the reactor walls since the melting temperature of even the most infusible materials do not exceed a few thousand degrees.

Scientists are trying to solve the problems of plasma confinement and thermal insulation by employing inhomogeneous magnetic fields. A charged particle moving along a magnetic line of force to a region of higher field strength is reflected by the field as a light ray is reflected by a mirror. Such reflecting magnetic fields have been called *magnetic mirrors*.

The plasma is located in a vacuum chamber. Inside the chamber a magnetic field is produced with a flux density decreasing toward the centre of the chamber. This type of magnetic field compresses the plasma near the centre of the chamber and separates it from the chamber walls. Thus the inhomogeneous magnetic field serves as a thermal insulator. A chamber with magnetic thermal insulation is said to be a *magnetic trap*.

The creation of reliable thermal insulation is a formidable task. One of the causes of instability of a plasma is the diffusion of the charged particles. As a result of collisions between themselves the particles change their motion in the plasma and some of them escape through the magnetic insulation. Other causes of plasma instability are fluctuations of the plasma volume, nonuniformity of temperature and density of the nuclei in the plasma. These factors alter the configuration of the external magnetic field and facilitate particle escape from the plasma.

The plasma in a fusion reactor is heated to the ignition temperature T_0 . During the time of existence of the plasma, τ , called the *period of confinement*, an amount of nuclei proportional to $N\tau$ will react (N is the density of nuclei in the plasma). The quantity $N\tau$ is called the *confinement parameter*.

The power of a fusion reactor can be divided into two components. Charged particles produced in the thermonuclear reaction are slowed down in the plasma itself. This deceleration of charged particles yields about 20% of the power. About 80% (the second component) is carried off by neutrons.

For a plasma of a given composition and volume V there is a minimal value of the confinement parameter $(N\tau)_0$ for which the first power component compensates the power required for maintaining the plasma at the suitable temperature. The quantity $(N\tau)_0$ is called the *Lawson criterion*. For a deuterium-tritium plasma ($T_0 \approx 10^8$ K) $(N\tau)_0 = 3 \times 10^{14}$ s/cm³ and for a deuterium plasma ($T_0 \approx 5 \times 10^8$ K) $(N\tau)_0 = 10^{16}$ s/cm³. Ignition of a deuterium-tritium plasma therefore occurs at lower temperatures and lower values of the Lawson criterion than ignition of a deuterium plasma. For this reason deuterium-tritium plasmas will be employed in the first thermonuclear reactors.

Investigations on controlled thermonuclear fusion of nuclei were initiated in the Soviet Union at the beginning of the 1950's. The theoretical and experimental studies of the properties of plasma were carried out by such outstanding scientists as Academicians I. V. Kurchatov and L. A. Artsimovich. As a result of several decades of work it seems that the design of power thermonuclear reactors may be feasible in the near future.

One of the best studied models of a fusion reactor is the Tokamak installation. The name is derived from the first letters of the Russian words "tok" (current), "kamera" (chamber) and "magnitnaya katushka" (magnetic coil).

The Tokamak consists of an air-tight toroidal chamber with two concentric walls (Fig. 8.6). The inner steel wall and outer copper wall are separated by a vacuum gap and are insulated from each other electrically. Magnetic coils producing a longitudinal magnetic field in the chamber are mounted on the copper wall. The chamber and magnetic coils are placed on a magnetic core with the primary coil. The Tokamak is essentially a transformer with a one-turn secondary coil (the plasma).

Before being filled with gas (deuterium or deuterium-tritium mixture) a high vacuum is created in the chamber. Af-

ter introduction of the gas at low pressure the primary coil is energized and breakdown and ionization of the gas take place. The electric current flowing in the ionized gas heats it to a high temperature.

Magnetic thermal insulation is produced by superimposing two magnetic fields. The first and major magnetic field is that created by the electric current in the plasma. It

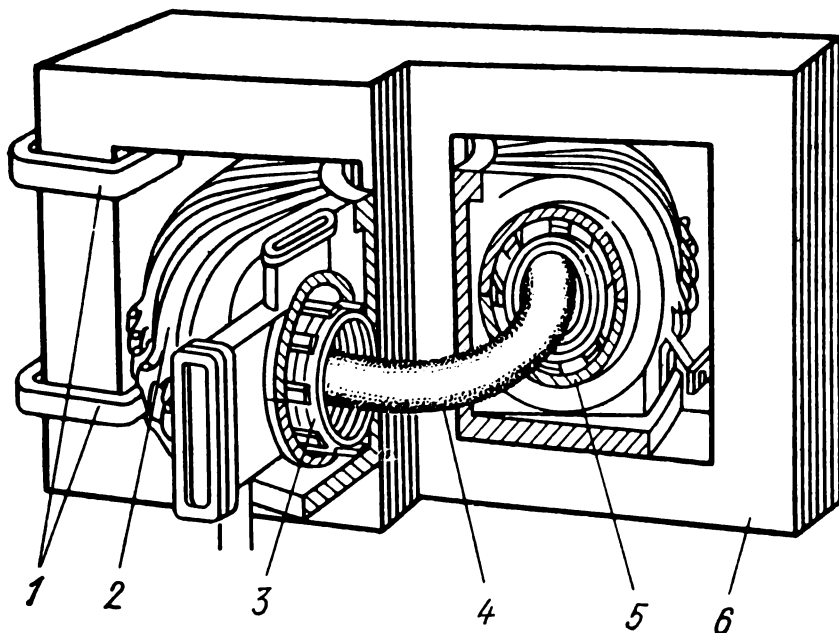


Fig. 8.6 Tokamak installation

1—primary winding; 2—magnetic coil; 3—steel casing; 4—plasma; 5—copper jacket; 6—iron core

compresses the plasma radially and confines it in the chamber. The second, controlled, magnetic field, produced by passing an electric current through the magnetic coils, is used for stabilization of the plasma.

Studies carried out on installations of the Tokamak type showed that the confinement time τ increases with increase of the plasma cross section. In the Tokamak-10 (USSR) and PLT (USA) the sectional area of the chamber is approximately 0.5 m^2 and plasma volume about 5 m^3 . With the Tokamak-10 (or briefly T-10) a plasma temperature of 10^7 K and confinement parameter $N\tau = 4 \times 10^{12} \text{ s/cm}^3$ have been attained. To obtain a self-sustaining thermonuclear reaction the temperature of the plasma will have to be increased about 10 times and the confinement parameter 50 times.

At present Tokamak-type devices are being designed in the USSR, USA and Japan with chambers having cross sections between 3 and 12 m² and plasma volumes between 60 and 400 m³. The plasma temperature and confinement parameter in these devices should not differ substantially from the ignition temperature and Lawson criterion.

Thermonuclear reactors will find wide application as energy sources. Various ways of transforming the energy of future thermonuclear electric stations are being studied in various laboratories. According to one proposal neutrons emitted from the plasma are slowed down in a thick layer of matter surrounding the chamber (blanket). The heat produced in the blanket is removed by a heat carrier. If liquid lithium is pumped through the blanket the slow neutrons may induce the ⁶Li (n, t)⁴He reaction and hence tritium which is burnt up in the plasma can be reproduced.

In a hybrid type of reactor the blanket is made of ²³⁸U. Neutrons with energies $E > 1$ MeV induce fission of ²³⁵U and an energy of 200 MeV per fission is liberated. In this kind of reactor the second power component increases by several times. Plutonium, which is a nuclear fuel for fission reactors, can also be produced in the blanket. Indeed neutrons can elicit, along with fission, the (n, γ) reaction in ²³⁸U: ²³⁸U (n, γ) ²³⁹U. Subsequently ²³⁹U decays into ²³⁹Pu:



New problems have been posed as a result of development of powerful lasers. One might inquire, for example, whether it might not be possible to raise the temperature of a frozen deuterium-tritium pellet to the thermonuclear ignition temperature by irradiating it by laser light pulses and not employing confining magnetic fields. Neutrons from a lithium deuteride pellet irradiated by laser pulses were first recorded in 1963 by a group of Soviet scientists headed by Academician N. G. Basov. The neutrons were formed in a thermonuclear reaction. These results have been confirmed in the USA and France.

What takes place in the pellet? Under the action of a 10^{-10} s laser pulse the surface layer of the pellet evaporates and goes over to the plasma state and the plasma is subse-

quently heated to several tens of millions of degrees. The thermonuclear reaction develops during a time $\tau \sim 10^{-9}$ s. A rapid growth of the plasma pressure takes place and the pellet ultimately breaks up into numerous fragments. One of the problems being studied in connection with the laser thermonuclear technique is how to transform the explosion energy into heat.

Laser thermonuclear fusion will be energetically profitable only if the explosion energy exceeds the amount of energy expended. The energy gain depends on the energy of the light pulse, which determines the initial temperature of the plasma, and also on the method of irradiating the pellet.

On unilateral irradiation of the pellet the confinement parameter $N\tau$ does not exceed 10^{14} s/cm³ (confinement time $\tau \sim 10^{-9}$ s, density of nuclei $N \sim 5 \times 10^{22}$ nucl./cm³). A confinement parameter of this magnitude is sufficient only for compensation of the expended energy. The amount of energy liberated greatly increases if a small sphere of a frozen deuterium-tritium mixture is irradiated from all sides by using many lasers. A sphere irradiated in this way changes into a plasma blob exerting a pressure of 10^{11} atm. Under such conditions the density of the plasma and hence the energy gain increase by hundreds of times.

Laser thermonuclear fusion heretofore has been investigated only in the laboratories. According to theoretical estimates in order to obtain an appreciable energy gain, powerful lasers with light pulse energies of 10^5 - 10^6 J are required, these energies exceeding by 10^2 - 10^3 times those obtainable from present-day lasers. The construction of a laser set-up capable of yielding such high energies is one of the major problems to be solved.

The amounts of deuterium and lithium in nature are enormous and the solution of the controlled thermonuclear reaction problem would signify that mankind has acquired a practically inexhaustible energy source.

8.8 Transuranic Elements

Natural elements fill the periodic table up to uranium ($Z = 92$). Those elements which are beyond uranium in the periodic table are called *transuranic*. They are all radioactive

and have half-lives which are small compared to the age of the earth. It is because of this that the transuranic elements have decayed long ago and are not encountered on the earth under natural conditions.

Thorium, protactinium, uranium and the transuranic elements comprise the actinide group. In the periodic table the actinide elements are arranged below the lanthanides which form a group of 14 elements. There are also 14 elements in the actinide group. Up to 1940 only the first three actinides found in nature, i.e. thorium, protactinium and uranium, were known. The remaining 11 elements of the actinide group (Table 8.1) have been produced in nuclear reactions.

Table 8.1
Transuranic Elements

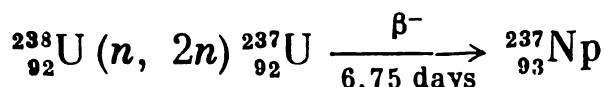
Element	Symbol	Atomic number	Mass numbers of isotopes	Year of discovery
Neptunium	Np	93	231-241	1940
Plutonium	Pu	94	232-246	1940
Americium	Am	95	237-246	1944
Curium	Cm	96	238-250	1944
Berkelium	Bk	97	243-250	1949
Californium	Cf	98	244-254	1950
Einsteinium	Es	99	246-256	1953
Fermium	Fm	100	250-256	1954
Mendelevium	Md	101	255-256	1955
Nobelium	(No)	102	253-255	1957
Lawrencium	Lr	103	257	1961
Kurchatovium	Ku	104	260	1964
Nielsborium	Ns	105	—	1970

Most isotopes of the transuranic elements are β -emitters. This property has been used to obtain isotopes of the transuranic elements. The first isotope of a chemical element with an atomic number $Z = 93$ was obtained by the American physicist McMillan in 1940. Natural uranium, consisting of the isotopes $^{235}_{92}\text{U}$ (93.3%) and $^{238}_{92}\text{U}$ (0.7%) which are α -emitters, was irradiated with neutrons. Among others, the reaction $^{238}_{92}\text{U} (n, \gamma) ^{239}_{92}\text{U}$ occurred; this was followed by β -decay of the $^{239}_{92}\text{U}$ with a half-period of 23 minutes in accord-

ance with the reaction



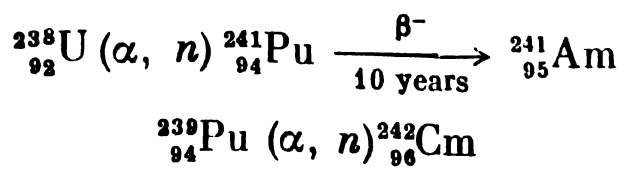
Thus a new element with $Z = 93$ was formed and called neptunium. At present 11 isotopes of neptunium with mass numbers ranging between 231 and 241 are known. The most suitable for studying the chemical properties of neptunium is the isotope $^{237}_{93}\text{Np}$ which has a half-life of 2.2×10^6 years. It is produced as a result of the series of transformations



^{237}Np is a member of the radioactive series with mass numbers $A = 4n + 1$. In the decay products of β -active neptunium isotopes the atomic number is raised to 94. The chemical element with an atomic number $Z = 94$ has been named plutonium.

Of all plutonium isotopes the most interesting from the scientific and practical viewpoints is ^{239}Pu with a half-life of 24 000 years. Under the action of neutrons ^{239}Pu undergoes fission and energy is liberated. Due to this property ^{239}Pu is used as a nuclear fuel in atomic power stations.

Extensive investigations of the transuranic elements have been carried out by a group of American scientists at the University of California in Berkeley (Seaborg, McMillan and others). They obtained new elements by bombarding heavy targets ($A \sim 240$) with deuterons or α -particles accelerated in the cyclotron. Thus americium Am and curium Cm were produced as a result of the transformations



Recently, beams of ^{12}C , ^{14}N and ^{16}O nuclei have been used to obtain transuranic elements. In this case Z increases after the reaction by 6-8 units. Einsteinium Es, fermium Fm, mendelevium Md, lawrencium Lr and other chemical elements were produced by this technique. As an example, irradiation of ^{238}U by ^{14}N nuclei accelerated to 100 MeV induced

the reaction



Soviet physicists (G. N. Flerov and others) have produced a number of isotopes with atomic numbers of 102, 104 and 105. The element with atomic number 104 has been called kurchatovium (Ku) in honour of Academician I. V. Kurchatov and the element with $Z = 105$ nielsborium in honour of N. Bohr.

CHAPTER 9

COSMIC RADIATION

9.1 Nature of Cosmic Radiation

The *primary cosmic radiation* is a stream of high energy particles falling upon the earth from outer space. It can be divided into two components, the galactic cosmic radiation (GCR) and solar cosmic radiation (SCR).

The GCR consists of light nuclei of which 91.5% are protons, 7.8% α -particles and the rest are nuclei with atomic numbers ranging from 3 to 30. The energies of the primary particles vary between 0.1 and 10^8 GeV/nucleon and the mean energy of the GCR is approximately 3.5 GeV/nucleon. The energy of a primary particle is equal to the energy referred to a nucleon multiplied by the mass number of the particle.

According to a theory of the Soviet physicists V. L. Ginzburg and I. S. Shklovsky the GCR arises in explosions of supernovae and novae occurring in the Galaxy. In these explosions enormous amounts of particles are thrown out into space. The interstellar space is permeated by a magnetic field. There are two theories in which it is assumed that the magnetic field may play a role in the acceleration of the cosmic ray particles.

According to one of the theories cosmic ray particles are accelerated just as electrons are in a betatron. It is assumed that the magnetic field in interstellar space is time-varying. In some spatial regions it increases and in others decreases. The energy of particles in the increasing magnetic field is enhanced under the action of the electric field induced by the varying magnetic field. Energy is imparted quite rapidly but the energy gain is not very high.

The second, so-called statistical mechanism of acceleration proposed by Enrico Fermi in 1949, is based on the assumption that the interstellar magnetic fields are very

inhomogeneous. In some regions the field strength is much greater than in the surrounding regions. These magnetic field blobs which resemble magnetized "clouds" move in space. If a charged particle collides with a moving cloud it is reflected by it. Such collisions are similar to those between a light and heavy particle. If the kinetic energy of a light particle is smaller than that of the heavy particle the light particle will acquire energy. Cosmic particles are accelerated in an analogous way. On reflection from a cloud it acquires energy, just as a light particle does from a heavier one. The statistical acceleration mechanism is a much slower process than the betatron mechanism. However, theoretical estimates show that precisely in the statistical mechanism cosmic particles can be accelerated up to 10^8 GeV/nucleon.

The magnetic fields in outer space are oriented randomly. The cosmic particles thrown out into space at certain parts of the Galaxy cover enormous distances. They are repeatedly scattered by the magnetic fields in various directions and, hence, most of the cosmic ray particles do not have any predominant direction. This is the reason why the GCR is isotropic and the particles strike the earth in all directions with equal intensity. The flux density of the primary cosmic particles does not depend substantially on time and is of the order of 1.0×10^4 particle/ $m^2 \cdot s$.

The SCR is caused by solar flares and consists mainly of protons with energies up to 50 GeV. The SCR is time-dependent. Observations carried out over a period of many years have shown that there is a periodic change in the SCR intensity which is repeated every 11 years. The solar activity is maximum about six years and is followed by the period of the quiet sun.

During the period of maximum solar activity short flares occur. During these outbursts intense jets of protons are ejected by the sun. The total flux density of the particles is 10^{13} part./ $m^2 \cdot s$ and the flux density of protons with energies between 1 and 50 GeV is about 2×10^{10} part./ $m^2 \cdot s$.

Low-energy electrons and protons which fill the interplanetary space are also continuously being emitted from the surface of the sun. This radiation which moves with a speed of 300 km/s is called the *solar wind*. The proton and

electron density in the solar wind is not high and is approximately 10^7 part./m³.

In recent years the investigation of outer space has become of interest not only from the theoretical point of view but also from a practical one. Thus artificial satellites are used for telecommunication and television.

Spacecrafts and artificial satellites of the earth are constantly subjected to the action of the cosmic radiation. At high intensities the radiation may damage the scientific apparatus or have a deleterious effect on the health of the astronaut. Therefore in order to choose suitable radiation protection and also the best trajectory and time of flight, a knowledge is required of the composition of the cosmic radiation and the time and energy distribution of the cosmic particles in circumterrestrial space (the space near the earth) and in interplanetary space. The dose rate of the GCR in interplanetary space is estimated to be 2 mrad/h. In circumterrestrial space the GCR dose rate grows with the distance above the surface of the earth. It also depends on the angle of inclination of the plane of the artificial satellite orbit with respect to the plane of the equator. This dependence is due to two factors. Part of the GCR which falls upon the opposite side of the earth is absorbed and does not contribute to the dose rate. Secondly, the magnetic field of the earth deflects charged particles and this may decrease the dose rate of the GCR at certain points of measurement. For example, if the plane of the orbit is inclined at an angle of 60°, the equivalent dose rate rises from 1.0 mrem/h (at a height of 200-600 km above the surface of the earth) to 3.0 mrem/h (at a height of 7000-8000 km).

The dose rate of the SCR during solar flares may be much higher. According to calculations made by American scientists the equivalent dose of the SCR at unprotected points may reach 1.8×10^4 rem; in the control compartment of the Apollo spacecraft it was 343 rem. Thus forecasting of solar flares is required before prolonged space flights are undertaken. Such forecasting should ensure that the flight proceeds during a period of minimal intensity of the SCR.

Fast primary particles colliding with nuclei in the upper layers of the atmosphere split them. Secondary cosmic rays

are formed which consist of protons, neutrons, pions and other particles. Most of the primary particles are absorbed in the top layers of the atmosphere and only a few (with energies exceeding 10^4 GeV) can pass through the atmosphere and retain an energy of about 1 GeV.

At heights of 20-30 km the primary particles cause chain multiplication of particles. The nucleons and pions created by the primary particles have energies which are sufficiently high for them to induce further particle production in subsequent collisions with nuclei. In this way *nuclear showers* are formed in the atmosphere. They occupy comparatively small volumes in the atmosphere. They begin to disappear as soon as the energy of the secondary nucleons is reduced to several tens of mega-electronvolts. The remaining proton energy is spent in ionization of the air.

Part of the neutrons is absorbed in the $^{14}_7\text{N}$ (n, p) $^{14}_6\text{C}$, $^{14}_7\text{N}$ ($n, \alpha p$) $^{10}_4\text{Be}$ and other reactions in which radioactive atoms are produced. Other neutrons are slowed down and absorbed by nuclei in (n, γ) reactions.

More extensive showers of secondary particles originate from neutral pions. On decay they produce two photons with a total energy of not less than 135 MeV (rest energy of the π^0 -meson). In the field of a nucleus the photon may create an electron-positron pair (Fig. 9.1). These electrons and positrons with energies of over 62.5 MeV passing near a nucleus experience bremsstrahlung and the photons thus emitted may produce further electron-positron pairs etc. Thus *photon-electron showers* are formed in the atmosphere. This particle multiplication in showers occurs in a sequence of repetitive cycles. Each cycle consists of two stages: the photons are first transformed into electrons and positrons and the latter then produce photons.

A photon-electron shower develops as long as the photons produced expend their energy in the production of electron-positron pairs. With decrease of photon energy the photoelectric effect and Compton effect become predominant and the shower begins to die out. Photon-electron showers extend over areas of several square kilometres. At a height of around 15 kilometres the cosmic radiation contains mainly electrons, positrons and photons. Only a few of these shower particles reach the surface of the earth. At sea level,

electrons and positrons comprise less than 30% of the total cosmic radiation.

A part of the charged pions decay without having interacted with nuclei. Muons and neutrinos are formed in the decay of these particles:

$$\pi^\pm \rightarrow \mu^\pm + \nu$$

Since the pion energy may reach several giga-electronvolts the muons move with a velocity close to that of light. The penetrating power of muons in matter is very high.

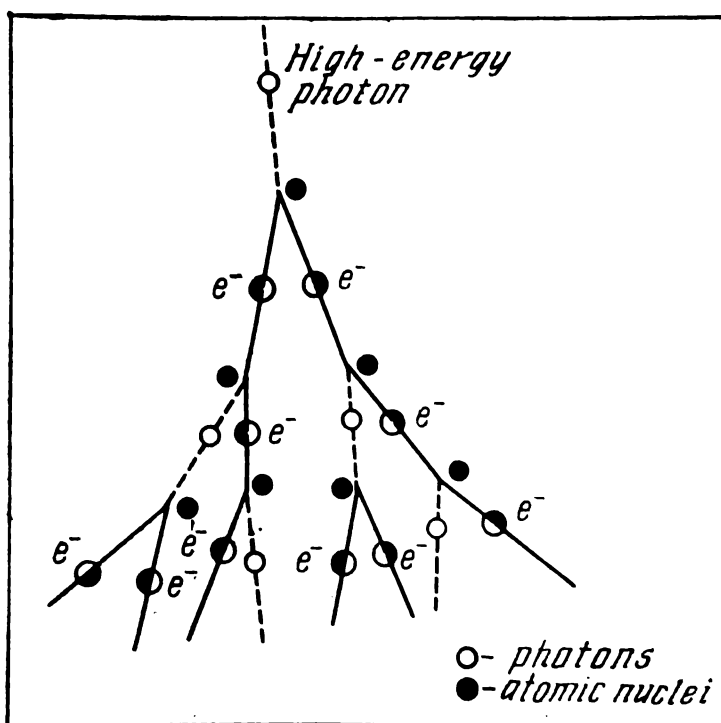


Fig. 9.1 Formation of electron-positron shower in the atmosphere

From a height of 20-30 kilometres, at which they are formed, the muons can not only reach the surface of the earth but penetrate deep into its crust. The high penetrating power of muons can be ascribed to a number of their properties. First of all, muons (similar to electrons) do not react readily with atomic nuclei and hence are not absorbed by them. The main mode of interaction between muons and nuclei is electromagnetic interaction. However, since the muon mass is 207 greater than the electron mass their radiative losses are tens of thousand times smaller. At sea level, about 70% of the cosmic ray particles are muons.

9.2 Radiation Belts of the Magnetosphere

Since 1957 artificial satellites of the earth and spacecrafts are being launched in the Soviet Union and in the USA. Precise and sensitive apparatus for measuring radiation are carried by many of these vehicles. The data obtained in recent years have contributed significantly to our understanding of the circumterraneous space.

The earth is an enormous magnet. The space surrounding the earth in which its magnetic field exists is called the

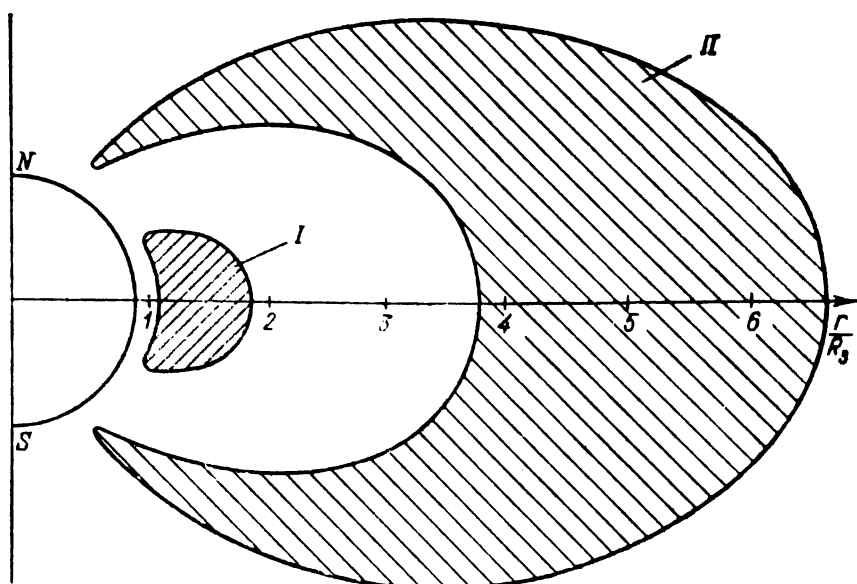


Fig. 9.2 Inner (I) and outer (II) radiation belts in the magnetosphere

magnetosphere. It extends over distances of tens of thousands of kilometres. Data obtained by means of various space vehicles have shown that the magnetosphere and interplanetary space are filled with a plasma consisting mainly of protons and electrons. The density of the charged particles in the magnetosphere is not uniform. There are two big regions, which are effectively magnetic traps in the magnetosphere, in which the density of the charged particles is enhanced (Fig. 9.2). These regions are called the *outer* and *inner radiation belts*. In the equatorial plane the boundaries of the inner radiation belt are at 500 to 6000 km from the earth's surface. The boundaries of the outer radiation belt are at 20 000 and 60 000 km. The inner belt is

filled with 30-100 MeV protons and electrons with energies below 100 keV. The outer belt contains mostly electrons with energies of several hundred keV.

The charged particles in the radiation belts move between the magnetic poles of the earth along the lines of force. Near the poles the magnetic lines of force become denser and the charged particles are reflected from the poles as from a mirror.

The protons and electrons in the inner radiation belt originate from neutrons. The latter are formed in nuclear reactions between the primary particles which penetrate the radiation belt and nuclei of the atmosphere. Neutrons can move freely in the magnetosphere and finally decay into protons and electrons, part of which are contained in the inner belt. Some of the charged particles in the radiation belts originate from the interplanetary plasma. Those plasma particles which enter the magnetosphere are accelerated and contained in the belts. The time-average of the charged particle density in the radiation belts is constant. Obviously the escape of particles from the belts is offset by the entrance of new particles.

The magnetic field near the earth's surface is not homogeneous. In this part of the magnetosphere several *magnetic anomalies* have been observed, the magnetic flux density being relatively low. In the magnetic anomalies the particle flux densities are unusually high and hence they have been called radiation anomalies. The most prominent are the anomaly in the southern part of the Atlantic Ocean and that near the shores of the Antarctica. These anomalies are related to the radiation belts: the south Atlantic to the inner belt and the Antarctic to the outer belt. The radiation belts in the regions of the radiation anomalies are only 200-300 km above the earth's surface. The density of the air at such heights is still perceptible.

A charged particle is contained in the radiation belt over a given period of time. Thus the average lifetime of a charged particle in the inner belt is one year. When a particle enters the magnetic anomaly it is swept out of the radiation belt by the atmosphere.

Information on the radiation dose rates near the earth's surface has been obtained by studying the radiation belts.

The dose rates have been found to depend on the location in the belts. The highest rate is observed in the inner radiation belt where it exceeds 10^8 rem/h. The peak rate is found near the centre of the belt where it is 10^6 rem/h. In the outer belt the dose rate grows from 30 rem/h at the outer boundary to 10^3 rem/h at the centre of the belt.

9.3 Elementary Particles

Elementary particles are particles with an unknown internal structure. The concept of elementariness is conditional and depends on the level of our knowledge. Less than 70 years ago the atom was regarded as an elementary entity although we now know it possesses a complex structure. At present nucleons are still referred to as elementary particles notwithstanding the fact that models of their structure have been proposed.

Theoretical physics predicts the existence of antiparticles for the majority of particles. A particle and its antiparticle have the same mass, spin, charge and magnetic moment but the last two quantities differ in sign.

When a slow particle and its antiparticle interact they annihilate and other particles are formed. An example of a particle and antiparticle is an electron-positron pair. The absolute values of the magnetic moments of the electron and positron are the same. However, the magnetic moment of the positron is directed along the spin whereas that of the electron is directed opposite to the spin. On annihilation a positron and an electron are transformed into photons with a total energy of not less than 1.02 MeV.

Two elementary particles, the photon and neutral pion, do not have antiparticles. In this case the particle and antiparticle are identical. Antiparticles are usually denoted by writing a bar over the symbol of the particle (Table 9.1). Some antiparticles are denoted by special symbols (e.g., the positron, negative pion etc.). The elementary particles are usually divided into four groups, the photons, leptons, mesons and baryons. A brief description of each of the groups follows below.

Photons are particles of the electromagnetic field. They have a unit spin and are therefore bosons. The interaction

between photons and charged particles is of an electromagnetic nature.

Leptons are light fermions (spin 1/2) and include the neutrino, electrons, negative muons and their antiparticles. Leptons can interact with each other and with other particles. A characteristic feature of the leptons is that they annihilate and are produced in pairs and therefore the number of leptons is constant. This law is expressed by ascribing to each lepton a *lepton charge*. It is -1 for antileptons and $+1$ for leptons. The total lepton charge of a system, similar to the electric charge, is the sum of the lepton charges of all the particles. In all kinds of transformations the total lepton charge is conserved, such is the formulation of the *law of conservation of lepton charge*. As an example consider the decay of a negative muon,

$$\mu^- = e^- + \nu + \bar{\nu}$$

There is one lepton charge in the left-hand side of the equation. For the lepton charge to be one in the right-hand side three leptons must be formed in the muon decay, viz. an electron, neutrino and antineutrino. In a similar way it can be shown that an antineutrino is emitted in β^- -decay and a neutrino in β^+ -decay.

The interaction of the strongly penetrating neutrinos with matter is 10^{10} times weaker than that of charged leptons. One of the reactions induced by the antineutrino is that involving interaction with the proton,

$$p + \bar{\nu} \rightarrow n + e^+$$

Detection of the products of this reaction has confirmed Pauli's hypothesis on neutrino emission in β -decay.

Mesons. This group includes particles with zero spin and masses between those of leptons and nucleons (pions, kaons). They are strongly absorbed by baryons. On the other hand their decay products are leptons. Thus the meson group is intermediate between leptons and baryons.

Baryons. These are particles possessing a nuclear (baryon) charge. Baryons have a nuclear charge of $+1$ and antibaryons a nuclear charge of -1 . It has been possible to produce antibaryons (antiprotons, antineutrons etc.) only by employing such powerful accelerators as the proton synchrotron.

Table 9.1

Elementary Particles

Group	Particle	Symbol		Rest mass	Spin	Electric charge	Baryon charge	Lepton charge	Lifetime, τ	Decay products of particle
		particle	anti-particle							
Photons	Photon	γ	γ	0	1	0	0	0	Stable	—
Leptons	Neutrino	ν	$\bar{\nu}$	0	1/2	0	0	1	”	—
	Electron	e^-	e^+	1	1/2	-1	0	1	”	—
	Muon (mu-meson)	μ^-	μ^+	206.7	1/2	-1	0	1	2.2×10^{-6}	$e^- + \nu + \bar{\nu}$
Mesons	Pion (pi-meson)	π^0	π^0	284.2	0	0	0	0	1.8×10^{-16}	$2\gamma; \gamma + e^+ + e^-$
	Kaon (K-meson)	π^+	π^-	273.2	0	1	0	0	2.55×10^{-8}	$\mu^+ + \nu$
		K^+	K^-	966.3	0	1	0	0	1.23×10^{-8}	$e^+ + \nu + \pi^0; \mu^+ + \nu$
		K^0	\bar{K}^0	274.5	0	0	0	0	0.910×10^{-10}	$\pi^+ + \pi^0; 2\pi^0$
Baryons	Nucleons	Proton	\bar{p}	1836.4	1/2	1	1	0	Stable	—
		Neutron	\bar{n}	1838.5	1/2	1	1	0	1013	$p + e^- + \bar{\nu}$

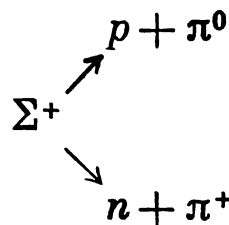
Table 9.1 (continued)

Group	Particle	Symbol	Rest mass	Spin	Electric charge	Baryon charge	Lepton charge	Lifetime, s	Decay products of particles
	particle	anti-particle							
Ba- ryons	Lambda hyperon	Λ	2182	1/2	0	1	0	2.6×10^{-10}	$p + \pi^-$ $n + \pi^0$
	Sigma hyperon	Σ^+	2327	1/2	1	1	0	0.8×10^{-10}	$p + \pi^0$ $n + \pi^+$
		$\bar{\Sigma}^0$	2333	1/2	0	1	0	$< 10^{-14}$	$\Lambda + \gamma$
		Σ^-	2342	1/2	-1	1	0	1.7×10^{-10}	$\pi^- + n$
	Xi hyperon	Ξ^0	2570	1/2	0	0	0	3.4×10^{-10}	$\Lambda + \pi^0$
		Ξ^-	2585	1/2	-1	1	0	1.7×10^{-10}	$\Lambda + \pi^-$
Omega hyperon		$\bar{\Omega}^-$	3278	3/2	-1	1	0	0.7×10^{-10}	$\Lambda + K^-$
		Ω^-							

Note: The masses, spins and lifetimes of antiparticles and particles are the same. The charges of particles and antiparticles are equal but opposite in sign. Masses are expressed in units of the electron rest mass m_e , spins in \hbar units and electric charge in e units.

The antiproton and antineutron were first detected by American physicists in 1955-1956 with the Brookhaven proton synchrotron.

Baryons, like leptons, are created and annihilate in pairs. Therefore the total baryon charge of a system of particles is conserved in all types of transformations. A particular case of this law of conservation is the law of conservation of nucleons. An example of the law of conservation of baryon charge is the decay of the sigma-plus hyperon,



The sigma-plus hyperon can decay along two channels. In each case the baryon charge at the left and right is one since pions have neither baryon nor lepton charge.

The decay products of some elementary particles are presented in the last column in Table 9.1. The decay scheme of antiparticles is the same as that for particles with the difference that particles in the decay products are replaced by antiparticles and vice versa. On such substitution the electric, lepton and baryon charges should be conserved. Decay of the sigma-minus hyperon and antihyperon, for example, proceeds according to the equations



Over 200 particles and antiparticles have been discovered; only a part of them is presented in Table 9.1. A unified classification encompassing the multifarious elementary particles, something resembling the periodic table of elements, is one of the tasks facing theoretical physicists at present.

CHAPTER 10

NEUTRON PHYSICS

10.1 Properties of Neutrons

The neutron was discovered in 1932 by the English physicist Chadwick who proved theoretically and experimentally that beryllium bombarded by α -particles emits neutral particles with a mass close to that of the proton. Because it does not possess an electric charge the particle was called the *neutron*.

The neutron mass can be measured in various ways. In one type of experiment the deuteron is split into a proton and neutron by γ -quanta,

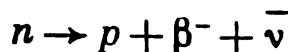


The minimum γ -quantum energy required for splitting the deuteron is 2.225 MeV. According to the Einstein equation this corresponds to a mass defect $\Delta M = 0.00239$ amu. The deuteron and proton masses have been determined by mass-spectrometry measurements and are $m_d = 2.01355$ amu and $m_p = 1.00727$ amu. From the expression for the mass defect we get

$$m_n = m_d - m_p + \Delta M = 1.00866 \text{ amu}$$

The value of the neutron mass generally accepted at present is $m_n = 1.0086652$ amu.

The difference between the masses of the neutron and proton is greater than the mass of the electron. Because of this the free neutron is radioactive. It disintegrates into a proton, electron and antineutrino,



The measurement of the neutron half-life is a formidable experimental problem. One of the difficulties is that neu-

trons during their movement in matter are continuously being absorbed by the nuclei in times which are much small or than the half-life of the neutron. A neutron beam is passed through a cylindrical vacuum chamber. On passing through the chamber part of the neutrons decays. The decay products (protons and electrons) are separated by an electric field. They are deflected in opposite directions, perpendicular to the chamber axis and are then recorded. The proton and electron counters are connected to a coincidence circuit. The coincidence rate $\Delta N/\Delta t$, which is equal to the rate of neutron decay, and the number of neutrons traversing the chamber per unit time, N , are measured. On the basis of these data the decay constant can be evaluated. $\lambda = (\Delta N/\Delta t) (1/N)$. The most precise measurements yield for the half-life a value of 14.7 min.

All nuclei, except the hydrogen nucleus, contain neutrons. Bound neutrons in the nucleus, in contrast to free neutrons, can exist an infinitely long time.

10.2 Neutron Sources

Characteristics of the sources. Neutrons are produced in nuclear reactions and in spontaneous fission of nuclei. Neutron sources are classified in accordance with the type of reaction involved, mode of obtaining the bombarding particles etc.

A neutron source is characterized by its *intensity* P and *neutron energy spectrum* $f(E)$. The *source intensity* P is the number of neutrons emitted by the source per unit time. It can vary in a broad range, from 10^6 to 10^{12} neutr./s or higher. For some sources, such as a nuclear reactor, the *neutron flux density* φ is a more convenient characteristic. In powerful nuclear reactors φ may be as high as 10^{16} neutr./ $m^2 \cdot s$. The *neutron energy spectrum* is the distribution in energy of the neutrons emitted by the source. The spectrum of some sources is discrete and that of others, continuous.

Besides P and $f(E)$ another characteristic used is the *neutron yield* Y . This is the fraction of α -particles which induces an (α, n) reaction in the source. If the rate of en-

trance of particles into the source is N part./s, the source intensity will be

$$P = YN$$

(α, n) Reaction. Some sources in which neutrons are produced in the (α, n) reaction are the radium-beryllium (Ra-Be), polonium-beryllium (Po-Be) and plutonium-beryllium (Pu-Be) sources. The ^{210}Po , ^{226}Ra or ^{239}Pu α -emitting atoms are mixed uniformly with beryllium atoms and the mixture is enclosed in an air-tight metal capsule. One type of Ra-Be source, for example, consists of an capsule containing a fine beryllium powder suspended in an aqueous solution of a radium salt.

Radium, polonium and plutonium emit α -particles with energies between 4.8 and 7.7 MeV. This energy is sufficient for the α -particles to surmount the potential barrier of the beryllium nucleus which is approximately 4 MeV high. However, most of the α -particles interact with the atomic electrons and are slowed down to energies less than 4 MeV. Thus only one in about $(1-1.5) \times 10^4$ α -particles penetrate the beryllium nucleus and induce the $^9\text{Be} (\alpha, n) ^{12}\text{C}$ reaction. The neutron energy spectrum of the Ra-Be, Po-Be and Pu-Be sources are continuous, the energies varying between 1 and 13 MeV. The mean neutron energy is about 4-5 MeV.

The neutron yield of Ra-Be, Po-Be and Pu-Be sources depends on the way of preparation of the mixture, on the size of the beryllium grains in the mixture, uniformity of mixing of the α -emitter and beryllium etc. Ordinarily it is expressed by the rate of neutron emission from the source referred to 1 Ci of the radioactive substance. The neutron yield of a well prepared Ra-Be source may be as high as 2×10^7 neutrons per second per Ci of radium. It should be mentioned that some of the disintegration products of radium (radon, polonium, bismuth) are also α -emitters and about 6/7 of the neutron yield is due to them. Because of the long half-life of radium (1620 years) the neutron yield of a Ra-Be source is practically constant. A shortcoming of this source is its high gamma-activity. The sources are kept in special containers which absorb γ -rays.

None of the disintegration products of polonium are α -emitters and hence the neutron yield of a Po-Be source per

Ci of polonium is about seven times smaller than that per Ci of radium. In practice the Po-Be source is more convenient since for equal activities the γ -equivalent of the Po-Be source is approximately 5×10^3 times smaller than the γ -equivalent of the Ra-Be source. On the other hand, the half-life of polonium is only 138.4 days. Hence, the activity of polonium and therefore the intensity of the source considerably decrease with time. The alloy PuBe_{13} is usually used in Pu-Be sources. The source intensity is stable [$T_{1/2} ({}^{239}\text{Pu}) = 2.4 \times 10^4$ years] and is 1.4×10^6 neutr./s·Ci.

Photoneutron sources. Many radioactive substances emit γ -quanta whose energies exceed the neutron binding energy in ${}^9\text{Be}$ nuclei (1.665 MeV) and D nuclei (2.225 MeV). This fact is exploited to obtain neutrons in the $\text{D}(\gamma, n)\text{H}$ and ${}^9\text{Be}(\gamma, n){}^8\text{Be}$ reactions. In a photoneutron source the capsule with the radioactive substance (${}^{24}\text{Na}$, ${}^{72}\text{Ga}$ etc.) is embedded in the target (Be, D_2O). The neutron energy is

$$E_n = \frac{A-1}{A} (E_\gamma - \varepsilon_n)$$

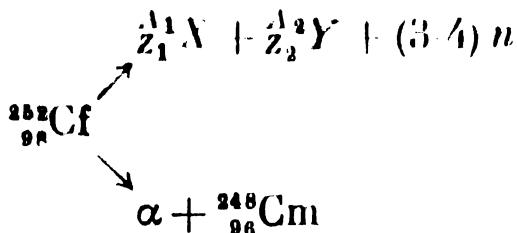
where ε_n is the binding energy of the neutron in the target nucleus.

If a radioactive substance emits a single γ -line with an energy E_γ , which exceeds the threshold of the (γ, n) reaction, the energy spread of the neutrons produced in the source will not be very high. However, since the neutrons are slowed down in the source itself the energy spread of the neutrons is correspondingly increased.

The neutron yield in photoneutron sources depends on the cross section for the (γ, n) reaction, σ_n , and on the thickness of the target, δ . The cross section for beryllium and γ -quantum energies $E_\gamma > 1.7$ MeV is 0.5-1 mb. For a beryllium target thickness of 1 cm the neutron yield is close to 10^{-4} . The intensity of photoneutron sources does not exceed 10^7 - 10^8 neutr./s. Photoneutron sources are employed in laboratories and as standard neutron sources. The precautions which must be taken in work with photoneutron sources are the same as in work with Ra-Be sources.

Spontaneous fission of nuclei. The nuclide ${}^{162}\text{Cf}$ can be used to obtain fission neutrons. The nuclide decays along two

channels,



Spontaneous fission ($T_{1/2} = 86$ years) occurs in 3% of the nuclei. One gram of californium emits about 3×10^{12} neutr./s. The useful lifetime of a californium source is determined by its α -decay ($T_{1/2} \approx 2.6$ years) into curium nuclei which accounts for 97% of the decays of the ^{252}Cf nucleus.

Charged particle accelerators. The neutron flux densities from the Ra-Be, Po-Be and (γ, n) sources are quite low. The progressing acceleration technique has offered experimental physicists powerful and convenient neutron sources. Neutrons are obtained by directing accelerated charged particles (protons and deuterons) onto a target containing light atoms for which the neutron binding energy is small (deuterium, tritium, lithium). The reactions $^7\text{Li}(p, n)^7\text{Be}$ (reaction threshold energy 1.88 MeV), $D(d, n)^3\text{He}$ and $T(d, n)^4\text{He}$ are induced in the target. These reactions are employed to obtain monoenergetic neutrons. The neutron yield is particularly high for deuterium- or tritium-containing targets bombarded with fast deuterons.

Nuclear reactor. Another powerful source of neutrons is the nuclear reactor (see Part two). The neutrons are produced as a result of fission. The neutrons are guided out of the reactor into the laboratory through special tubes. The spectrum of neutrons from a reactor is continuous. Its shape depends on the composition of the reactor.

10.3 Neutron Spectrometers

Neutron energy spectra are measured with neutron spectrometers. We shall consider one type of slow-neutron spectrometer, the so-called time-of-flight spectrometer.

The time-of-flight spectrometer consists of a neutron source (nuclear reactor, fast-particle accelerator), neutron counter and time analyzer. A beam of slow neutrons ($E_n < 1$ eV) from the nuclear reactor is directed to a rotating

mechanical chopper (Fig. 10.1). This is a cylinder with alternating layers of aluminium and cadmium. Thermal neutrons freely pass through aluminium but are completely absorbed by cadmium. During each half-revolution the direction of the aluminium layers (which are effectively slits for the neutrons) coincides for an instant with the direction of the neutron beam and thus a neutron pulse is

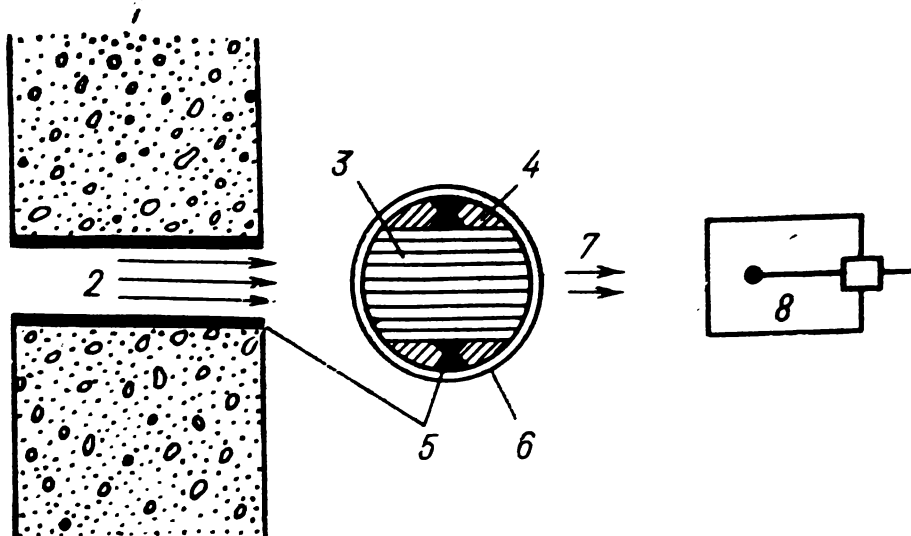


Fig. 10.1 Time-of-flight spectrometer

1—concrete shield; 2—collimated thermal neutron beam; 3—aluminium and cadmium layers; 4—aluminium; 5—cadmium; 6—steel casing; 7—neutron pulse; 8—neutron detector

transmitted by the chopper. All the rest of the time the neutron beam is absorbed by the cadmium.

The mechanical chopper transforms a continuous neutron beam into a sequence of pulses. Short neutron pulses are obtained by rotating the cylinder at a speed of 30 000 rpm which corresponds to 1000 pulses per second.

The neutron pulse then enters a detector (proportional counter, scintillation counter etc.) located at a distance L from the chopper. This distance L is called the *flight path*. Since the neutrons in the bunch have different velocities the neutrons spread out along the flight path. A neutron with a velocity v covers the flight path in a time $t = L/v$ which is called the *time of flight*. The fastest neutrons reach the detector in a time t_1 after the opening of the slit in the mechanical chopper and the slowest ones after a time t_2 . Thus, the time of flight of neutrons in a pulse, t , varies

between t_1 and t_2 . The time can be measured with a time analyzer which is switched on synchronously with the opening of the chopper.

Electric pulses produced by the neutrons in the detector are sent into a time analyzer. In each k th channel neutrons with times of flight between t_k and $t_k + \Delta t$ are recorded. Since $\Delta t/t_k \ll 1$, the neutron velocity for this particular time interval is $v_k = L/t_k$ and therefore the energy $E_n^{(k)} = m_n L^2/2t_k^2$. The total number of neutrons with energies $E_n^{(k)}$ is recorded in the k th channel. The ratio of the number of pulses in the k th channel to the number recorded in all channels is denoted by $f(E_n^{(k)})$. The neutron energy spectrum can be plotted on the basis of this function. The channel width, $\Delta t = (t_2 - t_1)/k$, depends on the number of channels in the time analyzer. In modern analyzers the number of channels may be several thousand; neutron energy spectra can therefore be measured with a high degree of accuracy.

Neutrons with energies exceeding 1 eV are weakly absorbed by cadmium. For such neutrons the cadmium and aluminium in the mechanical chopper are replaced by nickel which has a large neutron scattering cross section. Nickel reflects the neutrons and does not transmit them through the chopper. Periodic transmission of the neutrons is attained by making slits in the nickel.

Charged particle accelerators of continuous operation (linear accelerators, cyclotrons) can be rapidly switched on and off. Thus short particle pulses can be obtained. The charged particles produce a pulse of fast neutrons ($E_n > 0.1$ MeV) in the target. The neutrons are first slowed down in a slab of some light substance (paraffin etc.) and then reach the starting point of the flight path. In this case the neutron source consists essentially of the accelerator, slowing down substance (moderator) and target.

The spectra of fast neutrons ($E_n > 0.1$ MeV) can also be measured by other means. One method is based on the ability of fast neutrons to suffer elastic scattering and is called the *recoil nucleus method*. A neutron scattered elastically into some angle θ imparts a fraction of its energy to the recoil nucleus and moves with a velocity v_2 (Fig. 10.2). The recoil nucleus moves with a velocity v at an angle φ with

respect to the initial neutron velocity v_1 . Angle φ is called the recoil angle. The equation relating the energy E_r and mass number A of the recoil nucleus to the neutron energy E_n and recoil angle φ can be derived from the laws of conservation of energy and momentum and is

$$E_r = \frac{4A}{(A+1)^2} E_n \cos^2 \varphi \quad (10.1)$$

If E_r , φ and A are known the neutron energy may readily be calculated. In cloud or bubble chambers and in photographic plates recoil nuclei form visible tracks. The track

length depends uniquely on the energy of the recoil nucleus. Thus E_r can be found by measuring the track length. The energy spectrum of fast neutrons can be determined by measuring the track distribution for a given recoil angle which is the angle between the incident beam and the track. The neutron detectors are usually filled with hydrogen-containing substances. In this case the fast-

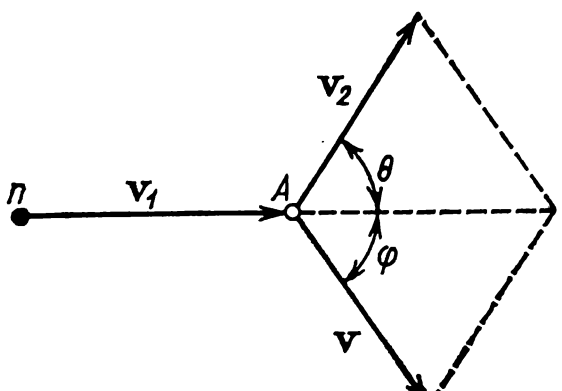


Fig. 10.2 Elastic scattering of neutron by a nucleus of mass number A

neutron energy spectrum is determined by measuring the recoil proton tracks ($A = 1$). The length of these tracks is the largest compared to those of other particles. With increase of track length the experimental errors decrease.

Fast-neutron spectra can also be determined by measuring the energies of recoil protons in ionization chambers or proportional counters filled with hydrogen or methane and also by using scintillation counters with organic phosphors (stilbene etc.). According to equation (10.1) the energy of the recoil protons varies between zero ($\varphi = \pi/2$) and E_n ($\varphi = 0$), where E_n is the initial neutron energy. The energy distribution of the recoil protons is first determined and the neutron energy E_n is then derived. If the recoil proton distribution is measured for all neutron energies, one can readily determine the fast-neutron spectrum.

10.4 Neutron-Induced Nuclear Reactions

The main reactions induced by neutrons are elastic and inelastic scattering and absorption of neutrons.

The behaviour of the cross section for the (n, b) reaction depends on the energy range. Because of this neutrons are divided into thermal ($E_n < 1$ eV), medium (1 eV $< E_n < 0.1$ MeV) and high energy (or fast) neutrons ($E_n > 0.1$ MeV). Correspondingly, the energy is divided into three ranges: thermal, medium and fast. Medium neutrons with energies between 1 and 1000 eV are called resonance neutrons and the respective energy range the resonance range. Sometimes thermal and resonance neutrons are united in a single group of so-called slow neutrons.

Elastic scattering. This reaction is analogous to an elastic collision between two balls. In elastic encounters a redistribution of kinetic energy between the neutron and nucleus occurs without any attendant alteration of the internal state of the nucleus taking place.

Elastic scattering of neutrons is divided into potential and resonance scattering. The wave properties of the neutron is of foremost importance in potential elastic scattering. The neutron is reflected from the surface of the nucleus as a wave. Resonance elastic scattering involves the compound nucleus. The total neutron elastic scattering cross section $\sigma_s = \sigma_{sp} + \sigma_{sr}$, where σ_{sp} and σ_{sr} are the cross sections for potential and resonance elastic scattering. In the vicinity of the resonance peaks $\sigma_{sr} \gg \sigma_{sp}$ and far from the peaks $\sigma_{sp} \gg \sigma_{sr}$.

In the high energy region the potential scattering cross section, σ_{sp} , like the cross section for compound nucleus formation, σ , approaches the geometrical sectional area of the nucleus πR^2 . The experimental data on the total cross section $\sigma_t = \sigma + \sigma_{sp}$ for energies $E_n > 15$ MeV yield a value for the proportionality coefficient α in the formula for the nuclear radius R (see formula 3.4) which is equal to 1.4 fermi.

The elastic scattering cross sections σ_s for most substances depend on the neutron energy only in the high-energy range and are almost constant in the thermal and intermediate ranges. An exclusion is hydrogen. In the thermal range the

cross section σ_s for hydrogen (Fig. 10.3) sharply drops from 80 to 20 b, remains constant in the intermediate region and then again falls down to 4-5 b in the high-energy region

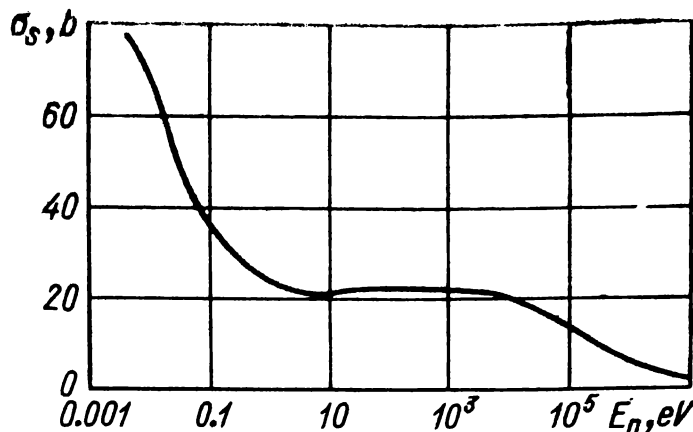
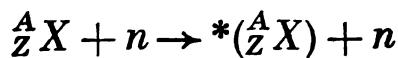


Fig. 10.3 Dependence of cross section for scattering of neutrons by hydrogen, σ_s , on neutron energy E_n

Inelastic scattering. Fast neutrons may experience both elastic and inelastic scattering as exemplified by the equation



As a result of this reaction the target nucleus is transferred to the excited state. The inelastically scattered neutron

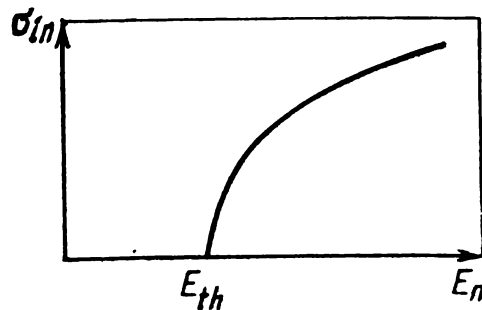


Fig. 10.4 Dependence of inelastic cross section σ_{in} on neutron energy E_n

imparts to the nucleus a part of its kinetic energy which is exactly equal to the excitation energy. On transition to the ground state the excited nucleus emits γ -quanta.

Inelastic scattering is a threshold reaction, the threshold energy being, according to formula (8.3), $E_{th} = \frac{A+1}{A} W_1$.

where W_1 is the energy of the first excited state of the nucleus. With growth of the mass number, W_1 is reduced from several million electronvolts to 100 keV or even less. Hence inelastic scattering of neutrons occurs only in the high energy region and mainly on heavy nuclei.

The inelastic scattering cross section (Fig. 10.4) begins to exceed zero at the threshold energy. It reaches a maximum at energies between 10 and 15 MeV (Table 10.1).

Table 10.1

Inelastic Scattering Cross Section for 14 MeV Neutrons

Element	$\sigma_{\text{In}}, \text{b}$	Element	$\sigma_{\text{In}}, \text{b}$
Fe	1.43	Hg	2.47
Cd	1.89	Bi	2.56
Au	2.51	Pb	2.29

Neutron absorption. In the (n, b) reaction a neutron is absorbed and particle b is produced. Absorption of neutrons takes place in such reactions as (n, γ) , (n, α) , fission, $(n, 2n)$. If account is taken for all types of processes which may be involved in the absorption of neutrons, the total absorption cross section may be written as

$$\sigma_a = \sigma_\gamma + \sigma_\alpha + \sigma_f + \sigma_{2n} + \dots$$

where σ_γ is the radiative capture cross section, σ_α the cross section for the (n, α) reaction, σ_f the fission cross section and σ_{2n} the cross section for the $(n, 2n)$ reaction.

In most nuclei only radiative capture of neutrons is observed up to 5 MeV ($\sigma_a = \sigma_\gamma$, Table 10.2). However, the (n, α) reaction ($\sigma_a = \sigma_\alpha$) is characteristic for the $^{10}_5\text{B}$ and $^{7}_3\text{Li}$ nuclei and in the $^{235}_{92}\text{U}$ nucleus radiative capture and fission are two competing reactions ($\sigma_a = \sigma_\gamma + \sigma_f$).

In the thermal region the cross section for most nuclei varies as $1/v$,

$$\sigma_a = c/v \quad (10.2)$$

Table 10.2

Reaction Cross Sections for 0.025 eV Neutrons (in barns)

Nucleus	σ_t	σ_s	σ_a	σ_y	σ_f	σ_a
^9Be	7	7	0.01	0.01	—	—
^{12}C	4.8	4.8	0.0034	0.0034	—	—
^{10}B	4014	4.0	4010	0.5	—	4009.5
^{238}U	704	10	694	112	582	—

In handbooks of nuclear physics the values of the cross section for 0.025 eV, σ_{a0} , are usually given. The corresponding neutron velocity is $v_0 = 2200 \text{ m/s}$. At this velocity, i.e. when $v = v_0$, the cross section according to formula (10.2) is $\sigma_{a0} = c/v_0$. Thus the constant $c = \sigma_{a0}v_0$. Hence

$$\sigma_a = \sigma_{a0}v_0/v$$

If the neutron energy E_n is expressed in electronvolts,

$$\sigma_a = \sigma_{a0} \sqrt{0.025/E_n}$$

Example. Find the absorption cross section for natural boron and 0.085 eV neutrons if the absorption cross section $\sigma_{a0} = 755 \text{ b}$

$$\sigma_a = 755 \sqrt{0.025/0.085} = 410 \text{ b}$$

An excited compound nucleus may expel two neutrons if its excitation energy is not less than the total binding energy of two neutrons in the nucleus. The threshold energy of the $^9\text{Be}(n, 2n)^8\text{Be}$ reaction is 1.75 MeV. For the majority of nuclei the threshold energy of the $(n, 2n)$ reaction lies between 8 and 10 MeV. The energy dependence of the σ_{2n} cross section is similar to that of the inelastic scattering cross section σ_{in} with the difference that σ_{2n} begins to differ from zero at higher energies than σ_{in} does.

10.5 Neutron Detection

On passing through matter neutrons do not ionize directly the atoms and molecules as charged particles do. For this reason neutrons are detected on the basis of the secondary

effects which they produce in interacting with nuclei. These include the (n, α) reaction, (n, p) reaction, radiative capture, inelastic scattering, fission of heavy nuclei and elastic scattering on light nuclei.

All methods of neutron detection can be divided into two groups. In the first group neutrons are detected by the charged particles or γ -quanta they produce in nuclear reactions. Prompt information on the neutrons in a certain volume can be obtained by these methods. In the second group the information from the detectors can be obtained only after a certain time of irradiation of the detector (radioactive tracers, photographic plates). In one type of detector radioactive nuclei are formed (radioactive labelled atom technique) and in another, tracks are created (photographic plates). A figure of merit of a neutron detector is its efficiency. Each type of detector is most efficient in some certain energy range.

(n, α) Reaction. The exoergic (n, α) reaction on light nuclei ($^{10}_5\text{B}$, ^6Li) can readily be induced by neutrons. The reaction products create the primary ionization in the detector. Boron has found particularly wide application for neutron detection. The relevant reaction is $^{10}_5\text{B}$ (n, α) ^7_3Li . The 2.8 MeV of energy released in the reaction is carried off by the α -particle (1.5 MeV), recoil ^7_3Li nucleus (0.8 MeV) and γ -quantum (0.5 MeV).

The ^{10}B absorption cross section at 0.025 eV is 4010 b. For energies up to 10 keV it varies as $1/v$.

The counting rate due to reaction between the neutrons and boron atoms is proportional to $\int \sigma_a \varphi dv$. Since for ^{10}B the cross section $\sigma_a \sim 1/v$ and the neutron flux density $\varphi = nv$, the counting rate is proportional to $\int n(v) dv$, or the neutron density, which is the number of neutrons per unit volume of the detector. Boron detectors are especially efficient for measurement of slow neutrons ($E_n < 1$ keV).

Boron is introduced into the ionization chamber or other types of gas-filled detectors as the gas BF_3 . Alternatively, the electrodes may be coated with a layer of a boron-containing substance. Natural boron contains 18.8% of the isotope ^{10}B and 81.2% of ^{11}B which is a weak neutron absorber.

The average absorption cross section for the nuclei of natural boron is therefore 755 b. The efficiency of boron counters can therefore be enhanced by using boron enriched in ^{10}B . Another way of increasing the efficiency is to surround the detector with a moderator. Slowing of the neutrons increases their probability of being absorbed by the boron.

In scintillation counters boron can be introduced into the phosphors. The light flashes are caused by the α -particles and ^7Li nuclei. The resolution and efficiency of scintillation neutron counters are higher than in gas-filled counters.

An energy of 4.8 MeV is released in the $^6\text{Li}(n, \alpha)\text{T}$ reaction. The electrodes of gas-filled detectors can be coated with lithium or the latter may be introduced into the phosphors of scintillation chambers etc. Lithium detectors are less efficient since the cross section for absorption by ^6Li is only 945 b at 0.025 eV and the content of the isotope in natural lithium is merely 7.5%.

(n, p) Reaction. In the $^3\text{He}(n, p)\text{T}$ reaction an energy of 0.8 MeV is released. The cross section σ_p varies as $1/v$. For a neutron velocity $v_0 = 2200$ m/s the cross section $\sigma_{p0} = 5500$ b. Spherical chambers and counters are filled with helium at a pressure of about 10 atm. At such pressures the efficiency of spherical chambers with respect to thermal neutrons is close to unity.

Inelastic scattering and radiative capture. The γ -quanta emitted by excited nuclei after radiative capture of inelastic scattering of neutrons are usually recorded by scintillation counters.

Fission of heavy nuclei. The ^{235}U nucleus can be split into two nuclei (fission fragments) by neutrons of any energy. The electrodes of an ionization chamber, which in this particular case is called a fission chamber, is coated with a thin layer of a chemical compound containing uranium, for example with uranium dioxide. Some of the fission fragments produced in the layer as a result of neutron capture can enter the gas and ionize it. Fast neutrons can be measured with threshold fission chambers. In such chambers thin layers of a compound containing ^{238}U or ^{232}Th etc. are deposited on the electrodes. Threshold fission chambers record fast neutrons with energies exceeding the fission threshold which is 1.0 MeV for ^{238}U and ^{232}Th .

Recoil protons. Fast neutrons are recorded by the recoil proton technique. Some of the detectors are filled with hydrogen-containing gases (hydrogen, methane). In other detectors the electrodes are coated with a hydrogenous substance.

Fast neutrons can also be detected in chambers filled with argon, helium or other gases. A thin paraffin layer is placed before the entrance of the fast-neutron detector. The neutrons knock protons out of the paraffin which are then recorded by the detector.

Neutrons can also be detected by the recoil protons produced in a cloud chamber or bubble chamber filled with gaseous or liquid hydrogen respectively. Scintillation counters with organic phosphors which contain sufficient amounts of hydrogen can be employed to count recoil protons.

Radioactivation technique. The (n, b) reaction frequently involves the formation of β -active nuclei. The transformation of a stable nucleus into a radioactive nucleus in the (n, b) reaction is characterized by the activation cross section σ_{act} . This is the cross section for those (n, b) reactions in which radioactive nuclei appear. To illustrate, in the $^{107}\text{Ag}(n, \gamma)^{108}\text{Ag}$ reaction the stable ^{107}Ag nucleus is transformed into the radioactive ^{108}Ag nucleus, the activation cross section σ_{act} being equal to the radiative capture cross section σ_γ .

The amount of radioactive nuclei produced in a certain volume of matter depends on the neutron flux density φ , activation cross section σ_{act} , decay constant λ , volume of matter and time of neutron irradiation. If the number of nuclei per square metre of a thin target of total area S is N_s and the number of radioactive nuclei accumulated in the target after the beginning of irradiation is N then the rate of formation of radioactive nuclei $N_{rn} = \sigma_{act}N_s\varphi S$ and the disintegration rate is λN . The quantity N will increase until equilibrium is reached between the formation and disintegration of the radioactive nuclei, $\lambda N = \sigma_{act}N_s\varphi S$. After saturation of the target with radioactive nuclei is attained, and this occurs after about five half-life periods, the activity of the target, $a = \lambda N$, is measured. The neutron flux density can then be found from this *saturation activity*: $\varphi = a/\sigma_{act}N_sS$.

In the radioactivation technique neutrons are detected by the radioactivity they induce. Usually thin foils of various materials are employed (Table 10.3). An advantage of the method is that the foils do not take up much space (an area of 5 cm² and thickness of about 0.05 mm are sufficient) and they are not sensitive to γ -rays.

Table 10.3

Properties of Some Radioactivation Reactions

Target element	Activation cross section at $E_n = 0.025$ eV, barns	Reaction	Reaction products	Threshold energy, MeV	Half-life
^{197}Au	98	(n, γ)	^{198}Au	—	2.7 days
^{107}Ag	45	(n, γ)	^{108}Ag	—	2.3 min
^{109}Ag	116	(n, γ)	^{110}Ag	—	253 days
^{115}In	155	(n, γ)	^{116}In	—	54 min
^{27}Al	—	(n, p)	^{27}Mg	2.2	9.45 min
^{32}S	—	(n, p)	^{32}P	1.0	14.2 days
^{12}C	—	$(n, 2n)$	^{11}C	10.2	20.4 min
^{14}N	—	$(n, 2n)$	^{13}N	10.6	10.1 min

Radioactivation foils in which β^- -active nuclei are produced in the (n, γ) reaction are used for detection of thermal and resonance neutrons. If the foil is shielded by a cadmium sheath, which absorbs practically all thermal neutrons, it will be activated only by the resonance neutrons. Without the cadmium sheath radioactivation will be induced by both resonance and thermal neutrons. The ratio of the foil activities without and with the cadmium absorber, a and a_r , is called the *cadmium ratio*

$$R_{\text{Cd}} = a/a_r$$

The resonance neutron flux density is proportional to the activity with the cadmium absorber in place, a_r , and the thermal neutron flux density is proportional to the difference of the activities

$$a_{\text{th}} = a - a_r = (R_{\text{Cd}} - 1) a_r$$

From this equation it can be seen that $(R_{\text{Cd}} - 1)$ is proportional to the ratio of the thermal to resonance neutron flux

densities. The higher the cadmium ratio the smaller the fraction of resonance neutrons and vice versa.

The radioactivation technique can also be used for threshold detection. In this case the irradiated foil consists of substances (Table 10.3) whose nuclei become β -active as a result of the (n, p) or $(n, 2n)$ threshold reactions. The radioactivity of the foil is proportional to the flux density of neutrons possessing energies exceeding the threshold value.

Example. A $^{197}_{79}\text{Au}$ foil ($\rho = 19\ 300\ \text{kg/m}^3$) 0.01 mm thick (δ) and $10\ \text{cm}^2$ in area (S) is irradiated by a beam of thermal neutrons. The activation cross section for gold $\sigma_{\text{act}} = 98\ \text{b}$. Find the neutron flux density if the saturation activity of the foil $a = 650\ \text{decays/s}$.

The number of nuclei per square metre of the foil

$$N_s = \frac{\rho \delta}{A} N_A = \frac{19\ 300 \times 0.01 \times 10^{-3}}{197} \times \\ \times 6.02 \times 10^{26} \approx 5.9 \times 10^{23} \text{ nucl./m}^2$$

The thermal neutron flux density is then

$$\varphi = \frac{a}{\sigma_{\text{act}} N_s S} = \frac{650}{98 \times 10^{-28} \times 5.9 \times 10^{23} \times 10 \times 10^{-4}} \approx \\ \approx 1.13 \times 10^9 \text{ neutr./m}^2 \cdot \text{s}$$

10.6 General Law of Attenuation of the Neutron Flux Density. The Macroscopic Cross Section

Neutrons moving in matter are scattered and absorbed by the nuclei. Let a parallel (collimated) beam of monoenergetic neutrons fall perpendicularly onto a plane target of thickness δ (see Fig. 5.4 in which the γ -quanta should be replaced by neutrons). Those neutrons which react are removed from the beam. At some depth x the flux density of the primary neutrons is reduced to some value $\varphi(x)$. The decrease of the neutron flux density, $d\varphi$, in a thin layer dx is the product of the yield $\sigma_t N dx$ by $\varphi(x)$,

$$d\varphi = -\sigma_t \varphi(x) N dx \quad (10.3)$$

where $\sigma_t = \sigma_s + \sigma_a$ is the total cross section of the reaction and N is the density of the nuclei in the target. The minus sign indicates that the neutron flux is reduced in the layer.

Dividing both sides of the equation by φ and integrating from zero to x we get

$$\ln \varphi(x) = -N\sigma_t(x) + C$$

The integration constant C can be found from the boundary condition that at $x = 0$, $\varphi = \varphi_0$ and hence $\ln \varphi_0 = C$. Inserting this expression for C in the previous equation we get

$$\ln(\varphi/\varphi_0) = -N\sigma_t x$$

Taking the antilogarithms we obtain the law of attenuation of a parallel beam in a plane target:

$$\varphi(x) = \varphi_0 \exp(-N\sigma_t x) \quad (10.4)$$

The flux density $\varphi(x)$ drops off exponentially with increase of the depth x . The flux density of primary neutrons at a given depth in the target depends on the cross section σ_t and density of the nuclei N .

The cross section σ_t can be measured experimentally. One of the methods for measuring σ_t is based on the law of attenuation of the neutron flux density. If the neutron flux densities at the entrance, φ_0 , and exit, $\varphi(\delta)$, from the target are measured, it follows from equation (10.4)

$$\sigma_t = -\frac{\ln[\varphi(\delta)/\varphi_0]}{N\delta}$$

where δ is the target thickness. This method has been called the *transmission method* since the transmission coefficient $T = \varphi(\delta)/\varphi_0$ is measured and the total cross section σ_t is derived from it. Methods for measuring the partial cross sections σ_s and σ_a have also been developed. Data pertaining to neutron cross sections are presented in special manuals and handbooks of nuclear constants.

The attenuation of a parallel beam in a target (equation (10.4)) depends on the total cross section for all the nuclei in a cubic metre:

$$\Sigma_t = N\sigma_t$$

σ_t can be expressed in terms of the partial cross sections, $\sigma_t = \sigma_s + \sigma_a$. Hence

$$\Sigma_t = \Sigma_s + \Sigma_a$$

Any cross section

$$\Sigma_i = N\sigma_i \quad (i = t, s, a) \quad (10.5)$$

is called a *macroscopic* cross section whereas the σ_i cross sections are called *microscopic* cross sections.

In practical calculations the total and partial macroscopic cross sections are used. They can easily be calculated if the microscopic cross sections, density and composition of the target material are known.

There is one nucleus in each atom. Therefore the nuclear density can be calculated by means of formulae (1.1) and (1.2).

The macroscopic cross section for some i th process in a chemical compound is

$$\Sigma_i = N_1\sigma_{i1} + N_2\sigma_{i2} + \dots + N_n\sigma_{in} \quad (10.6)$$

Here $i = t, s, a$; $k = 1, 2, 3, \dots, n$ denotes the different types of nuclei in the molecule.

Example. Calculate the macroscopic cross section for 1 eV neutrons in water ($\rho = 1000 \text{ kg/m}^3$, $\mu = 18$). The cross section for hydrogen and oxygen at this energy is $\sigma_{sH} = 20 \text{ b}$, $\sigma_{aH} = 0.175 \text{ b}$; $\sigma_{sO} = 4 \text{ b}$, $\sigma_{aO} = 0$.

For the density of the oxygen and hydrogen nuclei we obtain from formula (1.2), taking into account that $n_H = 2$ and $n_O = 1$,

$$N_H = 2 \times 10^3 \times 6.02 \times 10^{26} / 18 = 6.68 \times 10^{28} \text{ nucl./m}^3, \\ N_O = N_H / 2 = 3.34 \times 10^{28} \text{ nucl./m}^3$$

Inserting into formula (10.6) the densities of the hydrogen and oxygen nuclei and also the respective microscopic cross sections, we get

$$\Sigma_s = 6.68 \times 10^{28} \times 20 \times 10^{-28} + 3.34 \times 10^{28} \times 4 \times \\ \times 10^{-28} = 147.4 \text{ m}^{-1} = 1.474 \text{ cm}^{-1}, \\ \Sigma_a = 6.68 \times 10^{28} \times 0.175 \times 10^{-28} + 1.17 \text{ m}^{-1} = \\ 0.0117 \text{ cm}^{-1}.$$

$$\Sigma_t = 147.4 + 1.17 \approx 148.6 \text{ m}^{-1} = 1.486 \text{ cm}^{-1}$$

In nuclear physics manuals and handbooks the microscopic cross sections are expressed in barns instead of square metres. It is therefore convenient to calculate the macroscopic cross sections in barns. Since $1 \text{ m}^3 = 10^{28} \text{ b}$, a density of $10^{28} \text{ nucl./m}^3 = 1 \text{ nucl./m} \cdot \text{b}$. In order to express the nuclear densities N and N_k in $\text{nucl./m} \cdot \text{b}$, the right-hand sides of formulae (1.1) and (1.2) should be reduced 10^{28} times:

$$N = 0.0602 \frac{\rho}{A}, \quad N_k = 0.0602 n_k \frac{\rho}{\mu} \quad (10.7)$$

If the densities for the hydrogen and oxygen nuclei are calculated by formulae (10.7) the cross section calculations will now be as follows:

$$N_H = 6.68 \text{ nucl./m} \cdot \text{b}, \quad N_O = 3.34 \text{ nucl./m} \cdot \text{b},$$

$$\Sigma_s = 6.68 \times 20 + 3.34 \times 4 = 147.4 \text{ m}^{-1} = 1.474 \text{ cm}^{-1},$$

$$\Sigma_a = 6.68 \times 0.175 = 1.17 \text{ m}^{-1} = 0.0117 \text{ cm}^{-1},$$

$$\Sigma_t = 147.4 + 1.17 \approx 148.6 \text{ m}^{-1} = 1.486 \text{ cm}^{-1}$$

It follows from equation (10.3) that the reaction rate per unit volume

$$-\frac{d\varphi}{dx} = \Sigma_t \varphi$$

is proportional to the neutron flux density. Replacing the total cross section by the sum of the partial cross sections we may write

$$\Sigma_t \varphi = \Sigma_s \varphi + \Sigma_a \varphi$$

The first term yields the number of scattered and the second the number of neutrons absorbed per m^3 of the material per second.

10.7 Neutron Diffusion

Mean free path. As discussed above, neutrons interacting with matter are scattered and absorbed by the nuclei. Those materials which predominantly scatter and only weakly absorb neutrons ($\sigma_s \gg \sigma_a$) may be termed *scattering* materials. Those for which $\sigma_a \gg \sigma_s$ are called *absorbing* substances. This division into scattering and absorbing substances

is of course conditional. In some energy range a substance may be scattering and in another range, absorbing. Boron, for example, is a good absorber of slow neutrons but only weakly absorbs fast neutrons.

The path of a neutron in a scattering substance is a zig-zag line (Fig. 10.5) consisting of straight lines of free flight

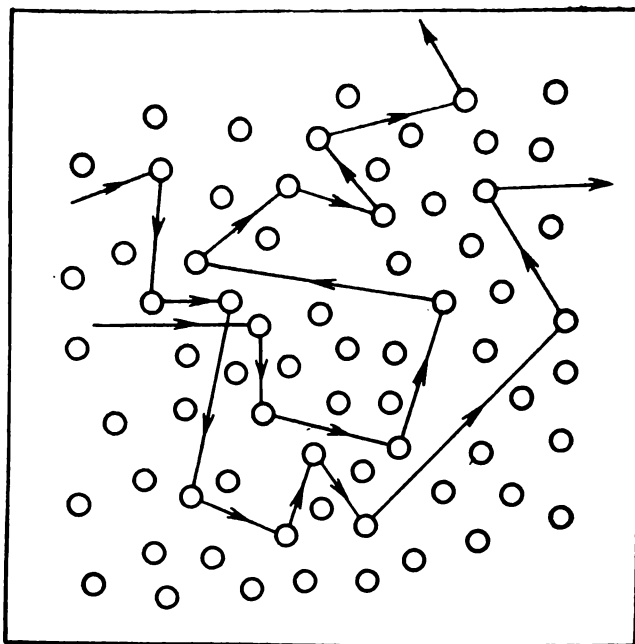


Fig. 10.5 Neutron paths in a scattering substance

between collisions. The distance a neutron covers between two consecutive collisions is the *scattering free path* (or scattering length). The scattering lengths are not the same, the distance covered between collisions being smaller in some cases than in others. After a number of scattering collisions the neutron is absorbed by the medium. The total path length traversed by a neutron after its appearance in the medium and up to its absorption is called the *absorption free path* (absorption length). Just as the scattering length, it is different for different neutrons. Some are absorbed after a few scattering events and others after a larger number of collisions. In absorbing media most of the neutrons are absorbed after a few collisions with the nuclei. In such media the neutrons do not migrate over a considerable distance.

In practical problems it is not the history of each separate neutron that is of interest but the migration of a large

number of neutrons in a scattering medium. The movement of neutrons in such conditions resembles in many respects that of gases or liquids which is described by the laws of diffusion. When gas molecules collide there is a general movement from sites of higher density to sites of lower density. The behaviour of neutrons is similar to that of gases. The main difference is that neutron diffusion is due to scattering collisions with nuclei of the medium. It should be noted that a collision between neutrons themselves is a rather rare event because the neutron density is from 10^{12} to 10^{14} times less than that of nuclei.

The general movement of many neutrons in media may be characterized by the mean scattering length λ_s and mean absorption length λ_a . They are related to the macroscopic cross sections by very simple equations:

$$\lambda_i = 1 / \Sigma_i, \quad i = s, a \quad (10.8)$$

In the theory of neutron diffusion it is assumed that all neutrons of a given energy have the same mean scattering length λ_s and cover the same mean distance λ_a before they are absorbed. The total mean free path is expressed by a formula similar to that for the partial cross sections,

$$\lambda_t = 1 / \Sigma_t \quad (10.9)$$

From formulae (10.8) and (10.9) it follows that

$$\lambda_t = \lambda_s \lambda_a / (\lambda_s + \lambda_a)$$

The physical meaning of λ_t will be clear if we consider the attenuation law for a parallel beam of monoenergetic neutrons in a plane-parallel plate. The total mean free path of the neutrons is simply the thickness of a layer which reduces the primary neutron flux density by e times. In scattering media $\lambda_s \ll \lambda_a$ and hence $\lambda_t \approx \lambda_s$. On the contrary, in absorbing media $\lambda_t \approx \lambda_a$. Thus the mean free paths for 0.025 eV neutrons in beryllium are $\lambda_s = 1.15$ cm, $\lambda_a = 810$ cm, $\lambda_t = 1.15$ cm, and in natural boron $\lambda_s = 1.2$ cm, $\lambda_a = 1.1 \times 10^{-3}$ cm and $\lambda_t \approx 1.1 \times 10^{-3}$ cm.

Average cosine of the scattering angle. The direction of a neutron scattered elastically by a nucleus is different from the initial direction, the angle between the initial and final velocities being anything between 0 and 180° . In central

collisions the neutron is scattered through an angle $\theta = 180^\circ$ and in noncentral collisions the angle θ lies in the range $0 \leq \theta < 180^\circ$. Only if neutrons are scattered by protons the scattering angle cannot exceed 90° , $\theta < 90^\circ$.

Neutron scattering is said to be *isotropic* if the scattering probability is the same for any direction. As a rule, however,

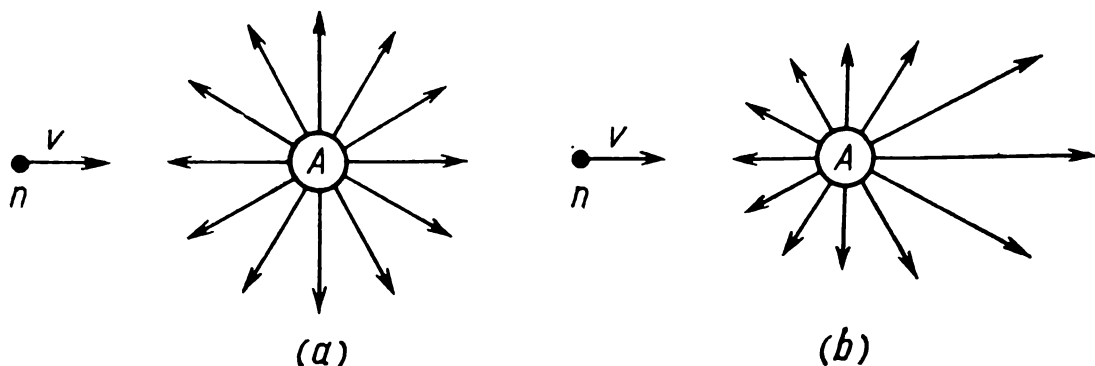


Fig. 10.6 Isotropic (a) and anisotropic (b) scattering of neutrons

nuclei scatter most neutrons at angles $\theta < 90^\circ$ and fewer at $\theta > 90^\circ$. This type of scattering is said to be *anisotropic*. Isotropic and anisotropic scatterings are diagrammatically depicted in Fig. 10.6. The arrows show the direction of the scattered neutrons, and the lengths of the arrows are proportional to the probability $f(\theta)$ that a neutron is scattered through an angle θ .

Anisotropy of neutron scattering is characterized by the mean cosine of the scattering angle, $\bar{\mu} = \overline{\cos \theta}$. For isotropic scattering $\bar{\mu} = 0$ and for anisotropic scattering $\bar{\mu} > 0$. If

Table 10.4

**Average Cosines of the Neutron Scattering Angles
for Various Nuclides**

Nuclide	$\bar{\mu}$	Nuclide	$\bar{\mu}$
H	0.67	^{12}C	0.056
D	0.53	^{16}O	0.042
^9Be	0.074	^{238}U	0.0028

the neutron energy is not high, $\bar{\mu}$ depends only on the mass number A ,

$$\bar{\mu} = 2/3A$$

The anisotropy of neutron scattering is particularly high in hydrogen and deuterium (Table 10.4). With increase of the mass number A the mean cosine $\bar{\mu}$ tends to zero and hence it may be considered that for $A > 10$ scattering is approximately isotropic.

Diffusion coefficient. A net flow of neutrons from one part of space to another will occur spontaneously only if there is a difference in the neutron densities.

The movement of neutrons from one site to another is impeded by the medium since the neutrons collide with nuclei of the medium and change the direction of their motion. The higher the density of nuclei the more difficult it is for the neutrons to travel over even comparatively small distances. The net displacement depends on the difference between the neutron flux densities at the two sites under consideration.

The movement of neutrons in a medium is characterized by the *neutron flow*, J , defined by the equation

$$J = -D \frac{d\phi}{dx} \quad (10.10)$$

The first factor depends on the properties of the medium and is called the *diffusion coefficient*. It is inversely proportional to the number of scattering collisions of neutrons per unit length in the medium,

$$D = \lambda_s/3 (1 - \bar{\mu})$$

The neutron flow resistance is higher for media with small diffusion coefficients (water, beryllium). Even thin layers of such substances considerably weaken the neutron flux.

The second factor ($-d\phi/dx$) takes into account the effect of the rate of variation of the flux density on neutron diffusion. The larger the difference between the neutron flux densities at two different sites, the higher is the rate of diffusion between the two points. The minus sign indicates that neutrons flow from higher to lower neutron flux densities.

There is a difference in the movement of fast and slow neutrons. Fast neutrons are slowed down since their energies are much greater than the energy of thermal motion of atoms of the medium. On the contrary, the energy of thermal neutrons is comparable to that of the atoms and hence they may either be decelerated or accelerated depending on the relative energies of the neutrons and atoms.

10.8 Neutron Slowing-Down

Elastic and inelastic scattering. Neutron sources emit fast neutrons. The fate of the neutrons depends on the composition and size of the medium. As a result of elastic and inelastic encounters with nuclei the neutrons are slowed down. In finite-size media part of the slowed neutrons moving near the surface leak out of the medium. All these factors affect the spatial and energy distribution of the slowed neutrons.

In heavy substances fast neutrons are slowed down to energies of 0.1-0.4 MeV as a result of inelastic collisions with nuclei, and then are either absorbed by the medium or escape from it. In an inelastic collision a fast neutron may spend the greater part of its energy in excitation of the nucleus. The lower energy limit for inelastic slowing-down is comparable to the first excited level of the heavy nucleus.

In light substances elastic slowing-down of neutrons occurs. In such media fast neutrons transfer practically all of their kinetic energy to the nuclei after several dozens of elastic encounters and are slowed down to thermal energies. Elastic slowing of fast neutrons by heavy nuclei is not effective because only a very small part of the neutron energy is imparted to a heavy nucleus in an elastic collision with it. If a medium consists of light and heavy nuclei both elastic and inelastic scattering will contribute to neutron slowing-down. The contribution of each of the processes depends on the volume content of each of them. If the volume contents are nearly the same most of the neutrons are first slowed down by inelastic collisions to energies of 0.1-0.4 MeV and then by elastic collisions down to thermal energies.

Slowing parameter. The energy lost by neutrons in elastic scattering depends on the type of collision between the neu-

tron and nucleus and also on the mass of the nucleus. Maximum neutron energy loss ΔE_{\max} occurs in the case of a central collision with the nucleus (scattering angle $\theta = 180^\circ$, recoil angle $\varphi = 0$). According to equation (10.1)

$$\Delta E_{\max} = E_{\text{nuc}} = E_1 - E_2 = 4AE_1/(A + 1)^2$$

where E_1 and E_2 are the initial and final energies of the neutron. A neutron colliding head-on with a hydrogen nucleus ($A = 1$) loses all its energy; in a central collision with a carbon nucleus ($A = 12$) 28% of the neutron energy is imparted to the nucleus, and in a collision with a uranium nucleus ($A = 238$) only 1.6%. Thus the amount of energy lost by a neutron in an elastic collision decreases with increase of the mass number A .

Neutrons experience, as a rule, noncentral collisions ($0 < \varphi < 90^\circ$) for which $\Delta E < \Delta E_{\max}$. The mean energy loss per collision, $\overline{\Delta E}$, is half of the maximum value ΔE_{\max} ; $\overline{\Delta E}$ is not a convenient quantity to be used in practice since it depends on the initial neutron energy and decreases as the neutrons are slowed down. The quantity used in practice is the mean logarithmic neutron energy loss per collision, the *slowing-down parameter* ξ ,

$$\xi = \overline{\ln E_1 - \ln E_2} = \overline{\ln (E_1/E_2)}$$

The slowing parameter depends only on the mass number A and is the same in any energy range. Values of ξ for a number of substances are presented in Table 10.5.

Table 10.5

Slowing Parameter

Nuclide	A	ξ	Nuclide	A	ξ
H	1	1.000	C	12	0.158
D	2	0.725	Na	23	0.084
Be	9	0.209	U	238	0.0085

The formula for the slowing-down parameter is very simple for mass numbers $A > 9$:

$$\xi = 2/(A + 2/3)$$

Since the slowing-down parameter does not depend on energy it is quite simple to calculate, for example, the mean number of collisions j experienced by a neutron slowed down from an energy E_1 to E ,

$$j = \frac{\ln (E_1/E)}{\xi}$$

In this formula $\ln (E_1/E)$ can be replaced by the difference,

$$\ln (E_1/E) = \ln (E_0/E) - \ln (E_0/E_1)$$

where E_0 is a prescribed constant. The value $E_0 = 2 \times 10^6$ eV is frequently employed in the calculations. The quantity $u = \ln (E_0/E)$ is called the *neutron lethargy*. With slowing-down of the neutrons it increases and in the thermal range ($E = 0.025$ eV) $u_{th} = 18.2$.

Let us rewrite the formula for j in the form

$$j = (u - u_{th})/\xi$$

and calculate the mean number of collisions on slowing-down the neutrons from $u = 0$ to $u_{th} = 18.2$ in hydrogen, beryllium and carbon. From Table 10.5 we find $\xi_H^{th} = 1.000$, $\xi_{Be} = 0.209$ and $\xi_C = 0.158$. The mean numbers of collisions are then

$$j_H = 18.2, \quad j_{Be} = 87, \quad j_C = 115$$

Moderators. Each slowing neutron collides with nuclei of the scattering substance on the average $\Sigma_s = 1/\lambda_s$ times per metre path length and its lethargy is increased by $\xi \Sigma_s$. The latter quantity is the *slowing-down power of the substance*. The higher the slowing-down power the faster neutrons lose their speed.

Another characteristic of moderating substances is the *neutron slowing-down coefficient*

$$k_m = \xi \Sigma_s / \Sigma_{a,th}$$

where $\Sigma_{a,th}$ is the thermal neutron absorption cross section. The slowing-down coefficient is proportional to the ratio

of the specific rates of formation and absorption of thermal neutrons. The rate of formation of thermal neutrons increases with increase of the slowing-down power and decrease of the absorption cross section. Light substances which possess high values of the slowing-down power and of the neutron slowing-down coefficient are called *moderators*.

Values of the neutron slowing-down power and slowing-down coefficients for a number of substances are presented in Table 10.6. The best moderator is heavy water ($k_m = 20\,000$). However, heavy water is expensive and water or graphite is usually used.

Table 10.6

Physical Characteristics of Moderators

Moderator	Density, kg/m^3	Slowing-down parameter, ξ	Slowing-down power, m^{-1}	Slowing-down coefficient
Water	1000	0.924	135	70
Heavy water	1100	0.515	18.8	20 000
Beryllium	1800	0.209	15.4	159
Beryllium oxide	2800	0.174	12.9	180
Diphenyl mixture	1060	0.886	16.1	118
Graphite	1670	0.158	6.4	170

The slowing-down power of alloys or chemical compounds can be calculated by the formula

$$\xi \Sigma_s = \xi_1 \Sigma_{s1} + \xi_2 \Sigma_{s2} + \dots + \xi_n \Sigma_{sn}$$

The subscripts $i = 1, 2, \dots, n$ correspond to the various nuclei in the alloy or compound; the $\xi_i \Sigma_{si}$ are the respective slowing-down powers.

Example. Find the slowing-down power of diphenyl for 1 eV neutrons. The density of diphenyl is 900 kg/m^3 and its molecular mass $\mu = 154$. From formula (10.7) we determine the density of the hydrogen and carbon nuclei:

$$N_H = 10 \times \frac{900}{154} \times 6.02 \times 10^{-2} = 3.5 \text{ nucl./m.b}$$

$$N_C = 12 \times \frac{900}{154} \times 6.02 \times 10^{-2} = 4.2 \text{ nucl./m.b}$$

Since $\sigma_{sH} = 20$ b, $\sigma_{sC} = 4.8$ b, $\xi_H = 1$ and $\xi_C = 0.158$ we find that the slowing-down power of diphenyl is

$$\begin{aligned}\xi\Sigma_s &= 1 \times 3.5 \times 20 + 0.158 \times 4.2 \times 4.8 = \\ &= 73.2 \text{ m}^{-1} = 0.732 \text{ cm}^{-1}\end{aligned}$$

Energy spectrum of slowing-down neutrons. Slowing neutrons have a certain distribution in energy. In general it depends on the properties and size of the moderator, distribution of the fast neutron sources in the moderator and on the absorption of the neutrons. The shape of the energy spectrum is simplest for an infinite-size moderator and a uniform distribution of the fast neutron sources. In this particular case the energy spectrum of slowing neutrons is called the *Fermi spectrum* and can be expressed by the formula

$$\varphi(E) = \frac{Q}{\xi\Sigma_s} \frac{1}{E}$$

If the slowing-down power in the medium-energy region is constant, $Q/\xi\Sigma_s = B = \text{const}$ and

$$\varphi(E) = B/E$$

Slowing-down length. Before a fast neutron becomes thermal it moves a certain distance away from the source. This distance is different for each neutron: some neutrons are thermalized near the source and others at appreciable distances from it. The mean distance from the source at which the neutrons are thermalized is the *slowing-down length* L_s . If the neutron source is located at a distance $\delta < L_s$ from the boundary surface of the medium, part of the slowing neutrons will escape from the medium.

The distance a fast neutron travels from the source depends on three quantities, on the diffusion coefficient, slowing-down power of the substance and initial energy of the neutron. If the diffusion coefficient D is small, fast neutrons cannot migrate far away from the source. The slowing-down length will also be smaller if the slowing-down power $\xi\Sigma_s$ of the substance is high. Finally the neutron slowing-down length increases with the initial energy of the neutrons.

If the scattering cross section of the medium depends weakly on the neutron energy, the square of the slowing-

down length, called the *neutron age* and denoted τ , can be determined from the equation

$$L_s^* = \frac{D}{\xi \Sigma_s} u_{th}$$

Since the diffusion coefficient D is inversely proportional and the macroscopic cross section is directly proportional to the density of the substance, ρ , the neutron age $L_s^* \sim 1/\rho$. Thus the slowing-down lengths, L_{s0} and L_s , in a given substance with different densities, ρ_0 and ρ , are related by the equation

$$L_s = L_{s0} \rho_0 / \rho$$

The density of a solid depends on the technology of its production and does not vary appreciably with temperature. The density of graphite, for example, varies between 1650 and 1800 kg/m³ and that of beryllium, between 1750 and 1850 kg/m³. The density of a liquid does not depend on how it was produced but pronouncedly decreases with heating. Thus the density of water at 100 atm drops from 1000 to 726 kg/m³ as the temperature is raised from 20 to 300°C.

The most exact information on the neutron slowing-down length can be obtained by direct measurements (Table 10.7) since for most moderators the scattering cross section depends on the neutron energy. The slowing-down length in a moderator whose density ρ differs from the table value ρ_0 can be calculated by means of the formula given above.

Table 10.7

Experimental Values of the Slowing-Down Length
for 2 MeV Neutrons

Moderator	Density, 10 ³ kg/m ³	Slowing- down length, 10 ⁻² m	Moderator	Density, 10 ³ kg/m ³	Slowing- down length, 10 ⁻² m
Water	1.0	5.2	Beryllium	1.85	9.3
Heavy wat- er	1.1	11.2	Beryllium oxide	2.8	12.0
Graphite	1.67	17.7	Diphenyl mix- ture	1.06	9.6

10.9 Thermal Neutrons

Neutron temperature. The energy of thermal neutrons migrating in a medium is about the same as the energy of thermal motion of the nuclei. After numerous elastic collisions with nuclei of the medium, an equilibrium velocity distribution of the thermal neutrons becomes established. The velocity distribution of gas molecules, and hence of thermal neutrons, is Maxwellian (see Fig. 1.1). The neutron kinetic energy corresponding to the most probable neutron velocity v_p is

$$E_n = m_n v_p^2 / 2 = k T_n$$

By analogy with the gas temperature T_n is called the *neutron temperature*. Inserting the value of the Boltzmann constant $k = 8.61 \times 10^{-5}$ eV/K, we get

$$E_n = 8.61 \times 10^{-5} T_n \text{ eV}$$

It is more difficult to measure the neutron temperature than the temperature of a gas. The velocity distribution of the neutrons is first measured with a neutron spectrometer. The most probable neutron velocity is then found and the neutron temperature is then calculated.

The neutron temperature T_n depends on the temperature of the medium T , on the slowing-down power $\xi \Sigma_s$, absorption cross section σ_a and size of the medium. Absorption of thermal neutrons by the medium may be regarded as effectively draining the particles out of the medium. The absorption cross section for moderators varies as $1/v$ and hence a neutron with a velocity $v < v_p$ is absorbed with a higher probability than one with $v > v_p$. This higher absorption of slow neutrons results in the peak of the spectrum being displaced toward higher neutron velocities.

In diffusion theory of thermal neutrons it is assumed that all thermal neutrons have the same energy, and the capture cross section and diffusion coefficient are averaged over the thermal neutron spectrum.

Diffusion length. A thermal neutron moves from the site of its origin to the site of its absorption on the average by a distance L , the *thermal neutron diffusion length*. This quanti-

ty depends on the diffusion coefficient D and macroscopic absorption coefficient of the thermal neutrons, Σ_a

$$L^2 = D/\Sigma_a \quad (10.11)$$

The relation between the diffusion length and neutron temperature T_n is

$$L^2 (T_n) = L_0^2 \sqrt{T_n/293}$$

where L_0^2 is the square of the thermal neutron diffusion length at 293 K and T_n is expressed in kelvins (K).

Leakage of thermal neutrons from the medium occurs from a surface layer with a thickness L . Those thermal neutrons which originate at a distance exceeding the diffusion length L are ultimately absorbed by the medium.

The main diffusion characteristics of moderators measured at $T_n = 293$ K are shown in Table 10.8. The absorption cross section and diffusion length of thermal neutrons depend on impurities in the moderator. Admixtures of water or heavy water are particularly efficacious. Thus an admixture of 0.2% water or heavy water reduces L from 159 to 110 cm.

Table 10.8

Diffusion Characteristics of Moderators

Moderator	Density, 10^3 kg/m^3	Thermal neutron absorption cross section σ_a , b	Diffusion coefficient D , cm	Diffusion length L , cm
Water	1.0	0.664	0.163	2.72
Heavy water	1.1	1.14×10^{-3}	0.960	159
Beryllium	1.85	0.01	0.533	21
Graphite	1.67	3.2×10^{-3}	0.900	58
Beryllium oxide	2.8	0.01	0.560	30
Diphenyl mixture	1.06	3.354	0.140	3.7

Migration length. Neutrons migrating in a medium move away from the point of their origin. Fast neutrons are first slowed down into the thermal energy region and then move around until they are absorbed by the medium. The mean distance between the point of origin and point of absorption is proportional to the migration length defined by the

formula

$$L_m = \sqrt{L_s^2 + L^2}$$

Escape of neutrons from a finite-size medium is determined by the migration length. The larger it is the thicker is the surface layer from which neutron leakage occurs.

10.10 Nuclear Fission

In 1938 the German chemists Hahn and Strassmann found that barium could be detected in uranium samples bombarded with neutrons. The appearance of barium, which

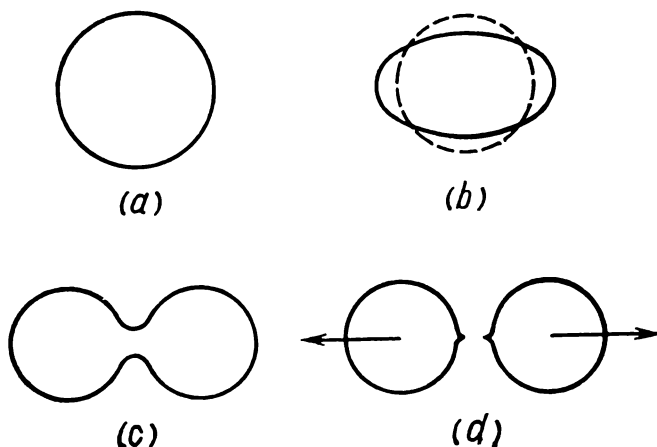


Fig. 10.7 Nuclear fission according to the liquid drop model
 a—undeformed nucleus; b—weakly deformed nucleus; c—highly deformed nucleus
 d—fission fragments

is an element in the middle of the periodic table, was subsequently ascribed to the division of ^{235}U into two nuclei (fission fragments) induced by the neutrons.

This nuclear fission can be explained by the drop model of the nucleus. Both coulomb and nuclear forces are active in the nucleus. Coulomb repulsion between protons tends to split the drop-like nucleus into fragments. On the other hand, the surface forces due to nuclear interaction between nucleons overcome the coulomb repulsion and maintain the nucleus as an entity.

Suppose a neutron is absorbed by the nucleus. The shape of the nucleus begins to change and passes through a number of stages. A spherical nucleus (Fig. 10.7a) may first become

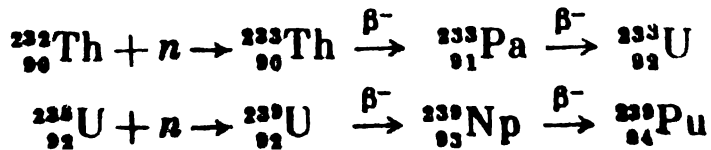
ellipsoidal (Fig. 10.7b). Surface forces tend to bring the nucleus back to its original shape. If the excited nucleus becomes spherical again, γ -quanta are emitted and the nucleus returns to the ground state. If, however, the excitation energy exceeds the fission threshold energy W_f , the nucleus will assume a dumbbell shape (Fig. 10.7c) and may divide into two fragments under the effect of the repulsive Coulomb forces (Fig. 10.7d).

After capture of a neutron by a heavy nucleus, a compound nucleus is formed with an excitation energy W_{ex} which is approximately equal to the sum of the neutron binding energy in the compound nucleus and the kinetic energy of the neutron (see Sec. 8.3). Fission of the compound nucleus may occur if W_{ex} exceeds the fission threshold of the compound nucleus. In heavy nuclei ($A = 230-240$) W_f is about 5.5-5.9 MeV.

Heavy nuclei in the ground state can undergo spontaneous fission. For nuclei with $A \leq 240$ this is a rather rare event. Spontaneous fission of ^{235}U nuclei, for example, is 2.5×10^8 times less probable than α -decay.

Natural uranium consists of two main isotopes, ^{235}U (0.7%) and ^{238}U (99.3%). The difference in the fission properties of these two isotopes can easily be understood if one compares the values of W_{ex} and W_f . On capturing a thermal neutron the ^{235}U nucleus is transformed into a ^{236}U nucleus with an excitation energy of 6.4 MeV and a ^{236}U fission threshold of 5.8 MeV. Thus the ^{235}U nucleus can be made to undergo fission by neutrons of any energy. The fission threshold for the ^{238}U nucleus $W_f \approx 5.8$ MeV whereas the excitation energy after capture of a thermal neutron by ^{238}U is only 4.8 MeV. This means that the ^{238}U nucleus can be split only by neutrons with energies exceeding 1.0 MeV.

Thermal neutrons can also induce fission in ^{233}U and ^{239}Pu . The ^{233}U , ^{235}U and ^{239}Pu nuclei and materials containing them are called *fissile materials*. ^{233}U and ^{239}Pu are not found in nature and are obtained artificially in accordance with the transformation sequences



Thorium and ^{238}U , which are used to obtain fissile materials, are called *nuclear fuels*.

Fission fragments. It has been found by chemical analysis that the fission fragments consist of nuclides with mass numbers lying between 72 and 161. The fragment yield per thermal neutron-induced fission of ^{235}U as a function of the mass

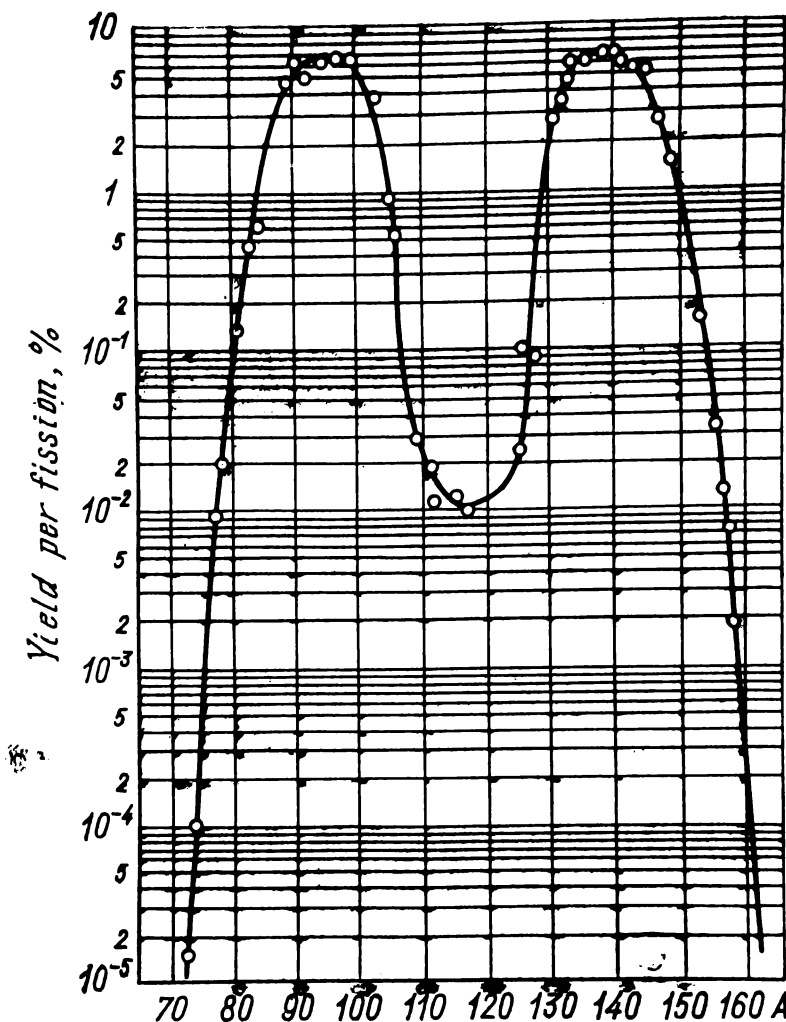


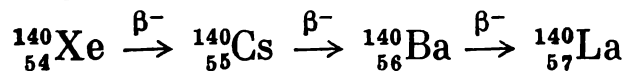
Fig. 10.8 Yield of fission products per ^{235}U fission induced by thermal neutrons

number is depicted in Fig. 10.8. The fragment yield per fission event is defined as the number of fission events involving the formation of the given fragment to the total number of fission events. Two groups of fission fragments are particularly pronounced on the curve. The first group of fragments produced with a high probability consists of compar-

atively light nuclei with mass numbers between 80 and 110. The second group consists of heavier nuclei with mass numbers between 125 and 155. A light and a heavy fragment are produced in 99% of fissions. Symmetric fission into two fragments with almost equal masses ($A = 110-125$) is a very rare event. The fraction of such fissions is about 1%. Hence fission almost invariably involves the formation of a light and heavy fragment.

Nuclear fission can proceed along approximately 30 channels. Thus about 30 different pairs of light and heavy fragments appear on fission of nuclei.

Fission fragments are β^- -active since there is an excess of neutrons. An example are the $^{94}_{38}\text{Sr}$ and $^{140}_{54}\text{Xe}$ fragments produced with a yield of about 7%. The mass numbers of stable strontium and xenon nuclei do not exceed 88 and 136 respectively. The $^{94}_{38}\text{Sr}$ nucleus has therefore an excess of six neutrons and $^{140}_{54}\text{Xe}$ nucleus an excess of four neutrons. Fission fragments can thus be the beginning of a radioactive sequence of β^- -decays. As a rule there are three disintegrations in the sequences which terminate with the formation of a stable nucleus. An example of such transformation chains is that involving the formation of lanthanum:



About 180 radioactive nuclides are formed in a nuclear fuel as the result of fission and subsequent disintegration of the fragments. Fission fragments and the products of their radioactive decay are called *fission products*.

Fission neutrons. In each fission v neutrons are emitted on the average. This number v is the *neutron yield per fission*. It depends on the energy of the absorbed neutron (Table 10.9).

Fission neutrons can be prompt or delayed. Prompt neutrons are emitted at the instant of fission, whereas delayed neutrons are emitted a certain time after fission.

Over 99% of fission neutrons are prompt neutrons. The energies of most of them are between 0.1 and 10 MeV. In many applied problems (calculation of the slowing-down length of fission neutrons, mean number of elastic scatterings per slowing etc.) account of the energy distribution of prompt neutrons considerably complicates the calculations. For simplification it is usually assumed that the energy of

Table 10.9

Neutron Yield per Fission

Nuclide	E_n	
	0.025 eV	1.8 MeV
^{233}U	2.52	2.71
^{235}U	2.41	2.74
^{238}U	—	2.70
^{239}Pu	2.92	3.21

all prompt neutrons is the same and equal to the mean energy of 2 MeV. This energy is the constant E_0 used in determining the lethargy.

Delayed neutrons comprise less than 1% of the fission neutrons. Some fission fragments (^{87}Br , ^{88}Br etc.) after β^- -decay form daughter nuclei with excitation energies exceeding the neutron binding energy. The β -decay is immediately accompanied by the emission from the daughter nucleus of a neutron whose time of appearance thus depends on the half-life of the parent fission fragment. Depending on the half-life of the fragments delayed neutrons are divided into six groups (Table 10.10).

The delay times of the different neutron groups vary from a fraction of a second to tens of seconds. The largest contribution to the yield of the delayed neutrons βv is from the

Table 10.10

Delayed Neutron Groups of the ^{235}U Nuclide

Group number i	Fragment half-life, s	Fraction of fission neutrons emitted as delayed neutrons of group i (β_i)	Kinetic energy of delayed neutrons, MeV
1	0.2	0.00027	—
2	0.6	0.00074	0.42
3	2.3	0.00253	0.62
4	6.2	0.00125	0.43
5	22.7	0.00140	0.56
6	55.7	0.00021	0.25
		0.0064	

third, fourth and fifth groups. The total fraction of delayed neutrons emitted per fission of ^{236}U is $\beta = 0.00640$ and the mean delay time is 12.4 seconds.

Despite their small yield delayed neutrons are of great importance for controlling fission chain reactions. Under certain conditions they ensure that safe build-up of the chain process will occur (see Part Two).

The absorption cross section of fissioning nuclei is the sum of the cross sections for fission σ_f and radiative capture σ_γ ,

$$\sigma_a = \sigma_f + \sigma_\gamma = \sigma_f (1 + \alpha)$$

Hence $1/(1 + \alpha)$ of the neutrons absorbed by nuclei induce fission. The neutron yield per absorption act, η , which is equal to the number of neutrons produced per neutron capture in a fissioning nucleus, is

$$\eta = v\sigma_f/\sigma_a = \gamma/(1 + \alpha)$$

In the thermal (Table 10.11) and high energy regions, $\eta > 2$ for all fissioning nuclei. However, in the medium energy region it is only 1.5 for the ^{235}U and ^{239}Pu nuclides. Therefore, neutron multiplication induced by medium-energy neutrons is less efficient.

Table 10.11

Neutron Yield per Absorption of Thermal Neutrons, η

Nuclide	σ_f, b	σ_γ, b	σ_a, b	$1 + \alpha$	η
^{233}U	527	54	581	1.10	2.29
^{235}U	582	112	694	1.19	2.07
^{239}Pu	746	280	1026	1.38	2.12

Energy of fission. The mean binding energy per nucleon in nuclei with mass numbers $A \sim 100$ (see Fig. 3.4) exceeds by about 0.85 MeV that in the uranium nucleus. This means that as a result of fission an energy of 0.85 MeV is released per nucleon. The energy released per nucleus is therefore $W_f = 235 \times 0.85 \approx 200 \text{ MeV}$.

Most of the energy W_f is imparted to the fragments as kinetic energy. Some of the energy is emitted as prompt

γ -radiation and also as the energy of the β^- - and γ -rays emitted in the subsequent radioactive disintegration of the fission fragments; finally, a perceptible amount of energy is carried off by the fission neutrons and neutrinos. The energy balance of fission expressed in MeV is given in the following table

Kinetic energy of fission fragments	169
Energy of	
prompt γ -quanta	5
fission neutrons	5
decay β -particles	7
decay γ -quanta	6
neutrinos	11
<hr/>	
Total	203

Besides these energy components some energy goes into the γ -quanta emitted after radiative capture of part of the fission neutrons. This component depends on the composition and size of the fission medium and on the average is ~ 8 MeV per nuclear fission. Thus approximately 211 MeV of energy is released in the medium as a result of fission of a nucleus. All of this energy except that of the neutrino, i.e. about 200 MeV, can be transformed into heat. To generate a power of 1 kW about 3.1×10^{13} fissions per second would be required. An amount of energy equivalent to 2000 kW over a year could be attained by "burning" a kilogram of a fissionable material.

10.11 Nuclear Fission Chain Reaction

The abundant emission of neutrons in fission of a nucleus enhances the possibility that fission will be induced in another nucleus. Suppose three neutrons are emitted in each fission. Each of these neutrons may induce fission and create three new neutrons. These neutrons can be called neutrons of the first generation. They can then generate $3^2 = 9$ second generation neutrons. In the third generation there will be $3^3 = 27$ neutrons etc. (Fig. 10.9). Roughly, this is how multiplication of neutrons proceeds. The pattern of chemical chain reactions is essentially the same and hence the process outlined above is called a neutron or fission chain reaction. A small amount of neutrons is required to start a chain reaction.

If neutron multiplication actually took place as sketched in Fig. 10.9 there would be $3^{50} \approx 10^{26}$ neutrons in the fiftieth generation of a single neutron. In reality not all neutrons induce fission. Some are lost as a result of radiative capture and others leak out of the fission medium. These losses affect the course of the chain reaction.

Fission chain reactions take place in media containing the fissionable substance, moderators, structural materials

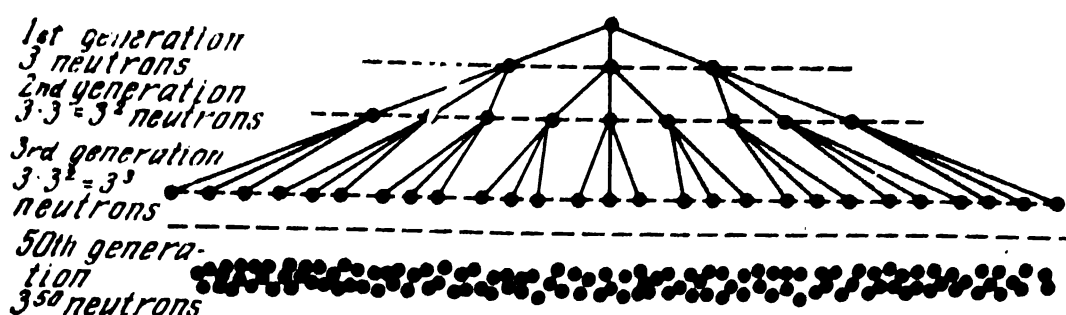


Fig. 10.9 Neutron multiplication in a nuclear fission chain reaction

(aluminium, zirconium, stainless steel etc.) and neutron absorbers. The fast fission neutrons interact with all these materials and hence elastic and inelastic slowing and absorption of neutrons occur along with nuclear fission. If the amount of moderator is not large the fast neutrons will be absorbed before being slowed down to thermal energies. In this case most of the fission reactions will be induced in the high-energy region. This kind of chain reaction is said to be a *fast neutron-induced fission reaction*.

As the amount of moderator is increased, elastic slowing of neutrons becomes more pronounced and relatively more fissions are induced at lower energies. At certain concentrations of the moderator most nuclei are split by medium-energy or thermal neutrons (*medium or thermal neutron-induced chain reaction*).

Thermal neutrons are most readily absorbed by fissionable nuclei. The fission cross section in the thermal region is hundreds of times greater than that in the fast region. This fact is exploited by slowing-down fast neutrons to thermal energies without loss and then using the slow neutrons for fission.

Assume for simplicity that the medium consists of only two components, the moderator and uranium, and a thermal-neutron chain reaction is taking place. The concentration of the moderating nuclei N_m will considerably exceed that of the uranium nuclei N_U in such a medium. The concentration of uranium nuclei in the medium will therefore be close to N_U/N_m . The inverse ratio N_m/N_U shows how many moderator nuclei there are per uranium nucleus. The number of uranium nuclei per cubic metre is the *nuclear concentration*.

In a ^{235}U -C medium a chain reaction induced by thermal neutrons takes place when $N_U/N_C \approx 3 \times 10^{-5}$ or $N_C/N_U \approx \approx 3 \times 10^4$ for ^{235}U nuclei.

Consider a thermal-neutron chain reaction in an infinite medium. Multiplication of neutrons can conveniently be viewed as a sequence of reproduction cycles. Each such cycle consists of four consecutive stages, viz. absorption of the thermal neutrons, fission of the ^{235}U nuclei, fast neutron-induced fission of ^{238}U nuclei and resonance absorption of neutrons.

Let the neutron density of the first generation (beginning of multiplication cycle) be n_1 . We shall find the number of second generation neutrons (end of multiplication cycle). All n_1 thermal neutrons are absorbed in an infinite medium, θn_1 thermal neutrons being absorbed by the uranium. The quantity θ is the *thermal-neutron* (or simply, *thermal*) *utilization factor* and expresses the fraction of thermal neutrons absorbed by the uranium fuel. It is always less than one because some of the neutrons are absorbed by the moderator. It is evident that θ approaches unity as the uranium concentration is increased.

On the average each of the θn_1 neutrons produces η fission neutrons and hence the number of fast neutron is $\eta \theta n_1$. Since thermal neutrons are absorbed by both ^{235}U and ^{238}U nuclei, the neutron yield η will depend on the isotopic content of uranium and can be found from the formula

$$\eta = v \frac{x \sigma_f^{(5)}}{x \sigma_a^{(5)} + (1-x) \sigma_a^{(8)}}$$

where x is the mass content of ^{235}U in uranium; $\sigma_f^{(5)}$ and $\sigma_a^{(5)}$ are the thermal-neutron fission and absorption cross

sections for ^{235}U ; $\sigma_a^{(n)}$ is the thermal-neutron absorption cross section for ^{238}U . If the mass content of ^{235}U in uranium exceeds the natural content (7.14×10^{-3}) it is said that *uranium is enriched* in ^{235}U . Enrichment of uranium is a process by which x is made to exceed the natural value.

Fast neutrons with energies above 1.0 MeV may induce fission of ^{238}U nuclei and the density of the fast neutrons will rise to $\epsilon\eta\theta n_1$. The *fast fission factor* ϵ characterizes the neutron multiplication due to ^{238}U fission induced by fast neutrons.

Some of the slowing neutrons can be captured by ^{238}U resonances. The density of thermal neutrons, n_2 , will therefore be less than the density of fast neutrons,

$$n_2 = \psi\epsilon\eta\theta n_1$$

where ψ is the *probability that resonance capture will not occur* and is the fraction of fast neutrons which become thermalized.

Multiplication of neutrons in an infinite medium is characterized by the infinite *multiplication factor* k_∞ . It is equal to the ratio of the thermal-neutron densities in the second (n_2) and first (n_1) generations,

$$k_\infty = \psi\epsilon\eta\theta$$

The multiplication factor k_∞ can also be defined as the ratio of the number of fissions induced by neutrons of the second generation to the number of fissions induced by neutrons of the first generation. The factor k_∞ thus characterizes the development of a chain reaction in an infinite medium. If $k_\infty < 1$ the neutron density will decrease from generation to generation and the chain reaction will be damped. The chain reaction is self-sustained at $k_\infty = 1$ and developing at $k_\infty > 1$.

Consider an example of the neutron population in a multiplication cycle. Suppose that 100 thermal neutrons are absorbed in a unit volume of an infinite reproducing medium, 93 of them being absorbed by uranium. Thus $\theta = 93/100 = 0.93$. We shall assume that $x = 0.00714$ (natural uranium) and hence the neutron yield $\eta = 1.32$. A result of the capture of the 93 neutrons will be the formation of $93 \times 1.32 \approx 123$ fast neutrons. If 3 of the 123 fast neutrons

split the ^{238}U nucleus, about 8 more fast neutrons will appear. The total number of fast neutrons is $123 - 3 + 8 = 128$. The fast multiplication factor $\epsilon = 128/123 \approx 1.04$. Suppose that 19 neutrons are absorbed by ^{238}U resonances during slowing-down and 109 neutrons become thermal. The probability that resonance capture does not occur $\psi = (128 - 19)/128 \approx 0.852$ and $k_\infty = 109/100 = 1.09$ or $k_\infty = 0.93 \times 1.32 \times 1.04 \times 0.85 = 1.09$.

The factors ϵ and ψ are equal to one in a reproducing medium which does not contain ^{238}U and hence

$$k_\infty = \eta\theta$$

In a finite-size medium the multiplication factor is called the *effective factor* and denoted k_{eff} . Some of the neutrons escape from such media through the outer boundaries (neutron leakage) and do not participate in the fission chain reaction. Thus during slowing-down and diffusion of thermal neutrons the neutron density in the second generation will also be reduced because of leakage. Consequently $k_{\text{eff}} < k_\infty$ and the relation between the two factors can be written as

$$k_{\text{eff}} = k_\infty p$$

where p is the fraction of neutrons absorbed in the medium.

With increase of size of the medium the role of neutron leakage will become less significant. The value of p approaches unity in this case and the effective multiplication factor k_{eff} approaches k_∞ .

Let us return to our numerical example of the neutron population. Suppose that on the average 5 slowing and 4 thermal neutrons escape from each unit volume of a finite-size medium. Since at the beginning of the slowing-down process there were 128 fast neutrons, we get $p = (128 - 9)/128 = 0.92$. The effective multiplication factor $k_{\text{eff}} = k_\infty p = 1.09 \times 0.92 = 1.00$.

A self-sustaining or developing fission chain reaction in a finite medium can take place if $k_{\text{eff}} \geq 1$. Depending on the magnitude of k_{eff} a medium is said to be subcritical ($k_{\text{eff}} < 1$), critical ($k_{\text{eff}} = 1$) or supercritical ($k_{\text{eff}} > 1$). The mass of the fissionable material and size (volume) of a critical medium are called the *critical mass* and *size*. If a chain

reaction is caused by thermal neutrons the critical volume is the largest and the critical mass the smallest.

The fission cross section in the fast region does not exceed 2 b. In order to increase the absorption of fast neutrons the concentration of fissionable material in the medium must be increased.

Let us now consider briefly multiplication induced by fast neutrons in an infinite medium. Part of the neutrons of a generation is absorbed in the first collisions with the nuclei. Most of the neutrons, however, suffer inelastic collisions with heavy nuclei and are slowed down to 0.1-0.4 MeV and then absorbed by the medium. Let θ be the fraction of fast neutrons of a generation which are absorbed by uranium (plutonium) and η the neutron yield per absorption. Then in an infinite medium the multiplication factor

$$k_{\infty} = \theta\eta$$

Since the absorption cross section for structural materials in the fast region is much less than that for the fissioning nuclei, we may put $\theta \approx 1$ and therefore

$$k_{\infty} \approx \eta$$

A medium consisting of pure ^{238}U cannot be critical. The absorption cross section σ_a for ^{238}U and energies exceeding 1 MeV is not more than 1 b. At the indicated energies the inelastic scattering cross section $\sigma_{in} \approx 3$ b. The decrease of the number of neutrons with energies $E_n > 1$ MeV is due to absorption and inelastic scattering of the fast neutrons. Therefore $\theta = \sigma_a/(\sigma_a + \sigma_{in})$ and

$$k_{\infty} = \eta\sigma_a/(\sigma_a + \sigma_{in})$$

Since $\theta \approx 0.25$ and $\eta \approx 3$, the multiplication factor $k_{\infty} \approx 0.75$.

In order to attain a chain reaction with medium-energy neutrons, the amount of moderator is chosen so as to slow down most of the fast neutrons to the resonance energies (1-10³ eV) at which they are captured by the fissionable material. In a ^{235}U -C medium, for example, the N_C/N_{U} ratio varies between 200 and 500.

Fission chain reactions are divided into *controlled* and *uncontrolled*. The latter are used for military purposes (ex-

plosions of atomic and thermonuclear bombs). A thermonuclear bomb consists of an atomic bomb located in the centre and surrounded by the thermonuclear fuel (mixture of lithium, deuterium and tritium) (Fig. 10.10). An atomic bomb consists of three parts, of two stationary hemispheres and a central mobile part (the igniter). All three parts are made of ^{235}U or ^{239}Pu . When the bomb is ready for action the igniter is kept in the upper position and the system is in the subcritical condition. With a conventional type of explosive the igniter is introduced into the atomic bomb and evokes its explosion. This results in a very high temperature being created in the thermonuclear fuel and a thermonuclear chain reaction is thus initiated. The envelope of the bomb confines the thermonuclear fuel in a certain volume until the thermonuclear reaction occurs.

Nuclear explosions can also be used for peaceful purposes (technological processes in mining and building industries, scientific research). Underground explosions have been used in the USSR to close down some faulty oil gushers. The nuclear charge is buried at a great depth near the oil well and the explosion stops the oil flow. An artificial storage reservoir for water with a volume of about 20 million cubic metres and also a condensate reservoir of 50 thousand cubic metres at a depth of over 1000 metres have also been built with the aid of underground nuclear explosions.

It is planned in the future to use nuclear explosions in the construction of some large hydraulic works and to open deep deposits of minerals. In the project of the Pechoro-Kolvin-sky canal, which will be 112.5 km long, it is envisaged that part of the water of the northern rivers will be diverted into the Volga river watershed and a 65 km section of the northern canal will be made by nuclear excavation. Nuclear explosions

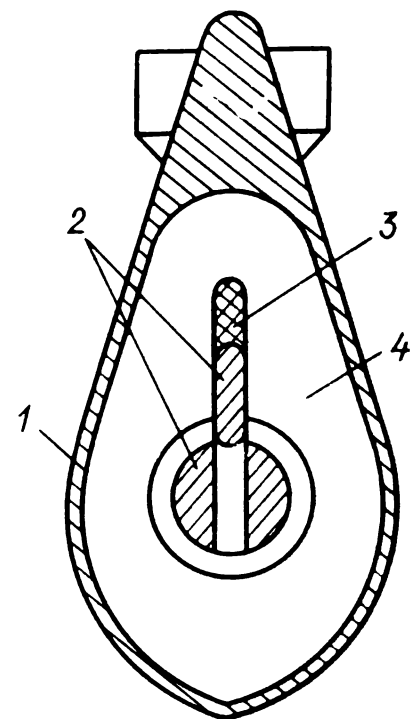


Fig. 10.10 Sketch of thermonuclear bomb
 1—bomb casing; 2—uranium;
 3—explosive; 4—thermonuclear fuel

may be economically profitable and can speed up civil engineering work but they must be applied with the observance of certain precautions to ensure that there will be no harmful effects on the population or environment.

Systems in which controlled fission chain reactions take place are called nuclear reactors. They are considered in the second part of the present book.

PART TWO

NUCLEAR REACTORS

CHAPTER 11

DESIGN AND CLASSIFICATION OF REACTORS

11.1 Reactor Design

A self-sustaining controlled nuclear fission chain reaction was first achieved in December, 1942. The nuclear reactor, designated CR-1, was built by a group of physicists at Chicago University headed by E. Fermi. The reactor consisted of spheres of natural uranium and its dioxide arranged between graphite blocks. The fast neutrons released in the fission of ^{235}U were slowed down by the graphite to thermal energies and in turn induced further fissions. Reactors of the CR-1 type, in which most of the fissions are induced by thermal neutrons, are called *thermal reactors*. There is much more graphite in this type of reactor than uranium.

In the Soviet Union theoretical and experimental studies on the start-up, operation and control of reactors were conducted by a group of physicists and engineers under the leadership of Academician I. V. Kurchatov. The first Soviet reactor F-1 was put into operation in December 25, 1946 and more than 30 years of research has now been carried out on it at the Kurchatov Atomic Energy Institute. The reactor, which is a sphere about 7.5 m in overall diameter, consists of a stack of graphite blocks. The graphite is perforated and uranium rods are imbedded in the slots. Experience obtained from the reactor was used for designing more powerful industrial reactors. In 1949 a reactor producing plutonium was put into operation and in June 27, 1954

the first atomic electric power station in the world with a gross power of 5 MW began to operate in Obninsk.

At present several hundred various types of reactors are operating throughout the world. A schematic diagram of a thermal reactor is shown in Fig. 11.1. The reactor consists of

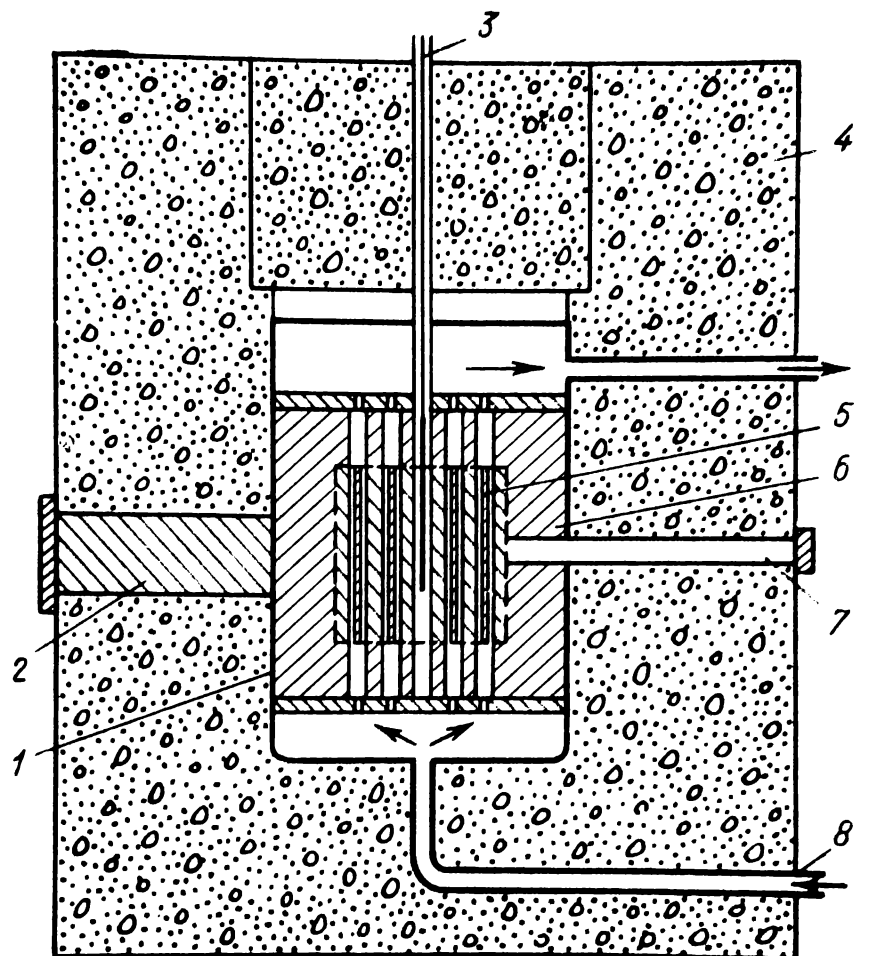


Fig. 11.1 Thermal neutron nuclear reactor

1—reactor vessel; 2—thermal column; 3—absorption rod; 4—radiation shield (concrete); 5—fuel assembly; 6—reflector; 7—experimental channel; 8—cooling system

several zones, each of which serves a definite purpose. The central part containing the fissile material is called the *core*. It is made up of the moderator blocks with slots in which *fuel channels* (FC) are housed. A fuel channel is a metal tube containing the *fuel elements*. A fuel element consists of a uranium-containing slug packed in a metal casing (the fuel element jacket). The fuel elements are grouped in the fuel channel length-wise and form a common construction called

the *fuel assembly* (FA). Inlet and outlet pipes for circulation of the coolant, special thermal expansion compensators are incorporated in the fuel channel. The coolant is pumped into the FC from a high-pressure chamber. The FA and moderator are cooled by the coolant passing through the fuel channels. The heated coolant then passes through an outlet pipe to the collecting tank.

The heat generated in the core causes thermal expansion of fuel channels and may cause their rupture and leakage. Mechanical stresses due to heating of the fuel channel are removed by special thermal compensators.

Thermal neutrons split the ^{235}U nuclei; heat is released and fast neutrons are emitted. The fast neutrons are slowed down in the moderator, return into the fuel elements and the same process is repeated. Thus the fuel element slugs are sources of heat and fast neutrons whereas the moderator is effectively a source of thermal neutrons. Fuel element slugs are made from fissionable materials (uranium, uranium oxide and others). Such materials are called *nuclear fuels*.

The chain reaction in the core depends on the value of k_{eff} . The reactor is also dependent on the reactivity ρ . Mathematically

$$\rho = (k_{\text{eff}} - 1)/k_{\text{eff}}$$

i.e. it equals the relative deviation of the effective multiplication factor from unity. When k_{eff} is close to unity

$$\rho \approx k_{\text{eff}} - 1$$

The reactivity of a subcritical system is negative, that of a critical system is zero, and for a supercritical system it is positive.

The operating parameters of a *critical reactor* ($k_{\text{eff}} = 1$, $\rho = 0$) are termed "critical". Such parameters are the core dimensions (critical size R_{cr}), the mass of the fissile materials (nuclear fuel) loaded into the core (critical mass or critical load M_{cr}), the volume of the core (critical volume V_{cr}) etc.

Fuel channels with a mass of nuclear fuel M tens of times greater than the critical mass M_{cr} are inserted into the core. How is this excess mass of fissile material ($M_0 = M - M_{\text{cr}}$) used?

The reactor operates at a specified power level for a definite period of time τ_0 called the *operating period*. At the end of the operating period the core is reloaded. Part or all the fuel channels may be replaced by new ones.

Due to fission and radiative capture during the operating period a mass ΔM of the nuclear fuel is expended. The ratio of ΔM to the total uranium (plutonium) mass M is termed the *nuclear fuel burn-up factor* z .

Radioactive decay products accumulate in the nuclear fuel and the absorption of neutrons by the products results in a decrease of the reactivity. The reactivity also depends on the temperature of the nuclear fuel, moderator and reflector. Variations of reactivity resulting from core heating are termed *temperature effects*. For instance, with a rise of the core temperature the density of the materials in the core and reflector decreases. The neutron migration length and neutron leakage from the core consequently are enhanced and this in turn reduces the reactivity.

The excess of fissile material M_0 introduced into the core raises the reactivity to a value (ρ_0) sufficient to start up the reactor, and also to compensate the temperature effects, fuel burn-up and neutron absorption by fission products.

A *control and safety system* is employed to ensure safe operation of the reactor. The safety control system (SCS) consists of detectors, amplifiers, control instruments, mechanical devices, control rods. The SCS can compensate any excess reactivity, start up the reactor, maintain steady-state operation, change from one power level to another and finally shut down the reactor when required.

Control of the chain reaction by the safety control system is performed as follows. The current in the ionization chambers housed in the channels of the safety control system is proportional to the neutron flux density and thus to the power level of the reactor. Depending on the current the amplifier can generate an electric signal which actuates the drive mechanism operating the control rods. In Fig. 11.1 one type of control rods is shown, an absorption rod. A rod of this type is made of materials with a high neutron absorption cross section (materials containing boron, cadmium and others) and is placed in the channel of the safety control system. The fraction of neutrons absorbed depends on how far

the control rod is inserted into or withdrawn from the core. The farther the rod is moved in, the greater is the number of neutrons incident on it and hence the greater the number of neutrons absorbed.

The value of the effective multiplication factor depends on how far the control rod is inserted into the core and can be less, equal or greater than unity. To illustrate the effect of the control rod on the state of the core let us take a numerical example. Assume that in a certain position 5% of the neutrons are absorbed, in the second position it is 3% and in the third, 1%. Now suppose that when the control rod is withdrawn the effective multiplication factor of the reactor is 1.031 ($\rho = 0.03$). This means that each thousand of neutrons increases up to 1031 neutrons per multiplication cycle. If the control rod is in the first position, it will absorb $0.05 \times 1031 \approx 51$ neutrons of the total 1031 neutrons. The number of neutrons taking part in the second multiplication cycle will not be 1031 but $1031 - 51 = 980$ neutrons. The effective multiplication factor of the reactor with the control rod in the first position is thus $k_{\text{eff}} = 980/1000 = = 0.98$ ($\rho = -0.02$) and hence the chain reaction in the core is damped out. In the second position $1031 \times 0.03 \approx \approx 31$ neutrons of the 1031 are absorbed by the control rod. A self-sustaining chain reaction will now be maintained in the core. The reactor is supercritical when the control rod is in the third position and the power level increases.

The chain reaction in an operating reactor is regulated by three types of control devices: the automatic control rods, shim rods and safety rods.

An inserted shim rod balances the excess reactivity ρ_0 . Release of the reactivity is attained by varying the position of the automatic control rods. For example, during steady-state operation the reactivity decreases due to fuel burn-up and accumulation of fission products. The attendant reduction of reactivity is compensated by withdrawing the automatic control rods from the core at such a rate that the core remains permanently critical. The control rods move vertically in the core between an upper and lower extreme position. When the control rods reach the top position they are rapidly moved downwards to the lower limit and simultaneously the shim rods are partially pulled out of the core.

When such a coordinated shift of rods takes place a small fraction of the excess reactivity is transferred from the shim rods to the control rods. The latter gradually rise to the upper position and the reactivity release cycle is repeated.

Note that the rods in the core absorb a certain fraction of neutrons. This quantity depends only on how far the rods are inserted into the core but not on the power level of the reactor itself. Thus, in the numerical example considered above a rod in the second position absorbs 31 per 10³¹ neutrons irrespective of the power level of the reactor.

Periodic reactor shutdown is required for routine maintenance requirements, reactor charging etc. Besides, in situations which may lead to accidents, the reactor also has to be shut down. Such situations may be caused by an unforeseen increase in power level, pressure drop in the coolant loop etc. In such cases the safety control system is triggered off and the chain reaction is suppressed in a short time. In case of serious accidents the current in the ionization chamber or signals from other control devices actuate the safety control system which drives all three types of rods (safety, shim and control) into the core and the reactor becomes sub-critical. The safety rods are used only to shut down the reactor. Prior to shutdown they are withdrawn from the core.

Such technological characteristics as the temperature, coolant flow rate and pressure, leakproof of fuel elements etc. are checked under steady-state operation conditions. By constantly monitoring the characteristics one can detect construction failures and take measures to eliminate them. For instance, in the case of a fuel element leakage, fission fragments appear in the coolant. The rupture in the fuel channel casing can be detected by measuring the radioactivity of the coolant at the outlet and the channel can be replaced.

The reactor instrumentation is arranged on a panel. The operators receive full information on all characteristics. Controls at the disposal of the operators permit them to start-up or shut down the reactor as required.

To reduce neutron leakage a *reflector* is closely fit around the core and serves to prevent neutrons from escaping from the core. As a large fraction of the neutrons are reflected back into the core the number of neutrons participating in

the chain reaction is increased. Reflectors are made from materials with high scattering properties and low absorption cross sections. Nickel, thorium, ^{238}U and others are suitable materials.

The core and reflector are of a cylindrical, spherical or rectangular shape and are housed in the reactor vessel. A thermal shield consisting of several layers of water and thin steel sheets is placed before the thick reactor vessel. Most gamma-quanta escaping from the surface of the reflector are absorbed in the shield. The thermal shield reduces the heat load on the thick-walled vessel which operates under high pressure and reduces thermal stresses in its walls caused by nonuniform absorption of intense gamma-rays.

Gamma-rays and neutrons, which are dangerous for the operators, may escape through the surface of the reactor vessel. To keep the dosage of neutron and gamma-quanta irradiation at a permissible level the core vessel is surrounded by a radiation shield. The shield is composed of materials with high gamma-quantum absorption properties (iron and lead) and materials which slow down and absorb neutrons (water, boron, concrete and others).

Heat is removed from the core by a circulating coolant (water, gas, sodium etc.). The heat can be used to generate steam and drive the turbogenerator of an atomic electric power station or of a vehicle. Figure 11.2 shows how thermal power is transformed into electric power in the two-loop installation used in the first atomic power station. The primary circulation loop includes the fuel channels, steam generator, circulating pumps and piping. The secondary circulation loop is composed of a steam generator, turbogenerator, condenser, feed pumps and piping.

In the primary loop water is pumped at a pressure of 100 atm. On passing through the fuel channels the water is heated from 190°C to 280°C . The heat is spent in producing steam in the steam generator of the secondary loop. The steam sets the turbogenerator in motion and then enters the condenser from which the feed pumps drive the water once more into the steam generator.

The water irradiated by neutrons in the core becomes radioactive and therefore the primary loop is contained in a radiation-proof casing. The secondary loop works in much

the same manner as that of a conventional electric power plant.

When liquid sodium is used as the coolant three loops are employed. Radioactive sodium circulates in the first loop, nonradioactive sodium or some other coolant (but not water) circulates in the second loop and steam is produced only in the third loop. Due to the presence of the second loop contamination of the water by radioactive sodium is excluded

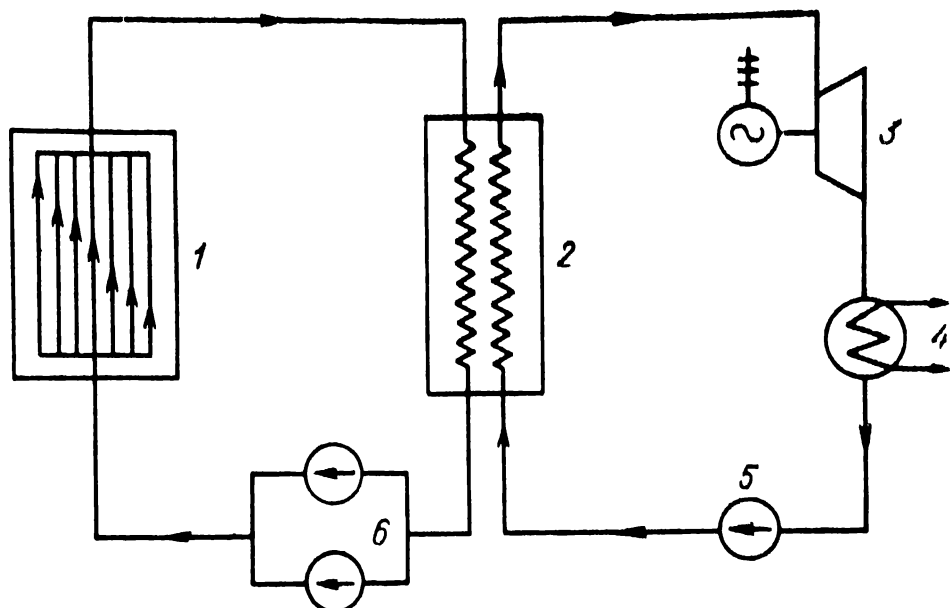


Fig. 11.2 Schematic diagram of transformation of heat into electric energy at the first atomic power station

1—reactor; 2—steam generator; 3—turbogenerator; 4—condenser; 5—feed pump; 6—circulating pumps

in case of leakage in the steam generator. In one-loop systems a steam-water mixture is produced in the core. The steam is then separated from the water in a separator. In some designs the steam is fed directly from the separator to the turbogenerator. In other one-loop systems the steam is directed to superheater channels in the core and then to the turbogenerator.

11.2 How Reactors Are Used

Thermal neutron beams for experiments are extracted from the thermal column. A thermal column is a big block of graphite (see Fig. 11.1). Neutrons that enter the thermal col-

umn are slowed down to thermal energies and emerge as thermal neutrons. Special experimental reactors are designed to study the action of neutrons and gamma-quanta on materials and the properties of irradiated materials. Experimental reactors are used as powerful sources of neutrons and gamma-quanta for various experiments (to study interactions of neutrons and gamma-quanta with materials, the effect of irradiation on physical and mechanical properties of materials, the biological effect of irradiation on a living organism etc.). Samples of materials under study are irradiated in special experimental channels in the reactor. For physical experiments neutron beams are extracted via channels extending from the core through the shielding into the laboratory (see Fig. 11.1). Artificial radioactive materials for commercial use are also produced in experimental reactors.

Neutron fluxes of very high density can be produced in powerful experimental reactors. The heat released in the core is usually removed by water. As the heat is not used to generate electric power the temperature at the outlet as a rule does not exceed 100 °C. Experimental reactors in which water is the coolant as well as the moderator are termed water-water reactors and are designated WWR.

Power reactors can be used as sources of heat in atomic electric power stations and for propulsion of mobile systems. At present more than 150 atomic electric power stations and atomic-powered ships are operating in the Soviet Union. Among them are the first atomic power station, the atomic-powered ice-breakers "Lenin", "Arctic", "Siberia", and the Novovoronezh, Beloyarsk, Leningrad, Kolsk atomic power stations.

Present-day atomic power engineering mostly uses ^{235}U . The natural reserves of ^{235}U are not abundant and cannot provide enough fission fuel for a long time. However, the world supply of ^{238}U and ^{232}Th , which can produce fission fuel (^{239}Pu , ^{233}U), is considerable.

Fissionable materials produced from nuclear raw materials will considerably increase power resources. Many scientists are searching for effective ways of producing ^{239}Pu and ^{233}U and manufacturing acceptable nuclear fuels based on them.

The fissionable materials ^{239}Pu and ^{233}U can be produced in three ways. One way is to accelerate protons to energies of the order of 0.5-1 GeV and direct them to heavy-element targets (tungsten, bismuth, lead, uranium). A (p, mn) reaction ($m = 15-40$) takes place in the target. Then the neutrons hit the nuclear raw material and are absorbed.

A second way is to obtain ^{239}Pu and ^{233}U in a hybrid reactor with a nuclear raw material blanket (see Sec. 8.7). Both methods are still being studied.

The third method of obtaining fissionable materials in the reactor has been studied in more detail. In this case fuel burn-up and breeding occur simultaneously.

The nuclear fuel breeding cycle breaks up into several steps. In the first, fuel assemblies containing nuclear fuel are loaded in the breeding zones (reflector, core). The fuel element slugs in reflector assemblies are made of nuclear raw materials whereas the slugs in the core fuel elements are made of a fissionable material and a nuclear raw material (enriched uranium dioxide, $\text{UC} + \text{PuC}$ etc.). In step two, the fuel assemblies discharged from the reactor at the end of the operating period undergo chemical processing and the fissionable material, nuclear raw material and fission products are extracted.

In step three, nuclear fuel is produced and the fuel assemblies are fabricated. After that the next nuclear breeding cycle begins.

Let us examine how nuclear fissionable material is produced in a reactor. When a neutron is captured in the fissionable material, $\eta = v/(1 + \alpha)$ fission neutrons emerge (see Sec. 10.10). A fraction of these η neutrons with an energy $E > 1 \text{ MeV}$ split the ^{238}U nuclei. As a result for every absorbed neutron in the fissionable material the number of fast fission neutrons increases to $\epsilon\eta$. One of the $\epsilon\eta$ neutrons is needed to maintain the chain reaction, C neutrons escape or are lost in radioactive capture in the structural materials, moderator or coolant. The remaining neutrons can be effective in breeding. The *conversion factor* (or *breeding ratio*)

$$\text{CF} = \epsilon\eta - (1 + C)$$

is the ratio of the number of fissionable atoms produced to the number of fissionable atoms burned.

Let us assume that m kg of fissionable material is burned in the first breeding cycle and CFm kg of new material are produced in the same cycle. Burning of CFm kg will produce $(CF)^2m$ kg of fissionable material etc. In the n th cycle the amount of fissionable nuclear material will be $(CF)^n m$ kg and the total amount of nuclear material burned

$$M_n = CFm + (CF)^2m + \dots + (CF)^n m \quad (11.1)$$

The series (11.1) is a geometric progression with a ratio equal to CF . If $CF < 1$, then with increase of the number of cycles the sum of the progression tends to

$$M = m/(1 - CF) \quad (11.2)$$

From (11.2) it follows that for $CF < 1$ only a fraction of the nuclear material can be used. In operating thermal neutron power reactors $CF = 0.5-0.8$ and hence only 2-5-fold gain of fissionable material is possible.

Breeding is possible in reactors only if $CF > 1$. In breeder reactors all fissionable material produced can be burned up. Thus, if $CF > 1$, the sum of the series (11.1) tends to infinity as the number of cycles increases.

The conversion factor is a function of η , ϵ and C . In thermal reactors the value of η for ^{235}U and ^{239}Pu is about 2.1; for ^{233}U it is about 2.3 (see Table 10.10). The fast fission factor ϵ in this type of reactor does not differ greatly from unity.

Hence, a thermal breeder reactor is feasible. However, since more than 5-7% of neutrons escape and are absorbed in the construction materials, moderator and coolant in thermal reactors, the breeder can operate only on ^{233}U . The difference $\eta - 1$ in the case of fast neutrons increases greatly. Moreover, the number of fissioning atoms in the nuclear material is appreciable in the fast region. Such fissions increase the number of neutrons participating in breeding. Hence, they increase CF . In fast neutron breeding CF may be as high as ~ 2 .

Fissionable material can be produced in two fuel cycles: with either uranium or thorium. Plutonium-239 is the fissionable material obtained in the uranium cycle and ^{233}U is the initial nuclear raw material. The designation of this cycle is $^{239}\text{Pu-}^{233}\text{U}$.

In the thorium cycle (^{233}U - ^{232}Th) fissionable material is ^{233}U and the nuclear raw material is ^{232}Th . In nature there are no ores containing ^{239}Pu or ^{233}U . Therefore ^{239}Pu and ^{233}U are obtained in thermal reactors with ^{235}U nuclear fuel. Since ^{236}U is not produced in breeders and is not abundant in nature it will gradually be replaced by plutonium and ^{233}U .

The uranium cycle is most effective in fast neutron breeder reactors for two reasons. The value of η for ^{239}Pu is approximately 20% greater than that for ^{233}U . The cross section of ^{238}U fission by fast neutrons is about 3 times greater than the cross section for ^{232}Th , and the value of ϵ in the ^{239}Pu - ^{238}U cycle is 1.1-1.3. In the thorium cycle such high values of ϵ are impossible. The thorium cycle is more efficient in thermal, graphite-moderator, gas-coolant breeder reactors. A considerable decrease in the loss of neutrons (leakage, radiative capture) in the thermal neutron thorium cycle results in CF attaining a value of 1.1-1.15.

The accumulation of nuclear fuel and hence the increase in the power of an atomic station can be characterized by the doubling time. This is the time it takes for the amount of nuclear fuel (or the power level of an APS) to double. The doubling time depends on the operating period, conversion factor, burn-up, nuclear fuel chemical processing time etc. The doubling time is about 6-8 years for powerful fast neutron breeders with a conversion factor of 1.4-1.6 and a burn-up $z \approx 10\%$.

Before building a power reactor the characteristics, composition, size etc. are first studied theoretically and the most acceptable variant is chosen.

The theoretical calculations are followed by experimental investigations which are aimed at determining more precisely the physical characteristics (multiplication factor, critical load etc.) and checking the reliability of the fuel elements. For this purpose a special experimental or pilot reactor is built. As the power level and heat release in such reactors are low, there is no need for an intricate coolant system. An experimental reactor is simple in construction and not expensive, high pressures are not necessary. Materials that are chemically active are replaced by inert materials which have equivalent physical properties. For example, sodium is replaced by aluminium.

The reliability of the fuel element design is tested in *loop* channels of the experimental reactor. The construction of these channels is similar to that of fuel channels. They are connected to a self-contained coolant loop which is not part of the heat removal system of the core. Such coolant loops are termed *experimental loops*. The experimental reactor is used as a source of neutrons which induce fission in the fuel elements under investigation. Normal operating conditions for the fuel elements (pressure, temperature, coolant flow etc.) are set up in the loop channels.

At the last stage of investigation another reactor is built to determine the physical and technological characteristics of the reactor as a whole.

The first power reactors were, to a certain degree, both research and experimental reactors. Various experiments in neutron physics and for studying the performance of the reactor are conducted with some reactors, whereas the means of lowering the cost of electricity etc. are studied in others. For example, the reactor at the first APS generates heat to obtain steam. On the other hand neutron beams and gamma-rays can be extracted for carrying out physical experiments. There are also experimental loops for testing fuel elements. The reactor itself is the prototype of the reactors at the Kurchatov Beloyarsk APS.

11.3 Homogeneous and Heterogeneous Reactors

Homogeneous reactors. In a homogeneous reactor the fuel and the moderator are intimately mixed. The core of a homogeneous reactor is of a comparatively simple construction. It is usually a cylindrical or spherical vessel packed with a homogeneous mixture. Such mixtures are solutions of uranium salts, suspensions of uranium oxides in light or heavy water, a solid moderator impregnated with uranium, melted salts.

Homogeneous reactors have not been extensively used because of high corrosion of structural materials in liquid fuels and the constructional complexity of reactors with solid homogeneous mixtures. Moreover, large loads of weakly enriched uranium must be used in homogeneous reactors etc.

Heterogeneous reactors. The deficiencies of homogeneous reactors can be overcome to a great extent by constructing a more intricate core. In a heterogeneous reactor the nuclear fuel is isolated from the moderator and packed in fuel elements. The fuel channels permeating the moderator form a space lattice. A unit cell is the least part of the space lattice which retains all geometric properties of the lattice. Square or triangular arrays are the types of lattice most often used

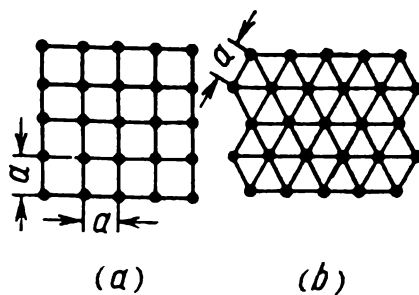


Fig. 11.3 Square (a) and triangular (b) fuel channel lattices

(Fig. 11.3). The lattice spacing a is characteristic of the lattice and is the distance between neighbouring fuel channels. Fuel elements are fabricated either as rods, tubes or plates and the nuclear fuel slugs possess similar shapes. They are "canned" in a jacket to contain the fission product and prevent it from being washed away by the coolant. Hence, the activity of the primary loop is determined not by the fission products but by the activity of the coolant. It is much simpler to inspect and repair the equipment of the primary loop in a heterogeneous reactor than in a homogeneous reactor. In case of fuel element rupture the fuel channel is replaced to prevent radioactive fission products from circulating with the coolant in the primary loop.

Between the jacket and slug there is always an air gap as it is practically impossible to achieve an air-tight fit. Air is a poor heat conductor and hence at high heat release rates the temperature of the nuclear fuel rises sharply due to this air gap. For example, a $10 \mu\text{m}$ air gap at a $2 \times 10^6 \text{ W/m}^2$ heat flux density causes the temperature of the nuclear fuel to rise by 600°C . In order to eliminate the effect of the air gap on the temperature of the nuclear fuel the gap is filled with a thermal conductor (helium, sodium, eutectic Na-K). In some cases diffusion welding gives good thermal contact

between the jacket and the nuclear fuel. A local impairment in thermal contact can cause irregular heating of the nuclear fuel and buckling of the fuel element.

A centring unit is used to adjust the fuel assemblies along the axis in the channel. A fuel channel in the reactor of the first atomic power station (Fig. 11.4) consists of 4 tubular fuel elements spaced from each other by graphite sleeves. Thermal expansion compensators and a device for adjusting or withdrawing the fuel channels from the core are mounted at the top of the channels. Water flows downward in the central tube to a distributing chamber at the bottom and is then heated in its upward flow through the four tubular elements. The fuel channel in block I of the Novovoronezh APS consists of 90 rod fuel elements (Fig. 11.5) housed in a hexahedral casing. Such large fuel channels are called *cassettes*. The transverse dimensions of a hexahedral cassette are characterized by the diameter of an inscribed circle d . For the cassette in Fig. 11.5 d is 145.5 mm. In powerful reactors the number of fuel elements runs as high as several thousand and cassettes simplify the design of the core and reduce the loading time at the end of an operating period.

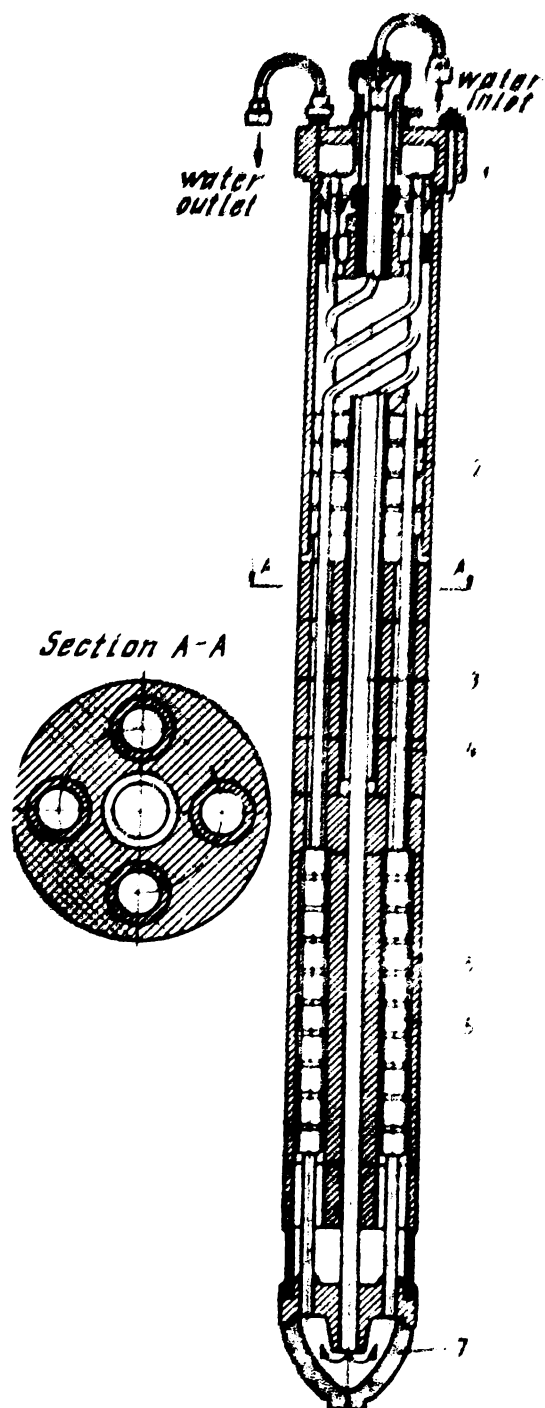


Fig. 11.4 Vertical section of the fuel channels in the reactor of the first atomic power station
 1—upper head; 2—steel bushings;
 3—pipe $\phi 15 \times 0.6$ mm; 4—pipe
 $\phi 9 \times 0.4$ mm; 5—graphite bushings;
 6—fuel element; 7—lower head

Fig. 11.4 Vertical section of the fuel channels in the reactor of the first atomic power station
 1—upper head; 2—steel bushings;
 3—pipe $\phi 15 \times 0.6$ mm; 4—pipe
 $\phi 9 \times 0.4$ mm; 5—graphite bushings;
 6—fuel element; 7—lower head

Reliable operation of a reactor depends to a great extent of the design of the fuel elements. In the case of leakage of the casing or buckling of the fuel elements the reactor is shut down. Emergency shutdowns, especially of powerful reactors, are extremely undesirable since they involve irregular supply of electric power to the consumers.

A certain pressure is set up in the primary loop of an APS. This pressure is sustained by the fuel channel or by the vessel of the reactor. Accordingly heterogeneous reactors are divided into *channel reactors* or *vessel reactors*. For example, in

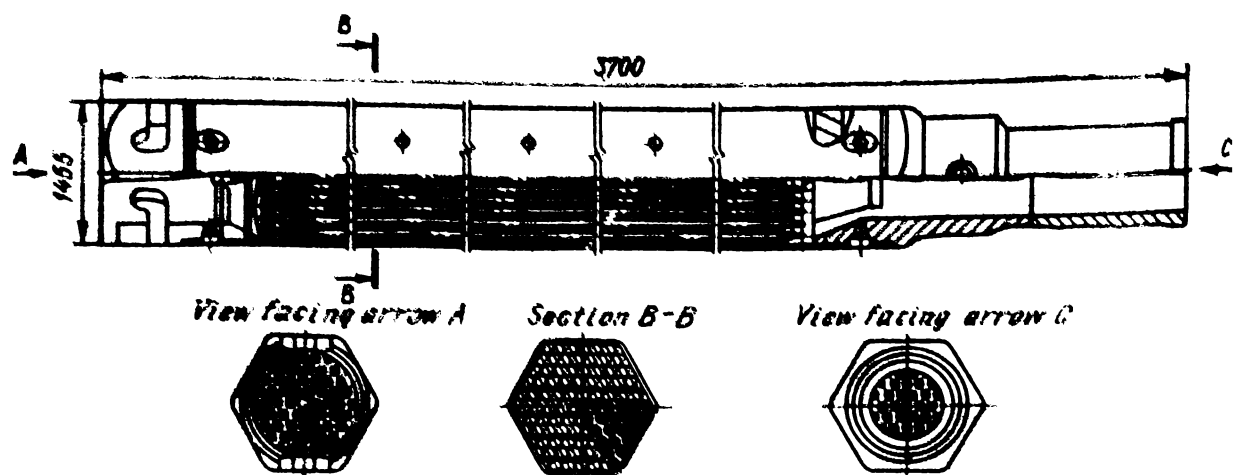


Fig. 11.5 Cassette of Novovoronezh APS reactor

the channel reactors of the Lenin APS in Leningrad the coolant circulates in the fuel channel under a pressure of 65 atm. At the Novovoronezh APS the pressure of the water is 100-160 atm and is sustained by the reactor vessel.

Channel reactors are characterized by one very important peculiarity: they can be recharged under steady-state operation conditions. Recharging without shutdown of the reactor prolong the uninterrupted operation of the power plant.

One of the shortcomings of heterogeneous reactors is the short lifetime of the fuel elements in the core. Irradiation substantially alters the composition of nuclear fuel and also its mechanical and physical properties. For this reason the core is reloaded at the end of each operating period.

11.4 Thermal, Fast and Intermediate Neutron Reactors

Thermal neutron reactors. Nuclear fission in the core is induced by neutrons of diverse energies. However, in each reactor neutrons of a definite energy range are predominantly responsible for fission. Hence, there are three types of reactors: thermal reactors, fast reactors and intermediate reactors. The thermal reactor core consists of a moderator, nuclear fuel, coolant and structural materials. Most fast neutrons in this type of reactor are slowed down to thermal energies and then absorbed in the core.

To reduce the amount of nuclear fuel in thermal reactors, structural materials with low radiative neutron capture cross sections are used. Among these are aluminium, magnesium, zirconium. The low loss of neutrons in the moderator and structural materials render it possible to use natural uranium and slightly enriched uranium.

For heavy-duty power reactors it is not always possible to find suitable structural materials possessing low absorption cross sections. In this case the casings, channels and other parts of the construction may be made of materials which strongly absorb neutrons such as stainless steel. To compensate for this additional loss of thermal neutrons highly enriched uranium (up to 10%) is used.

In thermal reactors the fission products absorb a considerable fraction of the neutrons. To compensate for this loss a certain additional amount of nuclear fuel is placed in the core prior to start-up. The longer the operating period and the higher the specific power of the reactor, the greater must be this additional amount of nuclear fuel.

Fast neutron reactors. The core and reflector in fast reactors are made of heavy materials. Moderating nuclei in the core are contained in the nuclear fuel [uranium carbide (UC), plutonium dioxide (PuO_2) etc.]. Measures are taken to reduce the concentration of the moderator in the core to a minimum as light nuclei soften the energy spectrum of the neutrons. Before being absorbed fission neutrons slow down, as a result of inelastic collisions with heavy nuclei, to energies of only 0.1-0.4 MeV.

The fission cross section in the fast energy range does not exceed 2 b. Therefore for a chain reaction to take place with

fast neutrons there must be a high concentration of fissionable material in the core. This concentration is tens of times greater than that in the core of a thermal reactor. Why then are the expensive fast reactors being designed and built? For every neutron captured in the core of a fast reactor about 1.5 times more neutrons are emitted than in the core of a thermal reactor. Hence, for processing nuclear material in a fast reactor a much larger fraction of neutrons can be used. That is the main reason why extensive investigations in the application of fast neutron reactors are being carried out.

The reflectors in fast reactors are made of heavy materials such as ^{238}U and ^{232}Th . They return fast neutrons with energies higher than 0.1 MeV back into the core. Neutrons captured by the ^{238}U or ^{232}Th nuclei produce the fissionable nuclei ^{239}Pu and ^{233}U .

The power level of a reactor is regulated by mobile fuel assemblies and fuel elements with slugs of natural uranium or thorium. In small reactors mobile reflectors are more effective as regulators. In this case the chain reaction is regulated by varying the neutron leakage. If the reflector is withdrawn from the core, neutron escape increases and as a result the chain reaction is damped, and vice versa. Mobile reflectors at the boundary of the core are the most effective.

In practice structural materials for fast reactors can be chosen without taking into account their absorption cross sections which in the fast neutron energy range are negligible compared to the fission cross sections. For the same reason neutron capture by fission products has little influence on the nuclear fuel load.

Intermediate neutron reactors. The concentration of fissionable material in the core of an intermediate reactor is such that before being absorbed fast neutrons are slowed down to energies of 1-1000 eV. For example, the ratio of beryllium nuclei to ^{235}U nuclei in reactors of this type varies between 150 and 250.

Intermediate reactors are comparatively rare for two reasons. Firstly, the nuclear fuel load is high compared to that of thermal reactors. Secondly, in the cores of such reactors not more than 1.5-2.0 neutrons are emitted per neutron capture. Consequently breeding is impossible in intermediate reactors whereas it is possible in fast neutron reactors.

Intermediate reactors are used as experimental reactors since it is possible to obtain high neutron flux densities. For example, the peak neutron flux density in the CM-2 reactor (USSR) is 3.3×10^{19} neut./m²·s.

11.5 Classification of Power Reactors with Respect to Coolants and Moderators

Water coolant reactors. Three combinations of coolants and moderators are used in presently operating reactors. In one type water is both the coolant and the moderator; another type uses water as the coolant and graphite as the moderator; in the third type the moderator is heavy water whereas the coolant is either heavy water or light water. In the Soviet Union the first type of reactors are called water-water power reactors (WWPR); the second type are graphite-water reactors (GWR), and the third heavy water reactors (HWR). We should note that in the literature the WWPR and GWR are also termed light water reactors and uranium-graphite reactors respectively.

The energy density per unit core volume (unit nuclear fuel mass) is characterized by the specific power P . This is the average power obtained from 1 litre of the core or 1 kg of the nuclear fuel. The specific power for WWPR and GWR lies in the range from 45 to 60 kW/kg.

Water coolant reactors can be subdivided into non-boilers (or pressurized-water reactors), and boilers (boiling-water reactors). In APS with non-boiling water reactors the temperature of the water in the primary loop is below the boiling temperature. In the secondary loop saturated water vapour is obtained at a pressure of 12-45 atm with a temperature up to 300 °C. Such conditions are encountered, for example, in the WWPR at the Novovoronezh APS.

In boilers the steam-water mixture is produced in the core. The pressure of the water in the primary loop is reduced to 70 atm. At this pressure water boils in the core vessel at a temperature of 280 °C. In comparison with non-boilers, boiler reactors have a number of merits. The pressure in the vessel of a water boiler is lower and no steam generator is incorporated in the APS.

To obtain steady performance of boilers the operation conditions are chosen in such a way as to ensure that the steam content in the steam-water mixture does not exceed a certain permissible value. For example, in the WWPR of the Dresden APS (USA), the steam content at the core outlet is 5%. If the value of the steam content is higher, the performance of the reactor may be unstable. This instability is due to the fact that the steam displaces the water in the core and thus increases the neutron slowing-down length L_s . When boiling is too vigorous the value of L_s increases to such a degree that a negative reactivity is produced and the power level of the reactor begins to fall.

A reduction in power level decreases the boiling rate, steam content and hence the slowing-down length. As a result reactivity is enhanced and subsequently the power level and intensity of boiling begin to rise. The power level oscillations are dangerous for both the reactor and personnel.

Such dangerous power level oscillations do not occur when the steam content is below the permissible value and steady state operation of the reactor becomes self-adjusting. Thus, a reduction in power level and a decrease in boiling intensity enhance the reactivity and the reactor returns to the initial power level. The steam content at the core outlet is a function of specific power. Thus, for a reactor with a given core size the maximum steam content which ensures steady operation of the boiling WWPR limits the power level of the reactor. This explains why the release of power per unit volume is smaller in a boiler WWPR than in a non-boiler WWPR. This is a significant deficiency of boiler WWPR.

Overheating of water vapour to 510 °C has been achieved in the Beloyarsk APS channel reactors. In contrast to vessel water boilers, the main moderator in the Beloyarsk reactor is graphite and boiling water in the loops does not cause dangerous power oscillations.

In the Soviet Union two types of power reactors are generally used: the non-boiler WWPR and the water boiler, graphite channel reactor HPCR (high power channel reactor).

Present-day atomic electric power stations consist of independent operating units. Each unit of the APS is self-contained. It consists of a power reactor and a system for con-

verting thermal energy into electric energy. The designation of a reactor indicates the type of reactor and the electric power level of the specific unit of the APS in megawatts. For example, WWPR-440 indicates that a WWPR is installed in the unit and its electric power level is 440 MW; HPCR-1000 means the APS contains an HPCR unit with an electric power level of 1000 MW. The thermal power of the reactor is termed the unit power of the reactor and the electric power of a unit is called its unit power. Specifications of a power reactor often include the power of a unit and not the unit power of the reactor.

Graphite-gas reactor (GGR). The moderator in graphite-gas vessel reactors is graphite and the coolant is a gas (helium, carbon dioxide etc.). Compared to the WWPR and GWR, gas coolant reactors are the safest type of reactor. This is explained by the fact that the gas practically does not absorb neutrons. Thus, a change in the gas content in the reactor does not affect the reactivity.

In Great Britain there are several atomic electric power stations with GGR using carbon dioxide as the coolant. The fuel element jackets and channels are made from magnesium alloys which weakly absorb neutrons. Consequently, natural or only slightly enriched uranium can be used as the nuclear fuel. Carbon dioxide is pumped through the reactor under a pressure of 10-20 atm. The temperature at the inlet is about 400 °C. The specific power of the reactor is only 0.3-0.5 kW/kg, i.e. about 100 times less than in the WWPR and GWR. In an improved GGR design the magnesium alloy jackets are replaced by stainless steel jackets and natural uranium is replaced by enriched uranium dioxide. These changes in the construction of the fuel elements allow the temperature of the carbon dioxide at outlet to be raised to 690 °C, and the specific power to be increased by about 3.5 times. The efficiency of the APS may reach 40%.

Reactors with organic coolants. Organic liquids (gas oil, diphenyl mixture etc.) possess good slowing-down properties and a high boiling point at atmospheric pressure. Therefore, the pressure can be significantly lowered by replacing water in the primary loop by an organic liquid, the outlet coolant temperature being in the range between 300 and 350 °C.

However, a serious shortcoming of organic coolants is their thermal and radiation instability. At high temperatures, or when exposed to radiation, organic liquids decompose or form more complex viscous liquids. To clean the organic liquid of impurities a purifier must be introduced into the primary loop and this complicates the construction of the power unit. Because of this organic liquids are seldom used in reactor engineering.

Liquid metal-cooled reactors. Liquid metal coolants (sodium, sodium-potassium alloys etc.) can efficiently remove heat from the reactor. Sodium is very suitable as a coolant. Its heat capacity is 4.5 times greater than that of a sodium-potassium alloy and its boiling point is 882 °C. Sodium becomes radioactive due to neutron capture in the core. To eliminate any possible contact between the radioactive sodium and water an expensive three-loop heat removal system is used. That is one of the reasons why sodium is not widely used as a coolant in power thermal reactors. Sodium is usually used to remove heat in fast or intermediate reactors with a specific power exceeding by 10-30 times that of thermal reactors.

11.6 Reactor Structural Materials

General requirements. Materials which are used in constructing reactors operate at high temperatures under irradiation by neutrons, gamma-rays and fission fragments. Therefore not all structural materials are suitable in nuclear engineering. When choosing materials for building reactors one must consider their radiation stability, chemical resistance, absorption cross section and other properties.

Fuel element jackets, channels, moderators (reflectors) are made of materials with low absorption cross sections. By using structural materials with low neutron absorption unproductive neutron losses can be avoided. Moreover, the nuclear fuel load can also be reduced and the conversion factor increased. On the other hand, materials with high absorption cross sections are suitable for the fabrication of absorption rods. A high cross section significantly reduces the number of rods required to operate the reactor.

Fast neutrons, gamma-rays and fission fragments damage the structure of materials. For instance, in solid substances fast neutrons dislodge atoms from the crystal lattice or displace them. As a result the plastic and heat conductivity properties are impaired. When irradiated, complex molecules dissociate into simpler molecules or into atoms. For example, water dissociates into oxygen and hydrogen. This effect is known as *radiolysis*.

Radiation instability is less pronounced at high temperatures. The mobility of the atoms is so great that the probability that the dislodged atoms return to their sites in the crystal lattice or that recombination of hydrogen and oxygen with the formation of a water molecule occurs is very high. Thus, in power non-boilers radiolysis is insignificant whereas in powerful research reactors a significant amount of the explosive oxyhydrogen gas is produced. Special devices are incorporated in such reactors for combustion of the gas.

Reactor structural materials come into mutual contact (e.g. the fuel element jacket with the coolant and nuclear fuel or the fuel channel with the coolant and moderator etc.). Of course, contacting materials must be chemically inert (compatible). Uranium and hot water are an example of incompatibility: they interact chemically.

The strength of most materials sharply declines with temperature. In power reactors the structural materials operate at high temperatures. This limits the choice of structural materials, especially of those parts that are subjected to high pressures.

Nuclear fuel. The nuclear fuel consists of materials containing fissionable substances such as ^{235}U , ^{239}Pu . Natural uranium, uranium oxide UO_2 , uranium alloys, plutonium oxide PuO_2 , are examples of nuclear fuels. In most of the reactors in existence the nuclear fuel is an uranium-containing compound.

Natural uranium consists of three isotopes, ^{238}U (99.282%), ^{235}U (0.712%) and ^{234}U (0.006%). It is not always acceptable as a nuclear fuel, especially if the structural materials and moderator have a high absorption cross section. In this case an enriched uranium fuel is employed. Thermal neutron power reactors operate with uranium enriched by less than 10%, whereas in fast and intermediate reactors the uranium

is usually enriched by more than 20%. Enriched uranium is obtained at special enrichment plants.

In the process of manufacturing enriched uranium from natural uranium the enriched and depleted (waste) uranium are separated. Fuel assemblies used in reflectors of fast breeders are prepared from depleted uranium.

Metallic uranium is comparatively rarely used as a nuclear fuel. It is stable only up to 660 °C. At this temperature there is a phase transition and the crystal structure changes. The volume of the uranium increases during the phase transition and this may cause disruption of the fuel element jacket. Prolonged irradiation at temperatures between 200 and 500 °C involves radiation creep, i.e. elongation of an irradiated uranium rod, and 1.5-fold increase of length has been observed.

Uranium metal swells, particularly at temperatures above 500 °C, and this also complicates its use. Nuclear fission produces two fragments with a total volume greater than that of the initial uranium atom (or plutonium atom). Some of the fission atoms are gases (krypton, xenon etc.) which accumulate in the pores of the uranium. This produces an inner pressure which increases as the temperature rises. Thus, because of the increase in volume of the atoms due to fission and of the increase in internal pressure, uranium and other nuclear fuels begin to swell. *Swelling* is the expansion of nuclear fuel resulting from nuclear fission.

Swelling depends on the degree of burn-up and on the temperature of the fuel elements. The number of fission fragments grows as the burn-up increases and the internal pressure of the gases rises together with the burn-up and temperature rise. Fuel element swelling may cause disruption of the fuel element jacket. Nuclear fuel is subjected to swelling to a less degree if it possesses high-grade mechanical properties. Uranium metal does not possess these qualities. The use of metallic uranium as a nuclear fuel limits burn-up, which is one of the main economical criteria in the designing of atomic power plants.

The irradiation stability and mechanical properties of the fuel can be improved by doping uranium, i.e. by adding small amounts of molybdenum, aluminium or other metals. These admixtures decrease the number of fission neutrons

produced per neutron captured by the nuclear fuel. This is why materials with low neutron absorption are chosen as alloying additions to uranium.

Some uranium compounds with high melting points such as its oxides, carbides or intermetallic compounds are good nuclear fuels. The most widely used is the ceramics, uranium dioxide UO_2 , with a melting point of 2800 °C and a density of 10.2 t/m³. Uranium dioxide does not undergo phase transitions and is less subject to swelling than uranium alloys. This allows one to raise the burn-up to a few per cent. Uranium oxide does not interact with zirconium, niobium, stainless steel and other materials at high temperatures. The main disadvantage of the ceramics is its low heat conductivity which is only 4.5 kJ/m·K; as a result at high power the melting point may soon be attained and this restricts the specific power of the reactor. For example, the peak heat flux density in the Soviet uranium oxide WWPR does not exceed $1.4 \times 10^8 \text{ kW/m}^2$, and in this case the peak temperature in the rod fuel elements is 2200 °C. Moreover, the hot ceramics is very brittle and is apt to crack.

Plutonium is a metal with low melting point of 640 °C, due to its poor plastic properties plutonium practically does not yield to mechanical processing. As plutonium is toxic the manufacturing technology of fuel elements is even more complicated. The nuclear fuel is usually manufactured from plutonium dioxide, plutonium carbide and uranium carbide mixture or plutonium alloys containing metals.

Dispersed fuels possess high heat conductivities and good mechanical properties. A dispersed fuel consists of fine particles of UO_2 , UC , PuO_2 and other uranium and plutonium compounds packed heterogeneously in a metal matrix made of aluminium, molybdenum, stainless steel or other metals. The material of the matrix determines the irradiation stability and heat conductivity of the dispersed fuel. For example, the dispersed fuel used at the first APS consists of uranium alloy particles containing 9% of molybdenum and embedded in magnesium.

Coolants. Heat produced in the core is removed by coolants (light water, heavy water, gas, sodium and others).

One of the most extensively used coolants is ordinary water. Natural water contains a minute amount of heavy water

(0.017%), various impurities and dissolved gases. Due to these impurities and gases water is chemically active with metals. Therefore before using water as a coolant it must be purified by evaporation and deaerated, i.e. freed from the gases.

Radioactive water circulates in the first loop. The radioactivity of water is mostly due to impurities which appear on corrosion of various parts in the primary loop and to impurities due to fissionable materials from the surface of fuel elements. The concentration of radioactive impurities can be decreased by filtering the water. Neutrons interacting with oxygen nuclei induce the reactions $^{18}\text{O}(n, \gamma)^{19}\text{O}$ and $^{16}\text{O}(n, p)^{16}\text{N}$ in which the radioactive nuclei $^{19}\text{O}(T_{1/2} = 29.4 \text{ s})$ and $^{16}\text{N}(T_{1/2} = 4 \text{ s})$ are produced. However, the activity of ^{19}O and ^{16}N is insignificant compared to that of the impurities.

The disadvantages of water as a coolant are its low boiling point (100 °C at a pressure of 1 atm) and its appreciable absorptivity of thermal neutrons. The first disadvantage can be overcome by raising the pressure in the primary loop. Absorption of thermal neutrons is compensated by using enriched uranium nuclear fuel.

The chemical and thermophysical properties of heavy water are not much different from those of ordinary water. Heavy water does not practically absorb neutrons and thus it is possible to use natural uranium as the nuclear fuel in reactors with heavy water as coolant. However, heavy water is not extensively used because of its high cost.

The most extensively investigated liquid metal coolant is sodium. Due to the presence of sodium oxide the sodium coolant reacts chemically with most metals at comparatively low temperatures. After thorough removal of the oxides sodium does not react with many metals (Mo, Zr, stainless steel etc.) up to temperatures of 600-900 °C.

The main gas coolant is carbon dioxide. Carbon dioxide is not expensive and its density and volume heat capacity are high compared to other gases. The corroding effect of carbon dioxide on metals is determined by the oxygen content. Oxygen is present in carbon dioxide as an impurity and is formed at high temperatures by dissociation of the CO_2 molecules into carbon monoxide CO and oxygen O_2 .

Moderators. Materials which have a large slowing-down power and a low absorption cross section are used as moderators. Light water, heavy water, graphite, beryllium are appropriate materials. The properties of water and heavy water were discussed above. Here we shall give a short description of the properties of graphite and beryllium.

Natural graphite contains up to 20% of impurities, boron included. For this reason it cannot be used as a neutron moderator. Reactor graphite is prepared from a mixture of oil coke and coal tar. The mixture is molded into blocks under high pressure and the blocks are thermally processed at a high temperature. The density of the graphite is 1.6-1.8 g/cm³. It sublimes at a temperature of 3800-3900 °C. When heated in air to 400 °C graphite ignites. Therefore in power reactors facilities are provided for maintaining a controlled inert gas atmosphere (helium, nitrogen) for the graphite moderator.

Beryllium is one of the best moderators. Its melting point is high (1282 °C), as is its heat conductivity. Beryllium is compatible with carbon dioxide, water, air and a number of liquid metals. Helium is produced in the threshold reaction $^9\text{Be}(n, 2n)^2\alpha$. Therefore intense irradiation with fast neutrons results in accumulation of the gas and the pressure it exerts leads to swelling of the beryllium. The high cost of beryllium limits its use. Reflectors and core water displacers in experimental reactors are made from beryllium.

Structural materials. Structural materials are used to make the fuel element jackets, channels, reactor vessels and other parts of the reactor. Some physical properties of the structural materials most widely used in nuclear engineering are listed in Table 11.1.

Pure aluminium and water are compatible at low temperatures. The jackets of fuel elements used in experimental reactors with a water coolant are mainly made of pure aluminium.

Magnesium alloys are weak neutron absorbers. They are compatible with carbon dioxide up to 450 °C and are used for manufacturing fuel element jackets in graphite-graphite reactors. In this type of reactor a widely branched surface for heat removal is required.

Zirconium alloys and deaerated water are compatible up

Table 11.1

Physical Properties of Structural Materials

Material	Density, 10 ³ kg/m ³	Absorption cross section Σ_a , m ⁻¹	
		thermal neutrons	fusion spectrum neutrons
Aluminium	2.7	1.3	2.5×10^{-3}
Magnesium	1.74	0.14	3×10^{-3}
Zirconium	6.4	0.76	4×10^{-2}
Stainless steel	8.0	24.7	1×10^{-1}

to 350 °C. As zirconium is a weak thermal neutron absorber, its alloys are used as the main material for fuel element jackets in water-water power reactors.

Stainless steel is characterized by its high strength and ability to resist corrosion in water and sodium at high temperatures. It is one of the most widely applied structural materials in reactor construction. The fuel element jackets for sodium coolant reactors, the channels and fuel element jackets of the channel graphite-water reactors of the first APS and the Beloyarsk APS are made from stainless steel.

Irradiation affects the corrosion of structural materials in contact with the coolant. Firstly, (n, γ) and other reactions alter the composition of structural materials. Atoms which chemically react with the coolant may appear at the surface of the structural material. The rate of chemical reactions at the surfaces, for example of the fuel element jackets, will consequently increase. Secondly, irradiation of water produces radiolysis products which chemically react with the structural materials.

Absorption rod materials. Absorption rods are made from materials which contain elements with high absorption cross sections (boron, cadmium, hafnium and others). Rods containing boron are the most commonly used type as boron is an exceptionally good neutron absorber. Pure boron, however, is unfit as material for control rods. It is nonresistant to irradiation, fragile and incompatible with coolants. Boron (up to 5%) is usually added to stainless steel (boron steel). Other materials that can be used in absorption rods are boron carbide B_4C , a $B_4C-Al_2O_3$ mixture etc.

CHAPTER 12

REACTOR PHYSICS

12.1 Neutron Multiplication Factor

The "infinite" multiplication factor k_∞ of a thermal neutron chain reaction is the product of four factors (see Sec. 10.11): the thermal utilization factor θ , the average number of neutrons released per neutron absorbed in uranium (reproduction factor) η , the fast fission factor ϵ , the resonance escape probability ψ .

The thermal utilization factor. The moderator and nuclear fuel in a homogeneous core are irradiated by a thermal neutron flux of uniform density φ . Let us assume that the homogeneous mixture consists of the moderator and nuclear fuel and for definiteness let uranium be the nuclear fuel. Our purpose is to determine how the thermal utilization θ is affected by dilution of the uranium with the moderator, by enrichment of the uranium and by the temperature of the neutrons. The number of thermal neutrons absorbed per second in a unit volume of the homogeneous mixture is $\Sigma_a \varphi = (\Sigma_a^m + \Sigma_a^U) \varphi$ which includes $\Sigma_a^U \varphi$ in uranium; (Σ_a , Σ_a^m and Σ_a^U are the macroscopic absorption cross sections of the mixture, the moderator and uranium in the mixture respectively). The thermal utilization factor θ is the fraction of thermal neutrons absorbed in the uranium:

$$\theta = \Sigma_a^U \varphi / \Sigma_a \varphi = \Sigma_a^U / (\Sigma_a^U + \Sigma_a^m)$$

Let us replace the macroscopic cross sections by the microscopic cross sections in accordance with formula (10.5) and rewrite the latter expression as

$$\theta = \frac{1}{1 + N_m \sigma_a^m / N_U \sigma_a^U} \quad (12.1)$$

Three conclusions can be drawn from formula (12.1):

(1) for a homogeneous mixture θ does not depend on the speed of the neutrons v and, hence, does not depend on the

temperature of the neutrons T_{m} , provided the cross sections σ_a of all components of the mixture are governed by the $1/r$ law:

(2) as the uranium concentration in the mixture increases, θ tends to unity. On the other hand, diluting uranium with the moderator leads to a decrease in θ ;

(3) the greater the enrichment of uranium, the larger are the cross section σ_a^U and thermal utilization factor θ .

Unlike a homogeneous core, a heterogeneous core is non-uniform for thermal neutrons since the cross sections of the

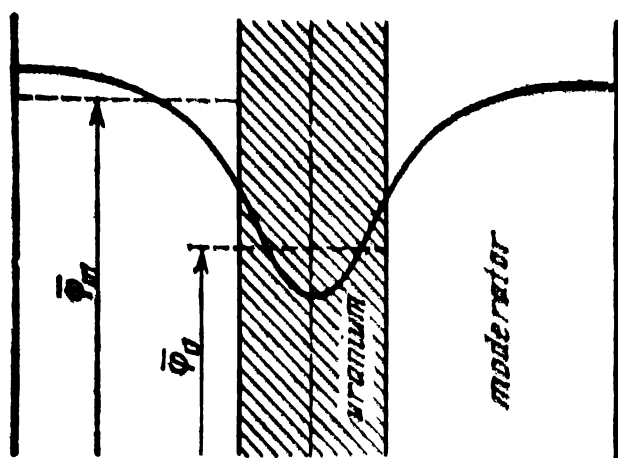


Fig. 12.1 Distribution of thermal neutron flux density in a cylindrical unit

moderator and structural materials of the fuel elements differ markedly. Let us find how the value of θ changes on transition from a homogeneous to a heterogeneous system. As an example we consider a cylindrical unit consisting of a uranium rod and the moderator (Fig. 12.1).

Fast neutrons lose their energy almost exclusively in the moderator as the uranium rod contains only heavy atoms. Hence, the moderator is a source of thermal neutrons. Thermal neutrons move from the moderator into the uranium rod. The variation of the thermal neutron flux density along the radius of the cylinder is shown in Fig. 12.1. The value of ϕ decreases on moving from the surface of the cylinder to the centre.

The mean thermal neutron flux density in uranium and in the moderator are denoted as $\bar{\phi}_U$ and $\bar{\phi}_m$. Nuclei of the mo-

derator in a heterogeneous reactor absorb $\bar{\varphi}_m/\bar{\varphi}_{h}$ times more thermal neutrons than the moderator in a homogeneous reactor does. Therefore, θ_{het} for a heterogeneous reactor is less than θ_{hom} for a homogeneous reactor with an identical core composition. Thus a transition from a homogeneous to a heterogeneous system reduces the utilization of thermal neutrons in a chain reaction. For example, in a square uranium-graphite lattice with a spacing $a = 30$ cm and a natural uranium rod with a diameter $d = 3$ cm the ratio $N_C/N_U = 215$, and $\theta_{het} = 0.885$. In a homogeneous mixture with the same ratio of carbon and natural uranium atoms the thermal utilization is $\theta_{hom} = 0.915$. In this particular example the efficiency of utilization of thermal neutrons decreases by 3% on transition to a heterogeneous system.

Neutron yield per absorption. Along with fissionable materials diluting agents are added to the nuclear fuel. They improve the mechanical properties and radiation resistance of the nuclear fuel and this in turn increases the degree of nuclear burn-up during an operating period. The neutrons absorbed in a nuclear fuel can be divided into two types. The first are those which induce nuclear fission, the others are those consumed as a result of radiative capture in uranium and all other components of the nuclear fuel.

Let v_f denote the number of neutrons released per fission of ^{235}U . If we denote by α_{nf} the fraction of neutrons captured by the nuclear fuel which induces fission, then the mean number of fission neutrons released per absorbed neutron (neutron yield per absorbed neutron)

$$\eta = \alpha_{nf} v_f$$

The total number of neutrons absorbed per unit volume of the fuel per second is $(\Sigma_a^U + \Sigma_a^d) \varphi$; of this number $\Sigma_f \varphi$ neutrons induce fission. Hence

$$\alpha_{nf} = \Sigma_f / (\Sigma_a^U + \Sigma_a^d)$$

where Σ_a^U and Σ_f are the macroscopic uranium absorption and fission cross sections respectively; Σ_a^d is the macroscopic absorption cross section of the nuclear fuel diluent.

Enriched uranium and diluting materials with low radioactive capture cross sections are used to increase the neutron

yield per absorbed neutron. Diluents with low radiative capture cross sections are especially important in breeders as the conversion factor depends not only on the uranium enrichment but also on the neutron absorption in the diluents.

Resonance neutron absorption. The resonance region consists of a region of resolvable resonance peaks and a region of peaks which cannot be resolved. The first region spans an energy range from 1 eV up to a certain E_b . The energy resolution of the measuring instruments is sufficient to distinguish any peak in this region. For energies exceeding E_b the distance between the resonance peaks is so small that the peaks cannot be separated. For heavy elements $E_b \approx 1$ keV.

In thermal reactors the dominant neutron resonance absorber is ^{238}U . Some neutron resonance energy levels E_r , the absorption cross sections $\sigma_{a,r}$ at peak value and the width Γ of these resonances for ^{238}U are presented in Table 12.1.

Table 12.1

Parameters of ^{238}U Resonance Peaks

E_r , eV	$\sigma_{a,r}$, b	Γ , MeV	E_r , eV	$\sigma_{a,r}$, b	Γ , MeV
6.68	22 030	26.3	36.8	39 820	59.0
21.0	33 080	34.0	66.3	21 190	43.0

Let us assume that the resonance neutrons are moving in an infinite system containing a moderator and ^{238}U . On encountering moderator nuclei the neutrons are scattered and on encountering ^{238}U nuclei they are absorbed. The first type of collision promotes the preservation of resonance neutrons and removes them from the dangerous range whereas in the second case the neutrons are lost.

The resonance escape probability (coefficient ψ) is a function of the nuclei density N_{238} and the slowing-down power of the medium $\xi\Sigma_s$:

$$\psi = \exp \left(- \frac{N_{238}}{\xi\Sigma_s} J_{\text{eff}} \right) \quad (12.2)$$

The quantity J_{eff} is termed the *effective resonance integral*. It characterizes neutron absorption by a nucleus in the re-

sonance region and is measured in barns. By using the effective resonance integral we can simplify quantitative calculations of resonance absorption without going into the details of the interactions involved when neutrons are slowed down. The effective resonance integral is usually determined experimentally. It depends on the ^{238}U concentration and the mutual arrangement of the uranium and moderator.

In a homogeneous mixture of the moderator and ^{238}U the effective resonance integral can be found with a good accuracy by the empirical formula

$$J_{\text{eff}} = 3.9 \left(\frac{N_m}{N_{238}} \sigma_s^m \right)^{0.415} \quad (12.3)$$

where N_m/N_{238} is the ratio of moderator to ^{238}U nuclei in the homogeneous mixture; σ_s^m is the microscopic scattering cross section of the moderator expressed in barns. As can be seen from formula (12.3) the effective resonance integral decreases with increase of the ^{238}U concentration. The more ^{238}U nuclei there are in the mixture, the less probable is the absorption of slowing-down neutrons by a moderator nucleus. Let us illustrate this effect with a numerical problem. Suppose that 1000 neutrons are slowed down in the resonance range and that for every 1 cm^3 of the mixture there is only one ^{238}U nucleus with which each of the 1000 neutrons can collide in the slowing-down process. If the concentration of ^{238}U nuclei in the mixture is increased, the probability for each neutron to collide with a given ^{238}U nucleus will be less since some of the neutrons will be absorbed by other nuclei. The influence the absorption in some ^{238}U nuclei exerts on the absorption by other nuclei is termed *screening of resonance levels*.

Example. Find the effective resonance integral in a homogeneous natural uranium-graphite mixture with $N_{\text{C}}/N_{238} = 215$. The graphite scattering cross section $\sigma_s^{\text{C}} = 4.7 \text{ b}$. Substituting the values of N_{C}/N_{238} and σ_s^{C} into formula (12.3) we get

$$J_{\text{eff}} = 3.9(215 \times 4.7)^{0.415} = 69 \text{ b}$$

In a homogeneous medium all ^{238}U nuclei are in the same conditions with respect to the resonance neutron flux. In a

heterogeneous medium the uranium is separated from the moderator and this substantially affects resonance neutron absorption. Firstly, a fraction of the resonance neutrons becomes thermal in the moderator without colliding with uranium nuclei; secondly, almost all resonance neutrons that reach the surface of the fuel element are absorbed in a thin surface layer. Inner ^{238}U nuclei are screened by the surface nuclei and are less effective in resonance neutron absorption, the screening increasing with increase of the fuel element diameter d . Therefore the ^{238}U effective resonance integral in a heterogeneous reactor is a function of the fuel element diameter d :

$$J_{\text{eff}} = a + b/\sqrt{d}$$

The constant a characterizes resonance neutron absorption in the surface ^{238}U nuclei, and the constant b that in the inner ^{238}U nuclei. For each type of nuclear fuel (natural uranium, uranium oxide and others) the constants a and b are measured experimentally. For natural uranium rods ($a = 4.15$, $b = 12.35$)

$$J_{\text{eff}} = 4.15 + 12.35/\sqrt{d} \quad (12.3')$$

where J_{eff} is the effective resonance integral in barns; d is the rod diameter in cm.

Example. Find the ^{238}U effective resonance integral for a natural uranium rod with a diameter $d = 3$ cm:

$$J_{\text{eff}} = 4.15 + 12.35/\sqrt{3} \approx 11.3 \text{ b}$$

A comparison of the two latter examples shows that when the uranium and moderator are separated neutron absorption markedly decreases in the resonance region.

The coefficient ψ depends on the ratio

$$N_{238} J_{\text{eff}} / \xi \Sigma_s = \Sigma / \xi \Sigma_s$$

which reflects the competition between two processes in the resonance region, viz. neutron absorption and slowing-down. The cross section Σ by definition is similar to the macroscopic absorption cross section in which the effective resonance integral J_{eff} replaces the microscopic cross section. It also describes the decrease of the number of slowing-down neu-

trons in the resonance region. Resonance neutrons absorption increases with increase of the ^{238}U concentration.

Indeed, from formula (12.3) it follows that $\Sigma = N_{238} J_{\text{eff}} \sim \sim N_{238}^{0.585}$. The greater the ^{238}U nuclei concentration the less is the fraction of neutrons that are slowed down to thermal energies. The neutrons slowing-down influences resonance absorption. Neutrons which collide with moderator nuclei escape from the resonance region. The higher the slowing-down power $\xi \Sigma_s$, the more intensive is this process. Thus for a given ^{238}U concentration the resonance escape probability is greater in a uranium-water medium than in a uranium-carbon medium.

Example. Calculate the resonance escape probability for homogeneous and heterogeneous natural uranium-graphite media. In both media the ratio of carbon to ^{238}U nuclei $N_{\text{C}}/N_{238} = 215$. The diameter of the uranium rod $d = 3$ cm. Taking into account that $\xi_{\text{C}} = 0.159$ and $\sigma_{\text{a}}^{\text{C}} = 4.7$ b, we get

$$N_{328}/\xi\sigma_{\text{s}}^{\text{C}} N_{\text{C}} = 1/0.159 \times 4.7 \times 215 = 0.00625 \text{ b}^{-1}$$

The effective resonance integrals for homogeneous and heterogeneous systems with a given composition and rod diameter were computed in the previous two problems. Substituting the two quantities into formula (12.2) we find the coefficients for a homogeneous system ψ_{hom} and a heterogeneous system ψ_{het} :

$$\psi_{\text{hom}} = e^{-6.25 \times 10^{-3} \times 68} = e^{-0.425} \approx 0.65,$$

$$\psi_{\text{het}} = e^{-6.25 \times 10^{-3} \times 11.25} = e^{-0.0705} \approx 0.93$$

At the beginning of this section we cited the values of the thermal utilization factors θ for homogeneous and heterogeneous media for which $N_{\text{C}}/N_{238} = 215$: $\theta_{\text{hom}} = 0.915$ and $\theta_{\text{het}} = 0.885$. The product $(\psi\theta)_{\text{hom}} = 0.595$, and $(\psi\theta)_{\text{het}} = 0.823$. Thermal neutron absorption in uranium is somewhat lower in a heterogeneous than in a homogeneous medium. However, this loss is significantly offset by the decrease in resonance neutron absorption, and the neutron multiplication properties of the medium are improved. In a heterogeneous medium 930 out of each 1000 fast neutrons

become thermal as compared to 650 in a homogeneous medium. Thus, in a heterogeneous medium an additional 280 neutrons are retained in the slowing-down process.

Multiplication by fast neutrons. In thermal reactors with slightly enriched uranium ($x < 5\%$) the concentration of ^{238}U is many times greater than that of ^{235}U . The fission of ^{235}U nuclei induced by fast neutrons is so insignificant that it can be neglected. However, the number of ^{238}U fissions induced by neutrons with energies $E_n > 1.0 \text{ MeV}$ may be great, and they have a marked influence on the course of the chain reaction.

In a homogeneous core the ^{238}U nuclei are surrounded by many moderator nuclei. Fission neutrons passing through the surrounding materials collide with light nuclei with a high probability and are slowed down to energies below the ^{238}U fission threshold. As a result the multiplication factor in a fast homogeneous reactor differs little from unity.

In a heterogeneous reactor fast neutrons initially move in the fuel elements among ^{238}U nuclei. Therefore, in a heterogeneous reactor the probability of a collision with a ^{238}U nucleus and its fission is much greater than in a homogeneous reactor. The probability depends on the path of the neutron in the nuclear fuel, i.e. on the size of the fuel element, the ^{238}U concentration and the lattice spacing a . In a thick fuel element the neutron path is longer than in a thin fuel element, and the multiplication factor in the first case is thus greater than in the second. If the lattice spacing a is much greater than the fast neutron scattering length in the moderator, λ_s , most of the fast neutrons enter another fuel element after having been slowed down to energies $E_n < 1.0 \text{ MeV}$. Therefore the fast fission factor ϵ for lattices with spacings $a \gg \lambda_s$ is determined only by the size and composition of the fuel element. As an example, for natural uranium rods with a radius R cm

$$\epsilon \approx 1 + 1.75 \times 10^{-2} R$$

In water-water reactors the fuel elements are inserted in a close-packet lattice ($a \ll \lambda_s$). Such an arrangement of fuel elements decreases thermal neutron absorption in the water. In a close-packed lattice fission neutrons penetrate several fuel elements before being slowed down below the fission

threshold energy for ^{238}U . The multiplication factor is highest for fast neutrons in water-water power reactors. For a hydrogen nuclei- ^{238}U ratio $N_{\text{H}}/N_{^{238}\text{U}} > 3$, the fast fission factor can be calculated by the approximate formula:

$$\epsilon \approx 1 + 0.22 (N_{^{238}\text{U}}/N_{\text{H}})$$

Example. Compute the fast fission factor: (a) for a uranium-graphite lattice with $a = 14$ cm and diameter of natural uranium rod $d = 3$ cm and (b) for a water-water power reactor with $N_{\text{H}}/N_{^{238}\text{U}} = 5$.

(a) The scattering length in graphite $\lambda_s = 2.5$ cm. Therefore the uranium-graphite lattice spacing $a \gg \lambda_s$. Hence,

$$\epsilon = 1 + 1.75 \times 10^{-2} \times 1.5 \approx 1.026$$

(b) The factor ϵ for a WWPR

$$\epsilon = 1 + 0.22 \times 0.2 = 1.044$$

The infinite multiplication factor. The neutron multiplication factor in an infinite thermal neutron reactor depends on the reactor's composition and structure. The dependence of the resonance escape probability ψ and of the thermal utilization θ on the moderator nuclei-uranium nuclei ratio $N_{\text{m}}/N_{\text{U}}$ in a homogeneous medium is shown in Fig. 12.2. As the ratio $N_{\text{m}}/N_{\text{U}}$ increases the thermal neutron absorption in the moderator increases and the thermal utilization θ decreases. At the same time the resonance escape probability smoothly tends to unity.

The infinite multiplication factor k_{∞} is proportional to the product $\psi\theta$ which determines the dependence of k_{∞} on the ratio $N_{\text{m}}/N_{\text{U}}$. For high uranium concentrations the thermal utilization factor θ changes insignificantly and therefore k_{∞} is proportional to ψ . In systems with low uranium concentrations the value of ψ is close to unity and the variation of k_{∞} is similar to that of θ . Thus the infinite multiplication factor k_{∞} initially increases, reaches its peak value and then decreases and tends to unity.

For natural uranium the neutron yield per absorption $\eta = 1.32$ and therefore for a chain reaction to take place the product $\psi\theta$ must be greater than

$$k_{\infty}/\eta = 1/1.32 = 0.76$$

Homogeneous mixtures containing natural uranium with graphite, beryllium or water are unsuitable for reactors as the maximum value of the product $(\psi\theta)$ for such mixtures is less than 0.76. For example, in a uranium-graphite mixture $(\psi\theta)_{\max} = 0.56$. In a homogeneous natural uranium-heavy water mixture the infinite multiplication factor k_{∞} can be greater than unity as the moderator is a poor thermal neutron absorber. In way of illustration, for solutions of natural uranium salts in heavy water with a ratio $N_D/N_U = 400$,

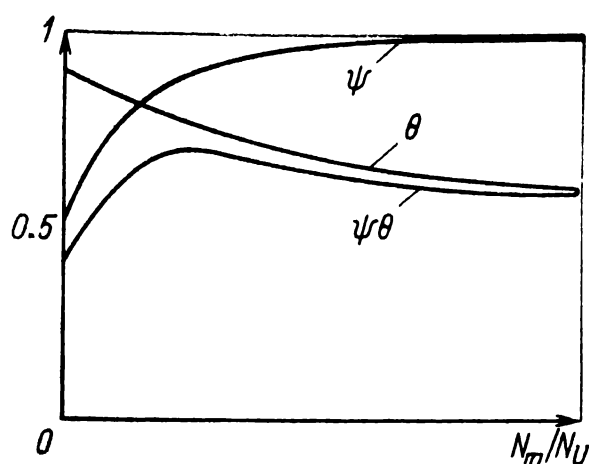


Fig. 12.2 Dependence of ψ , θ and $\psi\theta$ on uranium concentration in a homogeneous mixture

$\theta = 0.99$, $\psi = 0.79$ and $k_{\infty} = 1.03$. In research reactors water solutions of enriched uranium salts are used. The low value of $\psi\theta$ in such reactors is compensated by a high neutron yield η .

In a heterogeneous reactor the dependence of the multiplication factor k_{∞} on the lattice spacing a for fuel elements of a definite size is similar to the dependence of k_{∞} on N_m/N_U in a homogeneous mixture.

The consumption of neutrons due to resonance absorption is so low in a heterogeneous reactor that a chain reaction becomes possible with natural uranium and a graphite or beryllium moderator. For example, the highest $\psi\theta$ value in a square lattice with 30 mm diameter natural uranium rods in graphite is 0.830 at an optimal lattice spacing $a = 25$ cm. Therefore natural uranium is suitable as nuclear fuel for graphite-gas reactors.

12.2 Neutron Flux Density. Neutron Leakage

The reactor borders on media devoid of neutron sources. The neutron density in these media is lower than in the reactor. Therefore there is a leakage of neutrons through the outer surface of the reactor. The neutron flux density is not uniform through the reactor and is highest at the centre and drops towards the outer surface.

The volume flux density distribution can be found by applying the diffusion equation which is derived from the

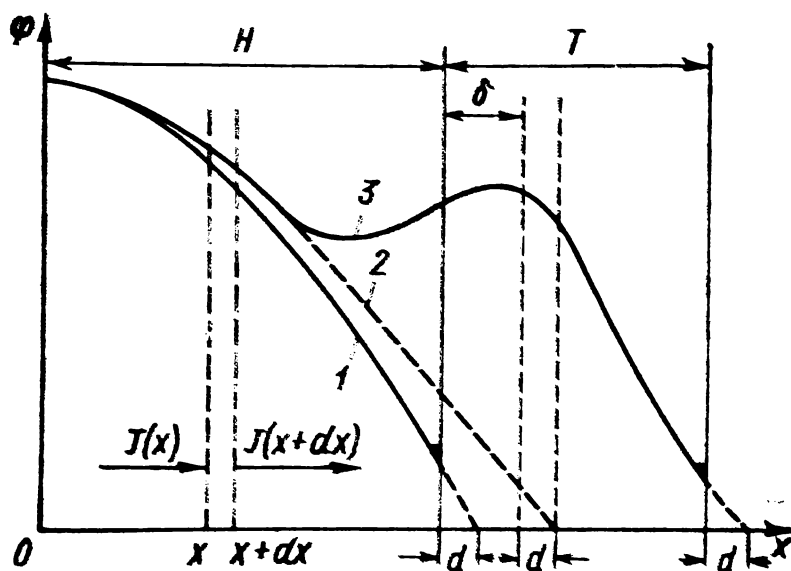


Fig. 12.3 Distribution of thermal neutron flux density with respect to thickness of a flat reactor
 1—reactor without reflector; 2—equivalent reactor without reflector; 3—reactor with reflector

neutron balance. In reactor theory the main features of neutron flux density distribution is often investigated for simple models. One of such models is a flat reactor without a reflector. The core of such a reactor is envisaged as an infinite flat slab $2H$ thick (Fig. 12.3) bordering on a vacuum.

Before writing down the neutron balance in a critical reactor, we choose the origin of coordinates in the plane of symmetry of the core and direct the x -axis perpendicular to the plane (Fig. 12.3). Consider a flat slab of a volume $dV = 1 \text{ m}^2 \cdot dx$ between the coordinates x and $x + dx$. We assume that as a result of nuclear fission thermal neutrons are emitted. The neutron balance for the volume dV can now be written down.

In dV there are $\Sigma_a \varphi dx$ neutrons absorbed per second and $k_\infty \Sigma_a \varphi dx$ other neutrons appear in the same time. To achieve a sustained chain reaction in volume dV , $\Sigma_a \varphi dx$ of the $k_\infty \Sigma_a \varphi dx$ neutrons must be absorbed again and the excess $(k_\infty - 1) \Sigma_a \varphi dx$ neutrons must leak out of volume dV through the surface.

Let us calculate the amount of neutrons passing through the surface of volume dV and equalize it to the neutron excess. We denote by $J(x)$ and $J(x + dx)$ the neutron fluxes at distances of x and $x + dx$ from the coordinate origin. The reactor has finite dimensions along the x -axis and the neutron flux is directed toward the edge of the reactor. Therefore $J(x)$ neutrons flow into volume dV and $J(x + dx)$ flow out of it. The neutron leakage from the flat slab is

$$dJ = J(x + dx) - J(x) = (k_\infty - 1) \Sigma_a \varphi dx$$

We divide the right and left sides of the last equation by $\Sigma_a dx$, and, taking into account formulas (10.10) and (10.11), we obtain the neutron diffusion equation for a flat reactor:

$$\frac{d^2\varphi}{dx^2} + \frac{k_\infty - 1}{L^2} \varphi = 0$$

Let us now give up the assumption regarding the energy of the source of thermal neutrons which was made in deriving the diffusion equation. After the fission of nucleus, fission neutrons, and not thermal neutrons, are emitted. The leakage of slowing-down neutrons decreases the excess of thermal neutrons. A more precise investigation of the neutron balance shows that the leakage can be taken into account by substituting the square of the migration length L_m^2 for the square of the diffusion length L^2 in the diffusion equation:

$$\frac{d^2\varphi}{dx^2} + \frac{k_\infty - 1}{L_m^2} \varphi = 0 \quad (12.4)$$

The quantity

$$x^2 = \frac{k_\infty - 1}{L_m^2} \quad (12.5)$$

is called the *material parameter*. The term is explained by the fact that it depends exclusively on the properties of materials the reactor is made from.

The solution of the diffusion equation (12.4) is

$$\varphi(x) = \varphi_0 \cos Bx$$

where φ_0 is the neutron flux density at the origin of coordinates ($x = 0$).

The neutron flux density $\varphi(x)$ must satisfy certain boundary conditions. If a tangent is drawn to the flux density curve near the surface of the reactor, it will intersect the x -axis (flux density $\varphi = 0$) at a distance d from the boundary (see Fig. 12.3). Let us equate to zero the flux density at the point $H_e = H + d$:

$$\varphi_0 \cos BH_e = 0$$

The cosine vanishes if

$$BH_e = \pi/2$$

Hence

$$B^2 = (\pi/2H_e)^2 \quad (12.6)$$

The quantity B^2 depends on the size and shape of the reactor. It is called the *size-shape factor* of the reactor.

The surface at which the extrapolated neutron flux density vanishes is termed the *extrapolated* boundary. It is located at the extrapolated distance $H_e = H + d$ from the centre of the reactor. The extrapolated additional distance in thermal neutron reactors is $d \approx 1$ cm. In cases when the thickness H is considerable, one may put, with a high degree of accuracy, $H \approx H_e$. It should be noted that when we formally equalize the neutron flux density to zero at the extrapolated boundary of the reactor under no circumstances does this mean that neutron flux density is actually zero at the boundary. The neutron flux density is nonzero both at the physical (real) and at the extrapolated boundary. The artificial extrapolated boundary is used in reactor theory as a mathematical device for simplifying theoretical investigations of the neutron flux density distribution within the body of the reactor.

The diffusion equation for spherical and cylindrical reactors is similar to equation (12.4). Let us place the origin of the coordinates in the centre of symmetry of a spherical or cylindrical reactor and solve the diffusion equation for these reactors.

In a spherical bare reactor of radius R neutron leakage through the spherical surface is radial. The neutron flux density will therefore be a function of a single coordinate, the radius r :

$$\varphi(r) = \varphi_0 \frac{\sin Br}{Br} \quad (12.7)$$

The size-shape factor

$$B^2 = (\pi/R_e)^2 \quad (12.8)$$

where $R_e = R + d$ is the extrapolated radius.

In cylindrical bare reactors neutron leakage occurs in two directions: through the end face and lateral surface. The neutron flux density in a cylindrical reactor varies along the z -axis and along the radius r of the reactor:

$$\varphi(r, z) = \varphi_0 J_0(B_R r) \cos B_H z \quad (12.7')$$

The size-shape factor of a cylindrical reactor of radius R and height H consists of two terms describing radial and axial leakage:

$$B^2 = R_R^2 + B_H^2 \quad (12.9)$$

where

$$B_R^2 = (2.405/R_e)^2, \quad B_H^2 = (\pi/H_e)^2$$

(here $H_e = H + 2d$ is the extrapolated height).

The function J_0 is the zero-order Bessel function. It is presented in tables or can be computed from the approximate ratio

$$J_0\left(\frac{2.405}{R_e} r\right) \approx \cos\left(\frac{\pi}{2} \frac{r}{R_e}\right)$$

It may be noted that the neutron leakage from a sphere and from a cylinder of equal volume differs. The size-shape factor of a sphere is less than that of a cylinder and hence neutron leakage from a sphere is smaller. This can be explained by the fact that the ratio of the surface to the volume is least of a sphere.

12.3 Parameters of a Critical Bare Reactor

In a critical reactor the following sustained chain reaction conditions are fulfilled: of the k_{∞} thermal neutrons formed in the multiplication cycle one thermal neutron is used to

sustain the chain reaction and the excess $k_\infty - 1$ neutrons leak out through the reactor surface. The mathematical relationship reflecting this condition follows from equation (12.4) and the diffusion equation. Inserting into these equations expressions for the neutron flux density and differentiating we obtain

$$B_{cr}^2 = (k_\infty - 1)/L_m^2 \quad (12.10)$$

where B_{cr}^2 is the size-shape factor of a critical reactor. Equation (12.10) is termed the *critical* equation. It relates the critical size and the neutron-physical characteristics of the reactor (k_∞ , L_m^2). For a given composition of the reactor there is a single value of the size-shape factor, $B^2 = B_{cr}^2$, which satisfies the critical equation.

To find the critical dimensions of a bare reactor with a given composition, the parameters are computed in the following order: k_∞ and L_m^2 , size-shape factor B_{cr}^2 [from formula (12.10)], critical size [from the formulas (12.6), (12.8), (12.9)]. In the case of a cylindrical reactor the ratio of the extrapolated height H_e to the extrapolated radius R_e must be given.

Critical equation (12.10) may be rewritten as follows:

$$1 = k_\infty / (1 + B_{cr}^2 L_m^2) \quad (12.11)$$

The equation for the effective multiplication factor for a non-critical reactor is written in the same way as (12.11):

$$k_{eff} = k_\infty / (1 + B^2 L_m^2) \quad (12.12)$$

Equation (12.12) coincides with the critical equation when $k_{eff} = 1$ and $B^2 = B_{cr}^2$. A comparison of equations (12.12) and (10.12) shows that the fraction of neutrons absorbed in the reactor is

$$p = 1 / (1 + B^2 L_m^2)$$

With increase of the size-shape factor B^2 the dimensions of the reactor and the quantity p decrease whereas the neutron leakage increases. For $B^2 < B_{cr}^2$ the reactor is supercritical and for $B^2 > B_{cr}^2$ it is subcritical.

Example. Calculate the critical size of a bare reactor with an aqueous solution of ^{235}U salts if the ratio of hydrogen to

^{235}U nuclei in the mixture is $N_{\text{H}}/N_{^{235}} = 1000$ and the density of the solution $\rho = 1000 \text{ kg/m}^3$.

$$\theta = 1 / \left(1 + \frac{N_{\text{H}}}{N_{^{235}}} \frac{\sigma_{\text{a}}^{\text{H}}}{\sigma_{\text{a}}^{^{235}}} \right) = 1 / \left(1 + 1000 \frac{0.33}{690} \right) \approx 0.675$$

For each neutron captured by ^{235}U , $\eta = 2.07$ neutrons are emitted. The multiplication factor in an infinite reactor

$$k_{\infty} = 2.07 \times 0.675 \approx 1.40$$

The diffusion length L in an uranium-water solution is insignificant in comparison with the slowing down length L_s , and the square of the migration length $L_m^2 \approx L_s^2 = 27 \text{ cm}^2$ (see Table 10.7).

From formula (12.8)

$$B_{\text{cr}}^2 = (k_{\infty} - 1)/L_s^2 = 0.40/2.7 \times 10^{-3} \approx 150 \text{ m}^{-2}$$

Let us compute the extrapolated size of a spherical and cylindrical reactor. According to formula (12.8)

$$R_e = \pi/B_{\text{cr}} = 3.14/12.2 \approx 0.26 \text{ m} = 26 \text{ cm}$$

Assume the diameter of the cylindrical reactor to be equal to its height, or $R_e = H_e/2$. Then from formula (12.9) it follows that

$$R_e = \sqrt{2.405^2 + (\pi/2)^2}/B_{\text{cr}} = 24 \text{ cm}$$

Subtracting the extrapolated additional length $d \approx 1 \text{ cm}$ from the values obtained we get

$$R_{\text{sph}} = 25 \text{ cm}, \quad R_{\text{cyl}} = 23 \text{ cm}, \quad H_{\text{cyl}} = 46 \text{ cm}$$

and hence $V_{\text{sph}} \approx 65 \text{ l}$, $V_{\text{cyl}} \approx 75 \text{ l}$.

Let us investigate how the hydrogen-uranium nuclei ratio in a critical bare sphere filled with an aqueous solution of ^{235}U salts, affects the critical radius R_{cr} , the ^{235}U critical mass M_{cr} and the thermal utilization factor (Fig. 12.4). With decrease of the ^{235}U concentration in the solution the critical radius increases monotonously, whereas the critical mass passes through a minimum at $N_{\text{H}}/N_{^{235}} \approx 800$.

The multiplication factor $k_{\infty} = \eta\theta = 2.07 \cdot 0$. Substituting this value into equation (12.11) and dividing the left-

and right-hand sides by 2.07 we get

$$0.48 = \theta / (1 + B_{cr}^2 L_m^2) = \theta p.$$

In critical reactors with different values of N_H/N_{235} the product of the thermal utilization factor θ and p is a constant.

In the first region ($100 \leq N_H/N_{235} \leq 800$), θ drops from 0.952 to 0.725, i.e. by 1.31 times. Hence, the leakage of fast

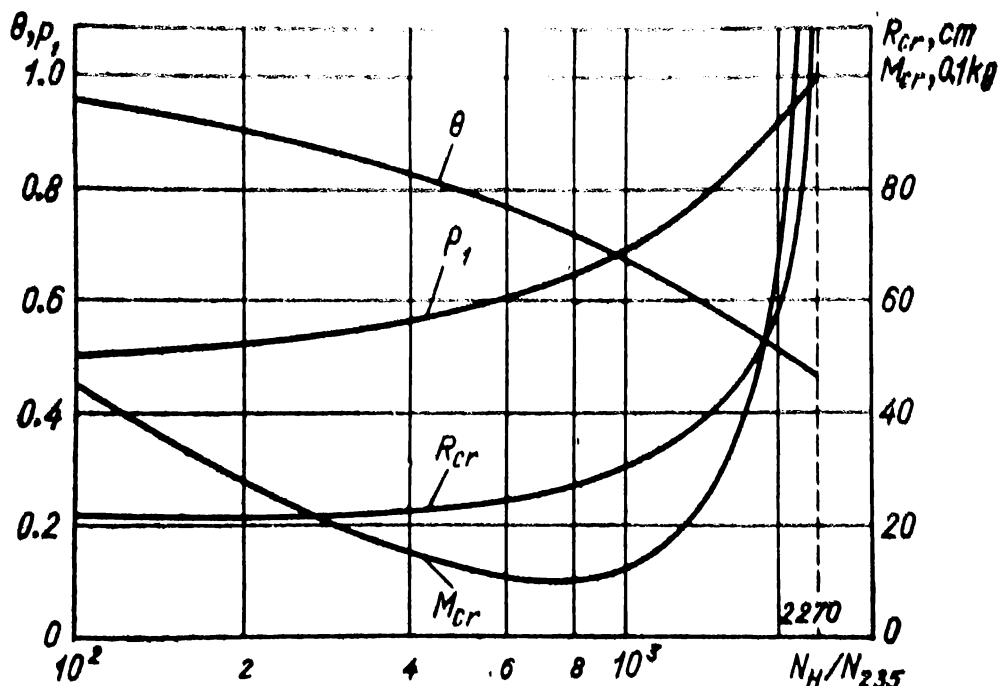


Fig. 12.4 Dependence of R_{cr} , M_{cr} , θ and p_1 on concentration of ^{235}U for a critical sphere containing aqueous solution of ^{235}U salts

neutrons must also be diminished by 1.31 times. This can be achieved by increasing the radius of the reactor from 21 cm to 27 cm. The ^{235}U concentration in the mixture drops eightfold whereas the volume of the mixture, V , increases only 2.15 times. Therefore the critical mass, which is proportional to $(N_{235}/N_H)R_{cr}^3$, decreases in the first region about 4 times.

Let us see how the critical volume and critical mass change in the second region ($N_H/N_{235} > 800$). Consider two solutions with N_H/N_{235} ratios of 1000 and 2000. The thermal utilization θ is 0.675 for the first solution and is reduced to 0.520 for the second, i.e. by 1.3 times. To keep the reactor critical

it is necessary to increase the radius of the sphere from 30 cm to 80 cm, thus increasing the volume 19 times. Therefore in the second region the growth of the critical volume is more rapid than the decrease of the ^{235}U concentration thus causing a significant increase in the critical mass.

How can one explain that in the first region the ^{235}U concentration in the solution diminishes faster than the volume increases, whereas in the second region, on the contrary, the ^{235}U concentration varies insignificantly in comparison to the increase in volume? As the ratio N_{H}/N_{235} increases in the first region, the thermal utilization θ experiences only a comparatively small decrease and the probability that leakage does not occur, p , grows rapidly. Therefore the drop in θ is compensated by a comparatively small increase of the critical radius (volume). In the second region the volume of the solution is so large that the probability of avoiding leakage is close to unity. This is why even a small drop in the thermal utilization θ must be compensated by a substantial increase of the reactor critical radius (volume).

Let us find the limiting value of N_{H}/N_{235} for which $k_{\infty} = 1$. In an infinite reactor all the neutrons are absorbed in the mixture ($p = 1$) and $\theta = 0.48$. It is not difficult to determine the ratio of hydrogen to ^{235}U nuclei in an infinite critical reactor. From equation (12.1)

$$\frac{N_{\text{H}}}{N_{235}} = \frac{1-\theta}{\theta} \frac{\sigma_a^{235}}{\sigma_a^{\text{H}}} = \frac{0.52}{0.48} \frac{690}{0.33} = 2270$$

The curves M_{cr} and R_{cr} tend to infinity as the ratio N_{H}/N_{235} approaches 2270. In an infinite reactor with a ratio $N_{\text{H}}/N_{235} > 2270$ a self-sustaining chain reaction is impossible.

For any ^{235}U -moderator media the dependence of the critical parameters on N_{M}/N_{235} is similar to that depicted in Fig. 12.4. The dependence may differ with respect to the position of the critical load minimum and the magnitude of the $N_{\text{M}} = N_{235}$ ratio in a critical infinite reactor. For example, the minimum critical mass of a sphere with a four kilogram homogeneous ^{235}U -beryllium mixture corresponds to a ratio $N_{\text{Be}}/N_{235} \approx 2 \times 10^4$.

12.4 Reactor with Reflectors

The specific energy release near the core surface is much less than within the core. The surface layer, in which a large mass of nuclear fuel is concentrated, is used inefficiently. Therefore it is economically profitable to supply a bare reactor with a reflecting layer. In such reflected reactors chain reactions can be sustained with a smaller load of nuclear fuel.

The effect of a reflector on the critical volume can be described by introducing an *effective increment*. This quantity shows to what extent the dimensions of a critical bare reactor must be reduced to keep the reactor critical after a reflector is installed. A bare reactor and a reflected reactor are considered equivalent if their core composition, structure and shape are identical and the effective multiplication factors of both reactors are equal. The half-thickness H of a reflected flat reactor and the half-thickness $H + \delta$ of an equivalent bare reactor are shown in Fig. 12.3.

In a spherical reactor the effective increment

$$\delta = R_0 - R$$

where R_0 is the radius of the equivalent bare reactor and R is the core radius of the reflected reactor.

In cylindrical reactors we discern two types of effective increments: one for the radius, δ_R , and the other for the height, δ_H :

$$\delta_R = R_0 - R, \quad \delta_H = (H_0 - H)/2$$

The effective increment for thermal neutron power reactors, in which the moderator and reflector are usually made from the same material, depends on the thickness of the reflector T and thermal neutron diffusion length L in the reflector.

The most efficient reflector layers are those arranged close to the core. Few neutrons emitted from the core reach those reflector layers which are located at large distances from the core boundary. The fraction of neutrons returned by distant reflector layers into the core is therefore small. Reflector layers at a distance of $1.5L_m$ from the boundary of the core (L_m is the migration length in the reflector) practically do

not participate in reflecting the neutrons. The limiting thickness of a reflector which exerts about the same effect as an infinite reflector is about $1.5L_m$. For example, the limiting thickness of a water reflector is 15 cm and that of a graphite reflector, 80 cm. The highest value of the effective increment δ for reflectors thicker than $1.5L_m$ depends on the relation between the slowing-down length L_s and the thermal neutron diffusion length L in the reflector. For $L > L_s$ (the reflector is beryllium, graphite etc.), $\delta \approx L$; for $L < L_s$ (water reflector), $\delta \approx L_s$.

It is difficult to calculate the critical dimensions of a reflected reactor precisely. To estimate the critical dimensions we must first determine the effective increment for a reflector of known composition and thickness. Then from the critical equation we find the critical dimensions R_e and H_e of an equivalent bare reactor. The critical dimensions of a reflected reactor are the differences $R_{cr} = R_0 - \delta_R$ and $H_{cr} = H_0 - 2\delta_H$.

Example. Find the critical size of a cylindrical reactor with an aqueous solution of ^{235}U salts surrounded by a 15 cm layer of water ($T = 15$ cm). The diameter of the core is equal to its height. The N_H/N_{235} ratio in the core is 1000. In Sec. 12.3 we computed the critical dimensions of a cylindrical bare reactor with $N_H/N_{235} = 1000$ ($R_0 = 23$ cm, $H_0 = 46$ cm). Now we must find the effective increments δ_H and δ_R . The thicknesses of the lateral and end reflectors are identical and $\delta_H = \delta_R = \delta$. The diffusion length in water $L \approx 3$ cm and the slowing-down length $L_s \approx 5$ cm. Therefore $\delta \approx L \approx 5$ cm. The critical dimensions of the reflected reactor are

$$R = R_0 - \delta = 23 - 5 = 18 \text{ cm},$$

$$H = H_0 - 2\delta = 46 - 10 = 36 \text{ cm}$$

The critical parameters of a reflected reactor depend similarly on the N_m/N_{235} ratio (see Fig. 12.4). The limiting thickness of a reflector made from graphite, heavy water, beryllium and other moderators, with the exception of water, reduces the critical load and volume several times. Water is a rather intensive thermal neutron absorber and therefore its efficiency as a reflector is relatively low. In our last

example a limiting water reflector would reduce the critical volume only 1.7 times.

The thermal neutron flux density in a reflected reactor (see Fig. 12.3) increases near the core edge, reaches its peak within the reflector and then falls. This type of variation of the thermal neutron flux density depends on the source and the thermal neutron absorption cross section. The flux density of slowing-down neutrons near the edge of the core and reflector changes insignificantly. Therefore the sources of thermal neutrons in this region in both the core and the reflector are practically the same. Neutron "bursts" are explained by the fact that thermal neutrons obtained by slowing-down epithermal neutrons ($E_n > 1$ eV) are absorbed to a lesser degree in the reflector than in the core. As a result, thermal neutrons accumulate in the reflector near the core at a higher rate. In some reactors of a small core size and with good reflectors, such as beryllium, the peak flux density may be in the reflector and not in the centre of the core.

The neutron flux density volume-nonuniformity coefficient (or shorter the volume-nonuniformity coefficient) is introduced to describe the uneven distribution of the flux density in the core:

$$k_V = \varphi_0 / \bar{\varphi}$$

where φ_0 and $\bar{\varphi}$ are the maximum and mean neutron flux densities in the core. In an infinite bare flat reactor the non-uniformity coefficient with respect to the thickness is

$$k_H = BH_0 / \sin BH_0$$

It depends only on the half-thickness of the reactor H and on the size-shape parameter B^2 . For a large reactor

$$H_0 \approx H_e, BH_0 \approx \pi/2 \text{ and } k_H \approx \pi/2 = 1.57$$

For a cylindrical reactor it is convenient to write the non-uniformity coefficient as the product of two factors:

$$k_V = k_R k_H$$

where k_R and k_H are nonuniformity coefficients with respect to the radius and height of the reactor.

The value of k_v is highest for a bare reactor. In a spherical reactor $k_v = 3.30$ and in a cylindrical reactor $k_v = 3.62$ with $k_R = 2.31$, $k_H = 1.57$. The nonuniformity coefficient k_v of a reflected reactor depends on the composition and size of the core and reflector. In large reactors it differs little from the nonuniformity coefficient k_v of the bare reactors. However, in small reactors with good reflectors the value of k_v falls to 1.7-2.0.

The power level of a reactor is proportional to the average neutron flux density $\bar{\varphi}$ and core volume V . The total number of fissions in a reactor per unit time is $\Sigma_f \bar{\varphi} V$, where Σ_f is the fission cross section in the core. A power level of 1 MW corresponds to 3.1×10^{16} fissions/s, and therefore the power of the reactor (in MW) is

$$P = \Sigma_f \bar{\varphi} V / 3.1 \times 10^{16}$$

Since $\bar{\varphi} = \varphi_0 / k_v$, we can rewrite

$$P = \Sigma_f \varphi_0 V / 3.1 \times 10^{16} k_v$$

Hence the power level of a reactor is inversely proportional to the nonuniformity coefficient k_v . In a bare reactor the fuel burn-up is very uneven: close to the surface the quantity $\Sigma_f \varphi$ is small compared to the $\Sigma_f \varphi_0$ at the centre. In a reflected reactor the nonuniformity coefficient k_v is smaller and the nuclear fuel is used more efficiently.

CHAPTER 13

REACTOR OPERATION

13.1 Reactivity and Reactor Period

The power level of a reactor is proportional to the number of nuclear fissions in the core per unit time. A reactor is said to be operating in the *steady* (or *stationary*) *state* if the number of nuclear fission per second is constant in the core. If the fission rate varies with time the *reactor operation is nonstationary*.

Let us find the power variation law assuming that the reactivity ρ is suddenly changed from zero to $\rho \ll 1$ at time t_0 . This time of sudden change may be regarded as zero time.

The average neutron density in the reactor n_0 will, during the lifetime of one generation of neutrons, τ , increase up to $n_1 = k_{\text{eff}} n_0$, during 2τ it will increase up to $n_2 = k_{\text{eff}}^2 n_0$, and during $m\tau$ to $n_m = k_{\text{eff}}^m n_0$ etc. The m th generation corresponds to time $t = m\tau$, and since the power level of the reactor $P(t)$ is proportional to neutron density $n(t)$, we get

$$P(t) = P_0 k_{\text{eff}}^{t/\tau}$$

Taking the logarithm of the equation we get

$$\ln \frac{P(t)}{P_0} = \frac{t}{\tau} \ln k_{\text{eff}}$$

Taking into account that $\rho \ll 1$ and that $k_{\text{eff}} \approx 1 + \rho$ (see Sec. 11.1) we can rewrite $\ln k_{\text{eff}}$ as

$$\ln k_{\text{eff}} = \ln (1 + \rho) \approx \rho$$

We thus obtain the law governing the variation of the power level

$$P(t) = P_0 \exp \left(\frac{\rho}{\tau} t \right) \quad (13.1)$$

where P_0 is the power level of the reactor at time $t = 0$.

After a time $T = \tau_p$ the reactor power increases e times. The quantity T is termed the **reactor period**. In practice one often uses the power doubling time T_d , which is the time it takes for the reactor power to double. The relation between T_d and T is $T_d = 0.693T$.

The lifetime of prompt neutrons τ_p in a thermal reactor is the sum of the slowing-down time for fast neutrons τ_s and thermal neutron diffusion time τ_d :

$$\tau_p = \tau_s + \tau_d$$

Taking into consideration that in a thermal reactor $\tau_s \approx \approx 10^{-4}$ s and $\tau_d \approx 10^{-3}$ s we may put $\tau_p \approx \tau_d$. When computing τ_d all thermal neutrons are considered to be moving at a mean speed v and to travel an absorption free path λ_a in the reactor:

$$\tau_d = \lambda_a/v$$

Let us assume that after fission only prompt neutrons with a lifetime $\tau_p = 5 \times 10^{-4}$ s are emitted and the reactivity $\rho = 0.0025$. Since the lifetime of a neutron generation $\tau = \tau_p$, the reactor period is $T = 5 \times 10^{-4}/2.5 \times 10^{-3} = 0.2$ s. In one second the reactor power increases $P(1)/P = e^b \approx 150$ times. It is practically unfeasible to automatically regulate a reactor in which the power varies at such a high rate. The reactor will be demolished before the safety control system can be brought into operation.

However, after fission not all neutrons are emitted promptly. The number of prompt neutrons per fission is $(1 - \beta)v_f$ and the number of delayed neutrons is βv_f . For the ^{235}U nuclide $v_f = 2.41$ and the fraction of delayed neutrons $\beta = 0.0064$. The mean time lag $\bar{\tau}$ is equal to the average lifetime of the fission fragments (the source of the delayed neutrons) which is 12.4 s.

The lifetime of delayed neutrons after decay of the fission fragments differs little from τ_p . Therefore the time it takes for the delayed neutrons to be absorbed in the reactor is

$$\bar{\tau}_d = \bar{\tau} + \tau_p$$

The lifetime of a generation of neutrons, τ , equals the arithmetic mean of the lifetimes of $(1 - \beta)v_f$ prompt and

βv_f delayed neutrons:

$$\bar{\tau} = [(1 - \beta) v_f \tau_p + \beta v_f \tau_p] / v_f \approx \tau_p + \beta \bar{\tau}$$

Substituting $\tau_p = 5 \times 10^{-4}$ s, $\beta \bar{\tau} = 0.0064 \times 12.4 = 0.08$ s, we obtain $\tau \approx 0.080$ s.

For $\rho = 0.0025$ the reactor period is 32 s and not 0.2 s, and the power level increases only by 3.1% in a second. At such power build-up rates it is easy to operate the reactor automatically.

Let us find in what reactivity range delayed neutrons affect the course of the chain reaction in a supercritical reactor. The energy of delayed neutrons ($E_d \approx 0.5$ MeV) is about one-fourth of the mean energy of prompt neutrons ($E_p = 2$ MeV). In the slowing-down to 0.5 MeV part of the prompt neutrons is absorbed or escapes from the reactor. Hence prompt neutrons are less valuable for the chain reaction than the delayed neutrons. The efficiency of βv_f delayed neutrons is equal to that of $\beta_{\text{eff}} v_f$ prompt neutrons. For the sake of convenience it is assumed that in each nuclear fission $\beta_{\text{eff}} v_f$ delayed neutrons with an energy of the prompt neutrons are emitted. The quantity β_{eff} is called the *effective delayed neutron fraction*. It is approximately 1.1-1.2 times greater than β .

After N neutrons of the first generation have been absorbed in the core, $k_{\text{eff}} (1 - \beta_{\text{eff}}) N$ prompt neutrons and $\beta_{\text{eff}} k_{\text{eff}} N$ delayed neutrons of the second generation are produced. By definition

$$k_{\text{eff}} = k_{\text{eff}} (1 - \beta_{\text{eff}}) + k_{\text{eff}} \beta_{\text{eff}}$$

The first term is the prompt neutron multiplication factor k_p and the second term is the delayed neutron multiplication factor k_d :

$$k_p = k_{\text{eff}} (1 - \beta_{\text{eff}}), \quad k_d = k_{\text{eff}} \beta_{\text{eff}} \quad (13.2)$$

If $k_p < 1$, the course of the chain reaction will be dependent on both prompt and delayed neutrons. In this case without the fission caused by delayed neutrons the chain reaction would cease. But if $k_p > 1$, the chain reaction can be sustained solely by prompt neutrons. In this case the lifetime of a generation is defined by the prompt neutron lifetime; the reactor power level grows at an extremely high rate with

a period $T = \tau_p(\rho - \beta_{\text{eff}})$ and the reactor becomes uncontrollable. A reactor with a factor $k_p = 1$ is termed a *prompt critical reactor*. The effective multiplication factor and reactivity of a prompt critical reactor can be computed from the first of equations (13.2) where $k_p = 1$ and $\beta_{\text{eff}} \ll 1$:

$$k_{\text{eff}} = 1/(1 - \beta_{\text{eff}}) \approx 1 + \beta_{\text{eff}}, \quad \rho \approx \beta_{\text{eff}}$$

The quantity β_{eff} is important when dealing with nuclear safety. In a supercritical reactor with a reactivity $0 < \rho < \beta_{\text{eff}}$ the chain reaction develops relatively slowly. A safe start-up to a predefined power level is usually carried out when the reactivity $\rho \ll \beta_{\text{eff}}$. Nuclear danger appears in a supercritical reactor with a reactivity $\rho > \beta_{\text{eff}}$.

Since the quantity β_{eff} is of such great importance it is taken as the *unit of reactivity*. In the literature it is called a *dollar* (doll).

Let $\rho = (k_{\text{eff}} - 1)/k_{\text{eff}}$ be the reactivity in absolute units; then

$$\rho (\text{doll}) = \rho / \beta_{\text{eff}}$$

Other reactivity units are as follows.

1. A *cent* is a hundredth part of reactivity. The reactivity on a percentage basis is

$$\rho (\%) = \rho \times 100$$

2. A *mil* is a thousandth part of reactivity ρ

$$\rho (\text{mil}) = \rho \times 1000$$

The relation between the reactivity in dollars, cents and mils is:

$$\rho (\text{doll}) = \rho (\%) / 100 \beta_{\text{eff}} = \rho (\text{mil}) / 1000 \beta_{\text{eff}}$$

Example. Express the reactivity $\rho = 0.0025$ in dollars, cents and mils if $\beta_{\text{eff}} = 0.007$.

The reactivity in dollars is

$$\rho = 0.0025 / 0.007 = 0.36 \text{ doll}$$

The reactivity in cents is

$$\rho = 0.0025 \times 100 = 0.25 \%$$

The reactivity in mils is

$$\rho = 0.0025 \times 1000 = 2.5 \text{ mils}$$

The power change in a supercritical reactor during a short time after an abrupt change in reactivity has occurred possesses a peculiarity which is not evident from equation (13.1). To clarify this point let us consider neutron multiplication in a subcritical reactor with a neutron source emitting Q neut./s located in the core. For the sake of simplicity we assume that the source emits simultaneously $Q\tau$ neutrons at time periods which are multiples of the lifetime of a neutron generation, τ .

Thus after a time τ the first $Q\tau$ neutrons produce $k_{\text{eff}}Q\tau$ second generation neutrons. At this moment the source is assumed to emit a second portion of $Q\tau$ neutrons. Hence in the time interval $\tau < t < 2\tau$ there are $Q\tau + k_{\text{eff}}Q\tau$ neutrons moving in the reactor. These neutrons in turn produce $k_{\text{eff}}(Q\tau + k_{\text{eff}}Q\tau)$ neutrons in the core. To compute the total number of neutrons in the time interval $2\tau < t < 3\tau$, one must add the $Q\tau$ neutrons of the third portion emitted by the source at time $t = 2\tau$.

$$Q\tau + k_{\text{eff}}Q\tau + k_{\text{eff}}^2Q\tau$$

Continuing reasoning in this way we can find the number of neutrons, N_m , in the interval $m\tau < t < (m + 1)\tau$

$$N_m = Q\tau (1 + k_{\text{eff}} + k_{\text{eff}}^2 + \dots + k_{\text{eff}}^m)$$

The series in parentheses is a geometric series with the ratio $k_{\text{eff}} < 1$. When m is large, the sum of the series tends to $N_m = Q\tau/(1 - k_{\text{eff}})$ and the number of neutrons per unit time interval tends to

$$N = N_m/\tau = Q/(1 - k_{\text{eff}}) \quad (13.3)$$

The quantity $1/(1 - k_{\text{eff}})$ is termed the *subcritical multiplication factor*. It is equal to the ratio of the number of neutrons, N , emitted per unit time as a result of fission and by the source in a subcritical reactor to the intensity of the neutron source, Q . For $k_{\text{eff}} = 0.99$ the subcritical multiplication factor is 100. If we place in a reactor a neutron source with an intensity $Q = 10^9$ neut./s, the neutron flux in the reactor will increase up to 10^{11} neut./s.

One can visualize a reactor with $k_{\text{eff}} < 1 + \beta_{\text{eff}}$ as being a prompt subcritical reactor with an internal delayed neutron source. For two or three minutes after start-up of a critical reactor, the concentration of delayed neutron sources reaches a stationary value since the number of delayed neutrons emitted in a steady-state reactor must equal the number of fragment sources produced newly as a result of nuclear fission. If Q designates the mean delayed neutron source density, then from formula (13.3) the power level of a critical reactor is found to be

$$P_0 = AQ/(1 - k_p) \quad (13.4)$$

where k_p is the prompt neutron multiplication factor, A is a proportionality constant. Inserting k_p from (13.2) into (13.4) and assuming $k_{\text{eff}} \approx 1$, we get

$$P_0 = AQ/\beta_{\text{eff}}$$

The mean rate of delayed neutron production at any given moment t is proportional to the nuclear fission rate at the time $(t - 12.4)$ s. Therefore if the effective multiplication factor is increased suddenly from 1 to $1 + \rho$ ($\rho < \beta_{\text{eff}}$), the delayed neutron production rate in the reactor will initially remain unchanged. Only a change in the prompt multiplication factor k_p influences the course of the chain reaction. After a time interval much greater than the prompt neutron lifetime, a new power level in the reactor sets in. If we take into account that the lifetime of prompt neutrons is not more than 10^{-8} s, we find that it should take only 0.01-0.1 s for a new power level to be reached. This time is so short that we may say that the power rise from P_0 to some P_{01} is practically instantaneous.

Inserting $k_{\text{eff}} = 1 + \rho$ into the first equation in (13.2) and taking into account that $\rho\beta_{\text{eff}}$ is small in comparison with ρ and β_{eff} , we obtain $k_p = 1 - \beta_{\text{eff}} + \rho$. From formula (13.4) find

$$P_{01} = A \frac{Q}{\beta_{\text{eff}} - \rho} = \frac{\beta_{\text{eff}}}{\beta_{\text{eff}} - \rho} P_0$$

The reactor power level at a time close to $t = 0$ and for $\rho = 0.0025$ abruptly rises to $P_{01} \approx 1.6P_0$. Subsequently

the subcritical multiplication factor $1/(\beta_{\text{eff}} - \rho)$ remains unchanged and the mean delayed neutron source density (and with it the reactor power level) varies according to law (13.1).

13.2 Reactivity Temperature Coefficient

Reactivity is a function of temperature since the heating or cooling of a reactor is accompanied by a change in core volume and of the physical properties of its materials. When a reactor is heated the density of the materials in the core and reflector falls, their temperature as well as that of the neutrons rises, and the reactor volume increases. Each of these effects influences the reactivity.

The diffusion length L and the slowing-down length L_s are inversely proportional to the density of the substance. Hence, reactor heating involves an increase in both quantities and thus enhances neutron leakage from the reactor. This effect is particularly pronounced in liquids. For example, the density of pressurized water heated from 100 °C to 300 °C decreases 1.5 times. The temperature of the neutrons also affects the diffusion length. The absorption cross section of the reactor materials $\sigma_a \sim 1/v$. Since the mean thermal neutron velocity grows with reactor heating the diffusion length L also increases.

Thus an increase in the diffusion and slowing-down lengths increases neutron leakage from the reactor and decreases the reactivity. An increase in the volume of a heated reactor, on the contrary, decreases neutron leakage and increases the reactivity. However, that is only one of the peculiar effects of the reactor temperature on reactivity. The second is the change in the thermal utilization factor.

In a heterogeneous reactor thermal neutron flux density is not uniformly distributed in the cell. The less the thermal neutron diffusion length in the moderator and nuclear fuel, the greater is the nonuniformity of the flux density φ and the smaller is the factor θ . The increase of the diffusion lengths in the moderator and nuclear fuel, which occurs when the reactor temperature rises, partially levels out φ over the cell and the thermal utilization factor becomes larger.

Let us examine the third effect the reactor temperature

exerts on the reactivity. When a substance is heated the resonance peaks broaden and slowing-down neutrons in the resonance region are absorbed more intensively. This effect is called *Doppler broadening*. Hence, with increase of temperature of the nuclear fuel and structural materials which contain resonance absorbers (^{238}U , Zr etc.) the resonance escape probability and reactivity decrease.

The reactivity changes caused by reactor heating are called *temperature effects*. They are described by the reactivity temperature coefficient α_t which is the change in the reactivity evoked by uniform heating of the reactor and raising of its temperature by 1° :

$$\alpha_t = d\rho(t)/dt$$

In a narrow temperature range α_t may be considered to be constant. In such ranges the dependence of the reactivity ρ on temperature is given by the linear equation:

$$\rho(t) = \alpha_t(t - t_0)$$

where t_0 and t are the initial and current temperatures of the reactor in centigrade degrees ($^\circ\text{C}$).

A negative temperature coefficient α_t ensures safe and stable steady-state operation of the reactor, as can be seen from the reactivity-temperature relationship. Let t_0 be the temperature of the reactor during steady-state operation. Under normal working conditions $t = t_0$ and $\rho = 0$. If for some reason the power of the reactor increases, its temperature will rise to $t > t_0$. The reactivity becomes negative and the power level returns to the initial level. With a fall in the power level the reactor cools to a temperature $t < t_0$ resulting in a positive reactivity and the initial power level is restored. Thus a reactor with a negative reactivity temperature coefficient is self-adjusting.

The behaviour of a reactor with a positive reactivity temperature coefficient is quite different. An accidental power rise results in positive reactivity and hence in a further increase in power, whereas a fall in the power level leads to reactor shutdown. Reactors with positive coefficients α_t are unstable. That explains why in designing a reactor one must aim at obtaining a negative coefficient α_t in the operating temperature range.

The negative temperature coefficient α_t is particularly large for water-water power reactors. Depending on the composition of the reactor, it varies between -2×10^{-4} and $-4 \times 10^{-4} \text{ K}^{-1}$. These values of α_t are mainly due to the decrease of the water density caused by reactor heating. Graphite-water and graphite-gas reactors with coefficients $\alpha_t \approx -10^{-4} \text{ K}^{-1}$ and also homogeneous and heterogeneous reactors with organic coolants and organic moderators are steady in operation.

A rise in the power level of the reactor evokes primarily a rise in the temperature of the nuclear fuel since about 90% of the fission energy is liberated in the fuel. Hence Doppler broadening occurs as soon as there is a change in the power level. It is also called the *power effect*. The *power reactivity factor* α_p is defined as the increase in reactivity per unit reactor power level increase:

$$\alpha_p = d\phi/dP$$

Stable reactor operation is ensured by a negative power reactivity factor. For example, in the WWPR-440 reactor $\alpha_p = 1.25 \times 10^{-5} \text{ 1/MW}$.

13.3 Changes in Nuclear Fuel Composition

The physical characteristics of the core depend not only on temperature. In an operating reactor the core composition changes: part of the nuclear fuel is burned up, fission products appear and plutonium is produced.

Nuclear fuel burn-up. In an operating period a certain mass ΔM of fissionable material is spent in nuclear reactions and radiative capture. The nuclear fuel burn-up is defined as

$$z = \Delta M/M$$

where M is the uranium (plutonium) load in the core. Fuel burn-up influences the duration of the reactor operating period, i.e. the uninterrupted time the fuel elements can perform in the core. A high fuel burn-up is economically profitable. It reduces the annual consumption of fuel elements in an APS and also the production expenses and expenses of fuel chemical processing. For example, a rise in burn-up from 1% to 4% increases the operating period and reduces the annual

consumption of fuel elements by a factor of 4. Fuel burn up is limited by the changes in the properties of the fuel. In present power reactors, fuel burn-up does not exceed 5%.

In a 1 MW thermal reactor 1.25 g of ^{235}U is consumed a day, i.e. the burning-up of 1.25 g of ^{235}U produces 1 MW·day of energy. In fast reactors radiative capture by ^{235}U is very small and the ^{235}U decrease is practically due to fission. Therefore in a fast reactor a 1 MW energy release per day corresponds to the burn-up of about 1.1 g of ^{235}U . From this it follows that the ^{235}U mass decrease in tons per operating period is

$$\Delta M = aP\tau$$

where P is the reactor power level in MW; τ is the operating period in days and $a = 1.25 \times 10^{-6} \text{ t/MW}\cdot\text{days}$ for thermal reactors and $1.1 \times 10^{-6} \text{ t/MW}\cdot\text{days}$ for a fast reactor.

Substituting ΔM in the burn-up equation we obtain

$$z = aP_{sp}\tau$$

where $P_{sp} = P/M$ is the specific power in MW/t.

Burn-up (z) can also be measured in MW·day/t. This unit is the amount of energy released by a ton of uranium (plutonium) a day at a specific power level of 1 MW/t. If the specific power is P_{sp} MW/t and the reactor operating period is τ days, the burn-up is

$$z = P_{sp}\tau \text{ MW}\cdot\text{day/t}$$

Reactor poisoning and slagging. Fission products absorb neutrons. In an operating reactor fission products accumulate in the core and this adversely affects the reactivity. All fission products can be divided into two groups. Nuclei with large absorption cross section comprise the first group and all other absorbing nuclei, the second group. Neutron absorption by nuclei of the first group is termed *poisoning of the reactor*, and neutron absorption by the nuclei of the second group is called *slagging of the reactor*.

The strongest absorber of neutrons is the fission product ^{135}Xe for which the absorption cross section is 3.5×10^6 barns at an energy of 0.025 eV. About 5% of the ^{135}Xe nuclei are produced immediately after fission and 95% in the

decay chain



The half-life of ^{135}Te is approximately 2 minutes and hence the ^{135}Te nuclei rapidly decay into ^{135}I nuclei. The half-lives of ^{135}I and ^{135}Xe are 6.7 and 9.2 hours respectively, i.e. the lifetime of ^{135}Xe is about 1.4 times longer than that of ^{135}I .

The rate of ^{135}I nuclei formation in 1 cm^3 of nuclear fuel is $\gamma_I \Sigma_f \varphi$, where $\gamma_I = 0.06$ is the ^{135}I yield; φ is the mean thermal neutron flux density in the nuclear fuel. The amount of ^{135}I decreases as a result of radioactive decay and radioactive capture of neutrons. The ^{135}I decrease rate is

$$\lambda_I N_I + N_I \sigma_a^I \varphi$$

where $\lambda_I = 2.9 \times 10^{-5} \text{ s}^{-1}$ is the ^{135}I radioactive decay constant; N_I is the concentration of ^{135}I nuclei in the nuclear fuel, nucl./ m^3 .

Since the cross section $\sigma_a^I = 7$ barns, and the mean thermal neutron flux density φ does not exceed 10^{20} neut./ $\text{m}^2 \cdot \text{s}$, the ^{135}I decay rate is much greater than the ^{135}I decrease due to neutron absorption. Thus the second term of the sum can be disregarded compared with the first term. After a certain time of reactor operation in the steady-state the rate of ^{135}I formation and disappearance in the core will be equal. From this condition one can find the ^{135}I equilibrium concentration in the nuclear fuel:

$$N_{0I} = \gamma_I \Sigma_f \varphi / \lambda_I$$

It is proportional to the mean thermal flux density φ . The higher the reactor specific power, the greater is the ^{135}I equilibrium concentration.

The equilibrium concentration for ^{135}Xe can be found in a similar way. The ^{135}Xe formation rate $\lambda_I N_{0I} + \gamma_{Xe} \Sigma_f \varphi$ is equal to the decrease rate $\lambda_{Xe} N_{0Xe} + \sigma_a^{Xe} N_{0Xe} \varphi$. Hence the ^{135}Xe equilibrium concentration in the nuclear fuel is

$$N_{0Xe} = (\gamma_I + \gamma_{Xe}) \Sigma_f \varphi / (\lambda_{Xe} + \sigma_a^{Xe} \varphi)$$

where $\lambda_{Xe} = 2.1 \times 10^{-5} \text{ s}^{-1}$ is the ^{135}Xe decay constant and $\gamma_{Xe} = 0.003$ is the ^{135}Xe yield.

For a flux density $\varphi > 10^{18}$ neut./m²·s, $\sigma_a^{Xe} \varphi > 3.5 \times 10^{-22} \times 10^{18} = 3.5 \times 10^{-4}$ s⁻¹, and the first term in the denominator for such thermal flux densities can be disregarded:

$$N_{0Xe} = (\gamma_{Xe} + \gamma_I) \Sigma_f / \sigma_a^{Xe}$$

The decrease of ¹³⁵Xe for a mean thermal flux density $\varphi > 10^{18}$ neut./m²·s is primarily due to radiative capture of neutrons by ¹³⁵Xe. If φ is greater than 10^{18} neut./m²·s reactor poisoning reaches its peak value and does not depend on the mean thermal neutron flux density.

Because of poisoning the reactor becomes unstable in operation, especially for the flux density $\varphi \geq 10^{18}$ neut./m²·s. Suppose that for some reason the reactor power (neutron flux density) accidentally increased. Neutron absorption by ¹³⁵Xe and the number of nuclear fissions will then increase. The neutron absorption leads to a drop in the ¹³⁵Xe concentration, and the fissions, to a growth of the ¹³⁵I concentration. The power increase is immediately followed by reactivity release due to additional ¹³⁵Xe burn-up. Thus an accidental rise in the power level releases reactivity and this in turn raises further the power. After a period of time when the safety control system has compensated the reactivity it begins to fall. ¹³⁵Xe is produced from the additional ¹³⁵I which was formed when the power increased and the reactivity became negative. A drop in power leads to a decrease in ¹³⁵Xe burn-up and this in turn diminishes the reactivity still greater. An accidental fall in the reactor power level first causes the reactivity to decrease and after some time compensation by the regulation system causes it to increase.

Usually the reactivity temperature coefficient $\alpha_t < 0$. For such values of α_t the instability of the reactor caused by poisoning is partially (or completely) brought under control by the reactor itself. But if $\alpha_t > 0$, steady-state operation can be maintained only by manipulating the control system.

The ¹³⁵Xe absorption cross section falls sharply at neutron energies exceeding 1 eV. Therefore ¹³⁵Xe accumulation in the core practically does not influence the reactivity in intermediate and fast reactors.

Slagging nuclei (slags) have a comparatively low absorption cross sections. The latter vary, depending on the slag, from 1 to 400 barns. As a result the reduction in the amount of slag in the core is slower than its formation due to nuclear fission and consequently the slag concentration in the nuclear fuel steadily increases reaching a maximum by the end of the operating period. Slags intensively absorb thermal and resonance neutrons. Therefore slag accumulation in nuclear fuels reduces the reactivity in thermal and intermediate reactors.

“Iodine well”. When a reactor is shut down the neutron flux density in the core falls to zero. The variation of the ^{135}Xe concentration in the core of a shutdown reactor is due to ^{135}I and ^{135}Xe β^- -decay. In a cubic metre of nuclear fuel $\lambda_I N_I$ ^{135}Xe nuclei are produced and $\lambda_{\text{Xe}} N_{\text{Xe}}$ nuclei decay per second. If the ^{135}I activity is higher than the ^{135}Xe activity ($\lambda_I N_I > \lambda_{\text{Xe}} N_{\text{Xe}}$), the ^{135}Xe concentration in the core will grow and vice versa.

The ^{135}I equilibrium concentration, $N_{0\text{I}}$, in an operating reactor is proportional to φ , whereas the ^{135}Xe equilibrium concentration, $N_{0\text{Xe}}$, is only slightly dependent on it, provided $\varphi > 10^{17}$ neut./ $\text{m}^2 \cdot \text{s}$. As a result, for flux densities $\varphi > 10^{17}$ neut./ $\text{m}^2 \cdot \text{s}$, $N_{0\text{I}}$ exceeds $N_{0\text{Xe}}$. Since $\lambda_I > \lambda_{\text{Xe}}$ over some period of time after shutdown, the inequality $\lambda_I N_I > \lambda_{\text{Xe}} N_{\text{Xe}}$ will hold. Therefore the ^{135}Xe concentration in a shutdown reactor at first grows until the ^{135}I and ^{135}Xe activities become equal. Subsequently ^{135}I decay cannot compensate the decrease of ^{135}Xe and the concentration of the latter begins to diminish. The time variation of xenon concentration, $N_{\text{Xe}}(t)$, and reactivity, ρ , after shutdown of a reactor, in which the flux density φ during operation was 10^{18} neut./ $\text{m}^2 \cdot \text{s}$ is shown in Fig. 13.1. The poisoning peak is reached 11 hours after the reactor is shut down and increases with the neutron flux density. The reactivity after shutdown of the reactor initially decreases, reaching a minimum when the ^{135}Xe concentration is maximum and then begins to grow. The curve depicting the variation of reactivity resembles a well, and the poisoning increase of the shutdown reactor is due to the build-up of ^{135}I in the operating reactor. The effect of poisoning on the reactivity of a shutdown reactor is therefore termed the iodine

well effect. No iodine well is observed in reactors with a flux density $\phi < 10^{17}$ neut./m²·s.

In the designing of a reactor the iodine well effect must be taken into account. In order to obtain a high specific power level, additional nuclear fuel is required to compensate for the iodine well effect. Otherwise to start up a reactor and to bring it up to the rated power level it would be necessary

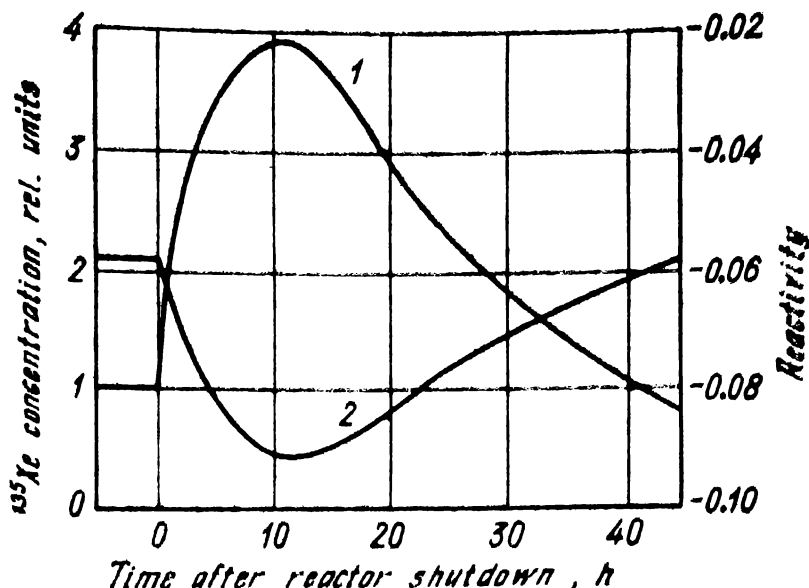


Fig. 13.1 Dependence of ^{135}Xe concentration (1) and reactivity (2) on time after shutdown of reactor. (Thermal neutron flux density before shutdown $\phi = 10^{18}$ neut./m²·s)

to wait several dozens of hours until all of the ^{135}Xe had almost completely decayed. It would be particularly difficult to start up a reactor shutdown near the end of the operating period.

Nuclear fuel breeding. In an operating reactor a fraction of the ^{238}U is transformed into plutonium. The fraction of neutrons absorbed in ^{238}U in a thermal reactor depends on the enrichment of the uranium and on the lattice spacing. The lower the uranium enrichment the more ^{239}U there will have to be in the core and the greater is the number of uranium atoms transformed into plutonium atoms. The lattice spacing affects neutron resonance absorption in ^{238}U . Fewer neutrons escape resonance capture in a lattice with closely arranged fuel elements. The value of the conversion factor increases if nuclear fuel is produced from natural uranium

or slightly enriched uranium and the fuel elements are in a close-packed lattice in the core.

Let us investigate how plutonium build-up in the core affects reactivity. The ratio of the ^{239}Pu and ^{235}U absorption cross sections of ≈ 1.5 and a ^{239}Pu nucleus replacing a ^{235}U nucleus in the nuclear fuel increases the thermal utilization factor α . The presence of plutonium raises the reactor reactivity, and the greater the value of the conversion factor the higher is the reactivity. For $\text{CF} > 0.8$ plutonium does not only compensate ^{235}U burn-up but also replenishes the reactivity excess. This can significantly prolong the operating period.

It is difficult to achieve nuclear fuel breeding in a thermal reactor since not more than two fission neutrons are emitted for each neutron captured in the core. In a fast reactor 2.5-3 neutrons are emitted per neutron captured. One neutron is used to maintain the chain reaction and the other 1.5-2 neutrons can be used for breeding plutonium. The CF of a fast reactor depends on neutron radiative capture in the nuclear fuel, on the structural materials and on neutron leakage. At present breeders are being designed in which unproductive neutron consumption will be reduced to a minimum. The conversion factor will be as high as 1.8, i.e. at the end of the operating period 1.8 kg of plutonium will be accumulated per kilogram of burned-up fissionable material (^{235}U , ^{239}Pu).

It should be noted that a mixture of ^{239}Pu and ^{240}Pu isotopes is obtained in the reactor and not pure ^{239}Pu . The fission threshold in ^{240}Pu is approximately 10 keV. If plutonium is in the reactor for a long period of time its fission properties deteriorate as a result of a fraction of ^{239}Pu being transformed into ^{240}Pu .

13.4 Control Devices of the Safety Control System

At the beginning of the operating period the reactor has an excess reactivity which is spent in the operating reactor on burn-up, poisoning, slagging and on eliciting the iodine well and temperature effects. The reactivity excess is compensated by the various devices of the safety control system (SCS).

The power level of thermal reactors is regulated by absorption rods, mobile fuel assemblies, burn-up absorbers etc. The effect of a specific control device on the reactivity is characterized by the *control device efficiency* Δk . This is the absolute value of the reactivity change caused by inserting the device (absorption rods, burn-up absorbers) into the core or by withdrawing the device (mobile fuel assemblies) from the core.

In graphite-water and graphite-graphite reactors, absorption rods are used in the SCS. These are divided into automatic control rods, shim rods and safety rods (see Sec. 11.1).

The automatic control rods are raised or lowered continuously during operation of a reactor. Faulty operation of the rod drive system may cause a control rod being accidentally withdrawn from the core. To exclude the possibility of the reactivity exceeding β_{eff} , the automatic control rod efficiency is kept below $0.7\beta_{\text{eff}}$, (0.5%). The rate of reactivity release by a moving automatic control rod lies in the range of 0.001-0.1%/s.

The total efficiency of a shim rod should be such that when fully inserted into the core the absolute value of the negative reactivity should be less than 1%. According to the "Nuclear Safety Regulations" after all the automatic control rods, shim rods and safety rods are dropped, the negative reactivity must be less than 5%.

Two mobile double-level emergency control cassettes are used in the SCS of the WWPR-440. The lower part contains fuel elements and the upper elements made from a boron alloy. The designs of all emergency control cassettes are similar and each cassette performs all three functions of the SCS control devices, viz. automatic control, reactivity compensation and emergency safety.

When a cassette is raised from the core the neutron absorbers are withdrawn and fuel elements take their place. In the event of an emergency the cassettes are dropped so that their upper parts are located in the core.

Another type of control device is the burn-up absorption rod which is kept in a fixed position in the core. It contains the nuclei of an absorber with a high absorption cross section. On capturing a neutron the nuclei of the burn-up absorber change into nuclei of elements with low absorption

cross sections. Boron is the most widely used burn-up absorber. For example, the concentration of boron in the burn-up absorbing rod in the WWPR-1000 is 1%.

A fraction of the reactivity excess in the WWPR-440 and WWPR-1000 is compensated by a system of boron control. Boron acid is dissolved in the coolant at a concentration of about 1% at the beginning of the operating period. During the operating period the boron in the absorption rod and water is gradually consumed. The reactivity release is spent in compensating the slow reactivity changes (nuclear fuel burn-up, poisoning etc.). The prime purpose of the burn-up absorbing rod and boron control system is to reduce the nonuniformity of heat release.

The efficiency of a control device depends on the composition and size of the device and the reactor, and on the depth of immersion of the device in the core. Let us assume that an absorption rod with a radius r_0 is inserted in the central channel of a bare cylindrical reactor with a radius R (Fig. 13.2). The rod disturbs (deforms) the neutron flux density. To describe the change in the neutron flux density that occurs when the composition or size of a reactor is changed, the term "neutron flux density perturbation" is usually used. Let us assume that the rod is "black" for thermal neutrons, i.e. it absorbs all thermal neutrons that strike its surface. The thermal neutron flux density is perturbed by lowering the rod into the core. The flux density φ (continuous curve in Fig. 13.2) falls near the surface of the rod. A steady power level (which is proportional to the mean neutron flux density) is sustained by slowly withdrawing the rod from the core. The mean flux density in the core remains constant when the rod is withdrawn as a result of automatic redistribution of the flux density in the core: the drop in the flux density near the rod is compensated by a small increase in the flux density at a large distance from the rod.

The efficiency of the control rod depends on the fraction of thermal neutrons striking its surface and on the change in neutron leakage subsequent to an increase in the neutron flux density near the surface of the core. The latter makes a noticeable contribution to the efficiency Δk in small-size reactors. In thermal reactors the efficiency Δk is determined mainly by thermal neutron absorption in the rod.

The volume from which thermal neutrons can reach the surface of the rod is proportional to $\pi L^2 H$ (L is the diffusion length and H is the height of the core). Most thermal neutrons at a distance from the rod exceeding the diffusion length L are absorbed in the core before they reach the rod. The number of thermal neutrons absorbed in the core is proportional

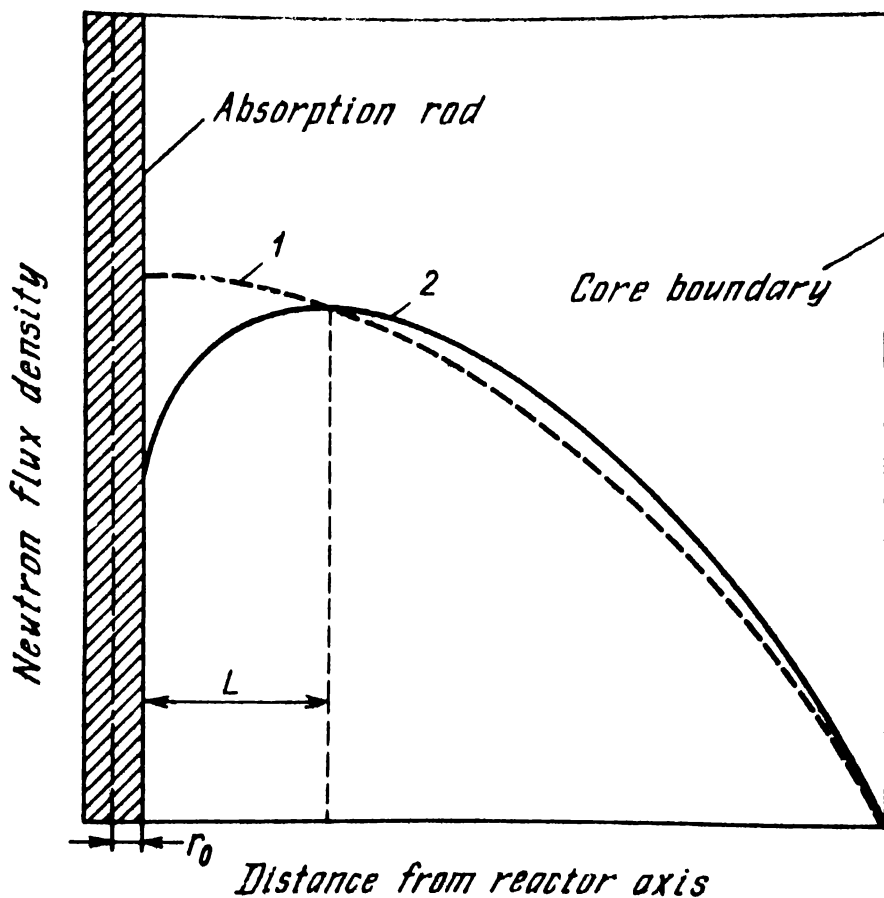


Fig. 13.2 Distribution of thermal neutron flux density in a core with a central absorption rod

1—rod withdrawn from core; 2—rod completely inserted into core

to the core volume $\pi R^2 H$, and the control rod efficiency Δk_0 is the ratio of the first volume to the second volume:

$$\Delta k_0 = b L^2 / R^2$$

The proportionality factor b depends on the nonuniformity of the neutron flux density along the radius and on the sizes of the rod and core. The rod efficiency is high in small thermal reactors. Absorption rods are least efficient in the WWPR since the diffusion length in a WWPR is about 1.5-2 cm.

The farther away the rod is from the axis of the core the less is its efficiency. The efficiency $\Delta k(r)$ of an eccentric rod is proportional to the square of the unperturbed neutron flux density. If the flux density at the centre is $\varphi_0 = 1$, then

$$\Delta k(r) = \Delta k_0 \varphi^2(r)$$

To compensate the reactivity excess in a power reactor some tens of shim rods are inserted into the core. Each shim rod influences the efficiency of the other shim rods. This interaction is termed *rod interference*. Let us assume that two rods are located at a distance a from each other and one of them is the central rod. If $a < L$ (see Fig. 13.2) the eccentric rod will be in a disturbed flux whose density is lower than that of the undisturbed flux and fewer neutrons are absorbed in it. In this case interference reduces the total efficiency of the two rods. If $a > L$ interference increases the total efficiency of the rods. As a rule the shim rods are evenly distributed in the core volume. The shim rod lattice spacing is chosen to be much greater than L . In this case the disturbed flux density for each shim rod is greater than the undisturbed flux density and the total efficiency of the shim rod system increases. Moreover, the shim rods are arranged in such a way that their effect on operation of the fuel elements is minimal. A defective shim rod arrangement may be the cause of underheating of some fuel elements and overheating of others.

The dependence of rod efficiency Δk on the depth of insertion in the core (Fig. 13.3) is called the *regulating characteristic*. At the top of a reactor the thermal neutron flux density is small and hence an initial immersion depth of about one fourth of the core height only slightly changes the reactivity. The rod is most efficient at depths between

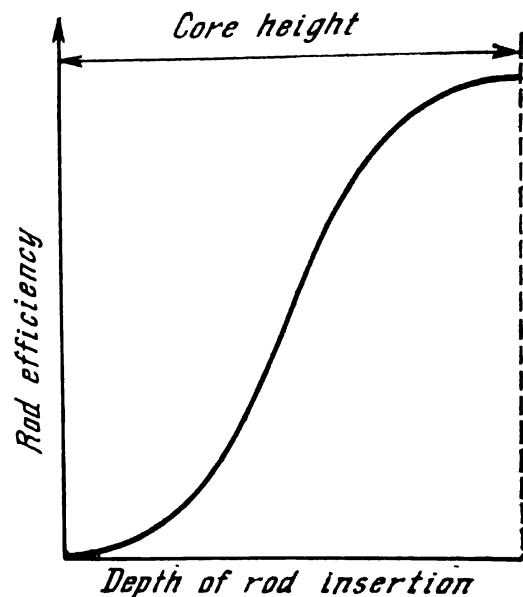


Fig. 13.3 Regulating characteristic of an absorption rod

$H/4$ and $3H/4$. Near the bottom of the core (as well as near the top) the change in reactivity is comparatively insignificant. This explains why rods are not inserted to full depth but about only down to $3H/4$. Rods are usually shifted in the middle region ($H/4$ - $3H/4$). In this range there is a linear relationship between the efficiency of the rod and depth of insertion. It is convenient to regulate the reactor power level in the linear range since the release of reactivity is proportional to the length of that part of the rod which is not in the core.

The rod efficiency is determined experimentally before start-up of the reactor and after the reactor is shut down. This procedure is called *rod calibration*. The measurements are carried out under steady-state conditions and at a low power level. The calibration rod inserted to a depth H is lifted from the core by a distance $\Delta H \ll H$ cm. The power begins to increase with a doubling time T_2 and the reactivity released by shifting the rod over ΔH can then be computed. After measurement of T_2 the reactor power is returned to the initial level by means of other rods. The calibration rod is then drawn out another ΔH cm, the reactor period is measured once again, the reactivity is computed etc. The function $\Delta k = f(z)$ is then plotted on the basis of the results thus obtained (see Fig. 13.3).

During the operating period the rods are moved according to a special program that provides for minimal distortion of the heat release field. This explains why the calibration of each rod is carried out with due regard for the working position of the other rods.

Another way to determine the regulating characteristics of a rod is to use an instrument called the reactimeter. The rod is inserted in a critical reactor. As the rod enters the core the reactimeter measures the reactivity of the sub-critical reactor.

The efficiency and regulating characteristics of emergency control cassettes are measured in much the same way. The difference is that a shift of a cassette releases reactivity as a result of the neutron absorbing rod in the core being replaced by the nuclear fuel. The path covered by an absorption rod in the core is about equal to the core height whereas that of the cassette is double the core height.

Heat is released in the control devices due to gamma-quantum absorption, whereas in materials containing boron the heat is due to α -particle absorption and absorption of ^7Li nuclei emitted in the $^{10}\text{B} (n, \alpha) ^7\text{Li}$ reaction. The amount of heat liberated in the control rods may reach a very high level. In that event they are cooled by a coolant which circulates in a separate self-contained loop. In reactors at the Beloyarsk APS the absorption rod moves in a metal pipe contained in another metal pipe of greater diameter. Water is pumped in the space between the inner and outer pipes. Heat from the absorption rods is transferred to the water as radiation. In WWPR, heat is transferred from the emergency control cassettes by the coolant in the first loop.

13.5 Reactor Start-Up and Shutdown

Physical start-up. *Physical start-up of a reactor* includes charging of the reactor (insertion of fuel assemblies into the core), approach to the critical level and the carrying out of experiments at the physical power level at which heating due to fission is not high. Let us examine the physical start-up of graphite-water reactors.

Prior to physical start-up the reactor is assembled without the fuel channels. The safety control system, radiation-monitoring instruments, ventilation system, sound emergency system and others are all tested. The safety control system includes equipment which is used to start a reactor and raise its power to the prescribed operating value.

The sensitivity of standard start-up equipment is comparatively low. The equipment begins to control the chain reaction at a certain power level termed the minimal controlled level (MCL), which is about $10^{-6} P_r$, where P_r is the rated reactor power. To regulate the chain reaction below the MCL, temporary start-up equipment is installed in the reactor which is capable of registering flux densities $\phi > 10^6-10^7 \text{ neut./m}^2 \cdot \text{s}$. The detectors of this temporary start-up equipment are mounted in several channels. Before admitting any active material into the fuel channel an artificial neutron source with an intensity of $Q \text{ neut./s}$ is placed at the centre of the core and the central channels are then loaded.

The neutrons emitted by the source can multiply in a sub-critical reactor. The neutron flux density $\varphi(r)$ at some point r is proportional to the ratio $Q/(1 - k_{\text{eff}})$. As the reactor approaches the critical point ($k_{\text{eff}} = 1$) neutron multiplication in the core and their flux density $\varphi(r)$ begin to increase

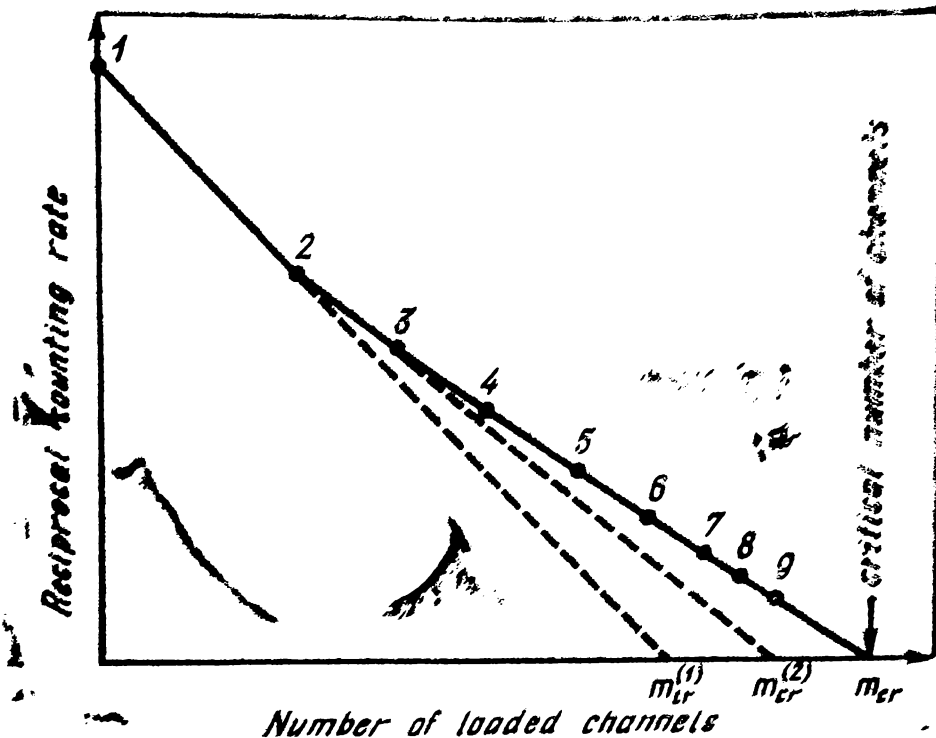


Fig. 13.4 Dependence of reciprocal counting rate on number of loaded fuel channels

at an infinite rate. The counting rate S of the detector mounted at point r in the core is proportional to the neutron flux density $\varphi(r)$. Hence, the closer k_{eff} is to unity, the greater is the counting rate S .

When determining the critical mass experimentally it is more convenient to use the reciprocal of the counting rate, $1/S$. This quantity is proportional to $1 - k_{\text{eff}}$ and on approach to the critical point it tends to zero.

Approach of the reactor to the critical point occurs as follows. Before the fuel channels are loaded (this is done outwards from the centre of the core to the edge) the counting rate is measured. The reciprocal of the counting rate is then calculated and the first point is plotted on the graph of $1/S$ as a function of number of loaded fuel channels (Fig. 13.4). Then m_1 fuel channels, which is not more than

30% of the computed critical amount, are loaded. The counting rate is observed and the second point of the reciprocal of the counting rate is plotted. It will be lower than the first point.

A straight line drawn through the two points intersects the abscissa axis at a point corresponding to $m_{cr}^{(1)}$ fuel channels. This value may be regarded as a first approximation for the critical number of fuel channels. The next load is chosen so as not to exceed $(m_{cr}^{(1)} - m_1)/4$. Again the counting rate is measured and the third point is plotted. The straight line drawn through points two and three intersects the abscissa axis at point $m_{cr}^{(2)}$. This is the second approximation to m_{cr} . Each following load is made smaller than $(m_{cr}^{(i)} - m_i)/4$, where $m_{cr}^{(i)}$ is the critical number of filled fuel channels in the i th approximation and m_i is the number of actually filled channels after the i th loading. When the subcritical multiplication constant reaches 25-30 ($k_{eff} = 0.96-0.97$) the fuel channels are loaded one by one. This renders it possible to determine the critical point rather accurately.

The determination of the critical mass is a very serious procedure. All possible measures are taken to ensure nuclear safety. The power level is controlled by a temporary, highly sensitive start-up device. The control rods of the SCS are withdrawn from the core in loading of the fuel channels. However, in the event of an emergency they are immediately dropped back into the core.

The reactivity excess needed to compensate burn-up, the temperature effects, poisoning and slagging is built up by loading m fuel channels in the core, m being tens of times greater than m_{cr} . For example, in the high power channel reactor-1000 (HPCR-1000) the ratio $m/m_{cr} \approx 70$. Prior to build-up of a reactivity excess the efficiency of the SCS control rods near the critical point is determined. Afterwards some of the shim rods are lowered into the core and more fuel channels are loaded until the reactor is brought up to the critical point in the presence of the neutron source. The efficiency of the rods is determined again and a second portion of shim rods is introduced into the core and more fuel channels are loaded etc.

After the reactor is fully loaded the efficiency of the SCS rods is checked; the distribution of heat release in the core

volume is measured and the effect on the reactivity of filling of the fuel and SCS channels with the coolant is determined. Finally the sequence in which the SCS rods will be moved in the operating reactor is determined.

The order in which a WWPR is assembled is different. The dry reactor without the coolant is first assembled; the neutron source is then lowered into the core and the level of the water in the core and reflector is gradually raised.

Power start-up. Gradual raising of the power level from the physical power level to a level which is sufficient to drive the turbines and carry out experiments is termed the *power start-up of an APS*.

Before power start-up the coolant is circulated through the loops and the equipment and regulation and control systems are checked. During the first stage of the start-up the power level is raised to the minimal controlled level, and the chain reaction is controlled by the temporary start-up equipment which is sensitive to low neutron flux densities at low temperatures. At power levels higher than the MCL the flux density and temperature are not low and therefore above the MCL the power level is controlled by standard start-up equipment; the temporary equipment is usually dismantled and the channels from which the detectors are removed can be used as fuel channels.

At a power level of (0.05-0.1) P_r the reactor and coolant loops are warmed up, the temperature effects measured and the accuracy of the instruments employed to measure the coolant flow rate and temperature is checked. After warming-up of the reactor and loops, the power level is gradually raised to the rated capacity. For example, the power level of unit II of the Leningrad APS was raised in several stages. The power level was initially brought up to 500 MW; ten days later it was increased to 750 MW, and finally raised to full power, 1000 MW.

The experimental results obtained during the physical and power start-up of the reactor are subsequently used to plan the operation routine of the reactor installed in an APS.

A reactor unit of an APS is shut down for reloading of the fuel channels, routine inspection or repairs and also in the event of an emergency. A shutdown reactor is started up by means of the standard start-up equipment.

The initial (zero) power level P_0 of a shutdown reactor is determined by spontaneous fission of the uranium nuclei and by fission due to photoneutrons. In power reactors P_0 is 10^{-7} - 10^{-6} W. If a neutron source is placed in the power reactor, P_0 rises to 10^{-3} - 10^{-2} W.

The power rise from the initial to rated level can be divided into 3 energy ranges: the start-up ($P_0 \leq P \leq 10^{-5}P_r$), minimal automatically controlled ($10^{-5}P_r \leq P \leq 10^{-2}P_r$) and operating range ($10^{-2}P_r \leq P \leq P_r$). The division into power ranges depends on the sensitivity of the start-up equipment.

In the start-up range only a high sensitivity detector, such as that used in the physical start-up of a reactor, is able to register the neutron flux density. Standard start-up equipment is used in an operating power reactor. It is less sensitive and begins to register the flux density only at the MCL near the end of the start-up power range. Raising the reactor to the MCL is not a simple matter since standard start-up equipment cannot control the flux density at power levels below the MCL. The broad range of uncontrollable changes in the power level makes it imperative to have a safe and reliable method for a build-up to the MCL. One of the most widespread ways is the step by step withdrawal of the automatic control rod inserted at a depth H into the core. The control rod is removed from the core in successive steps $\Delta H \ll H$. The steps are separated from each other by a time period τ_d . At one of the steps a subcritical reactor becomes supercritical. On the basis of the experimental results obtained in the physical start-up such values of ΔH and τ_d are chosen that the reactor is brought up to the MCL during a sufficiently safe period of time, say, $T \geq 30$ s.

For example, in the start-up of the first APS, paired control rods were withdrawn 4 times by 10 cm with a 1 minute delay. After the fifth rod shift the delay was increased to 3 minutes. Each shift involved a reactivity change of 4.5×10^{-4} . The neutron flux density growth rate was such that the whole start-up required from 8 to 10 minutes.

Start-up to the MCL is safer in a subcritical reactor with a neutron source since the critical point is reached in controlled conditions. For instance, a shutdown WWPR is brought up to the critical state by referring to the MCL. The detec-

tors of the highly sensitive start-up equipment are located in loops outside the WWPR body.

Reactor shutdown. There are two distinctive features in the power level change of a shutdown reactor that must be taken into consideration when running an atomic power reactor. It has already been mentioned that a reactor with a reactivity $\rho < \beta_{\text{eff}}$ can be treated as a prompt neutron subcritical reactor with a delayed neutron sources located in the core. After SCS control rods with an efficiency Δk are lowered, k_p drops from $1 - \beta_{\text{eff}}$ to $1 - (\beta_{\text{eff}} + \Delta k)$. The power level of the reactor falls from P_0 to some P_{01} in a very short time. According to formula (13.4) the power change is

$$P_{01} = P_0 \beta_{\text{eff}} / (\beta_{\text{eff}} + \Delta k)$$

After the rapid power change has occurred delayed neutrons begin to influence the power level. They are emitted by fission fragments formed in the core prior to the SCS control rod drop. As a result the power level slowly decreases in accordance with the law

$$P(t) = P_{01} e^{-t/T}$$

The period T of a shutdown reactor depends on the lifetime of the delayed neutron emitters. Short-lived fission fragments decay first and then the long-lived ones. Therefore T increases and after some time it is determined by the emitters with the longest lifetime which is about 80 s.

Delayed neutrons prevent an instantaneous stoppage of the chain reaction in a shutdown reactor. It is necessary to produce a negative reactivity as large as possible in order to evoke a fast change in the fission rate. In this case the fission rate in the core may drop practically to zero in the course of a few minutes.

Another characteristic of a shutdown reactor is the protracted decay of fission products in the core. Due to the decrease of concentration of the fission products the intensity of the radiation emitted by them also diminishes. The heat generated as a result of adsorption of fission product radiation in a shutdown reactor is called the *residual heat*. After a long run of the reactor the amount of residual heat released can be evaluated from the empirical formula

$$P_{\text{res}}(t) = 0.065 P_0 t^{-0.2}$$

where t is the time lapse after the SCS control rods drop, \propto P_0 is the power level of the reactor, kW. The formula is valid for time periods $t > 10$ s.

The level of the residual heat is proportional to the reactor power level P_0 and may remain high for a long time. For instance, two hours after shutdown $P_{res} \approx 0.01P_0$. Therefore the coolant is pumped through the reactor for a day or two to eliminate the possibility of fuel channel damage or destruction of other units of the reactor.

The residual heat in a nuclear power unit is usually removed by a special shutdown cooling system connected to the first loop. It is brought into operation after the SCS control rods have been dropped into the core.

13.6 Heat Generation and Heat Exchange in Reactors

Heat generation in a reactor. Fission energy is converted into thermal energy in various ways. About 90% of the heat is generated in the nuclear fuel (slowing-down of fission fragments and β -particles, absorption of gamma-quanta). The intensity of heat release in nuclear fuel is proportional to the fission rate per unit volume which for a thermal neutron reactor is $\Sigma_f \varphi$ (Σ_f is the macroscopic fission cross section of the nuclear fuel and φ is the thermal neutron flux density in the nuclear fuel). If the nuclear fuel concentration in the core is constant the intensity of heat evolution will be proportional to the flux density φ . The remaining 10% of the fission energy is liberated in other core components (moderator, coolant, structural materials) and in the reactor and radiation shielding as a result of γ -quantum absorption or slowing-down of fast neutrons.

The heat flux density as well as the neutron flux density is not uniform throughout the core. The peak value of the heat flux density is at the centre of the core, and the minimal value is near the border between the core and the reflector.

The heat flux density nonuniformity coefficient and neutron flux density nonuniformity coefficient are similar. At high k_R values the channel is unevenly heated. Thus a few central channels are heated to much higher temperatures than the others. In power reactors it is profitable to have the heat load the same in all channels. To achieve this the heat

release must be uniform along the radius. The reflector reduces to some extent uneven heating in the core. However, in large reactors the power level of the peripheral channels is about half that of the central channels.

To level out heat generation along the radius of the core the specific fission rate is increased near the boundary between the core and the reflector. This is done by increasing the ^{235}U concentration in the peripheral fuel channels. This equalizing of heat generation is termed *nuclear profiling*.

Uniform heat release along the radius is attained by dividing the core into several concentric zones. The amount of ^{235}U in the fuel channels is greater in those zones which are farther from the axis of the core.

Achievement of complete uniformity of heat release involves additional expenditure as it is necessary to fabricate nonstandard fuel assemblies. Moreover, the reactor design is more intricate, the nuclear fuel load is greater etc. This explains why at present the intensity of heat generation is not completely equalized throughout the core. The heat flux density nonuniformity coefficient k_R can usually be reduced only to 1.2-1.3. However, even this is enough to appreciably increase the mean nuclear fuel burn-up.

There are dozens of absorption rods in power reactors. The nonuniformity of heat release along the radius becomes less if the absorption rods are placed so that the lattice spacing decreases towards the centre.

In a reactor in which the heat production has not been levelled out, nuclear fuel burn-up at the end of the operating period is highest in the central fuel channel and lowest in the peripheral ones. If some of the central channels are removed towards the end of the operating period and replaced by the peripheral channels and if the latter are charged with fresh fuel elements, the reactivity excess and fission rate in the outer channels will increase. It is difficult to attain a value of k_R close to unity by this method of partial recharging. Nevertheless it greatly increases the burn-up of the nuclear fuel. The WWPR-440, HPRC-1000 and Beloyarsk APS reactors operate in this partial recharging regime.

The efficiency of a power installation depends on the mean temperature of the coolant at the reactor outlet which even in a partially heat-uniform reactor is lower than the

maximum temperature at the outlet of the central fuel channels. *Hydraulic profiling* can be employed to increase the efficiency of a reactor. A regulating head is mounted at the inlet of each fuel channel. The volume of the coolant passing through it is proportional to the power in the fuel channel. For such flow rates the exit temperature of the coolant will be the same for all fuel channels. By this method the mean exit coolant temperature can be made to approach the maximum temperature. Both nuclear and hydraulic profiling are employed in modern APS reactors.

Coolant flow rate. The coolant volume flow rate in a reactor with a power P is

$$V = P/c\Delta t$$

where c is the heat capacity per unit volume of the coolant and Δt is the difference between the outlet and inlet temperatures.

The volume flow rate V is inversely proportional to c . Heat is most readily removed by water, sodium etc. An increase in the volume flow rate involves an increase in the power spent in pumping, which is proportional to the square of the coolant flow velocity. Therefore in some cases to reduce the flow velocity the coolant is heated to a greater degree in the reactor. For example, when heat is removed by a gas Δt may be as high as 200-350 °C and for sodium it is 150-200 °C.

Heat transfer coefficient and heat flux density. The intensity of heat exchange between the fuel element surface and the coolant is determined by the heat transfer coefficient α . This is the amount of heat transferred through a unit surface per unit time when the difference between the temperatures of the surface and coolant is 1 °C. The heat flux density

$$q = \alpha (t_j - t) \quad (13.5)$$

where t_j is the surface temperature of the fuel element jacket, °C; and t is the temperature of the coolant, °C; α is the heat transfer coefficient, kW/m²·K.

The heat flux density in modern power reactors may be as high as several thousand kilowatts per m². The heat transfer coefficient α is proportional to $v^{0.8}$ (v is the coolant flow

velocity). Therefore at a constant value of q the temperature t_j falls as the velocity v grows. The upper velocity limit of the coolant is restricted by erosion of the surface of the fuel element jacket. A fluid flowing at a high velocity can wash out microscopic metal particles from the fuel element surface. Prolonged erosion may lead to rupture of the fuel element jacket. The maximum coolant velocity which does not evoke inadmissible surface erosion is less than 10 m/s. High values of the heat transfer coefficient for gas coolants are obtained by pumping the gas through the core at a velocity up to 60 m/s. The maximum gas velocity is chosen in such a way as to make both the heat transfer coefficient and the pumping power consumption as optimal as possible.

The temperature drop $\Delta t = t_j - t$ in non-boilers is limited either by film boiling or chemical instability of structural materials which are in contact with the coolant. In the WWPR and GWR film boiling can occur at low temperatures. The maximum temperature for liquid metals in reactors is significantly lower than the boiling temperature. In this case the temperature drop is limited by chemical instability of the structural materials.

Let us examine heat transfer in a WWRP or GWR with boiling water. As the wall temperature rises the temperature drop Δt will also rise. Steam bubbles begin to appear on the walls; they grow and then tear away from the surface. This causes additional agitation of the water near the wall and heat transfer improves. This regime of boiling is termed nucleate boiling. As the temperature difference grows, more and more bubbles appear at the wall surface. At a certain temperature difference a steam film appears instead of bubbles and nucleate boiling goes over to film boilings. Steam is a poor heat conductor. Hence in film boiling heat transfer is sharply impaired and the danger of overheating the fuel elements arises.

The danger of film boiling arises when nonboiling WWPR or GWR are shut down and the sudden pressure drop in the first loop is not accompanied by a corresponding reduction of the reactor power level and water temperature.

In the cores of boiling WWPR and GWR nuclear boiling occurs. The fuel elements operate under greater stress in a boiling reactor than in a non-boiler.

Temperature distribution. Due to heat generation and heat transfer in the core the temperatures of the coolant $t(z)$, of the fuel element jacket $t_j(z)$ and the nuclear fuel t_f depend on the height z . The dependence of the temperatures on the high z in a fuel channel containing a rod fuel element is shown in Fig. 13.5 for a reactor without end reflectors. The centre of symmetry of the channel is chosen as the origin of the coordinates. The coolant temperature $t(z)$ monotonously rises from the inlet temperature t_1 to the outlet temperature t_2 . The heating of the coolant $\Delta t = t_2 - t_1$ in a reactor of a given power level is dependent on the coolant flow rate V . The greater the flow rate V the less is the coolant heating.

The temperature of a fuel element jacket is, according to formula (13.5),

$$t_j = t(z) + q(z)/\alpha$$

The heat flux density $q(z)$ along the channel in a reactor without end reflectors, as well as the neutron flux density, vary according to a cosine law:

$$q(z) = q_0 \cos \frac{\pi z}{H+2d}$$

where q_0 is heat flux density at the centre of the channel; H is the height of the channel; d is the extrapolated correction.

The heat transfer coefficient α does not vary appreciably along the axis of the channel provided the state of coolant aggregation remains unchanged. Therefore the temperature of the jacket surface $t_j(z)$ depends on two quantities $t(z)$ and

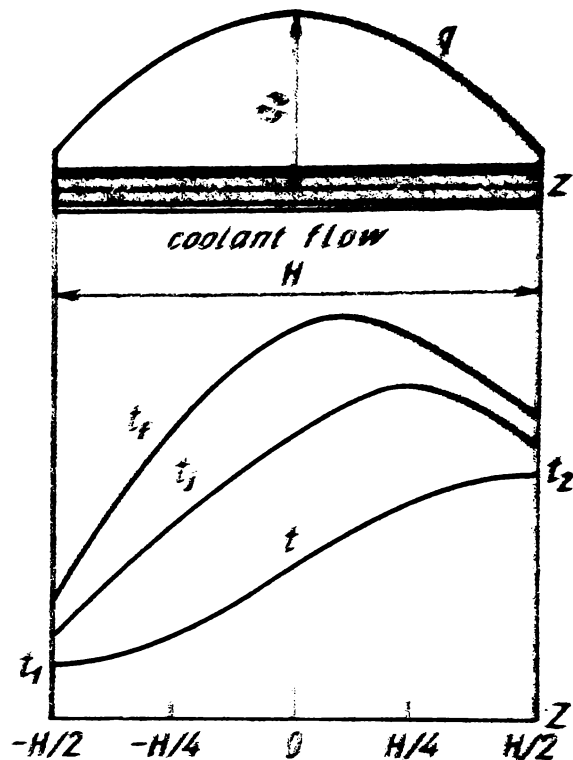


Fig. 13.5 Heat flux density q , temperatures of coolant t , fuel element jacket t_j and nuclear fuel t_f as functions of height in a fuel channel

$q(z)$. The first function monotonously increases with increase of z , whereas the second function (for $z > 0$) monotonously decreases. As a result of such variation of $t(z)$ and $q(z)$ the jacket wall temperature $t_j(z)$ is highest in the region from $z = 0$ to $z = H/2$. The maximum can be explained by the fact that the coolant temperature at the outlet is almost constant whereas the heat flux density falls sharply.

The permissible temperature of the jacket surface is determined by its corrosion resistance in the coolant, mechanical durability and by the possibility of film boiling in non-boilers.

The nuclear fuel temperature varies along the radius and reaches its maximum value $t_p(z)$ at the axis of a cylindrical fuel element. The difference between the temperatures $t_f(z)$ and $t_j(z)$ depends on the heat flux density $q(z)$, thickness of the fuel element jacket δ , slug radius R , jacket thermal conductivity λ_j and nuclear fuel thermal conductivity λ_f . It can be expressed by the formula

$$t_f(z) = t_j(z) + q(z) \delta / \lambda_j + q(z) R / 2\lambda_f$$

The variation of temperature $t_f(z)$, with a constant R , is influenced by two quantities, $t_j(z)$ and $q(z)$. The temperature of the jacket wall at first rises, reaches a peak and then falls. The heat flux density $q(z)$ is (for $z > 0$) a monotonously decreasing function of z . Therefore the maximum temperature at the axis of a cylindrical fuel element (see Fig. 13.5) is closer to the centre of the channel than the maximum temperature of the fuel element jacket.

The maximum temperature of the nuclear fuel and also the specific power are restricted by the melting temperature, nuclear fuel swelling and compatibility of the fuel element jacket and nuclear fuel.

CHAPTER 14

ATOMIC POWER ENGINEERING

14.1 Development of Atomic Power Engineering

At present the main sources of energy are organic fuels (coal, oil, shale, gas). The reserves of these fossil fuels in the earth's crust are limited and are gradually being exhausted. This explains why mankind is already confronted with the problem of replenishing its energy resources. The solution of this problem will also have a beneficial effect on the development of the chemical industry: fossil fuels may then be used as raw materials for manufacturing synthetic fibers, plastics, fertilizers etc.

One feasible way of replacing fossil fuels is to burn nuclear fuel in nuclear reactors. The natural supply of nuclear fuel and nuclear materials is so great that it can provide mankind with electric power for hundreds of years. The composition and properties of nuclear fuels are the objects of intensive research in many countries. Scientists and engineers are striving to find such compositions of nuclear fuels and the ways to burn them which will yield cheaper energy than we now obtain by burning organic fuel. The research is primarily aimed at designing efficient APS.

The first APS with an electric power output of 5MW was put into operation on June 27, 1954 in Obninsk. This first atomic power station was built by a team of scientists, engineers and technicians which included the well-known scientists I. V. Kurchatov, D. I. Blokhintsev, N. A. Dollezhal, A. K. Krasin and others. The successful operation of the first APS over many years has shown that atomic electric power plants can be safely operated. Reactor radiation shielding ensures safety of the APS personnel. The radiation dose in the vicinity of the plant has not been observed to exceed the natural dose. The first APS gave an impetus to the development of atomic engineering. Extensive studies

were begun in many countries to find acceptable APS designs in order to supplement the available energy resources.

Atomic scientists of many countries meet regularly in Geneva at international conferences to discuss the results obtained in their research and the prospects of atomic engineering. The first conference was held in 1955, the second in 1958, the third in 1964 and the fourth in 1971. At the time of the first conference only the first Soviet APS was in operation with an electric power level of 5000 kW. By the end of 1975, however, there were more than 100 stations with an aggregate capacity of 80 GW. In 1985 the APS electric power capacity is expected to reach 1250 GW and to provide one fourth of the demand in electric energy.

The Soviet Union possesses tremendous fossil fuel resources which can meet the demands for hundreds of years. However, the natural sources of coal, oil and other fuels are located only in a few distinct regions of the country and therefore transportation over long distances is required. Thermal electric power stations in the European part of the USSR use such expensive fuel transported from afar. This is one of the reasons why it is profitable to build APS in these regions to get cheaper electric energy. As atomic electric power gets cheaper APS will be built in other parts of the country as well. Several big multi-unit APS are already operating in the USSR. They will be enlarged and new APS will be constructed (Table 14.1). In 1977 the total APS capacity in the USSR was 7 GW; by 1980 it has risen to 13-15 GW.

In regions which are located at considerable distances from the gas, coal and oil sources it should be advantageous to build low-power APS. A four-unit atomic thermal and electric power plant is in operation in the small town of Bilibino (Magadan region). The electric power generated in each unit is 12 MV. The unit consists of a channel graphite boiler reactor with natural convective motion of the coolant. The heat power produced in the unit is 62 MW. The design of the reactor does not differ appreciably from that of the first APS. The Bilibino atomic power plant supplies electric power to some industrial plants and to the town itself. From 70 to 116 MW of hot water is used for heating factories and houses in the town.

Table 14.1

APS Operating or Under Construction in the USSR

Name	Type of reactor	Electric power level of APS unit, MW	Number of units in operation
First Kurchatov Beloyarsk	GWR	5	1
	GWR	100	2
	GWR	200	
	FN-600	600	
Novovoronezh	WWPR-210	210	
	WWPR-365	365	
	WWPR-440	440	
	WWPR-1000	1000	
	GWR	600	4
Siberian	HPCR-1000	1000	1
	FN-350	150	2
		(1.2 × 10 ⁵ t/day of water)	1
Kolsk	WWPR-440	440	2
Bilibino	GWR	12	4
Kursk	HPCR-1000	1000	1
(Smolensk)	HPCR-1000	1000	
(Kalinin)	WWPR-1000	1000	
(Rovno)	WWPR-1000	1000	
Chernobylsk	HPCR-1000	1000	
(South Ukrainian)	WWPR-1000	1000	
Armenian	WWPR-440	440	
	WWPR-440	440	
	HPCR-1500	1500	

* Brackets denote units and APS under construction.

Soviet scientists and engineers have designed an APS using a fast neutron breeder reactor, the FN-350 with a 350 MW electric power capacity of the unit and an APS with a reactor FN-600 with a power of 600 MW. On the basis of studies conducted in the designing of the FN-350 and FN-600 more powerful APS are being worked out with improved technology and better economical and nuclear fuel breeding characteristics.

Power reactors can be extensively used in desalting water. Industrial development in some regions of the world is inhibited by a lack of fresh water. The Donbas, some regions on the shores of the Caspian sea are examples of such regions in the USSR. There are two ways of supplying fresh water to these regions: by digging canals and pumping fresh water from rivers, or by building power facilities to desalt water. In the regions mentioned above there are great amounts of salt water. In some regions the first way seems to be the more economical and in others, the second.

The use of powerful reactors in desalination installations should facilitate the production of cheap fresh water. Hopefully the cost of the fresh water will be low enough to make it profitable to supply it to industrial centres or to use it for irrigation.

Atomic power desalination installations can serve three purposes. They will generate electric power, provide heat for buildings and desalt water. If the source of energy in the facility is a fast breeder it will reprocess ^{238}U into ^{339}Pu .

An atomic-power desalter has been built in Shevchenko on the shores of the Caspian Sea. It is equipped with a FN-350 breeder with a thermal power capacity of 1000 MW. The electric power level is 150 MW and $1.2 \times 10^6 \text{ m}^3$ of water can be desalinated daily.

Studies are being conducted with the aim of converting atomic energy into electric energy directly without making recourse to the steam generation stage. In such APS it should not be necessary to install costly steam generators, turbogenerators, circulating pumps etc. However, the application of such reactors is a complicated problem. The first fast neutron reactor-converter in the USSR, "Romashka", was put into operation in 1964-1965. A reflector transferred the heat generated in the core to a thermal element consisting of silicon-germanium thermocouples. The hot ends of the thermocouples facing the reflector are joined in pairs, the cool ends are connected to a common electric circuit.

Appreciable efficiency of the thermal element requires high temperatures which are limited by the thermal stability of the structural materials. In the "Romashka" the maximum temperature of the core did not exceed 1900 °C and the temperature of the reflector surface, 1200 °C. The

thermal power of "Romashka" was 40 kW, the electric power, 0.5 kW. From this it can be seen that the efficiency was rather low, about 1%. Further studies of thermoelectric reactors are aimed at raising their efficiency.

In another Soviet installation ("Topaz") a thermionic generator is used. The moderator is made of zirconium hydride, and the reflector, from beryllium. The electrogenerating channels, whose design is rather intricate, are located in the moderator. The main components of the channel are the electrodes (fuel element emitter and collector) separated by a small vacuum gap (interelectrode gap). The electrodes are commutated and connected to the consumer electric circuit.

A fraction of the heat released in the fuel element is spent in the ejection of electrons from the surface of the jacket; the remaining heat is removed from the core by the coolant (Na-K eutectic). The electrons from the emitter traverse the interelectrode gap, strike the collector and thus close the electric circuit. The thermal power of the reactor is 130-150 kW whereas the electric power does not exceed 10 kW.

The Soviet Union lends technical assistance to the Socialist countries in building atomic power stations. Soviet experts have participated in building on the basis of Soviet designs a 70 and 880 MW electric power APS in the German Democratic Republic, a 880 MW station in Bulgaria and 150 and 440 MW APS in Czechoslovakia. Atomic power stations with WWPR are being built in Rumania and Hungary.

An APS using a WWPR with a 440 MW electric power capacity has been built in Finland with the technical aid of the USSR. Our country has presented India the technical documentation for a 50 MW electric power fast reactor.

World fuel resources are distributed unevenly. Some countries are well supplied whereas others (Japan, Italy and others) experience an acute shortage.

This uneven distribution of fossil fuels in capitalist countries is related to the rise in prices of oil and gas and to the energy crisis of 1973-1974. This explains the growing importance of APS as a source of energy which can curb the import of organic fuels.

The highest rate of atomic power growth is in the USA (Table 14.2). In 1975 54 APS were in operation in the USA

with an aggregate capacity of 37.5 GW. By 1980 the number of APS will increase to 200. Emphasis in the USA is placed on APS with boiler and non-boiler WWPR with units up to 1100-1300 MW.

Table 14.2

APS Capacity in Some Countries as of January 1, 1976

Country	Number of APS	APS power capacity, GW
USA	54	37.50
Great Britain	14	6.10
France	9	3.03
German Federal Republic	8	3.47
Canada	1	2.65
Japan	10	5.48
Other capitalist countries	—	11.9

In Great Britain, vessel GGR with a carbon dioxide coolant and natural or enriched uranium are predominantly used. Plutonium is produced in the reactors with a $CF \approx 0.8$. The aggregate capacity of the 14 APS was 6.1 GW by the end of 1975. Five more APS are being built with an aggregate capacity of 6.2 GW.

In Canada heavy water reactors on natural uranium are mostly used. By 1985 the aggregate capacity of the Canadian APS will rise to 14 GW.

In all countries atomic engineering at present is based on the application of thermal neutrons. However, it is expected that in the future there will be a switch over to fast breeders.

Atomic electric power installations are being applied for propulsion of ships (ice breakers, submarines etc.). The atomic-powered ice-breakers *Lenin*, *Arctica*, *Siberia* of the Soviet arctic fleet are driven by power installations containing 2 WWPR. An atomic ice-breaker has one important advantage compared to the conventional ones: the latter must be refueled once a month whereas an atomic-powered ice-breaker can operate several years without any recharging of the reactors.

About thirty per cent of the useful atomic energy is utilized to generate electric energy. The other 70% is used in transport, in various technological processes (smelting of cast iron, steel and nonferrous metals, hot rolling of metals, etc.), in the chemical industry, for heating etc. In these cases also atomic power can save organic fuels.

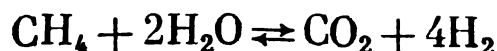
The most promising reactor for many technological processes are high-temperature gas-cooled reactors (HTGR) with a helium coolant. Such reactors are being designed in the USA, Great Britain, the Federal Republic of Germany and the USSR.

Energy installations with HTGR can be used as a source of heat in technology, to generate electric power, for central heating and so on. For example, helium heated to a high temperature first loses a fraction of its heat in technological apparatuses and is then directed to the electric power generating units.

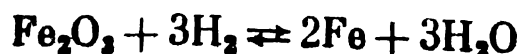
A 342 MW power plant with a HTGR is in operation in the USA. Helium heated from 404 to 775 °C circulates in the first loop. Water steam circulating in the second loop enters the turbine at a temperature of 538 °C. Single loop APS with HTGR are being designed at present.

Some technological problems which can be solved by using HTGR are as follows.

1. *The production of hydrogen from natural gas (methane).* Helium heated to about 950 °C together with a mixture of methane CH_4 and steam are admitted into a furnace. The chemical reaction in the heated mixture is



The hydrogen obtained in this way can be used in petroleum cracking, reduction of iron oxides (metallurgy), synthesis of ammonia (fertilizer manufacturing) etc. For instance, the reduction of ferric oxide may be written as follows,



2. *Coal gasification.* Helium enters the gasifier at a temperature of 1000-1200 °C. Part of the heat in gasifier maintains the chemical reaction yielding methane



14.2 Atomic Power Economics

One of the main economical characteristics of an APS is the cost of the electric energy generated. The cost of energy is made up of all capital and operating charges.

Let us examine what these charges are. A certain sum, say K rubles, is invested to construct the APS, i.e. to erect the building and reactors, buy equipment etc. These investments are termed capital charges. The building and equipment are used, say τ_c years. In that time they become unfit for further use or their further use is economically unprofitable. Therefore the capital expenditures must be compensated by selling electrical energy in equal portions of $K/\tau_c = aK$ rubles annually. The cost due to depreciation of the buildings is called the *capital component*.

As in other power stations there are charges for the operating personnel. Lubricants must be bought for the APS, a certain amount of electrical power is used etc. The annual personnel and operating charges are called *maintenance expenditures* M .

The capital component and maintenance expenditures do not depend on the annual electric energy output. Therefore they can be added together to yield the first term of the cost of electric energy

$$C_1 = aK + M$$

Now let us examine how the burning of nuclear fuel in the reactor contributes to the cost of power. Let the cost of the fresh fuel channels in the core be C_f . After an operating period of τ days the reactor is recharged. Almost all fissionable material in the replaced fuel channels is unused. Besides, due to plutonium build-up the value of the fuel channels is increased. These channels are sent to a chemical processing plant, where the fissionable material is reclaimed and used again as nuclear fuel. The sum annually spent on purchasing fuel channels for the APS is

$$C_2 = \frac{365}{\tau} (C_f - C_u)$$

where C_f and C_u are the costs of new and used fuel channels respectively, and τ is the operating period expressed in days.

The annual expenditure on nuclear fuel C_2 is called the fuel component of the cost of electric power. Unlike the capital component and maintenance expenditures it is a function of the amount of electric energy generated by the APS. As the amount of electricity supplied to the consumer increases the number of exhausted fuel channels also increases and the fuel component C_2 will be correspondingly higher.

The annual expenditure of an APS is

$$C = C_1 + C_2$$

This sum yields the cost of the electric energy produced a year.

Up to this point we have discussed only the total annual energy cost and have not considered the amount of electric energy supplied to the consumer. Thermal and electric energies are measured in kilowatt-hours. The cost of a kilowatt-hour is found by dividing the total energy cost C by the amount of electric energy expressed in kilowatt-hours generated by the APS in a year.

If the APS runs uninterrupted a whole year at its rated electric power capacity of P_{el} kW, it will generate bP_{el} kWh of electric energy, where $b = 8750$ is the number of hours in a year. However, the APS is usually shut down from time to time for preventive repairs, recharging of the fuel channels etc. Because of these shutdowns the annual energy output drops to nbP_{el} kWh. The coefficient n denotes the fraction of time the APS operates at its rated capacity during a year and is called the *use factor*. Thus the cost of a kilowatt-hour is

$$c = C/nbP_{el}$$

Only part of the reactor thermal power P_{th} is converted into electric power at an APS

$$P_{el} = \eta P_{th}$$

where η is the APS thermal conversion efficiency. Replacing the electrical power in the cost price formula by ηP_{th} we get

$$c = C/n\eta bP_{th}$$

To lower the cost of 1 kWh of electric energy the use factor n and the efficiency η should be increased. The factor

n can be increased by reducing the duration of planned shutdowns and by ensuring failure free operation of the APS. In big present-day APS n is approximately 0.7-0.85. To increase the APS efficiency η the plants are designed to possess high level steam characteristics (temperature, pressure). In many countries APS are being designed in which the steam is delivered to the turbine at 560°C and a pressure of 250 atm. The efficiency of such APS is 0.46. In single-loop APS using HTGR with the outlet temperature of helium of 900°C the efficiency will rise to 0.6. In present day APS it is 0.25-0.37.

Now let us investigate how the reactor thermal power capacity influences the cost of 1 kWh. For this purpose we examine separately the first constant component and the fuel component of the cost of a kilowatt-hour. For simplicity we assume $n = 1$ and $\eta = 1$:

$$c = C_1/bP_{th} + C_2/bP_{th}$$

Capital charges for construction of the reactor building are determined by the size of the building and not by the power level of the reactor to be installed. Irrespective of the thermal capacity of the reactor aK rubles must be returned annually. Therefore with an increase in the reactor thermal capacity the deductions required to cover the capital charges per kilowatt-hour of energy will decrease. This follows from the first term, C_1/bP_{th} .

The reactors of the second units at the Beloyarsk and Novovoronezh APS, for example, do not differ in size from those of the first units. However, their power capacity is 1.5-2.0 times greater. The buildings for the first and second units are the same. Therefore the capital component for the second units is significantly less than that for the first units. For example, an increase in the electric power of a unit at the Novovoronezh APS from 210 to 440 MW reduced the specific capital expenditures from 406 to 200 rubles per kWh.

Substitution of C_1 (see above) into the fuel component of the cost of a kilowatt-hour $c_2 = C_2/bP_{th}$, yields

Dividing and multiplying the product $bP_{th} \times \tau/365$ by the uranium load m_U we obtain

$$\frac{bP_{th}}{m_U} \frac{\tau}{365} m_U = \left(\frac{b}{365} P_{sp} \tau \right) m_U = z m_U$$

The first factor is the nuclear burn-up z per megawatt-day per ton (MW·day/t). Hence, the price of a kWh of electrical energy decreases with increase of the nuclear fuel burn-up. It is planned in the next ten years to utilize nuclear fuels with a burn-up as high as 4.5×10^4 MW·day/t (6%) or even higher.

Enrichment raises the cost of nuclear fuel. The fuel charges fall as the cost of the discharged fuel rises. Thus if the burn-up in the reactor is m kg and CFm kg of plutonium are produced, the difference $C_f - C_u$ will be the smaller the greater the value of CF . The latter factor, which reduces the electric power cost, is particularly significant in fast breeders which possess high CF values (1.5-1.8). The cost of a kilowatt-hour can be lowered by increasing the specific power of the reactor and raising its efficiency and burn-up. For example, the cost of a kilowatt-hour at the Novovoronezh APS was reduced from 2 kopecks (1964) to 0.635 kopecks (1976). The Novovoronezh APS electricity is 20% cheaper than that of the Voronezh heat and electric power plant which runs on coal. The cost of electricity from unit II of the Beloyarsk APS was 0.92 kop./kWh in 1974 and was the same as the cost of electricity of the Ural heat and electric power plant which has a power capacity close to that of unit II of the Beloyarsk APS.

Thus the main means of obtaining cheaper electric power at an APS is to raise the thermal conversion efficiency η , use factor n , thermal specific power of the reactor P_{th} , burn-up z and the conversion factor CF . It should be noted that intensive development of atomic engineering will stimulate the mass production of APS equipment and lead to the design of APS with higher thermal conversion efficiencies. By perfecting the production of various components of the reactor and simplifying the conversion of heat into electric power it will be possible to reduce further the cost of electricity generated in APS.

14.3 Research and Experimental Reactors

Research reactors. The first research reactors were designed primarily for the study of various problems in atomic engineering. Experiments in the field of neutron physics were carried out and the effects of prolonged fast-neutron or gamma-quanta irradiation on the properties of materials were investigated. Fuel elements for future atomic energy installations were tested in the loop channels of these early reactors.

There were some disadvantages in carrying out physical and technological experiments in a single reactor. Thus, substitution of loop channels could lead to radioactive contamination and this would considerably complicate the physical measurements. Moreover, the physical experiments had to be discontinued when the reactor was shut down for a faulty loop channel to be replaced. Finally, the volume of research in many various directions had increased greatly. For these reasons special reactors were designed, each for a specific field of research.

More than ten research reactors have been built in the Soviet Union. Some of them are used as neutron and gamma-quantum sources in physical experiments or in studies of the properties of materials. This type of reactor includes several water-water reactors operating in Moscow, Leningrad, Kiev and other cities of the Soviet Union. The amount of nuclear fuel used in WWR is not great and the reactors are simple in construction. The WWR contains experimental channels through which neutron beams can be extracted into the laboratory. The samples to be irradiated are placed in other channels and thermal neutron beams are produced in the thermal columns.

Since the absorption of thermal neutrons in water is high, all WWR use enriched uranium. An excess reactivity is set up in the reactor and used to compensate for poisoning, accumulation of slag, fuel burn-up and absorption of neutrons in the experimental channels.

In some types of research reactors fuel elements are tested and samples of various materials are irradiated. These reactors contain loop channels in which the fuel elements to be used in prospective reactors are tested.

In order to obtain higher neutron flux densities (about 10^{19} neut./ $m^2 \cdot s$) the power of the research reactors is made as high as 50-100 MW.

In the following we present short descriptions of a reactor for physical research WWR-M (Russian designation BBP-M) and of a reactor for technological studies MR (MP). The basic characteristics of these reactors are given in Table 14.3.

Table 14.3

Basic Characteristics of Research Reactors

Type of reactor	^{235}U load, kg	Core volume, l	Core height, cm	Uranium enrichment, %	Max. power, MW	Mean specific power, kW/kg ^{238}U	Peak thermal neutron flux density, 10^{18} neut./ $m^2 \cdot s$
WWR-M	4.0	12.5	50	20	10	2500	3
MR	7.0	600	100	90	20	2800	8

WWR-M reactor. The core of the reactor consists of fuel channels. In each channel there are three coaxial tubular fuel elements, the external one being a hexahedral tube and the two inner ones circular tubes. All three tubes are made of $(UO_2 + Al)$ cermet 0.9 mm in diameter and are enclosed in aluminium jackets 0.7 mm thick. Four kilograms of ^{235}U are loaded into the 12.5 litre hexahedral core (Fig. 14.1). Three fuel channels comprise sections which are mounted on the lower core lattice. The space between the sections is filled with beryllium displacers possessing the same shape and size as the sections.

Considerable thermal neutron bursts occur in the lateral beryllium reflector. It is precisely here that the horizontal and vertical experimental channels are situated. There are 9 horizontal channels in the reflector for exit of neutron beams and 11 vertical channels in which samples of materials are irradiated and radioactive substances produced. Two vertical channels are used as experimental loops to study the interaction between different materials and coolants under irradiation conditions.

The heat removal system consists of two loops. The temperature of the water at the core inlet varies between $24^{\circ}C$ and $36^{\circ}C$; at the outlet it lies between $32^{\circ}C$ and $45^{\circ}C$.

Part of the water circulates in the reflector and keeps the temperature of the beryllium below 60 °C. The heat in the first loop is conveyed to the service water in the second loop by means of four heat exchangers.

To compensate the excess reactivity five boron carbide rods are inserted into the core. One boron steel rod automatically regulates the power level.

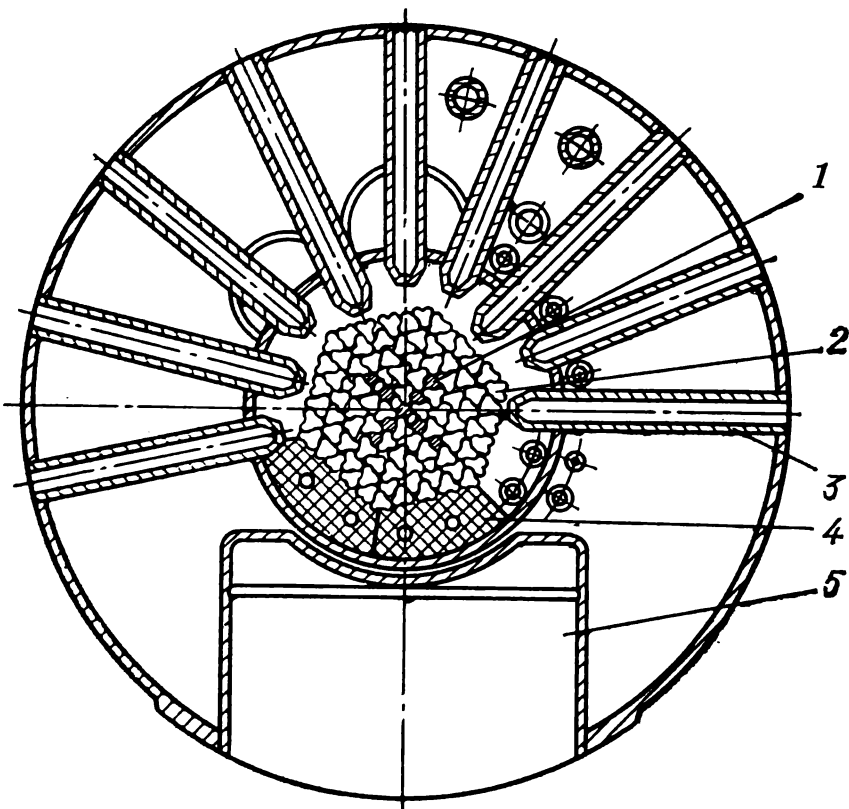


Fig. 14.1 Horizontal cross section of WWR-M reactor

1—absorption rod; 2—fuel section; 3—horizontal channel; 4—reflector; 5—thermal column

MR Reactor. Research reactors for testing fuel elements should be simple in construction and possess good physical characteristics (low ^{235}U loading level, high neutron flux density etc.). The MR reactor meets all these requirements. It is placed at the bottom of a pool (Fig. 14.2) under a layer of water. This provides good external observation under conditions of overloading of the core and loops. The thick layer of water also protects the operators from irradiation.

The core consists of fuel channels which contain the fuel assemblies (five concentric tubular fuel elements). Water at a pressure of 10 atm and temperature of 40 °C is pumped

into the fuel channels at the top of the reactor. The water moves downward in the space between the outer fuel element of the assembly and the jacket of the fuel channel. It then returns through the assembly to the upper outlet after being heated to 110 °C.

The space between the fuel channels is filled with beryllium displacers. Plugged ducts run along the axis of the beryllium

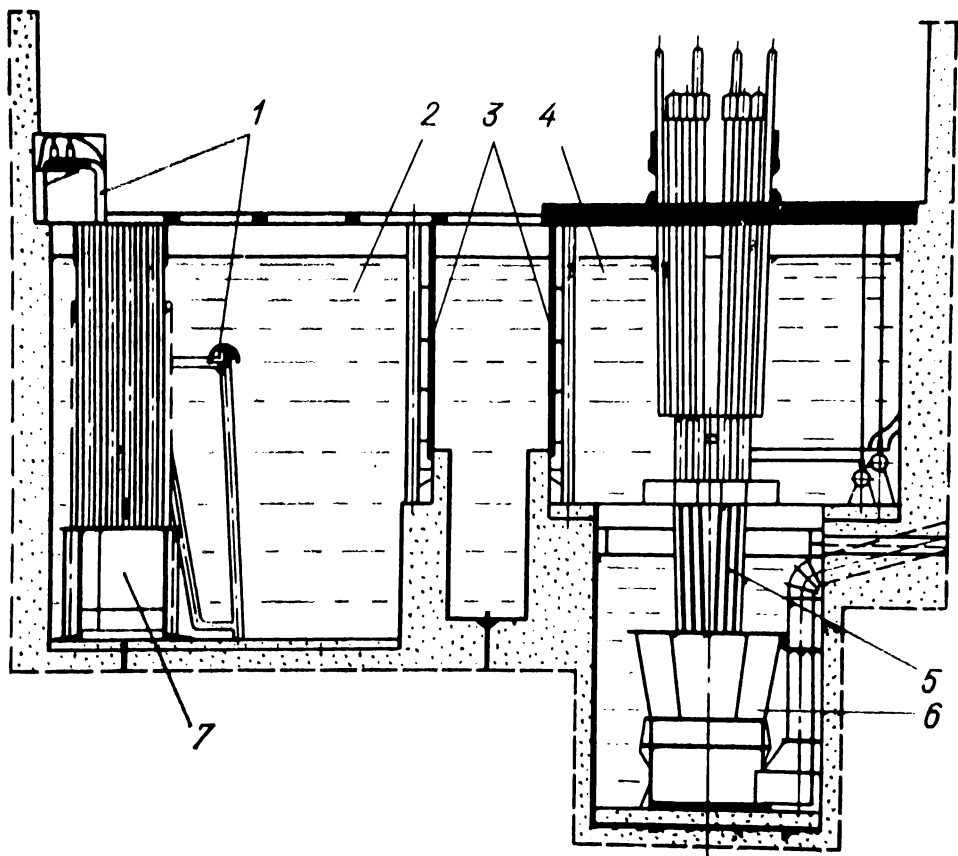


Fig. 14.2 Vertical sectional view of pool of the MR reactor and storage tank

1—loop channel removed from reactor; 2—storage tank; 3—lock gate; 4—reactor pool; 5—fuel channel; 6—MR reactor; 7—gamma-source chamber

displacers, and absorption rods or samples of materials to be irradiated can be placed in the ducts. The heat released in the moderator and reflector is removed by the water in the pool which circulates in the gaps between the moderator blocks.

The distance between the fuel channels in the core varies from 20 mm at the bottom of the core to 140 mm at the top.

The beryllium displacer together with the variable spacing keeps the tops of the fuel channels separated by a sufficient distance from each other.

A spherical water reflector 100 mm in diameter is located in the central part of the core. It is also called a neutron trap. The slowing-down capacity of this inner reflector is about 4 times that of a water-beryllium moderator. This explains the appearance of thermal neutron bursts in the inner reflector. The maximum neutron flux density in the nuclear fuel at a peak power level of 20 MW is 2.4×10^{18} neut./m²·s and in the trap, 8×10^{18} neut./m²·s.

The core is surrounded by two layers of reflectors. Beryllium blocks are arranged in the inner layer; the second layer consists of graphite blocks in an aluminium casing.

The reactor pool is connected to the storage pool through a lock. The surface of the pools is lined with stainless steel. By using two pools leakage of radioactive substances can be practically eliminated during a recharging of the channels. Fuel and loop channels removed from the core are transferred to the storage tank under a thick layer of water.

New constructions of fuel elements for future power reactors can be tested and changes in the properties of coolants caused by irradiation can be studied in the 13 MR loop channels. The design of the loop channels differs from that of the fuel channels. The heat of the loop channels is removed by a coolant moving upward through the channel. The loop channels viewed from the side resemble a U and therefore are called U-channels. A loop channel removed from the core and located in the storage tank is shown in Fig. 14.2.

The possibility of using organic coolants in nuclear engineering and the means of removing disintegration products from them are studied in the MR reactor. To attain a high efficiency in atomic electric power stations and to ensure efficient burn-up of the nuclear fuel it is necessary to have fuel elements which can operate over long periods of time under extreme temperature conditions. In the MR reactor there are two loop channels with helium as the coolant. The helium is pumped at a high velocity through the loops at a pressure of 100 atm. and is heated up to 850 °C. Heat removal with a steam-water mixture which is formed during bulk boiling can be investigated in the other loops.

Experimental reactors. Loop and test rig experiments cannot yield full information on the operation of the whole power reactor. To study the parameters, reliability and other features of the performance of power reactors, special experimental reactors are usually built. The fast neutron reactors FR-5, FR-10 and FER-60 (Russian designation, БР-5, БР-10, БОР-60) belong to this type. The numbers following the letters denoting the Soviet experimental reactors specify the thermal power of the reactor in megawatts.

The core of FR-5 consists of 80 hexahedral cassettes with stainless steel jackets. The jacket encloses a fuel assembly consisting of 19 rod fuel elements. Nuclear fuel pellets (plutonium dioxide) are encased in stainless steel tubes. Plutonium dioxide is compatible with the reactor structural materials and is resistant to irradiation; hence a high burn-up of the plutonium is permissible. The 17.5 litre cylindrical core is enclosed in a stainless steel vessel. Liquid sodium is pumped through the vessel and is heated in the core to between 375 and 500 °C.

The reactor reflector is made from nickel which has a large neutron scattering cross-section. The inner part of the nickel reflector consists of two mobile layers which are part of the safety control system. Flowing air removes the heat liberated in the reflector.

Valuable experimental data have been obtained with the FR-5 reactor operating at rated capacity. Plutonium dioxide burn-up up to 7% has been attained. Most of the fuel elements have endured prolonged operation at a coolant temperature of 500 °C and jacket temperature of 600 °C. However, at burn-ups exceeding 2.5% a few of the fuel elements developed leaks and fission products were washed out into the primary loop. Nevertheless, the leaks in the fuel elements and subsequent contamination of the sodium by the fission products did not interrupt normal operation of the reactor. Cold traps efficiently captured the solid fission fragments and removed the sodium oxides from the sodium.

The conversion factor of a breeder reactor depends on the composition of the nuclear fuel. A particularly high CF can be expected when the carbide mixture UC + PuC is used as the fuel. The carbide fuel was tested in the FR-5 reactor and proved to be suitable for breeder reactors. It has been

used in monocarbide fuel elements between 1965 and 1971. Monocarbide fuel elements retain their working capacity at burn-ups up to 5.5-5.9%.

Long-term operation of the FR-5 reactor has helped to solve some problems in the design of the FN-350 atomic power station. In particular, experience was gained in working with a sodium coolant in the core, various units of the reactor were tested etc.

To accelerate fuel element testing with a burn-up up to 10% and to check other elements of the construction the power of the FR-5 reactor was increased to 10 MW. The specific power of the FR-10 reactor loaded with plutonium dioxide fuel elements is 780 kW/l with a mean sodium temperature at the outlet of 500 °C.

The experimental fast reactor FER-60 is employed for testing constructional units and fuel elements for fast reactors with sodium coolants. The specific power in the FER-60 core may reach 1100 kW/l, the sodium temperature at the outlet being 580 °C. The construction of the FER-60 is such that nuclear fuels with burn-ups over 10% can be tested in the reactor.

14.4 Graphite-Water Reactors

Reactor of the first atomic electric power station. The source of energy at the first atomic electric power station is a water-cooled graphite reactor with a power output of 30 MW. The reactor rests on a concrete foundation (Fig. 14.3). The air-tight steel vessel is filled with hexahedral graphite blocks with spacings between to allow for thermal expansion of the graphite. The assembly is filled with low-pressure nitrogen which protects the graphite from ignition. The central part of the graphite assembly is threaded by 151 vertical ducts, each of 65 mm in diameter, in which the fuel channels are inserted. Shim and safety rods are located in 23 of the ducts.

The reactor core is a cylinder 170 cm high and 150 cm in diameter surrounded by lateral and end-face graphite reflectors 75 cm and 70 cm thick respectively. A 140 cm thick graphite shield for neutron protection covers the upper end of the reflector.

A cast iron plate is mounted on the top of the reactor vessel. Its thickness over the core is 150 cm, and over the reflector, 20 cm. The cast iron plate absorbs gamma quanta emitted by the core. A ring coolant collector is located above the

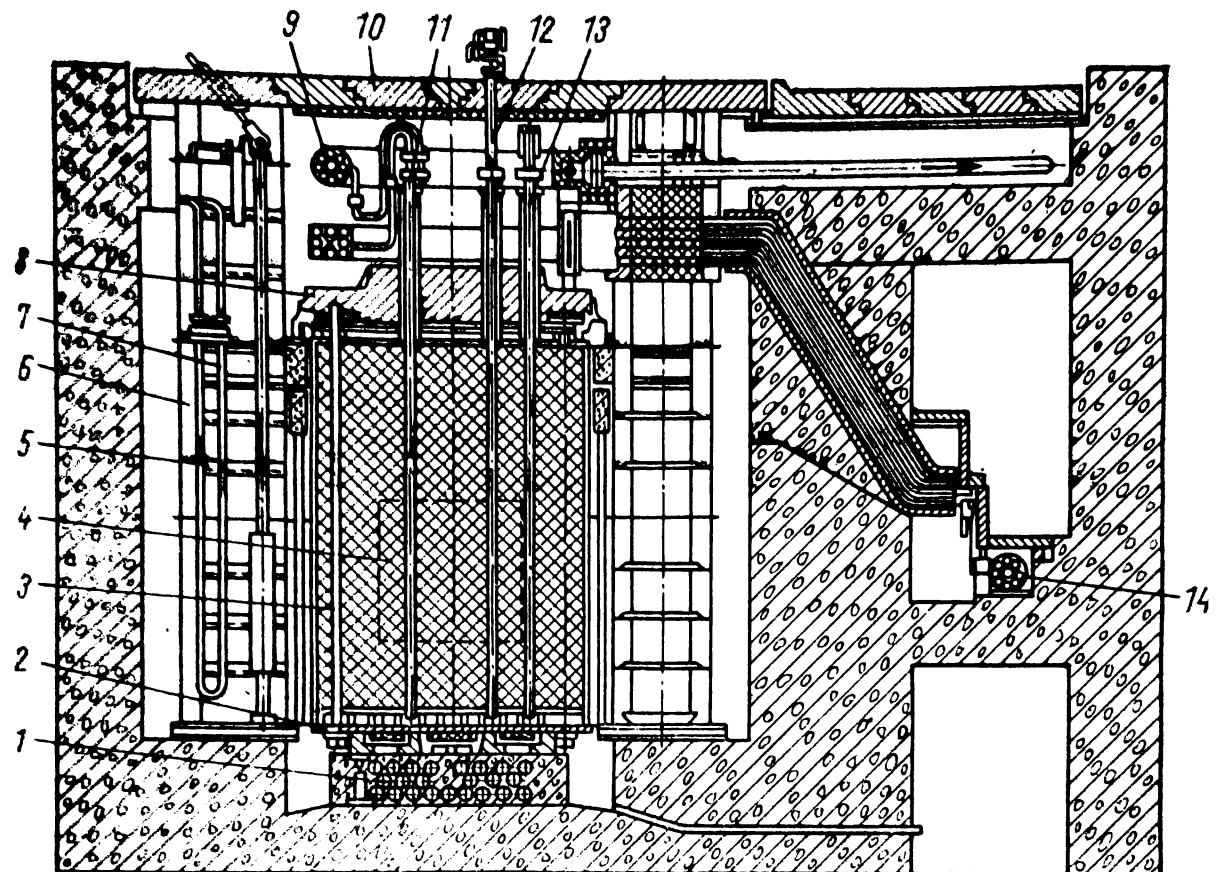


Fig. 14.3 Vertical sectional view of reactor of first APS

1—pipes for cooling of reactor foundation; 2—steel plate; 3—pipe for cooling of reflector; 4—reactor; 5—channel for ionization chamber; 6—water shield; 7—pipe coil for cooling of water shield; 8—cast iron plate; 9—coolant collector; 10—top cast iron shield; 11—fuel channel; 12—safety rod; 13—automatic control rod; 14—supply tank

iron plate. A supply tank is housed separately and enclosed in a light cast iron shield.

The reactor is located in a pit made of standard concrete and covered with a cast iron plate. The lateral radiation shield includes a ring-shaped tank with a one-metre layer of water and a concrete wall three metres thick. The water tank is adjacent to the reflector. Heat generated in the shield is removed by a subsidiary heat-transfer loop.

The fuel channel (see Fig. 11.5) consists of graphite distance bushings, housing four tubular fuel elements and a sup-

ply pipe. The total length of the fuel channel is 677.5 cm, including 170 cm of the active part.

The tubular fuel element consists of uranium alloy (9% molybdenum) pellets enriched to 5-7% and covered with magnesium. The nuclear fuel is enclosed in a 0.2 mm layer of stainless steel which contains the fission fragments within the fuel element. The inner 9 × 0.4 mm tube can endure a pressure of 100 atm in the primary loop. Each of the four tubes has a spiral device to compensate for thermal expansion. At the upper end all four fuel elements are connected to a common outlet chamber which is joined to the outlet collector.

Water pumped from the supply tank into the central tube of the channel flows down to the distributing chamber and cools the graphite. Then, on its way up, it cools the fuel elements and is heated from 190 °C to 280-290 °C at a pressure of 100 atm.

In case of a leak the water strikes the hot graphite and is converted into steam. The pressure in the gap between the fuel element and graphite then increases. From this change of pressure one can tell if the jacket of the fuel element is intact or not. Fuel channels with damaged fuel elements are cut off from the supply tank and removed from the core.

By using tubular fuel elements it is possible to avoid poisoning of the primary loop system by fission products which enter the graphite stack from the damaged fuel element.

The safety control system consists of 19 rods for manual control (MC), four paired automatic control rods (AC) and two safety rods (SR). The SR rods are located at a distance of 40 cm from the axis of the core. The manual control rods are arranged in two circles in the core with radii of 26 cm and 60 cm respectively. The paired AC rods are in the reflector; one pair is used for active operation and the other is kept in reserve.

The operator raises or lowers the MC rods with cables and servomotors from the control desk. The speed of removal is restricted by special devices.

There are several loop channels in the reactor for investigation of heat removal by overheated steam or free flowing water etc. In some experimental channels materials are

tested and in others radioactive substances are produced. Neutron beams can be extracted through the other channels and thermal column and transferred into the laboratory behind the radiation shield.

The reactor of the first atomic power electric station was the first pilot power-generating reactor in the world. For this reason it is used as an experimental power reactor. In particular studies on the application of water-cooled graphite channel reactors in atomic engineering have been carried out on it. These studies include the investigation of high nuclear fuel burn-up, selection of operation conditions in atomic power electric plants, radiation protection problems, testing of fuel elements etc. Since the reactor has such a broad range of application, it is operated at various power levels. Therefore the operation period is usually measured not in calendar days but rather in effective days. An effective day is the time it takes the reactor to burn up the same amount of ^{235}U that is burned up in the fuel elements when the reactor is operating at rated thermal capacity. The first operating period of the reactor was 75 effective days.

Reactors of the Kurchatov Beloyarsk APS. The data obtained during operation of the first APS were taken into account in the design of the reactors for the Beloyarsk APS (BAPS). The plant consists of self-contained units, each of which includes a channel reactor and steam power plant (steam generator, turbogenerator etc.). This system of independent units facilitates the operation of the APS and enhances its reliability in performance. Unit I reactor of the BAPS is similar in construction to that of the first APS. The fuel channels contain six tubular fuel elements with enriched uranium (1.8%) slugs.

The reactor is designed to produce superheated steam directly in the core. There are 998 fuel channels: 730 evaporative channels and 268 superheating channels. The steamwater mixture leaves the evaporative channels at a pressure of 130 atm with a 20-30% mass steam content. The heat removed from the evaporative channels is used in the steam generator to produce steam at a pressure of 100 atm. The steam is then directed to the 268 superheating channels where its temperature is raised to 520 °C. This superheated steam

enters the turbogenerator at a pressure of 90 atm. The efficiency of Unit I is 35-37% and the electric power of the unit is 100 MW.

The Beloyarsk APS Unit I was put into operation in May, 1964. The operating period of the reactor is two years.

The characteristics of Unit II reactor of the BAPS, which was put into operation in October, 1967, differ from those of Unit I reactor. The core sizes are identical but the electric power is twice as high, viz. 200 MW. This was achieved by introducing some minor changes in the construction of the fuel channels and heat removal system.

The heat transfer surface in the fuel channels was increased by increasing the inner diameter of the fuel elements. In the improved superheating channels the steam passes down the first three fuel elements where it is initially superheated. The steam then goes over the second three fuel elements where it is heated to 520 °C, and, at a pressure of 75 atm, enters the turbogenerator. The central coolant tubes are removed from the superheating channels thus improving the physical characteristics of the reactor. Automatic control rods are installed in place of the central tubes and this somewhat levels out the heat release in the core. The fuel slugs are prepared from uranium or cermet (uranium enrichment 3%). Cermet is also used in the mobile fuel elements in the superheating channels. These fuel elements are subjected to particularly great heat stresses.

A single-loop heat removal system is used in Unit II. Boiling water in the evaporative channels is pumped to a separator in which the steam is separated from the water and then directed to the superheating channels.

From 32 to 35 fuel channels in the reactors of Units I and II are recharged every 115 days (Unit I) and 85 days (Unit II). The average burn-up in the discharged fuel channels is 13.7 MW day/kg (evaporative channels) and 23 MW day/kg (superheating channels).

Investigations are being carried out at the BAPS on high burn-up and efficiency of superheating channels operating under improved steam conditions. Part of the evaporative and superheating channels are kept in the core until a burn-up of 20 and 38 MW day/kg is attained respectively. The superheater channels have been found to be highly reli-

able. Some were tested to see how they performed when the temperature of the steam at outlet was 300 °C.

High power channel reactor (HPCR). In the designing of an APS with a HPCR the problem was to improve the fuel cycle. To solve this problem it was necessary to develop new structural materials with low neutron absorption and with mechanical properties similar to those of stainless steel. Lowering neutron absorption in the structural materials makes it possible to use cheaper nuclear fuel with only 1.8 % enrichment.

In HPCR-1000 and HPCR-1500 (Table 14.4) the fuel channels are located in the graphite moderator. A cassette with upper and lower fuel assemblies is installed in each fuel channel. The fuel assembly consists of 18 rod fuel elements. Uranium oxide pellets are packed in the fuel element. The middle part of the pressure tube in the core is made from a zirconium alloy (Zr + 2.5% Nb) possessing high mechanical and corrosion resistance properties; the upper and lower parts of the pressure tube are made from stainless steel. The zirconium and steel parts of the tube are joined by welded adapters.

In an APS unit with a HPCR, energy is transformed in a single loop system. Boiling water from the reactor is passed through separators. Saturated steam (280 °C) under a pressure of 65 atm is then delivered to two turbogenerators each with a 500 MW electric power capacity. The spent steam is condensed and circulating pumps feed the water back into the reactor.

The HPCR-1000 is a standard graphite-water channel boiler reactor. It is designed for four-unit atomic power stations, viz., the Leningrad, Kursk, Chernobylsk, Smolensk stations. Two units with the HPCR-1000 were put into operation at the Lenin Leningrad APS, one in 1973 and the other in 1975.

The power of APS units with the HPCR-1500 is raised by increasing the power of the fuel channels. Special grids in the upper fuel assembly communicate an axial whirl to the coolant flow. This increases 1.5-fold heat removal and the channel power. The HPCR-1500 will be installed in the Ignalina APS in Lithuania.

Besides the HPCR-1000 and HPCR-1500 another high-

Table 14.4

Operating Characteristics of the HPCR and APS Unit

Characteristic	HPCR-1000	HPCR-1500	HPCRS-2000
Reactor thermal power, MW	3200	4800	5400
Unit electric power, MW	1000	1500	2000
Unit efficiency, %	31.3	31.3	37.0
Steam pressure at turbine inlet, atm	65	65	65
Steam temperature at turbine inlet, °C	280	280	450
Core size, m:			
height	7	7	6
diameter (or width × × length)	11.8	11.8	7.75 × 24
Uranium load, ton	192	189	226
Enrichment, %	1.8	1.8	1.8*
Number of channels:			
evaporative	1693	1661	1744
superheating	—	—	872
Average burn-up, MW·day/kg:			
in evaporative channel	18.1	18.1	20.2
in superheating channel	—	—	18.9
Size of fuel element jacket (diameter × thickness), mm:			
evaporative channel	13.5 × 0.9	13.5 × 0.9	13.5 × 0.9
superheating channel	—	—	10 × 0.3
Material of fuel element jacket:			
evaporative channel	+ Zr + + 2.5% Nb	+ Zr + + 2.5% Nb	+ Zr + + 2.5% Nb
superheating channel	—	—	Stainless steel

The uranium in superheating channels is enriched to 2.2%.

power channel reactor using steam superheated up to 450 °C (HPCRS-2000) has been designed. The core of the HPCRS-2000 is a rectangular parallelepiped. The construction of the evaporative and superheating channels in the HPCRS-2000 differs only slightly from those in HPCR-1000. However, the jacket of the fuel elements and evaporative channels are made from stainless steel and not of a zirconium alloy; the uranium is enriched to 2.2%.

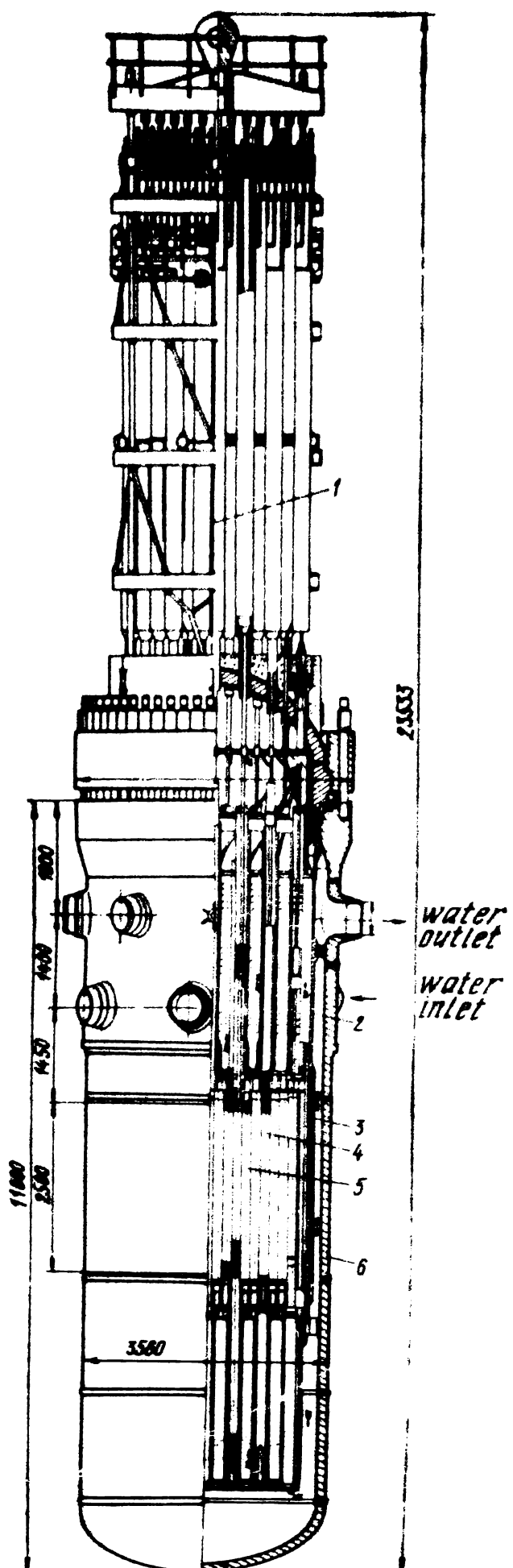


Fig. 14.4 General view of WWPR-440 reactor

1—upper unit with SCS drive mechanism; 2—pit; 3—removable basket; 4—emergency control cassettes; 5—core; 6—reactor body

The boiling water in the evaporative channels flows to the separator. The saturated steam in the separator then enters the superheating channel where it is heated to 450 °C and at a pressure of 65 atm is driven to two turbogenerators of 1000 MW each.

14.5 Vessel Water-Water Power Reactors (WWPR)

In present-day atomic engineering APS with WWPR play a prominent role. Water is both a good moderator and a good coolant and consequently WWPR with high specific power can be designed. The vessel reactors WWPR-210, WWPR-365, WWPR-440, WWPR-1000 and others have been designed in the Soviet Union.

The first two reactors, WWPR-210 and WWPR-365, have been operating for a long time in units I and II at the Novovoronezh APS (NVAPS) (Table 14.5). The experience gained during the long term operation of these reactors has provided valuable data which was taken into account in the designing of the production model WWPR-440. Investigations were carried out on the WWPR-210 and WWPR-365 to see if their thermal power could be raised without increasing the size of the core and also to see if the reactor could be regulated by adding absorbing substances to the coolant etc.

The WWPR-440 (Fig. 14.4) is operating in units III and IV at the NVAPS, the Kolsky APS, in power plants in the German Democratic Republic and Bulgaria. It will be installed at several APS being constructed in the USSR, in the socialist countries and in Finland.

The WWPR-440 core consists of 349 hexahedral cassettes some of which are used as control rods of the SCS. Each cassette contains 126 rod fuel elements (diameter 9.1 mm) arranged in a triangular lattice. The fuel element slugs (sintered uranium oxide enriched to 3.5%) are 7.5 mm in diameter and encased in a jacket 0.6 mm thick. The cassette shroud and fuel element jacket are made of zirconium alloyed with niobium (1%).

During the operating period, which is about 870 days, the WWPR-440 cassettes are partially recharged three times. Every 286-290 days one third of the cassettes is replaced.

Table 14.5

Operating Characteristics of the Novovoronezh APS
Units and WWPR

Characteristics	WWPR-210 unit I	WWPR-365 unit II	WWPR-440 units III and IV	WWPR-1000 unit V
Reactor thermal power, MW	760	1320	1375	3000
Unit efficiency %	27.6	27.6	32.0	33.0
Steam pressure at turbine, inlet, atm	29.0	29.0	44.0	60.0
Pressure in first loop, atm	100	105	125	160.0
Temperature of water, °C:				
at core inlet	250	250	269	289
at core outlet	269	275	300	324
Core diameter, m	2.88	2.88	2.88	3.12
Core height, m	2.50	2.50	2.50	3.50
Fuel element diameter, mm	10.2	9.1	9.1	9.1
Number of fuel elements in a cassette	90	126	126	317
Uranium load, ton	38	40	42	66
Mean uranium enrichment, %	2.0	3.0	3.5	3.3-4.4
Mean fuel burn-up, MW·day/kg	13.0	27.0	33.3	40

At first the cassettes are removed from the central region of the core and replaced by cassettes from the peripheral region. The vacant places in the peripheral region are loaded with fresh cassettes. Recharging is done under a 5 m layer of water which reduces the level of irradiation in the reactor hall below that of the permissible dosage.

The WWPR power reactivity factor is a negative quantity. At the Novovoronezh APS it is used to prolong the interval between recharging in the autumn and winter when power consumption is maximal. The reactor is switched to a self-regulating regime for a short time before being partially recharged. The reactor power level is slowly reduced thus releasing reactivity which compensates the additional nuclear burn-up.

The WWPR-440 core is housed in a thick-walled steel vessel of 3.8 m in outer diameter and 11.2 m in height. The vessel operates under a pressure of 125 atm and has two connecting pipes for inlet and outlet of the coolant. It is covered at the top by a shielding plate.

Neutrons and gamma radiation striking the inner vessel walls cause changes in the structural materials of the vessel and induce thermal stresses in the vessel. These effects depend on the radiation dose. To lower the dose water and steel shields are placed between the core and the vessel walls. The water shield is 20 cm thick and the steel shield 9 cm thick.

The WWPR-440 safety control system (SCS) consists of two independent systems: the emergency control cassette system (ECC) and the boron control system (see Sec. 13.4). The first system, which consists of 37 ECC, ensures reactor control in non-stationary regimes and reactor shutdown. A cassette of fuel elements is located at the bottom of the ECC and elements with a boron alloy at the top. The ECC are attached to rods which extend through the top of the vessel. They are moved vertically by electric motors and in case of an emergency can be plunged to the bottom of the reactor vessel. In this case the vacancy left by the fuel elements of the ECC is filled by the boron alloy absorber.

The boron regulating system compensates gradual reactivity changes due to burn-up of nuclear fuel, poisoning, slugging etc. The boron regulating system has simplified the reactor SCS and the number of ECC could be reduced from 73 (in the WWPR-365) to 37 (WWPR-440).

In each unit there are two loops. Water under a pressure of 125 atm circulates in the first loop. The water at a temperature of 269 °C moves downward in the annulus between the vessel wall and the core. Subsequently, moving upward, the water cools the fuel elements and is heated to 300 °C. The heat removed from the core generates saturated steam (pressure 44 atm, temperature 275 °C) in the steam generators which rotates the turbogenerators.

The WWPR-1000 core consists of 151 cassettes each with 317 fuel elements. Twelve guide tubes are distributed evenly in the cassette. A single drive mechanism moves a cluster of 12 absorption rods in the guide tubes of 109 central cas-

settes. Burn-up absorption rods are housed in the guide tubes of 42 peripheral cassettes. The slugs in the absorption rods are made of dispersed materials (Eu_2O_3 in an aluminium alloy matrix); the slugs of the burn-up absorption rods are made of boron in a zirconium matrix. The 7 mm diameter slugs of the absorption rods and burn-up absorption rod are enclosed in 8.2×0.6 mm stainless steel jackets. Besides the absorption rod and burn-up absorption rod systems a boron regulating system is also used in the WWPR-1000. By changing some of the parameters it has been possible to increase the power level of the WWPR-1000 unit compared to that of the WWPR-440 unit; thus the core volume was increased 1.65 times, the core specific power 1.3 times and the unit efficiency was also increased. The mean nuclear fuel burn-up for an operating period involving three partial rechargings is $40 \text{ MW}\cdot\text{day/kg}$.

The WWPR-1000 and equipment of the first loop with the radioactive coolant are housed in a concrete protective casing. This ensures safety in the event of a leakage in the primary loop.

14.6 Fast Neutron Reactors

Only a small fraction of the uranium is burned up in thermal reactors which are the main source of energy in atomic engineering today. By using fast reactors it should be possible to achieve complete uranium and thorium burn-up in the core. This explains the extensive studies which are being carried out in many countries on the intricate fast reactors. Before introducing fast reactors in atomic engineering on a large scale it will be necessary to solve a number of scientific and technological problems and to gain experience in the operation of industrial APS.

The first Soviet APS using a fast reactor, the FN-350 (Table 14.6), was put into operation on July 16, 1973 in Shevchenko on the coast of the Caspian Sea. Part of the thermal energy is spent in generating electric energy, the other part is used for desalting water.

The thermal energy of the FN-350 reactor is converted into electric energy in a three-loop system. Radioactive sodium in the first loop, which is heated from 300 to 500 °C is cooled

Table 14.6

Operating Characteristics of the FN-350 and FN-600 Reactors

Characteristics	FN-350	FN-600
Reactor thermal power, MW	1000	1430
APS electric power, MW	350 (or 150 MW and 1.2×10^5 t/day desalinated water)	600
Sodium temperature, °C:		
at reactor inlet	300	380
at reactor outlet	500	550
Parameters of steam at turbine:		
temperature, °C	440	500
pressure, atm	50	130
Burn-up, %	5	10
Operating period, days	250	450
Core size, cm:		
diameter	150	205
height	106	76
Reflector thickness, cm	60	40
Nuclear fuel	UO_2	UO_2
Fuel element diameter, mm	6.1	6.9
Number of fuel elements in a cassette	169	129

in heat exchangers by sodium in the second loop. The coolant in the third loop is water. Steam produced in the steam generator has a temperature of 440 °C and a pressure of 50 atm. Part of the steam is directed to the desalination facility, then condensed, degassed and again pumped into the steam generator.

The FN-350 reactor is housed in a stainless steel vessel of variable diameter with a wall 30 mm thick (Fig. 14.5). The diameter can be changed from 2.4 to 6.0 m. The top of the reactor is covered and the sides are surrounded by a casing which prevents leakage of radioactive sodium in the event of a rupture in the vessel. A steel cover over the top plate prevents leakage of radioactive substances through the cover. Argon under a pressure of 1.9 atm fills the gap above the sodium level.

A high-pressure chamber is installed in the lower part of

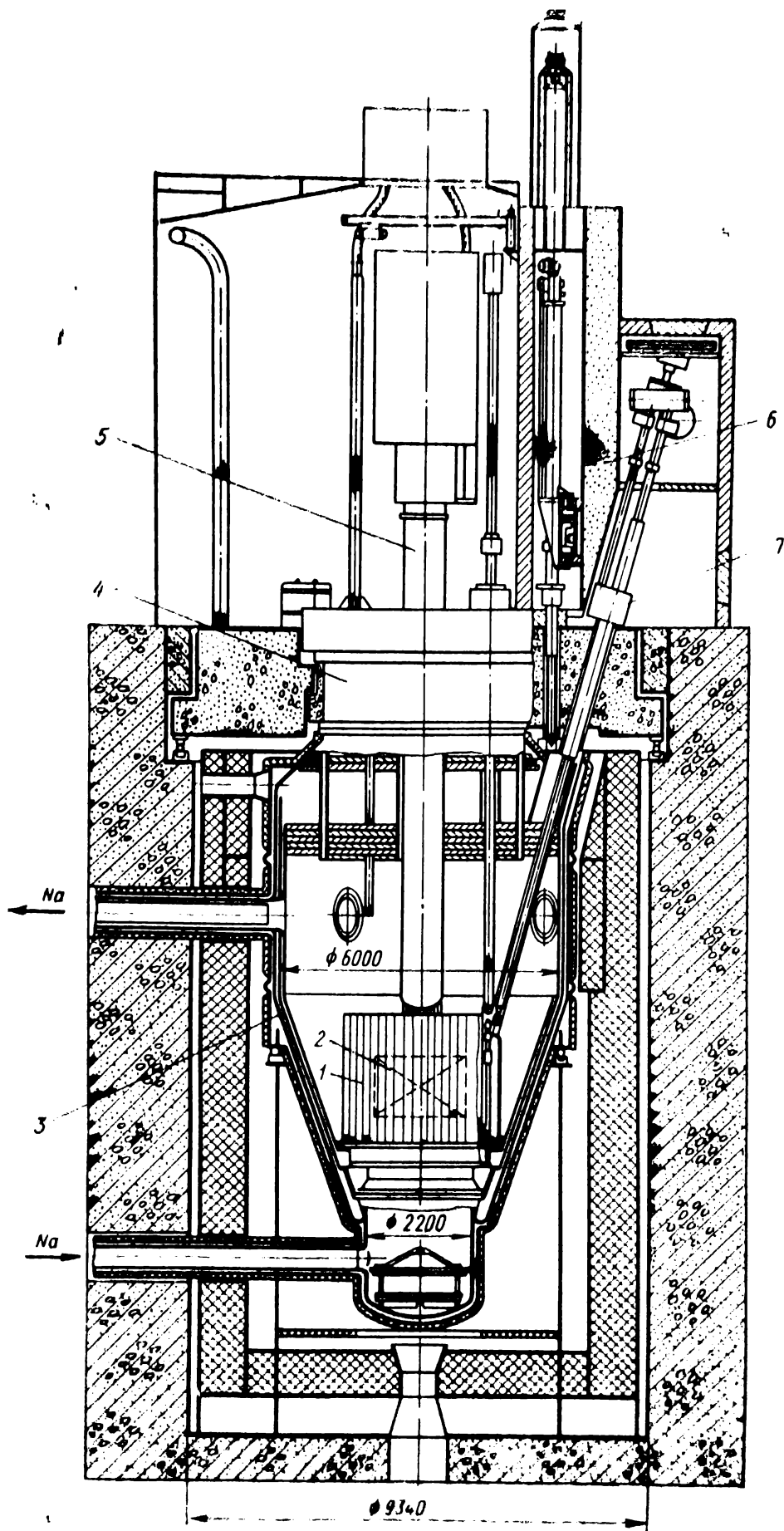


Fig. 14.5 Vertical sectional view of FN-350 reactor

1—reflector; 2—core; 3—reactor body; 4—rotating plugs; 5—central column with SCS drive mechanism; 6—unloading box; 7—unloading elevator

nism to the cap of any of the cassettes. The cassette to be removed is carried by the recharge mechanism to the elevator where it is deposited in a socket and then transported to the transfer device. The latter in turn directs the cassette to the transfer drum which sets it in storage where it is cooled before being discharged from the reactor. The transfer device then returns with a fresh cassette extracted from a second drum and the elevator and recharge mechanism insert the fresh cassette in the vacant socket. The reactor is controlled by two boron carbide automatic control rods, compensators consisting of boron carbide rod assemblies. Three such assemblies are used for emergency shutdowns.

A multilayer radiation shield is employed in the reactor. The first layer of the side shield (stainless steel-sodium) reduces the fast neutron flux density in the vessel by about ten times. The second layer (steel-ferric oxide) protects the concrete from intense neutron and gamma-quantum beams. The top shield consists of a layer of sodium, a steel plate, plugs and alternating layers of iron and graphite.

The second step in constructing powerful and economically efficient APS with fast reactors will be the FN-600 designed for unit III of the Beloyarsk APS. Various means of improving the economical characteristics of APS have been incorporated in the FN-600. Thus, the steam pressure and temperature, APS power capacity, fuel burn-up and operating period have all been increased (see Table 14.3).

The FN-600 reactor (Fig. 14.6), heat exchangers, pumps and other equipment of the first loop are housed in a tank filled with sodium. Pipes of the second loop are connected to the tank. Due to this use of tanks the equipment takes up little space and the first loop can be made leak-proof by simple means. The experience obtained in operating the FN-350 and FN-600 will help to choose optimal designs of the primary loops in more powerful fast reactors.

Some of the ideas used in the design of FN-350 will be used in the FN-600. Thus, the sizes of the cassettes and recharge mechanism will be the same etc. The diameter to height ratio D/H is 2.7 (see Table 14.3). By flattening the core in this way it will be possible to increase the sodium flow rate, reduce its heating in the reactor and also the maximum temperature of the protective casing.

APPENDIX

1. International System of Units (SI)

Physical quantities are expressed in certain units. In solving problems all physical quantities should be expressed in SI units (Table A.1).

Table A.1

Some SI Units of Measurement of Physical Quantities

Physical quantity	Name of unit	Unit symbol
length	metre	m
mass	kilogram	kg
time	second	s
temperature	kelvin	K
density	kilogram per cubic metre	kg/m ³
force	newton	N
pressure	pascal	Pa
work (energy)	joule	J
power	watt	W
quantity of electricity	coulomb	C
electric current	ampere	A
electric field strength	volt per metre	V/m
electric potential difference	volt	V
magnetic induction	tesla	T
activity (of radionuclides)	becquerel	Bq
absorbed dose	gray	Gy

Units differing by factors of 10 are denoted by prefixes. In the following the symbols of the prefixes are indicated in parentheses: giga (G)— 10^9 ; mega (M)— 10^6 ; kilo (k)— 10^3 ; centi (c)— 10^{-2} ; milli (m)— 10^{-3} ; micro (μ)— 10^{-6} . Example: 1 megawatt (MW) = 10^6 W; 1 microampere (μ A) = 10^{-6} A.

Some convenient units which do not differ by a factor of 10 and are not included in the SI are presented in Table A.2.

Table A.2

Some Units Not Included in the SI

Physical quantity	Name of unit	Unit symbol	Conversion factor to SI units
time	day	d	1 d = 8.64×10^4 s
volume	year	y	1 y $\approx 3.15 \times 10^7$ s
	litre	l	1 l = 1.0×10^{-3} m ³ (1 l = 1.0 dm ³ = 10 ³ cm ³)
energy	watt-hour	Wh	1 Wh = 3600 J
	electron-volt	eV	1 eV = 1.00×10^{-19} J
power	kilocalorie per hour	keal/h	1 keal/h = 1.163 W
pressure	millimetres of mercury	mm Hg	1 mm Hg = 133.3 Pa
	standard atmosphere	atm	1 atm = 1.01×10^5 Pa = 1 bar

2. Fundamental Constants

Velocity of light in vacuum $c = 2.998 \times 10^8$ m/sAvogadro's number $N_A = 6.02 \times 10^{23}$ molecules/kmoleBoltzmann's constant $k = 1.38 \times 10^{-23}$ J/K = 8.63×10^{-4} eV/KPlanck's constant $h = 6.626 \times 10^{-34}$ J.s = 4.13×10^{-15} eV.s $\hbar = h/2\pi = 1.05 \times 10^{-34}$ J.s = 6.56×10^{-10} eV.sElectron charge $e = -1.60 \times 10^{-19}$ C

Rest mass of

electron $m_e = 9.11 \times 10^{-31}$ kg $m_e = 5.49 \times 10^{-4}$ amuproton $m_p = 1.6726 \times 10^{-27}$ kg $m_p = 1.007276$ amuneutron $m_n = 1.6750 \times 10^{-27}$ kg $m_n = 1.008665$ amuAtomic mass unit 1 amu = 1.66×10^{-27} kg

Energy equivalent in MeV of

an atomic mass unit 931

electron mass 0.511

proton mass 938.2

neutron mass 939.5

3. Physical and Nuclear Properties of Some Elements

Element	Chemical symbol	Atomic number Z	Density ρ_0 at 20°C, 10 kg/m ³	Density of atoms, N , 10 ²⁸ m ⁻³	Thermal neutron scattering section, σ_s , b	Absorption cross section for 0.025 eV neutrons	
						σ_a , b	Σ_a , 10 ³ m ⁻¹
Aluminum	Al	13	26.97	2.7	1.4	0.23	0.014
Beryllium	Be	4	29.013	1.85	1.7	0.010	0.001
Boron	B	5	10.82	2.54	14.1	755	107
Hydrogen	H	1	1.008	8 \times 10 ⁻⁵	0.005	0.33	2.6 \times 10 ⁻³
Helium	He	2	4.003	1.6 \times 10 ⁻⁴	0.0025	—	—
Iron	Fe	26	55.85	7.85	8.47	2.53	0.21
Cadmium	Cd	48	112.41	8.65	4.63	2450	310
Potassium	K	19	339.096	0.87	1.34	2.1	0.028
Oxygen	O	8	16.00	1.33 \times 10 ⁻³	0.005	—	—
Cobalt	Co	27	58.94	8.71	8.90	37	3.3
Magnesium	Mg	12	24.32	1.74	4.91	3.6	0.063
Molybdenum	Mo	42	95.95	10.20	6.40	2.7	0.027
Sodium	Na	11	22.99	0.97	2.54	20.5	0.173
Nickel	Ni	28	58.69	8.9	9.13	4.8	0.013
Niobium	Nb	41	92.91	8.4	5.45	1.15	0.44
Lead	Pb	82	207.21	11.40	3.30	1.1	0.063
Thorium	Th	90	232.05	11.5	2.98	5.56	0.056
Carbon	C	6	12.01	1.67	8.38	0.034	0.212
Uranium	²³⁸ U	92	238.05	18.7	4.73	2.7	2.9 \times 10 ⁻⁴
Zirconium	Zr	40	91.22	6.44	6.94	33.3	0.128
					$\Sigma_f = 582$	$\Sigma_f = 27.9$	$\Sigma_f = 27.9$
					$\sigma_f = 0.18$	7.65×10^{-3}	7.65×10^{-3}

4. Physical Properties of Some Moderators

Property	Water H ₂ O	Heavy wa- ter D ₂ O	Beryllium Be	Carbon (graphite) C	Beryllium oxide BeO
Density at 20°C, 10 ³ kg/m ³	1.00	1.10	1.85	1.67	2.80
Atomic (molecular) mass	18	20	9	12	25
Density of atoms (molecules), 10 ²⁸ atoms (mol.)/m ³	3.34	3.31	12.35	8.37	6.75
Slowing-down power $\xi \Sigma_s$, 10 ² m ⁻¹	1.35	0.188	0.154	0.064	0.129
Absorption mean free path λ_a for $E_n =$ = 0.025 eV, 10 ⁻² m	45.1	26 500	810	3740	1610
Scattering mean free path λ_s for $E_n =$ = 0.025 eV, 10 ⁻² m	0.68	2.88	1.35	2.54	1.50
Diffusion length L for $E_n = 0.025$ eV, 10 ⁻² m	2.72	159	21	58	30
Slowing-down length L_s , 10 ⁻² m	5.2	11.2	9.3	17.7	12.0

5. Half-lives of Some Radioactive Substances

Substance	$T_{1/2}$	Substance	$T_{1/2}$
¹⁴ C	20.38 min	²¹⁰ Po	138.378 days
⁴⁰ K	1.28×10^9 years	²²⁶ Ra	1600 years
⁶⁰ Co	5.27 years	²³² Th	1.405×10^{10} years
¹⁰⁸ Ag	2.41 min	²³⁸ U	6.85×10^8 years
¹¹⁴ In	54.15 min	²³⁸ U	4.468×10^9 years
¹⁹⁶ Au	2.6946 days	²³⁹ Pu	2.4060×10^4 years
²¹⁰ Bi	5.012 days		

6. Values of e^{-x} and e^x Functions

x	e^{-x}	e^x	x	e^{-x}	e^x	x	e^{-x}	e^x
0.0	1.000	1.00	1.6	0.202	4.95	3.2	0.041	24.5
0.1	0.905	1.11	1.7	0.183	5.47	3.3	0.037	27.1
0.2	0.818	1.22	1.8	0.165	6.05	3.4	0.033	30.0
0.3	0.741	1.35	1.9	0.150	6.69	3.5	0.030	33.1
0.4	0.670	1.48	2.0	0.135	7.39	3.6	0.027	36.6
0.5	0.607	1.65	2.1	0.123	8.17	3.7	0.025	40.5
0.6	0.549	1.82	2.2	0.111	9.03	3.8	0.022	44.7
0.7	0.497	2.01	2.3	0.100	9.97	3.9	0.020	49.4
0.8	0.449	2.23	2.4	0.091	11.0	4.0	0.018	54.6
0.9	0.407	2.46	2.5	0.082	12.2	5.0	0.00740	148
1.0	0.368	2.72	2.6	0.074	13.5	6.0	0.00248	403
1.1	0.333	3.0	2.7	0.067	14.9	7.0	0.000912	1096
1.2	0.301	3.32	2.8	0.061	16.5	8.0	0.000315	2980
1.3	0.273	3.67	2.9	0.055	18.2	9.0	0.000123	8100
1.4	0.247	4.06	3.0	0.050	20.1	10.0	0.000045	22 000
1.5	0.223	4.48	3.1	0.045	22.2			

SUBJECT INDEX

Accelerator, linear resonance 154
Activity 79
Alpha-decay 70
Alpha-particle 50
Angstrom 14
Annihilation 200
Atom 5
 excited 29
 labelled 90
 metastable 47
Atomic mass unit 11
Atomic number 27
 effective 115
Avogadro's number 12

Barn 175
Becquerel 79
Betatron 161
Beta-decay 70
Beta-particle 70
Bohr postulates 28
Boltzmann constant 18
Boron control 316
Burn-up absorption rod 316

Cadmium ratio 220
Cassette 265
 emergency control 316
Chamber, bubble 150
 cloud 148
 diffusion 149
 fusion 218
 ionization 126
Channel, fuel 252
 loop 263
Characteristic, counting 137
 regulating 319
 volt-ampere 128

Coefficient, diffusion 227
 energy transfer 114
 heat transfer 329
 linear attenuation 109
 linear scattering 114
 mass attenuation 109
 neutron transmission 222
 reactivity temperature 307
 slowing-down 231
 transmission 83
 volume-nonuniformity 299

Compton effect 112
Conversion efficiency 141
Conversion factor 260
Coolant 277
Core 252
Cosine of scattering angle, average 226
Cost of electric power 340
Counter, Cherenkov 147
 Geiger-Muller 126, 138
 halogen 139
 proportional 126, 133
 scintillation 141
Counting rate 127
Cross section, macroscopic 223
 microscopic 223
 partial 129
 total 213
Curie 79
Cycle, multiplication 245
 thorium 261
 uranium 261
Cyclotron 156

Decay constant 77
Density of, nuclear fluid 67
 particles 13, 96
Detector, boron-containing 217

Detector,
 current 127
 efficiency 132
 pulse 127
 semiconductor 143

Deuterium 50

Deuteron 50

Diffraction of radiation 24

Disintegration diagram 75
 equation 73

Displacement law, radioactive 74

Dose, of absorbed radiation 117
 equivalent 118
 exposure 117
 maximum permissible 119
 rate 118

Effective cross section 175

Effective increment 297

Efficiency of control device 316

Electrode, collecting 129

Electron 14
 capture 86
 shell 28

Elementary, charge 14
 particle 200

Energy, atomic (nuclear) 57
 binding of, nucleus 54
 particle system 29
 of a body 21
 decay 73
 total 72
 fission 242
 ion pair formation 101
 kinetic 22
 level of, atom 29
 nucleus 58
 reaction 168
 rest 21

Enriched uranium 246

Enrichment of uranium 246

Equation of nuclear reaction 167

Extrapolated boundary 291

Factor, accumulation 115
 effective multiplication 247

fast fission 246

gas amplification 130

infinite multiplication 246

photomultiplier amplification
 142

power reactivity 309

radiation quality 118

size-shape 291

thermal utilization 245

use 341

Fermi 61

Filter, gamma radiation 70, 120

Fission fragment 239

Fluence, particle 98

Fuel channel 252

Fuel element 252

Gas, electronegative 129
 electropositive 129

Gamma, decay 70
 quantum 58
 radiation 23
 primary 108
 scattered 112
 secondary 114

Gray 117

Half-life 71

Half-value thickness 109

Impurity concentration 13

Integral, effective resonance 282

Internal conversion 87

Iodine well 313

Ion mobility 129

Ionization, gamma constant 120
 losses 100
 primary 126
 secondary 130

Isobar 50

Isomer, nuclear 50

Isotope 50
 content 12

Kilogram-mole 12

Lattice of fuel elements 264

Law of, conservation of,
 charge 75
 energy 72
 number of nucleons 75
 momentum 73
 radioactive decay 77

Length, diffusion 235
 migration 236
 slowing-down 233
Loop experimental 263

Magnetosphere 198
Mass, of atom 11
 atomic 11
 body 21
 critical 247
 defect 54
 molecular 11
 molecule 11
 nucleus 50
 rest 21
Mass spectrometer 51
Material parameter 290
Matter 11
 fissile 238
 radioactive 70
 tissue-equivalent 117
Maximum permissible uptake (MPU) 119
Mean annual permissible concentration (APC) 119
Mean free path of neutrons 224
Mendeleev periodic law 31
Mesic atom 66
Model, drop (nuclear) 65
 shell 67
Moderator 231
Molecule 11
Moseley's law 36
Muon 66

Neutrino 85
Neutron 49
 age 234
 delayed 240
 fast 213
 fusion 240
 flow 228
 intermediate 213
 prompt 240
 resonance 213
 slow 213
temperature 235
thermal 213
transmission coefficient 222

yield of nuclear reaction 177
 per absorption act 242
 per fission 240
Neutron-proton diagram 64
Nuclear, concentration 245
 forces 60
 fuel 239, 273
 burn-up 254
 isomerism 88
 photoelectric effect 180
 reaction 166
Nucleon 60
Nucleus, atomic 49
 compound 171
 daughter 71
 excited 58
 fissile 237
 magic 57
 parent 71
 radioactive 69
Nuclide 49
Number, atomic 27
 mass 49
 quantum 28, 41, 42

Pair production 113
Particle, flux 96
 density 96
 primary 108
Pauli exclusion principle 44
Phosphor 141
Photoelectric effect 26
 nuclear 180
Photographic plate 150
Photon 26
Pion 62
Planck constant 26
Plasma 182
Positron 14
Positronium 107
Potential, barrier 61
 well 61
Probability 15
 density 17
 resonance capture escape 246
Protective shield 120
Protium 50
Proton 35
Proton synchrotron 163
Pulse, voltage 127

Rad 117
Radiation, annihilation 107
 belt 198
 bremsstrahlung 106
 cosmic 193
 creep 274
 directional 96
 electromagnetic 23
 intensity 96
 integral 98
 ionizing 96
 monoenergetic 96
 protection 120
 Vavilov-Cherenkov 147
 X-ray 23, 35
Radiative, capture of particles 168
 energy losses 105
Radioactivation technique 219
Radioactive series 76
Radioactivity 69
Radioisotope 69
 fuel 91
 thermoelectric power generator 91
Radiolysis of water 273
Radius of nucleus 61
Range of particle, linear 102
 mass 104
Reaction, endothermic 169
 exothermic 169
 nuclear fission chain 243
 thermonuclear 183
 threshold 169
Reactivity 253
Reactor, breeder 261
 channel 266
 core 252
 critical 253
 experimental 262
 fast neutron 267
 heterogeneous 264
 homogeneous 263
 intermediate neutron 268
 nuclear 250
 operating period 254
 period 302
 poisoning 310
 power 259, 269
 prompt critical 304
 research 259
 start-up, physical 321
 thermal neutron 267
 thermonuclear 184
 vessel 266
Recombination of ions 129
Reflector 256
Residual heat 326
Resolving power of, instrument 52
 pulse detector 133
Resonance integral, effective 282
Rod, absorption 254
 automatic control 255
 burn-up absorption 316
 calibration of 320
 interference 319
 safety 255
 shim 255
Roentgen 117
 equivalent man 118

Safety and Control System (SCS) 254
Saturation current 130
Scattering, anisotropic 227
 elastic 167
 inelastic 167
 isotropic 227
Screen, protective 120
SCS operating devices 254
Sensitivity of detector 132
Size-shape factor 291
Slowing-down power 231
Slowing parameter 229
Solar wind 194
Source, gamma ray 120
 isotropic 115
 point 115
 neutron 206
Specific, energy losses 101
 ionization 100
Spectrometer 17
 time-of-flight 209
Spectrum, alpha-particle 84
 atomic 31
 beta-particle 84
 continuous 17
 discrete (line) 17
 Fermi 233
 of physical quantity 17

Spectrum,
mass 52
Maxwell 18
normalized 18
State of atom, excited 29
ground 29
State of nucleus, excited 58
ground 58
Stopping power 101
Structural material 277
Swelling 274
Synchrocyclotron 159
Synchrotron 162

Temperature, neutron 235
Thermal shield 257
Time, doubling 262
phosphorus emission 142

reactor power doubling 302
resolving 133
Transparency of phosphor 142
Transuranium elements 189
Tritium 50
Triton 50

Uncertainty principle 45
Unit, cell of reactor lattice 264
charge 14

Van de Graaf electrostatic generator 154
Velocity of light 21
Vul'f-Bragg equation 25

Waste uranium 274

